The effect of wood composition and compatibilisers on polyethylene/wood fibre composites

By

Anour N. Shebani

Dissertation presented for the degree of Doctor of Philosophy (Polymer Science)

at

Stellenbosch University

Promoter: *Prof Albert J. van Reenen*
Copromoter: *Dr. Martina Meincken*

December 2010

Declaration

I, the undersigned hereby declare that the work in this thesis is my own original work and that I have not previously in its entirety or in part submitted it at any university for a degree.

Signature: ……
Date: ……

Abstract

The effects of the macromolecular composition and content of different wood species on the properties of wood-polymer composites (WPCs) achieved when using poly(vinyl alcohol-co-ethylene) (EVOH) as a compatibiliser and linear low density polyethylene (LLDPE) as a matrix, were investigated. Four wood different species (*A. cyclops* (acacia), *E. grandis* (eucalyptus), *P. radiata* (pine) and *Q. alba* (oak)) with different macromolecular composition and contents and average particle lengths were used. WPCs filled with these species and WPCs filled with the same species but without extractives were prepared using 10% wood content and different amounts (0, 2, 5, 7 and 10%) of EVOH. An EVOH content of 7% was found to be optimum. Unextracted woods produced WPCs with higher mechanical properties and better resistance to ultraviolet (UV) degradation, while the extracted woods produced WPCs with lower water absorption (WA) rates and better thermal stability. Use of unextracted *A. cyclops* resulted in composites with superior mechanical and thermal properties compared with the other unextracted species, most probably due to its higher cellulose and lignin contents and a favourable average wood particle length (0.225 mm). *A. cyclops* composites also had higher WA and thickness swelling (TS) rates most likely due to the greater number of free hydroxyl groups present in these composites because of higher cellulose content. Composites containing wood species with a high lignin and extractive content, such as *A. cyclops* and *Q. alba*, exhibited higher resistance to UV degradation.

Poly(vinyl alcohol-co-ethylenes) (EVOHs) with different ethylene content (27, 32, 38 and 44%) and *A. cyclops* with different particle sizes (180, 250 and 450 μm) were used to prepare WPCs with 10% *A. cyclops* content. The effect of the contact area between the *A. cyclops* particles and LLDPE achieved when using EVOHs as compatibilisers on the properties of WPCs was also investigated. The greatest improvements in the mechanical and thermal properties of composites made with *A. cyclops* with particle size 180 μm were obtained when EVOH with 44% ethylene content was used. The greatest improvements in the composites made with *A. cyclops* with particle size 250 μm were achieved when EVOH with 38% ethylene content was used. Composites made with *A. cyclops* with particle size 450 μm exhibited better properties when EVOH with 27% ethylene content was used. All the composites that

had better mechanical and thermal properties, also exhibited better compatibility and interface adhesion.

Two successful approaches were used to impart more attractive ecological and economical advantages to WPCs. In the first approach, (0, 2, 5 and 7%) degraded LLDPE was used as a compatibiliser in WPCs at levels of 10, 30 and 50% wood content. The resulting mechanical properties, such as tensile strength and hardness, thermal and morphological properties of the compatibilised composites were slightly higher than those of noncompatibilised composites and virgin LLDPE. Elongation at break and impact properties of the compatibilised composites were lower than in virgin LLDPE, but higher than in noncompatibilised composites.

In the second approach, polyethylene (PE) and various functionalised polyethylenes (PEs) were synthesised by copolymerising ethylene and 10-undecen-1-ol using a soluble metallocene/methylaluminoxane catalyst at room temperature. The incorporation of functional groups increased with increasing comonomer content. WPCs with 10 and 30% wood content were prepared. The composites prepared with functionalised PEs had better mechanical, thermal and morphogical properties than the composites prepared with PE. Composites made with functionalised PE with higher hydroxyl groups content exhibited better properties than composites made with functionalised PE with lower hydroxyl groups content. Composites with 10% wood content exhibited better properties and performance than composites with 30% wood content.

Opsomming

Die gevolg van die makromolekulêre samestelling van verskillende houtspesies op die eienskappe van hout-polimeer saamgestelde materiale (HPS) wanneer poli(viniel alcohol-ko-etileen) (EVOH) as versoeningsmiddel gebruik word saam met linieêre lae digtheid poli(etileen) (LLDPE) as matriks is ondersoek. Vier houtspesies (*A. cyclops* (acacia), *E. grandis* (eucalyptus), *P. radiata* (pine) and *Q. alba* (oak)) met verskillende makromolekulêre samestelling and partikelgrootte-verspreiding is gebruik in die studie. HPS materiale is berei met hierdie vesels, beide voor en na ekstraksie van die houtpartikels met onderskeidelik warm water en oplosmiddels (alleen en in kombinasie). In hierdie HPS materiale is 10% hout gebruik en 0, 2, 5, 7 en 10% EVOH. ‘n EVOH inhoud van 7% is as optimum bepaal. Houtpartikels voor ekstraksie het HPS materiale met beter meganiese eienskappe en beter weerstand teen UV bestraling, terwyle partikels wat ekstraksie ondergaan het HPS materiale met laer water-absorpsie en beter hitte-stabiliteit to gevolg gehad het. Die gebruik van on-geekstraheerde *A. cyclops* het samegestelde materiale met die beste meganiese en termiese eienskappe tot gevolg gehad in vergelyking met die ander houtspesies (voor ekstraksie), as gevolg van die hoër sellulose en lignien inhoud van die spesie, sowel as ‘n voordelige partikelgrootte-verspreiding. *A. Cyclops* saamgestelde materiale he took hoër waterabsorpsie (WA) en dikte-swelling (DS) tempos gehad, weens die groter hoeveelheid vrye hidroksielgroepe teenwoording in die materiale, direk in verwantskap met die sellulose-inhoud. Saamgestelde materiale met ‘n hoë hoevellheid lignien en ekstraheerbare materiale (*A. cyclops* and *Q. alba)* het beter weerstand teen UV-degradasie geopenbaar.

Verskillende poli(viniel alkohol-ko-etileen) polimere (EVOHs) met wisselende etileen-inhoud (27, 32, 38 en 44%) en *A. Cyclops* met verskillende partikel-groottes (180, 250 en 250 μm) is gebruik om HPS materiale met 10% hout te vervaardig. Die gevolg van die kontak-area tussen die houtpartikels en die LLDPE wanneer EVOHs as versoeningsmiddel gebruik is, is ook ondersoek. Die beste verbetering in die meganiese en termiese eienskappe van die saamgestelde materiale met *A. cyclops* met partikel-grootte 180 μm is gekry met EVOH met 44% etileen-inhoud, terwyl die beste resultate met 250 μm partikels verkry is met ‘n EVOH met 38% etileen, en met 27% etileen in die geval van die 450 μm partikels.

Twee benaderinge om meer aantreklike ekologiese en ekonomiese eienskappe by die HPS materiale te bewerkstellig was suksesvol. In die eerste geval is gedegradeerde LLDPE as versoeningsmiddel gebruik. Die resulterende meganiese eienskappe van die HPS materiale met LLDPE as versoeningsmiddel was beter as die HPS mateirale daarsonder. Samegestelde materiale met 10, 30 en 50% hout is vervaardig. Die trekverlenging by die breekpunt sowel as die impaksterkte van die HPS materiale was laer as LLDPE alleen, maar beter as die nie-versoende HPS materiale.

In die tweede benadering is polietileen (PE) en gefunksionaliseerde PE gesintetiseer deur etileen en 10-undekeen-1-ol te koplimeriseer met ‘n oplosbare metalloseen/metiel alumoksaan katalis. Die hoeveelheid funskionele (OH) groepe is verhoog deur toenemend ekomonommer-inhoud. HPS materiale met 10 en 30% hout is vervaardig. Die saamgestelde materiale met funksionele PE het beter maganiese eienskappe gehad as die met gewone PE. Hoe hoër die hidroksielgroep-inhoud, hoe beter die eienskappe van die HPS materiale, terwyl die materiale met 10% hout beter eienskappe openbaar het as materiale met 30% hout.

Dedicated to:

♥ **My mother and father, who always supported me in every endeavor. They are the reason I'm here at all, and made me who I am today.**

♥ **My wife and son, who are my inspiration in everything I do and every choice I make.**

Acknowledgments

First and foremost, I would like to thank Allah/God for giving me strength, health, opportunity and courage to face my reality. I thank him also for blessing me.

I would like to express my sincere thanks and appreciation to thank my supervisor, Prof Albert J. van Reenen, for providing his excellent guidance, his fine ideas, and for the time and interest he invested into the project.

I would like to express sincere gratitude to my co-supervisor, Dr. Martina Meincken, for her interest and valuable input to this work. Her constructive comments and suggestions were always appreciated.

I sincerely thank the International Centre for Macromolecular Chemistry and Technology in Libya for financial support and encouragement.

I would like to profoundly thank Dr. M. J. Hurndall for her assistance and advice on the proofreading of this thesis.

I extend my thanks to the people at the department of forest and wood science at Stellenbosch University for wood supplying.

I am grateful to Dr Remy Bucher at Ithemba Labs for his assisting with XRD analysis.

I also would like to express my thanks to all the members of our polyolefins research group at the Institute of Polymer Science at the University of Stellenbosch for their friendship, fellowship, assistance, helpful suggestions, support and encouragement.

Last, but certainly not least, I would like to thank all my family for their continuous love, strong support and unlimited encouragement that I have received over the years. There are no enough words to thank them for providing in me the drive and the self confidence necessary to accomplish this task. Without them none of this would have been possible. My appreciation is also expressed to all my dear and wonderful friends for their friendship, help and support.

List of contents

List of figures

Chapter 2

Chapter 3

Chapter 4

Chapter 5

Chapter 6

Chapter 7

Chapter 8

List of tables

Chapter 2

Chapter 3

Chapter 4

Chapter 5

Chapter 6

Chapter 7

Chapter 8

List of appendices

List of publications

- A.N. Shebani, A. J. van Reenen, M. Meincken, The effect of wood extractives on the thermal stability of different wood species, Thermochimica Acta, 471, 43-50, 2008.

- A.N. Shebani, A. J. van Reenen, M. Meincken, The effect of wood species on the mechanical and thermal properties of wood–LLDPE composites, Journal of Composite Materials, 43, 1-2, 11, 305-1318, 2009.

- A.N. Shebani, A. J. van Reenen, M. Meincken, The effect of wood extractives on the thermal stability of different wood-LLDPE composites, Thermochimica Acta, 481, 1-2, 52-56, 2009.

- A.N. Shebani, A. J. van Reenen, M. Meincken, Using extractive-free wood as a reinforcement in wood-LLDPE composite systems, submitted to Journal of Composite Materials, 2010.

- A.N. Shebani, A. J. van Reenen, M. Meincken, The use of degraded LLDPE as a compatibiliser in wood-LLDPE composites, submitted to Polymer Degradation and Stability, 2010.

- A.N. Shebani, A. J. van Reenen, M. Meincken, The effect of the contact area on the morphogical, mechanical and thermal properties of wood-LLDPE composites, submitted to Journal of Applied Polymer Science, 2010.

List of abbreviations

AA	Acetic anhydride
AACA	2-Diallylamino-4,6-dichloro-s-triazine
ABAC	Abietic acid
Al/Zr	Aluminum/zirconium mole ratio
AN	Acrylonitrile
ASA	Alkyl succinic anhydride
BA	Butyl acrylate
BMI	N,N′-m-phenylene bismaleicimide
BO	Butylene oxide
Cp	Cyclopentadienyl
DMA	Dynamic mechanical analysis
DP	Degree of polymerisation
DS	Dimensional stability
DSC	Differential scanning calorimetry
DTG	Derivative thermogravimetric
E′	Storage modulus
E″	Loss modulus
EAB	Elongation at break
E/C	Ethanol/cyclohexane
EIC	Ethyl isocyanate
EPMA	Epoxylpropyl mechacrylate
ESC	Environmental stress cracking
ESCR	Environmental stress cracking resistance
E/VAC	Ethyl/vinyl acetate
EVOH	Poly(vinyl alcohol-co-ethylene)
EVOH27	Poly(vinyl alcohol-co-ethylene) 27% ethylene content
EVOH32	Poly(vinyl alcohol-co-ethylene) 32% ethylene content
EVOH38	Poly(vinyl alcohol-co-ethylene) 38% ethylene content
EVOH44	Poly(vinyl alcohol-co-ethylene) 44% ethylene content
EVOHs	Poly(vinyl alcohol-co-ethylenes)
FTIR	Fourier-transform infrared spectroscopy
GMA	Glycidyl methacrylate
HDPE	High density polyethylene
HEMA	Hydroxyethyl methacrylate
Hf	Hafnium
ΔH_f	Heat of fusion
ΔH_f^o	Heat of fusion of completely crystalline polymer
HMDIC	Hexamethylene diisocyanate
HT-GPC	High temperature gel permeation chromatography
HW	Hot water

IM	Injection moulding
IR	Infrared spectroscopy
LAC	Linoleic acid
LCBs	Long-chain branching
LDPE	Low density polyethylene
LLDPE	Linear low density polyethylene
LLDPEs	Linear low density polyethylenes
M_0	Mass of the sample before immersion in water
M_I	Mass of the sample after immersion in water
$\overline{M_n}$	Number average molecular weight
$\overline{M_w}$	Weight average molecular weight
MA	Maleic anhydride
MAA-CAAPE	Methacrylic acid-3-((4,6-dichloro-s-triazine-2-yl) amino)propyl ester
MAO	Methylaluminoxane
MAPE	Maleated polyethylene
MAPP	Maleated polypropylene
MFA	Microfibril angle
MI	Melt index
MMA	Methyl methacrylate
MOE	Modulus of elasticity
m-PEs	Metallocene polyethylenes
MW	Molecular weight
MWD	Molecular weight distribution
MWs	Molecular weights
NMR	Nuclear magnetic resonance
OACA	2-Octylamino-4,6-dichloro-s-triazine
OM	Optical microscopy
PE	Polyethylene
PEOH1, PEOH2 and PEOH3	Different functionalised polyethylenes
PEPPIC	Poly[ethylene(polyphenyl isocyanate)]
PF	Phenol-formaldehyde resin
PHA	Phthalic anhydride
PMAA	Polymethacrylic acid
PMPPIC	Poly[methylene(polyphenyl isocyanate)]
PO	Propylene oxide
POD	Photo-oxidation degradation
PP	Polypropylene
PS-PMAA	Polystyrene/polymethacrylic acid
PVAC	Polyvinyl acetate
PVC	Polyvinyl chloride
RHF	Rice-husk flour
SA	Succinic anhydride
SCBs	Short chain branches
SEM	Scanning electron microscopy
SMA	Styrene/maleic anhydride

T_0	Onset temperature in the decomposition of wood
T_{01}	Onset temperature in the first decomposition step of composites
T_{02}	Onset temperature in the second decomposition step of composites
T_1	First decomposition temperature of wood
T_2	Second decomposition temperature of wood
$\mathrm{Tan}\,\delta$	Damping coefficient or damping ratio
T_c	Crystallisation temperature
T_f	Final decomposition temperature of wood
T_{f1}	Final decomposition temperature of the first step of composites
T_{f2}	Final decomposition temperature of the second step of composites
Tg	Glass transition temperature
TGA	Thermogravimetric analysis
T_{h0}	Thickness of the sample film after immersion in water
T_{h1}	Thickness of the sample film before immersion in water
Ti	Titanium
T_m	Melting temperature
TOD	Thermo-oxidative degradation
TS	Thickness swelling
UV	Ultraviolet
WA	Water absorption
WF	Wood flour
WFs	Wood flours
WPC	Wood-polymer composite
WPCs	Wood-polymer composites
X_c	Degree of crystallinity
X_c^{corr}	Corrected degree of crystallinity
XRD	X-ray diffraction
Zr	Zirconium
2θ	Bragg angle

Chapter 1
Introduction and objectives

1.1 Introduction

Traditionally, composite materials combine two or more components with very different properties. Composite materials are widely used in many industries because they possess attractive properties [1]. Composites represent some of the most significant breakthroughs in a variety of industrial applications, (for example, aerospace, aircraft, physical infrastructure and automobile industries) [2] and there has been an increasing use of these materials. The field of composite materials has grown rapidly in recent years in terms of both industrial applications and fundamental research. One reason is because it is often very costly to produce new homopolymers [3]. Another reason is that composite materials can be made from waste polymers and wood, which contributes to reducing the waste disposal burdens of these materials. Composite materials can be man-made but they also exist in nature. Wood is a natural composite of cellulose fibres cemented together with lignin. Man-made composites can be polymer matrix composites, metal matrix composites and ceramic matrix composites. They are made by adding reinforcing fillers into a polymer, metal or ceramic matrix [4-5]. The most common of these are polymer matrix composites [5]. These composites consist of thermoplastic or thermosetting polymers reinforced by fibres (e.g wood fibre).

The use of wood based material, as reinforcement or filler for polymers, has attracted significant interest. Wood is generally light, inexpensive, allows easy fibre modification and it can be added to commodity matrices in considerable amounts, thus offering economically and ecologically advantageous solutions. Wood-polymer composites (WPCs) are produced with low costs. They have low density, good mechanical properties combined with renewability, reasonable processibility and biodegradability when compared to the neat polymer matrix [6-8]. This is because wood is obtained from natural resources, available in various forms and in large quantities. The presence of synthetic polymers in WPCs, on the other hand, provides better moisture and decay resistance.

The use of wood materials in WPCs does however, present several disadvantages. The use of wood as a filler or reinforcement in thermoplastics has been hampered by the limited thermal stability of wood, and the difficulties in obtaining good filler dispersion and strong interfacial

adhesion [9]. Other disadvantages of WPCs are wood's water adsorption and poor dimensional stability, which contrasts with that of solid thermoplastics, where this phenomenon is virtually nonexistent [10]. Furthermore, WPCs are often more brittle than the neat polymers [11-12], which limits their use in applications where these composites are likely to be subjected to impact forces. Some of these disadvantages are due to the natural incompatibility between the hydrophilic wood and hydrophobic polymers.

To address these problems, the polymer must be fully compatible with the chemical constituents of the wood: cellulose, lignin and hemicelluloses. The compatibility and the interfacial adhesion can be improved by using compatibilisers or coupling agents (hereafter referred as compatibilisers) or by modifying the wood surface. WPCs can be used in many different fields, including automotive, construction, marine, electronic and aerospace [13]. Classic applications for WPCs are decking, fencing, industrial flooring, timbers, railing, mouldings, roofing, window and door profiles, as well as automotive applications such as rear shelf trim panels, instrument panels, load floors and cab-back panels [14]. The future of WPCs will ultimately depend on many factors, including the availability and cost of the raw materials, product formulation, product quality, consumer perceptions (market demand) and research objectives or development efforts.

1.2 Motivation

The first motivation for this study was the need to understand the effect of wood's macromolecular composition and content on the properties of WPCs. To our knowledge, nothing is yet reported in the literature on studies carried to determine the effect of wood species with different macromolecular composition and content on the properties of WPCs. The properties of WPCs depend on the physical and mechanical characteristics of the polymer matrix, the macromolecular composition and content of the wood and the amount and nature of the compatibilisers used [3]. Although wood contains cellulose, hemicelluloses, lignin and extractives, its macromolecular composition and content cannot be defined precisely. Wood's macromolecular composition and content varies with species, between and within the trees of the same species, geographic location, climate, and soil conditions. The cellulose, hemicelluloses, lignin and extractives make up the wood cell walls and determine most of the properties of the wood. Although low in content, extractives can have an important effect on the processing and properties of wood/wood based products. Since the quantity of these components varies from species to species, species with different macromolecular composition and content are expected to impart different effects to the properties of wood and WPCs. This helps to formulate a WPC for a specific application.

The second motivation was to be able to impart more attractive ecological and economical advantages to WPCs. In this regard, two approaches were planned in order to achieve this, as described in the methodology section (Section 1.3).

1.3 Methodology

The first approach to attain ecological and economical improvements is to use a degraded polyolefin as a compatibilizer in a WPC system. It is believed that a degraded polyolefin can be an effective compatibiliser because it has the basic functional groups of a compatibiliser. The functional groups in degraded polyolefins (e.g. polyethylene (PE)) can interact with the polar groups (mainly hydroxyl groups) of cellulose to form covalent or hydrogen bonds, while the nonpolar part of degraded polyolefin interacts with the polymer matrix. Use of this approach will help to convert the polymer waste into useful products and reduce the production cost of WPCs.

The second approach is to minimise the raw materials. This can be performed by the synthesis of functionalised polyolefins with high molecular weight (MW) for use as a matrix in WPC systems without any treatment or using any type of compatibiliser. The incorporation of functional groups into polyolefin can provide polymers with improved adhesion, thermal, rheological, morphogical and optical properties, better affinity for dyes and improved compatibility with other materials [15]. A mixture of a polymer matrix and filler (two components system) will probably be less complicated than a mixture of polymer, filler and compatibiliser (three components system) in terms of compatibilisation and processing. Thus, it is appealing to try these two approaches in order to achieve more attractive ecological and economical advantages.

1.4 Objectives

The objectives of this study were the following:

1. To study the effect of different wood species with different macromolecular composition and content on the properties (mechanical, thermal and morphological properties, water absorption, thickness swelling behaviour and resistance to UV degradation) and performance of wood-linear low density polyethylene (LLDPE) composite systems when using poly(vinyl alcohol-co-ethylene) (EVOH) as a compatibiliser.

2. To investigate the differences in the compatibility and interfacial adhesion between the different wood species and LLDPE, achieving by the use of EVOH in each wood-

LLDPE composite system (prepared in the study carried out to address objective 1) and relate any inferior in their properties and performance to poor compatibility and interfacial adhesion.

3. To investigate the effect of the wood extractives on the properties and performance of wood-LLDPE composite systems (composites with superior properties and performance prepared in the study carried out to address objective 1).

4. To study the effect of the contact area between the wood particles and polymer matrix achieved by the use of EVOH, on the properties and performance (mechanical, thermal and morphological properties) of WPCs and performance. This will be studied using different poly(vinyl alcohol-co-ethylenes) (EVOHs) with different hydroxyl group contents, and wood particles with different particle sizes and lengths. Wood species will be selected based on the results achieved for objectives 1-3.

5. To investigate the possibility of using degraded LLDPE as a compatibiliser in WPC systems. Wood particle size will be selected based on the results achieved for objective 4.

6. To assess the attempted use of functionalised PE as a matrix and compatibiliser in a WPC system. Wood species and wood particle size will be selected based on the results achieving for objectives 1-5.

1.5 Outline of dissertation

This dissertation is structured in the following manner:

- **Chapter 1** comprises a general introduction, motivation and objectives of this study.

- **Chapter 2** provides background information about WPCs, including; some facts, concepts, and definitions; historical developments; characteristics of raw materials, such as woods, polymers and compatibilisers; properties and types of components used to produce WPCs; and their effects on the final properties, processing, applications and marketing.

- **Chapter 3** describes the results of an investigation into the effect of different wood species, with different macromolecular composition and content, on the properties and performance of wood-LLDPE composite systems when using EVOH as a compatibiliser.

- **Chapter 4** describes the results of an investigation into the differences in the compatibility and interfacial adhesion between the different wood species and LLDPE via EVOH in different wood-LLDPE composite systems.

- **Chapter 5** describes the results of an investigation into the effect of the wood extractives on the properties and performance of different wood-LLDPE composite systems.

- **Chapter 6** describes the results of an investigation into the effect of the contact area between the wood particles, and polymer matrix, via compatibilisers, on the properties and performance of wood-LLDPE composites.

- **Chapter 7** describes the possibility of using degraded LLDPE as a compatibiliser in WPC systems.

- **Chapter 8** describes an assessment of the attempt made to use functionalised PE as a matrix and compatibilisers simultaneously in wood-LLDPE composite systems. Chapters 3-8 address the objectives as set out in Section 1.3.

- **Chapter 9** presents general conclusions and recommendations for future research.

1.6 References

1. Frei J., Tamburini U., Munir Z., Journal of Applied Physics, 101, 114911-114918, 2007.
2. Bhattacharyya D., Bowis M., Jayaraman K., Composites Science and Technology, 63, 353-365, 2003.
3. Mamunya Y., Zanoaga M., Myshak V., Tanasa F., Lebedev E., Grigoras, V. Semynog C., Journal of Applied Polymer Science, 101, 1700-1710, 2006.
4. Bhargava A., Engineering Materials: Polymers Ceramics and Composites, 1st edition, Prentice Hall of India, New Delhi, 2004. 226-245.
5. Taj S., Munawar M., Khan S., Proc. Pakistan Academy of Science, 44, 129-144, 2007.
6. Nygard P., Tanem B., Karlsen T., Brachet P., Leinsvang B., Composites Science and Technology, 68, 3418-3424, 2008.
7. Ndiaye D., Fanton E., Therias S., Vidal L., Tidjani, A., Gardette, J., Composites Science and Technology, 68, 2779-2784, 2008.
8. Caraschi J., Leão A., Journal of Materials Research, 5, 405-409, 2002.
9. Haihong J., Pascal K., Journal of Vinyl and Additive Technology, 10, 59-69, 2004.
10. Lisperguer J., Droguett C., Ruf B., Nunez M., Journal of the Chilean Chemical Society, 52, 1073-1075, 2007.
11. Afrifah K., Hickok R., Matuana L., Composites Science and Technology, 70, 167-172, 2010.
12. Mengeloglu F., Matuana L., King J., Journal of Vinyl and Additive Technology, 6, 153-157, 2000.
13. Ashori A., Bioresource Technology, 99, 4661-4667, 2008.
14. Kharazipour A., Schöpper C., Müller C., Euring M., Review of Forests; Wood Products and Wood Biotechnology of Iran and Germany - Part III, 1st edition, University of Göttingen, Germany, 2009. 56-69.
15. Aaltonen P., Löfgren B., Macromolecules, 28, 5353-5357, 1995.

Chapter 2
Wood-polymer composites

Abstract

Facts, concepts, advantages and definitions of WPCs are highlighted. Background information and historical development of WPCs are provided. Characteristics of raw materials such as wood, polymers and compatibilisers are presented. This includes historical reviews, properties and types of each component used to produce WPCs and their effect on the final properties of WPCs. Processing, application and marketing of WPCs are also given attention.

Keywords: *WPCs, Woods, Polymers, Compatibilisers*

2.1 Historical and literature review

2.1.1 Introduction

The combination of wood materials with synthetic polymers to make WPCs has gained significant popularity in the last decade [1]. WPCs are also known as wood-plastic composites, wood-fibre plastic composites or green composites [2]. These composites can be divided into two main types; wood-polymer composites and wood-plastic composites [3]. Wood-polymer composites are normally prepared by impregnating wood with monomers and initiators or prepolymers [4-5]. Polymerisation reactions are normally initiated by gamma radiation, chemical catalysts or heat [3]. Wood-plastic composites, on the other hand, include wood-thermosetting composites and wood-thermoplastic composites [3, 6] and can be prepared by dispersing wood particles and additives in molten plastic [3, 7]. The abbreviation "WPCs" most often represents wood thermoplastic composites [3].

2.1.2 Advantages

The popularity of WPCs stems from the fact that WPCs take advantage of the properties of both wood and plastics. Wood represents a low-cost, renewable natural reinforcement that enhances mechanical properties such as strength and modulus, enhances heat deflection temperature under load, and produces composites with low density and at low cost [8-10]. Wood further offers several other advantages, including biodegradability, no associated health hazards, ease of surface modification, wide availability and relative nonabrasiveness [1, 11]. On the other hand, plastics provide good moisture and decay resistance [3]. Consequently,

WPCs have many advantages over pure plastics, such as improved stiffness, creep resistance, thermal stability [12] and resistance against biological deterioration [13]. This makes WPCs highly desirable in terms of its properties and economic and environmental aspects. WPCs are known to reduce the waste disposal burdens caused by manufacturing plastics and wood [14]. Recycled plastics and wood have both been shown to be acceptable as raw materials for WPCs [15]. Although it may be difficult to secure recycled raw material sources, many commercial WPC manufacturers use a combination of recycled wood and plastics [3, 16].

2.1.3 Definitions

The term WPC refers to any composite that contains plant fibres and thermosets or thermoplastics [17-18]. According to Schneider and Witt [19] WPCs have the feel and look of wood with the hardness, machineability and moisture resistance of plastics. WPCs are hybrid materials that combine the advantages of thermoplastics and wood or natural fibres [20]. WPCs can also be described as wood impregnated with polymers in order to strengthen the properties of the natural wood [21]. WPCs are mostly thermoplastically processible composites that consist of varying contents of wood, plastic and additives and are processed by shape-forming techniques such as extrusion, injection moulding (IM), rotomoulding or pressing [22]. Ellis and Sanadi [23] considered WPCs as unique materials where a natural composite (wood) is impregnated with monomers that are then polymerised in the wood to tailor the material for special applications.

2.1.4 Brief history

The uses of thermosetting polymers in the production of WPCs have a long history, while the use of thermoplastic polymers is a more recent innovation [20]. In the early 1900s, wood-thermoset composites were produced using phenol-formaldehyde resin and wood sawdust [6]. In 1916, Rolls-Royce made the first commercial product, which was a gear lever knob made of WPC [24].

WPCs were patented in Italy in the 1920s [25]. Between 1930 and 1960, many attempts were made to alter wood properties by impregnation with polymers [26]. In the early 1960s, results of studies by Kenaga, Kent and Meyer for making WPCs helped to initiate further research in Canada, Japan, Germany, France, Austria, the United Kingdom, Denmark, Czechoslovakia and South Africa [21]. The use of lignocellulosic fibres as the reinforcing material for thermoplastics was introduced in patents in the 1960s and 1970s in order to reduce the cost and improve the mechanical properties of composites [27]. WPC was re-born as a modern concept in Italy in the 1970s, and popularised in North America in the early 1990s [17, 28].

WPCs attracted interest both in academia and in industry in the 1980s due to their advantages over mineral filler-polymer composites [29]. Since the 1980s, WPCs have been extensively used for automotive applications, building products, packaging materials, and in other areas [30]. In the 1990s, the use of WPCs grew significantly. Polyethylene (PE) and polypropylene (PP) composites with up to 50% wood content were produced [7]. Better WPCs have now been developed, with a higher wood content, better interfacial properties, improved processing technologies and more effective additives.

2.1.5 Literature review

Papers and patents dealing with WPCs date back to the 1960s and 1970s [1, 4, 21]. Reviews of types of modified woods have also been published [31-33]. The use of in-situ polymerisation to produce WPCs was reported by Kenaga [34] and Hills [35]. Handa et al. [36] reported the physical properties of WPCs, while Spindler et al. [37] studied the resistance of WPCs to chemical corrosion. Baas [38] described microscopic studies on the interactions between plastic and the cell wall of beech. Munozescalona et al. [39] demonstrated the effect of the impregnation of six different tropical wood species with various vinyl monomers. The utilisation of partial-impregnation techniques to improve the economic viability of WPCs was explored by Du Plessis and Du Toit [40] and general information on WPC applications was given by Witt [41]. Okumura et al. [42] investigated the temperature dependence of viscoelastic properties of wood-poly(methyl methacrylate) (PMMA) composites prepared by various methods. Lya and Majali [43] reported the development of radiation processed WPCs based on tropical hardwoods. Moustafa et al. [44] investigated the impregnation and polymerisation of several samples of casuarina and other types of wood with methyl methacrylate (MMA) with some other specific multifunctional monomers, such as ethylene glycol dimethacrylate. Coutts and Campbell [45] studied the role of compatibilisers in wood fibre-reinforced cement composites.

In the 1980s and 1990s, authors paid more attention to property improvements in WPCs. Some authors [46-49] reported the improvement in WPCs when using different types of raw materials. The improvement of some mechanical properties (e.g. impact toughness) of WPCs by blending with rubber was also reported [50-51]. Other authors [52] introduced and discussed some facts and concepts about using WPCs in some applications such as structural automotive applications. A number of papers [53-54] reported the possibilities of using pure lignin or cellulose as reinforcements in WPC composite systems. The effect of compatibilisers on the properties of WPCs was also studied [55-57]. The effect of processing

received less attention, although some authors [58-60] described the development of compounding processes and studied their effects on the final properties of WPCs.

Since 2000, there has been a significant increase in the number of reports from scientists and engineers engaged in the development of these materials. More attention has been directed to the effects of processing on the final properties of WPCs [61-63]. New topics, such as resistance to environmental degradation [64-65] and the utilisation and behaviour of liquefied WPCs [66-67], have emerged. Some research [68-70] has been devoted to the improvement of the interfacial adhesion between the wood and the plastics by modifying the wood or adding compatibilisers. Several authors [71-73] have presented reviews of WPCs (e.g. uses of WPCs in construction, building, some environmental applications, the effect of additives, etc.). Some papers [74-75] have described the main differences between wood species and mineral fillers in terms of their ability to reinforce and enhance properties, while others [76-77] investigated the effect of adding clay or rubber to WPCs. The uses of waste wood and plastics in the production of WPCs to meet the demand for WPCs in various applications and to impart more attractive ecological and economical advantages have gained increased interest [78-79]. The main aim of most researchers [80-82] was to improve the properties of WPCs over those of the raw materials.

2.2 Characteristics of raw materials

2.2.1 Wood

2.2.1.1 Wood anatomy

The anatomy of wood is complex because wood is porous, it contains fibres and is anisotropic [24]. The general features of wood are shown in Figure 2.1a [83-84]. Wood is primarily composed of hollow, elongated, spindle shaped cells called tracheids or fibres [24]. The wood cell wall consists of two layers: the primary wall (thin outer layer) and the secondary wall (thicker inner layer) [85]. This structure is displayed in Figure 2.1b [83]. These layers consist mostly of cellulose, hemicelluloses and lignin, in varying amounts.

The cellulose chains crystallize into microfibrils, which run roughly parallel to the main fibre direction in the S_2 wall, while they are more horizontally orientated in the S_1 and S_3 walls. The grey lines in the secondary wall layers, as shown in Figure 2.1b, represent idealised cellulose microfibrils. The angle between these microfibrils is called the microfibril angle (MFA) and plays a crucial role in determining the mechanical properties of wood [83]. The lumen is the hollow centre of the fibres. Extractives are present throughout the cell wall structure and their type and amount depends on the wood species. The fibres dimensions are highly variable and

depend on wood type and the position in the tree [24]. The adjacent wood cells are bound together by lignin and hemicelluloses, and this layer between the cells is called the middle lamella.

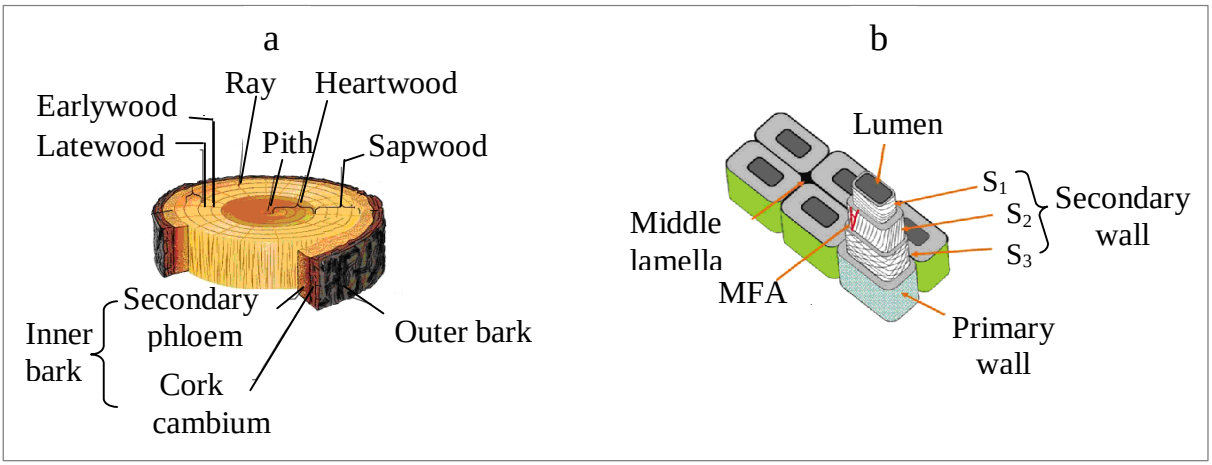

Figure 2.1 The main features and structure of wood [83-84].

2.2.1.2 Wood classification

Wood is classified by botanical and anatomical features rather than actual wood hardness into softwoods and hardwoods [24]. These terms are in common technical use, although the wood of some hardwoods is actually softer than that of many of the softwoods [86]. Softwoods include pines, yew, firs, cedars, spruces, etc., while hardwoods include species such as acacia, basswood, cottonwood, balsa, oak, maple, ash, eucalyptus, etc.

Hardwood fibres are often cheaper and more readily available than softwood fibres and they have been found to be more suitable for extrusion with respect to long-term mechanical properties [87]. This is important because the wood species chosen for WPCs, manufacturing often depends on its cost and availability [24].

The anatomical structure of hardwoods is more varied and complicated than that of softwoods, as they contain vessels that are not found in softwoods. The hollow and spindle-shaped elongated cells are called tracheids in softwoods and fibres in hardwoods.

Figure 2.2 shows that hardwoods contain vessels (the big black holes) and illustrates the three dimensional differences between hardwood and softwood cell structure [88-89]. Vessels appear as holes and are termed pores. The size, shape, and arrangement of these pores vary between different species [7]. Vessels are shorter than hardwood and softwood fibres but larger in diameter, as illustrated in Figure 2.3.

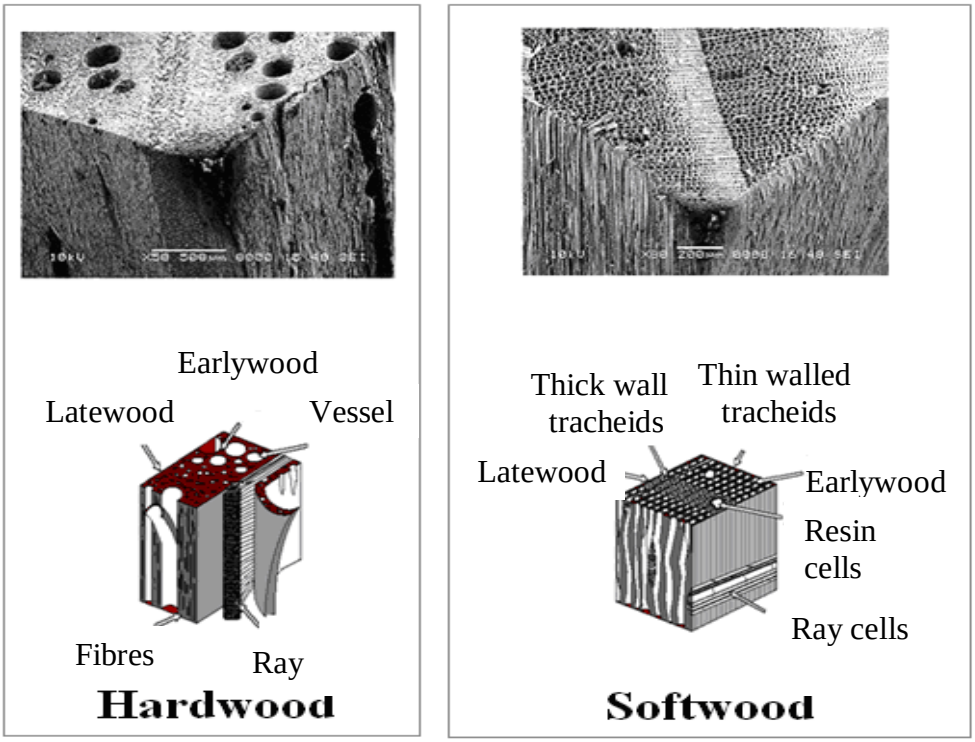

Figure 2.2 Anatomical structures of hardwood and softwood [88-89].

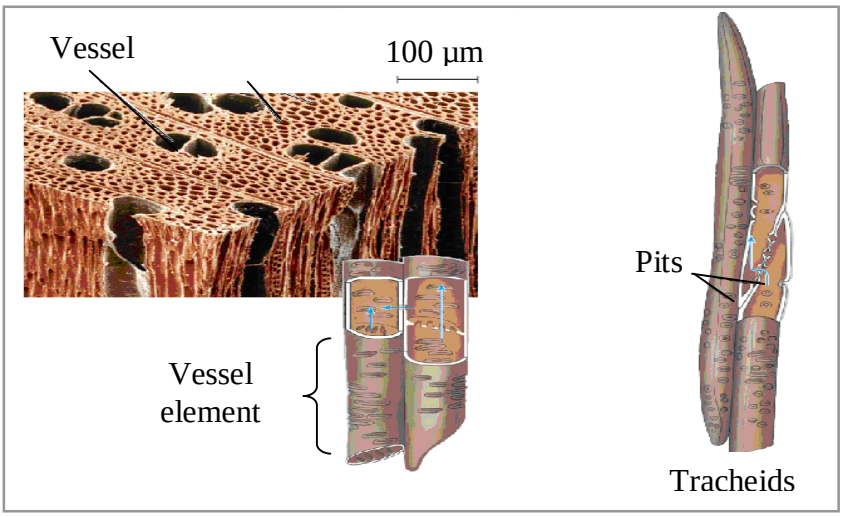

Figure 2.3 Relative sizes of vessel and tracheids in wood [90].

Hardwood fibres are shorter than softwood tracheids and average about half the width of the softwood tracheids, but are usually 2-10 times longer than vessel elements. The characteristics of these fibrous cells and their arrangement affect the wood's strength properties, appearance, resistance to penetration by water and chemicals, resistance to decay, and many other properties [91]. The major differences between hardwoods and softwoods are listed in Table

2.1. In the field of WPCs, it has been found that hardwood-PP composites have better performance and mechanical properties than softwood-PP composites [92-93]. For example, hardwood-filled composites tend to have better flexural strength and heat deflection than softwood-filled composites [94].

Table 2.1 The major differences between softwoods and hardwoods

	Softwoods	Hardwoods	Ref.
Structure of lignin	Lignin consists predominantly of guaiacyl (G) units	Lignin is more complex due to the presence of both guaiacyl (G) and syringyl (S) units	[87]
Extractives	Lower concentration of steryl esters and waxes	Higher concentration of steryl esters and waxes	[95]
Density	Lower	Higher	[96]
Structural	Greater uniformity	Less uniformity	[97]
Strength and stiffness	Lower	Higher	[98]
Flexibility	More flexible	Less flexible	[8]
Crack propagation	Stable	Unstable	[94]
Degradation	Higher rate	Slower rate	[99]
Water absorbency	lesser WA	more WA	[100]
Dimensional stability	Poor	Better	[101]
Fibre length	Range from 3 to 8 mm	Average about 1 mm	[87]
Fibre diameter	Smaller diameters	Larger diameters	[102]
Alkalis/acids attack	Less susceptible to attack	More susceptible to attack	[102]
Cost and availability	Expensive and less available	Cheaper and more available	[87]

2.2.1.3 Wood composition and components

Wood has an elemental composition of about 50% carbon, 6% hydrogen, 44% oxygen and trace amounts of nitrogen and several metal ions [7, 103]. The components that are presents in all wood types include carbohydrates (mainly as polysaccharides, i.e. cellulose, hemicelluloses such as xylanes, mannans, starch, pectic substance), phenolic substances (lignin, tannins, phlobaphenes, colouring matter and lignans), terpenes (resin acids, and volatile terpene and terpenoid compounds), aliphatic acids (fatty acids including acetic acid), alcohols (aliphatic alcohols and sterols), proteins and inorganic (ash) constituents [86].

Cellulose, as shown in Figure 2.4, is the principal component. On average it contributes about 50% to the dry mass of wood. It is an organic compound with the formula $(C_6H_{10}O_5)_n$ and is a highly crystalline, linear condensation polymer of D-anhydroglucopyranose (often abbreviated as anhydroglucose units or just glucose units) joined together by β -1,4-glycosidic bonds with a degree of polymerisation (DP) or (n) of 10000–14000 [8, 24]. The elementary unit contains three hydroxyl groups. Many wood properties depend on the cellulose chain length or the DP. Cellulose is organised in crystalline as well as amorphous regions.

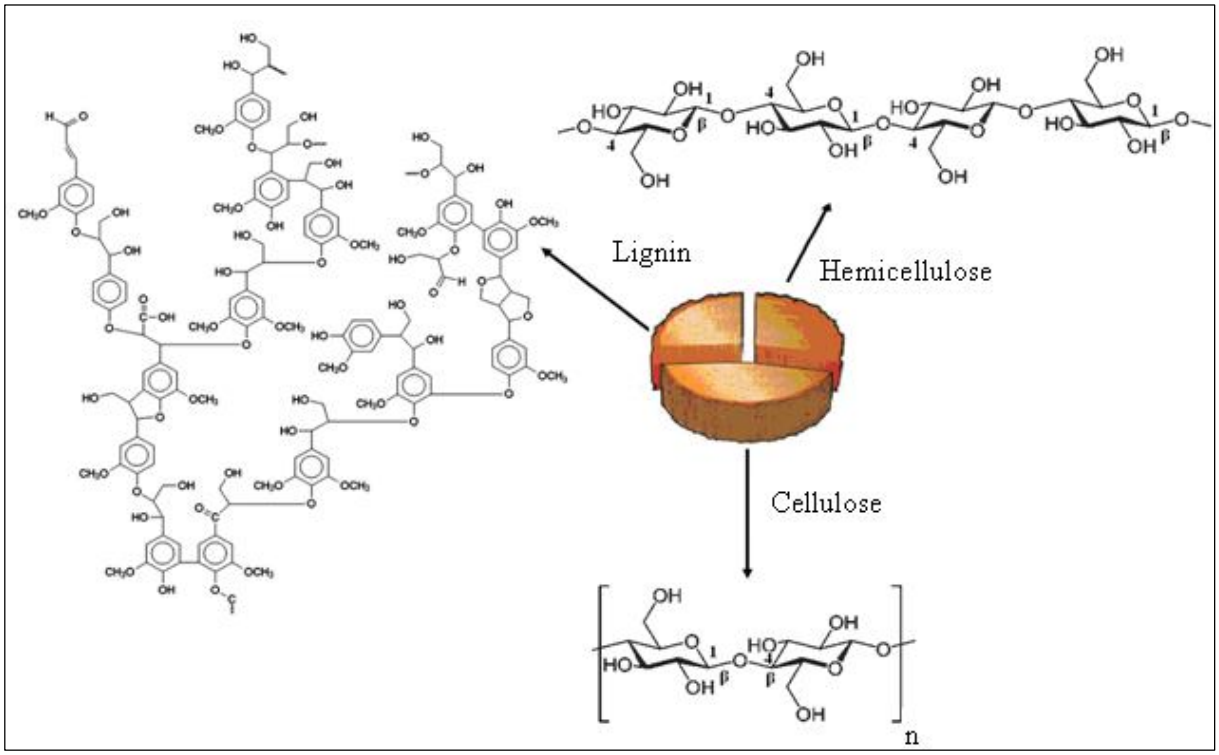

Figure 2.4 The major chemical components of wood [104].

In wood, cellulose is typically 60–90% crystalline by mass and its crystal structure consists of monoclinic and triclinic unit cells [24]. As shown in Figure 2.5 [105], the cellulose molecules are arranged into ordered strands called fibrils, which in turn are organised into the larger structural elements that make up the cell wall of wood fibres [8].

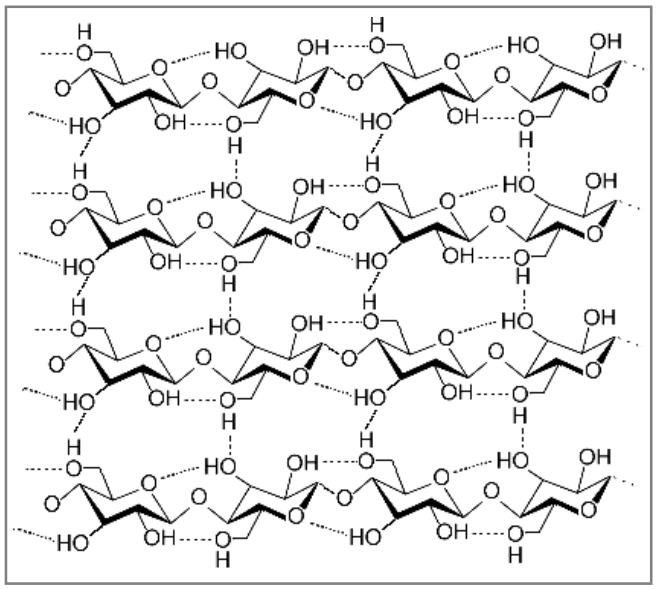

Figure 2.5 Fibril strand structure of cellulose showing intra- and inter-molecular hydrogen bonding [105].

The strands of cellulose in Figure 2.5 show the hydrogen bonds within and between cellulose molecules. The hydroxyl groups form hydrogen bonds within the macromolecule itself (intra-

molecular), and between other cellulose macromolecules (inter-molecular) and between different cellulose chains [106]. Overall, the molecular structure of cellulose is responsible for its super-molecular structure and this, in turn, determines many of its properties [8].

Hemicelluloses are the second most abundant class of polysaccharides found in nature after cellulose, comprising roughly 25–35% of most plant materials, with the amount varying according to the particular plant [107-108]. The general formulas are $(C_5H_8O_4)_n$ and $(C_6H_{10}O_5)_n$, which are called pentosans and hexosans, respectively [109]. Hemicelluloses are branched polymers of low MW with a DP of 80-200 [110-111]. Hemicelluloses are non-cellulosic heteropolysaccharides consisting of various different sugar units, arranged in different proportions, and having different substituents [109]. The hemicelluloses obtained from wood is mainly constituted of units of α-D-glucuronic acid, or 4-*O*-methyl-α-D-glucuronic acid and occasional units of α-L-arabinofuranose, α-D-xylopyranose or α-D-galactopyranose as side chains. Other side groups are acetyl groups, phenolic acids, ferulic, and coumaric acids [111]. Hemicelluloses are the amorphous cell-wall constituent, which occupies the space between the fibrils in both the primary and secondary wall. Hemicelluloses have the ability to bind non-covalently through hydrogen bonding to cellulose and to bind covalently to lignin. According to literature [112], the DP of hemicelluloses isolated from softwood is about 100 and for hardwood hemicelluloses are about 200.

Lignin, as shown in Figure 2.4, is a complex hydrocarbon polymer with both aliphatic and aromatic constituents [8]. Lignin is a three-dimensional, amorphous polymer with high MW and comprises various linked phenylpropane units. It is formed from hydroxyl and methoxy substituted phenylpropane units [113]. Lignin is a polymer of phenylpropane units: guaiacyl (G) units from the precursor trans-coniferyl-alcohol, syringyl (S) units from trans-sinapyl-alcohol, and p-hydoxyphenyl (H) units from the precursor trans-p-coumaryl alcohol. Lignin can be classified into two major groups: guaiacyl lignins and guaiacyl-syringyl lignins. Guaiacyl lignin is found in softwoods while guaiacyl-syringyl lignin is present in hardwoods. Guaiacyl lignin is composed principally of coniferyl alcohol units, while guaiacyl-syringyl lignin contains monomeric units from coniferyl and sinapyl alcohol.

Hardwood lignin has higher methoxy group content than softwood lignin [114]. Softwood lignins are more cross-linked than hardwood lignins [115]. Softwood lignin has a MW of about 90 000 or more, while the MW of hardwood lignin is lower [116]. The composition of lignin can vary with species and the quantity increases with plant age and stem diameter [114].

Wood extractives are a group of low MW organic compounds that may be extracted from wood by means of polar or nonpolar solvents [117]. Although extractives contribute only a few percent to the entire wood composition, they cover a wide range of chemical compounds. They comprise fats, waxes, fatty acids, tannins, gums, sugars, starches, resins, colouring matters, steryl esters, sterols, terpenoids, and other phenolic compounds [117-118]. The extractive content varies between 2% and 5% but can be as high as 15% [119]. The quality of wood can be affected by the amount and type of these extractives [120]. The type and the amount of extractives determine the possible use of wood in WPCs, e.g. wood from Manchurian Ash is commonly used for producing automotive interior panelling, because of its relatively high bulk density, high stiffness and low extractives content [121]. Extractives can be removed with a single solvent or a combination of solvents, such as ethanol, water, benzene, or a mixture (1:2) of ethanol/cyclohexane [118, 122-123]. The amount of the extractives depends on wood species, wood age, and the location in the tree. Extractives can be removed from finely-ground wood samples by Soxhlet extraction with any of the above solvent for periods ranging from 4 to 18 hours [111]. More information on extraction methods, testing procedures, solvents, etc. is available in texts on TAPPI test methods [118].

In conclusion, at a molecular level softwoods and hardwoods contain the same types of macromolecular compounds, i.e. cellulose, hemicelluloses and lignin. The type and amounts of building blocks (monomer) as well as the bonds between the monomers differ [124]. The fact that wood material had a biological function, created further differences at higher structural levels found in the tree. At an ultra-structural level, however, wood structure resembles that of a fibre reinforced composite, the reinforcing element being the cellulose microfibril units embedded in a matrix of the wood polymers lignin and hemicelluloses [125]. Like in any complex composite material, the supramolecular organization between cellulose, hemicelluloses and lignin in cell walls determines the properties of the plant fibres [126].

2.2.1.4 Effects of wood components on the properties of wood and wood-polymer composites

- **Mechanical properties**

Most of the attention has been given to the cellulose when it comes to mechanical properties of the wood components. This is because cellulose is the reinforcing material in the wood and therefore the component that mostly determines the properties of the wood material (flour) or wood fibre (pulp) [127]. Most of the mechanical properties of natural fibres depend on their cellulose type, because each type of cellulose has its own cell geometry and the geometrical

conditions determine the mechanical properties [8]. Tensile strength, modulus of elasticity (MOE) and elongation at break (EAB) provide an excellent measure of the degree of reinforcement provided by the fibre to a composite.

Cellulose is responsible for high tensile strength in wood due to its microfibrillar structure [24]. According to Bledzki and Gassan [8] and Bledzki et al. [128] an increase in a WPC's strength can be ascribed to higher cellulose and lignin content, as well as a better dispersion and adhesion of fibres to the matrix. Yang et al. [129] showed that the difference in the tensile strength between PP-rice-husk flour (RHF) and PP-wood flour (WF) composites can be attributed to the difference in the holocellulose (cellulose and hemicelluloses) content in RHF and WF. Karina et al. [130] found that Kenaf and banana fibre filled PP composites showed higher tensile strength due to the high cellulose content compared with acacia filled PP composites. Unger et al. [131] claimed that higher cellulose content in wood composition tends to increase the tensile strength, while higher lignin content tends to improve compression strength.

The MOE describes the stiffness of a material and is therefore one of the most important properties in engineering design. The MOE measures how well a material resists tension. A smaller MOE illustrates that less stress causes more strain, and vice versa. The MOE of wood fibres is approximately 40 times higher than that of PE [132]. A higher MOE in wood can be ascribed to a high cellulose content and low MFA [133]. The MOE of cellulose is about 132 GPa, which exceeds that of many metals, the MOE of lignin is about 2 GPa [134], and that of hemicelluloses are about 8 GPa [129]. WPCs often reach 1/3-1/2 of the MOE of wood [24].

In general, wood fillers with higher stiffness than the polymer matrix reduce the EAB [135]. As a result, the addition of wood particles to plastics causes a decrease in the EAB [136]. The dramatic drop of the EAB is due to the stiffening effect of wood particles [29]. This behaviour is typical of reinforced thermoplastics and has been widely reported [8, 135-136]. According to Bouafif et al. [137] the difference between two different WPCs in the EAB can be related to the difference in the wood dispersion and the presence of extractives. Good dispersion of wood particles in the polymer matrix and the presence of some lipophilic extractives result in a better EAB.

Hardness is an important property, especially in the flooring and furniture industries. Hardness is defined as the resistance of a material to deformation, usually indentations. WPCs usually show a greater hardness than pure polymers. Hardness of WPCs increases with an increase in the wood particle loading [138]. As the wood particle loading increases the

composite became stiffer and harder [9]. Investigations have shown that wood hardness is influenced by its density and moisture content [139-140]. Higher density increases the hardness, and as the moisture content level increases, the hardness decreases [140]. Others [7, 23] reported that the hardness of WPC can be due to the polymer hardness, polymer loading and polymer-wood interactions. According to Elvy et al. [58] the ultimate hardness values of a WPC depends on the intrinsic hardness of the wood species used.

The final important mechanical property that remains to be discussed is the impact strength. The impact resistance is the ability of a material and its structure to survive impact induced damages during an impact event [81]. The impact behaviour of WPCs in engineering applications is also a very important property, which may influence the design of WPCs. Impact behaviour is normally affected by the fibre type and content, matrix ductility and void content. The fillers are believed to reduce the polymer chain mobility and thereby reduce the ability to absorb energy during fracture propagation [135]. Karmarkar et al. [136] suggested two reasons for the decrease in the impact strength. The first is that the presence of wood particles in the polymer matrix provides points of stress concentration, thus providing sites for crack initiation. The second is the stiffening of polymer chains due to bonding between wood and the matrix.

- **Thermal properties**

Some authors have found that the crystallinity of the polymer matrix of WPCs can be higher than that of a pure polymer matrix because the wood particles act as sites for heterogeneous nucleation, which increases the crystallinity of the matrix [141-142], while other authors [72, 143-144] have found the opposite trend. According to Sailaja et al. [69] the reduced crystallinity as fibre loading increases may be due to the incorporation of wood particles and compatibiliser, which inhibits close packing of the matrix chains. This indicates strong interactions between the components in the WPC. Mamunya et al. [144] suggested that the interactions between polymer and wood lead to the binding of some macromolecular chains to the wood surface, which results in a decrease in the polymer's crystallisation rate near the wood surface because the polymer chains bound to wood seem to be excluded from the crystallisation during the preparation of the composite.

Hristov and Vasileva [143] claimed that the observed decrease in the values of crystallinity with the addition of wood particles can be directly related to the dilution effect of the wood particles. Most of these studies showed no real change in the melting temperature (T_m) and crystallisation temperature (T_c) of the polymer matrix.

Thermal stability is a crucial aspect in the development of WPCs as it affects the maximum service temperature of the composites. Wood as a filler is usually processed with plastics at temperatures below 200 ^{o}C due to its low thermal stability [24]. This, however, limits the type of plastics that can be used in WPCs and the applications for which they can be used. Thermal properties of wood vary depending on the chemistry and structure of the wood. Tserki et al. [145] reported that the lower thermal stability of some wood species can be attributed to a high lignin and hemicelluloses content, while the high thermal stability is due to the higher cellulose content. This is because the onset of degradation differs for the major wood components. Cellulose is the most thermally stable [24] and hemicelluloses are the least thermally stable [146-147]. A high lignin content seems to impart more stability to the wood at high temperatures due to its low degradation rate. The decomposition of lignin occurs over a wide temperature range [145]. On the other hand, the decomposition of the wood extractives in some wood species can continue up to 550 ^{o}C, overlapping with the decomposition of other wood components [148]. The decomposition of these extractives occurs in a broad temperature range and in two main stages: the first stage takes place below 250 ^{o}C and the second stage between 250 and 550 ^{o}C.

Polyolefins such as PE degrade in one single step due to the decomposition of carbon-carbon (C-C) bonds in the main chain. PE remains chemically stable until about 270-290 ^{o}C and at higher temperature the MW decreases [149]. The polyolefin degradation temperature range is quite broad. Most of the degradation occurs between 400 and 600 ^{o}C. In another words, PE degradation begins somewhere above 370 ^{o}C, by random scission reactions, and is completed above 500 ^{o}C. This degradation process normally occurs very slowly below 500 ^{o}C and very rapidly above 500 ^{o}C. PE decomposes into paraffinic and olefin compounds, particularly *n*-alkanes and *n*-alkenes, which are volatile and leave little or no residual char. However, the improvements in the stability of WPCs over pure wood or pure polymer indicate that the compatibility and interface adhesion is increased by mixing both components with compatibilisers [150].

- **Viscoelastic properties**

Dynamic mechanical analysis (DMA) is a technique which permits the determination of the viscoelastic behaviour of polymers and provides valuable insights into the relationship between structure, morphology and properties of composite materials [125]. The damping coefficient or loss coefficient or damping ratio (tan δ) is a particularly useful parameter, which can be used to provide information about the adhesion in a composite system [125, 133]. Tan δ is the ratio of the loss modulus (E″) to the storage modulus (E′). E′ is associated

with the elastic response of the composite and indicates the stiffness of the material. E″ is proportional to the amount of energy that has been dissipated as heat by the sample and represents its viscous response.

Tan δ is independent of the material's stiffness and hence is a very good parameter when the differences in viscoelastic response of the material are desired [151]. Branched and linear PE, for example, displays three well known transitions. It is common to label these observed transitions with decreasing transition temperatures as α-, β- and γ-transitions. The α-transition is due to deformation movements in the amorphous regions and consequent reorientation within crystallites. The β-transition can be assigned to the relaxation of chain units located in the interfacial region. Finally, the γ-transition can be interpreted as the reorientation of three, five or more chain units of the main backbone, known as crankshaft movements. The γ-transition is better known as the glass transition temperature (T_g).

The position of the primary γ-transition peak can provide information about the interaction between the polymer and wood at the molecular level. Any shift in this transition to higher temperatures in comparison to the pure polymer indicates better interfacial interaction between wood particle and polymer matrix, and a restriction in the mobility of the polymer matrix [152-153]. The shift in γ-transition should be proportional to the surface area of the filler, so the effect is expected to increase with increasing wood content [154]. According to Behzad et al. [155] an increase in the intensity or amplitude of this transition indicates that the number of molecular portions responsible for this transition has increased. The number of so-called "defects" in the crystalline region increases when fibres are present. According to Gatenholm et al. [156], weight or volume ratios of wood influence the T_g and E′ of WPCs. E′ and E″ can be affected by the type of filler and the strength of the interface that is formed via compatibilisers [157].

- **Water absorption, thickness swelling and dimensional stability**

In some WPC applications, such as building components/structural uses, dimensional stability (DS) is critical, particularly for outdoor use. It is important to understand the water absorption (WA) and thickness swelling (TS). When a WPC is exposed to moisture it absorbs water. As the WA rate increases the TS rate increases [79]. This has an undesirable effect on the DS, as it could have a deleterious effect on some mechanical and physical properties of the WPC [158]. Mechanical properties, such as stiffness and strength, can be negatively influenced [159] because the adhesion between polymer and wood becomes very weak when

the composite is wet. WA and TS are affected by the polymer type, wood content, and more significantly, the type and amount of compatibilisers. The presence of voids increases the WA and TS. The WA and TS increase with the wood filler content and immersion time until an equilibrium condition is reached [160].

The polymer matrix exhibits no WA and TS, while the wood particle induces significant WA and TS. This is obvious, because the polymer matrix (e.g. PE or PP) is hydrophobic, while wood is hydrophilic. The increase in the WA and TS, as the wood content increases can be explained by the water-wood interaction [154]. In spite of all the information mentioned above, not much attention has yet been paid to the effect of wood extractives on the WA and TS rates of WPCs during the WA test.

- **Resistance to ultraviolet radiation**

The effect of ultraviolet (UV) radiation on WPCs is important because some of the main applications of WPCs are outdoor applications. WPCs are likely to undergo degradation that limits their use. The photo-oxidative degradation (POD) of WPCs seems to be only a surface phenomenon, which promotes the environmental stress cracking (ESC) [64]. Some authors [161-162] found that some WPCs retained a higher percentage of their original mechanical properties after UV exposure compared to the unfilled polymer. It has been shown that the colour of WPCs lightens after weathering [65]. The results of Ndiaye et al. [163] clearly revealed that the presence of wood in polymer composites does not change the effects of POD in the polymer, but it can cause a significant improvement in the photo-stability of WPCs.

The POD mechanisms of wood and plastic are complex, but well documented in the literature. The POD of polyolefins has been intensively studied [164-175]. The detailed kinetics of oxidation has been investigated using various analytical techniques [164-166]. POD occurs mainly via a free-radical chain mechanism, initiated by the absorption of UV radiation by chromophores within the polymer [167]. It occurs as a heterogeneous process controlled by oxygen diffusion. The amorphous regions are more affected as oxygen diffuses into the amorphous phase, leading to chain scission and weakening of the intermolecular forces. According to Attwood et al. [167], the preliminary reaction is generally bond scission in the polymer chain or in some other molecule, initiating degradation. Subsequent reactions can typically include crosslinking and double bond formation. PE undergoes chain scission, branching and crosslinking, which take place as competitive reactions, while PP predominantly undergoes chain scission. Molecular structure, morphology, internal

impurities, specimen thickness, temperature, irradiation intensity and other climatic conditions can be considered as the most important factors influencing polyolefin POD.

PE is easily degraded by UV light due to the low dissociation energy of its chemical bonds: 410 kJ/mol for the carbon-hydrogen (C-H) bond and 339 kJ/mol for the C-C bond. The main products of PE POD are hydroxyl, carbonyl and vinyl groups [168]. Naddeo et al. [169] investigated the UV degradation of LLDPE and found that, following the initial small production of hydroperoxides, the degradation is dominated by the formation of carbonyl and vinyl species. Several different mechanisms have been proposed for the formation of these groups. It appears that the UV radiation leads to a breakdown of molecular chains and a reduction in molecular size, making the PE brittle. The kinetics of POD in PE is characterised by a superposition of two phenomena [169]. The first one corresponds to an exponential increase in the concentration of carbonyl groups with time and is observed when the kinetics are controlled by the diffusion of oxygen. The second one corresponds to a linear increase of the carbonyl concentration with time, it occurs in degraded samples, and is not controlled by diffusion. Weathering of PE results in an increase in crystallinity, which indicates that chain scission, has occurred [170]. Chain scission normally forms short chains that are more mobile and crystallize easily, and cause embrittlement.

The POD of wood is attributed to the degradation of its components. It takes place on the wood surface, primarily in the lignin component. It results in a characteristic colour change [24]. The POD process largely depends on the surface properties of the wood. It is well known that lignin is more susceptible than cellulose to POD [171]. About 80-95% of the degradation of wood by light can be due to the POD of lignin [172]. The POD process is slow, and results in a change in the colour and loosening or erosion of the fibre surface [7]. The change in the wood colour to yellow-brown reflects the chemical changes due to POD, and is mostly due to a breakdown of lignin and wood extractives [24].

According to Kutz [172], the key step involved in POD appears to be the photolysis and fragmentation of lignin, resulting in the formation of aromatic radicals. Further degradation of lignin and POD of other wood components such as cellulose and hemicelluloses occurs via these radicals. These radicals can be terminated by reacting with photo-degraded lignin fragments, producing yellow unsaturated carbonyl compounds, which explain why wood turns yellow when exposed to light. However, lignin undergoes POD via many different pathways. Ultimately, they all lead to the formation of chromophoric groups, such as carboxylic acids, quinones and hydroperoxide radicals that have a characteristic yellow

colour [68]. The POD of cellulose is based on the wavelength of the incident light [172]. The rate of POD in cellulose is high below 280 nm and very low above 340 nm. Free radicals can form through this process via the cleavage of glycosidic bonds in the presence of oxygen. Some radicals, especially hydroxyl radicals, are known to be important intermediates in this oxidative process [173]. The POD of cellulose also results in an increase in the carbonyl content. The carbonyl content increases with increasing the exposure time.

Wood extractives also play a role in the POD process of wood. Some extractives such as terpenes, terpenoids, phenol, lignans, tannins and flavonoids are very good light absorbers [24]. The presence of extractives may therefore exert a protective effect on the POD of wood. Depending on the composition of extractives, the colour of degraded wood becomes yellow, grey, and red-orange or brown [174]. The POD of wood proceeds more rapidly in the presence of moisture. This is because water molecules swell the wood and thereby open up previously inaccessible regions of the material, facilitating their degradation [171]. The POD of wood results in an increase in the cellulose content and a decrease in the lignin content at the surface, and it ultimately leads to deterioration of some physical, chemical and biological properties of wood [175].

It should be emphasised that the wood influences the properties of the WPC, not only by the type and composition of the wood used, but also by the geometry and aspect ratio of the wood particles [128]. For example, the improvements in composite strength are limited by the low aspect ratio of the wood particles [24]. Prachayawarakorn [176] claimed that good interfacial adhesion between wood particles and the matrix is associated with a high aspect ratio or longer length of the sawdust which makes the reinforcement transfer forces along the length of the reinforcement more efficient. The length of the wood particles and their variation affect the mechanical properties of WPCs significantly [138]. On the other hand, smaller sized wood particles result in lower WA and TS rates and better DS behaviour. Raj et al. [177] reported that small particles are not as easily dispersed as large particles because of a higher specific surface area that exposes more hydroxyl groups. Dányádi et al. [178] mentioned that very small or very large particles induce a separation or de-bonding at the interfaces. According to Bledzki et al. [128] short and narrow wood particles are preferable, because they provide a high specific surface area, which increases the adhesion between the wood and the polymer, and results in a homogenous distribution and better compatibility.

It is known that the specific surface area, which depends on the particle size distribution of the filler, determines the area of the contact surface between the polymer and the filler [176].

Since a higher specific surface area exposes more hydroxyl groups, a larger number of bonds can be formed and better interfacial adhesion between the wood and the matrix can be expected. A larger number of bonds between wood and matrix, on the other hand, will lead to better stress transfer [178].

The adhesion and compatibility between the wood and matrix is an important parameter to understand with regards to the stress transfer in WPCs. The efficiency of the stress transfer from the polymer to the wood particles is of fundamental importance in determining the mechanical properties of WPCs [179]. Weak interfacial adhesion prevents the wood particles from acting effectively as reinforcement by reducing the ability to transfer stress from the matrix to the wood particles and vice versa. It is possible to observe cracks through the wood particles when fracturing the WPCs [180], which can be an indication of stress transfer from the weaker matrix to the stronger wood particle. This is, however, only possible in the case of good compatibility and strong interfacial adhesion. This stress transfer occurs not only along the wood particle, but possibly also at the particle ends [181]. Insufficient adhesion and debonding between wood and the polymer matrix can lead to an increase in the number of voids present in the composite. This in turn causes an increase in the WA and TS of the WPCs, which has a deleterious effect on their mechanical and physical properties, as mentioned above in the WA and TS section.

Poorly compatible WPCs show relatively low strength and stiffness, poor impact properties and dimensional stability, whereas composites with strong interfaces have a high strength and stiffness but are somewhat brittle [14, 141]. Zhang et al. [182] reported that poor compatibility can cause an agglomeration of wood particles, weak interfacial adhesion, and unsatisfactory properties.

It is difficult to obtain good compatibility and interfacial adhesion between the hydrophilic wood and hydrophobic polymer due to the energy difference at their interfaces. The effective way to address this problem is to improve the polarity of the polymer or to reduce the polarity of the wood surface and decrease the energy difference at interfaces [183]. This can be accomplished by modifying the wood or adding a compatibiliser to the composite. Compatibilisers improve the interfacial bonding between wood and polymer matrix and facilitate the stress transfer at interfaces [184] by increasing the contact area between wood particles and polymer matrix. They enhance dispersion and improve the adhesion of the two components [185]. Overall, compatibilisers enhance the mechanical properties and thermal stability and reduce the WA of WPCs.

2.2.1.5 Types of wood used in the WPCs

Ashori [17] classified plant fibres according to which part of the plant they are obtained from. Plant fibres can originate from the stem, leaf, seed, fruit, root, grass, cereal straw and wood. According to Bledzki and Gassan [8] many types of plant fibres are used to reinforce plastics: hairs (cotton, kapok), fibre-sheafs of dicotylic plants or vessel-sheafs of monocotylic plants, e.g. bast (flax, hemp, jute, ramie), and hard-fibres (sisal, henequen, coir). WF has been produced commercially since 1906 and has been used in many and varied products including WPCs [24]. WF is a finely ground, dried wood product. It is fibrous in structure and acts as reinforcing materials for plastics. The most commonly used wood flours (WFs) for WPCs in the United States are pine, oak and maple [24]. Veneers and lumber have been used for many years to produce WPCs [19]. Other species, such as alder, yellow poplar, ash, maple, walnut, birch, basswood, red gum, beech, red and white pine has also been found useful for WPCs [186-187]. Species such as acacia [188], eucalyptus [136], RHF [129], Manchurian ash [121], spruce [180], aspen [189], bamboo [190] and coconut [191] are also used as fillers in WPCs. Woods particles used in WPCs have a large variety of shapes and can be used alone or in combinations. Ichazo et al. [192] tried to use mixture of some types of WF, for example, cedar, pine, oak and saki-saki for WPCs. Selection of the wood species is based on regional availability, familiarity and costs. The costs are variable and based on availability, particle size and shipping distance. Narrow particle size distributions and fine sizes tend to increase the costs [24].

2.2.2 The polymer matrix

Composites are normally categorized by their matrix characteristics, including type (metal, ceramic, polymeric-based organic or inorganic filler), origin (natural or artificial) and processability (thermoplastic or thermoset) [193]. As stated earlier in Section 2.2.1.4, due to the low thermal stability of wood, plastics that can be processed below 200 ^{o}C are generally used for WPCs. Thermoplastics offer several advantages such as low processing costs, design flexibility and ease of moulding over thermoset polymers. Nevertheless, several thermoset resins such as phenol-formaldehyde or diphenyl methane diisocyanate are also used in WPCs [7]. Some manufacturers use a combination of thermoplastics and thermosets as a matrix material [24]. The matrix serves the following functions: stress transfer in and out of the fibres, prevention of crack propagation through the fibres, and protection of the fibres from the environment [193]. The most common WPCs use polyolefins as a matrix, either PE or PP, due to their low cost and good processing compatibility with wood [17]. As shown in Figure 2.6 [24], the greater majority of WPCs use virgin and recycled PE as a matrix. All PE grades (low density polyethylene (LDPE), LLDPE and high density polyethylene (HDPE))

are used to produce WPCs [194]. The matrix is often selected based on its inherent properties, product requirements, availability, cost and the manufacturer's familiarity with the fillers [7]. For example, WPCs made with PE are used in exterior building components, while WPCs made with PP are used in automotive applications. WPCs made with poly(vinyl chloride) (PVC) are used in window manufacturing, decking, etc. The relative quantities of these polymers used in the manufacturing of WPCs are 70% for PE, 17% for PP and 13% for PVC. Polybutene [195], acrylonitrile butadiene styrene, polystyrene [36], polyesters, polyepoxide, PMMA [54], polybutylene succinate [196] and polyurethane [197] are also used as matrices for WPCs.

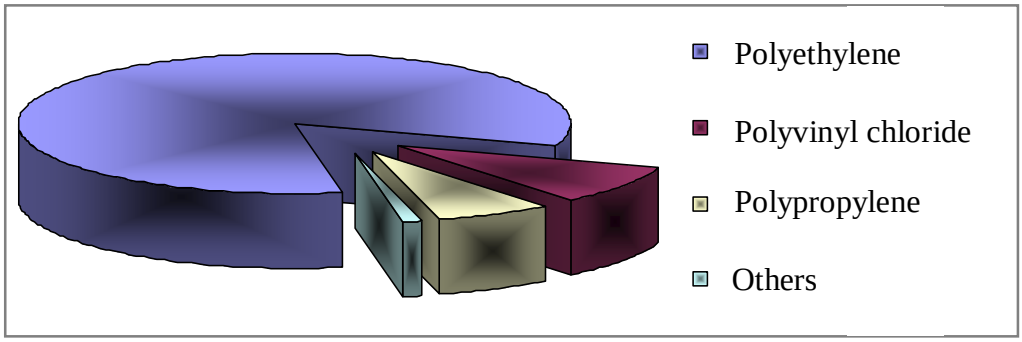

Figure 2.6 Plastics used in WPCs [24].

Like HDPE and LDPE, LLDPE melts and can be processed around 150-200 °C. Recycled LLDPE is available in a range of formats and costs [15]. In recent years the market for LLDPE has increased substantially and is now more than half the total for LDPE and for HDPE [198]. LLDPE is being used in many applications, replacing LDPE and HDPE in some areas [199]. This is because LLDPE combines the main features of both LDPE and HDPE and acts as an intermediary between HDPE and LDPE [200]. LLDPE combines the toughness of LDPE with the rigidity of HDPE. The linearity provides strength, while the branching provides the toughness. This may explain why LLDPE was a popular choice for many WPCs in the last decade [24, 70, 201-202].

Linear low density polyethylenes (LLDPEs) are produced at low pressure and temperature by compolymerisation of ethylene with various α-olefins, such as propene, butene, hexane and octane in the presence of a suitable catalyst [203], such as Ziegler-Natta or metallocene catalysts [204]. The first commercial process for producing LLDPE was high temperature solution polymerisation. Slurry processes are not widely used because the copolymer resins swell to various degrees, depending on the diluents and operating temperature. Philips loop reactors can be used to copolymerise ethene with 1-butene, 1-hexene, 1-octene and 4-methyl-1-petene in a solvent such as iso-butane at 60-75 ^{o}C to prevent swelling [205]. LLDPE is now

mostly made by gas-phase reactors with butene or hexene as the comonomer. In the gas-phase process, high temperatures and high comonomer content can result in sticky materials, which may cause problems and difficulties [203]. The order of reactivities of the comonomers is propene > 1-butene > linear α-olefins > branched α-olefins. MW and MW distribution (MWD), crystallinity and density of LLDPE are controlled by the catalyst selection and reaction conditions. Metallocene catalysts are more effective for the compolymerisation of ethene with α-olefins than Ziegler Natta catalysts [206]. The less effective Ziegler Natta systems tend to favour high ethylene insertion rates, yielding ill-defined, heterogeneous primary structures with low MW [204]. Metallocene PEs (often abbreviated to m-PEs) exhibit superior mechanical and optical properties as well as better organoleptic properties than PEs prepared by Ziegler Natta catalysts [198]. Properties of m-PEs such as low density, lower melt temperatures, and clarity and heat sealability can be related to the presence of copolymers rather than the narrow MWD (which has a more significant effect on toughness and melt flow properties) [207].

The term linear in LLDPE implies the absence of long-chain branching (LCBs) [202]. LLDPE is a copolymer containing short side-chain branches (SCBs) of 1-propene, 1-butene, 1-hexene or 1-octene. The SCBs tend to reduce the crystallinity, with little effect on the flow properties. The main advantages arising from the linearity and SCBs are a high tensile strength, impact strength, toughness, stiffness, environmental stress cracking resistance (ESCR), permeability, etc. [208]. Commercial LLDPE contains 8-12% butene or 1-hexene or 1-octene, with a nonrandom broad comonomer distribution [198]. Most of the LLDPE currently produced has a high MW and a relatively narrow MWD. LLDPEs are produced commercially with molecular weights (MWs) ranging from 20 000 to over 200 000 [208]. LLDPEs are available in a range of densities ranging from about 0.900 to 0.935 g/cm^3 [207]. Properties such as tensile strength are higher in LLDPE based on octene than in LLDPE based on hexene and LLDPE based on butene, respectively. The costs per unit mass of these LLDPEs are generally higher in LLDPE based on octene and butene [209]. It was found that compatibilisers, such as maleated PE (MAPE) improved LLDPE more than HDPE and LDPE, because the linear α-olefin structure of LLDPE helped to improve interfacial adhesion [182]. Due to all the above facts, LLDPE was chosen as a matrix for all composite systems in this study.

Metallocene catalysts can also be used to produce functionalised PE because they are able to polymerise monomers containing functional groups [210]. For example, it is possible to compolymerise ethylene or propylene with 1-undecen-1-ol, using stereorigid $Et[Ind]_2ZrCl_2$, $Me_2Si[Ind]_2ZrCl_2$, $Me_2Si[2\text{-}MeInd]_2ZrCl_2$, $(n\text{-}BuCp)_2ZrCl_2$/MAO and $Me_2Si[2\text{-}Me\text{-}4,5\text{-}$

BenzoInd]$_2$ZrCl$_2$ catalysts activated with methylaluminoxane (MAO) [210-211]. The structure of the catalyst plays an important role in incorporating polar groups into polyolefins [211]. A chiral structure of the catalyst with a dimethyl silane bridge connecting two indenyl ligands seems to favour the compolymerisation of functional monomers, while the non-bridged counterpart seems to polymerise the polar comonomer to a much lesser degree. The polymerisation activity is strongly dependent on the structural characteristics of the polar compound [210]. The interest in functionalised polymers is largely due to the significant improvements that can be achieved in their physical, mechanical and rheological properties. Such compolymerisation results in polyolefins with improved hydrophilicity and compatibility, which depends on the number and nature of the anchored functions.

Part of this study involves copolymerizing ethylene with different amounts of 1-undecen-1-ol, using bis(tert-BuCp)$_2$ZrCl$_2$/MAO in order to obtain different functionalised PEs with different amounts of hydroxyl groups, to be used as a matrix in a WPC system, without using any compatibilisers. This is important since many other researchers [144] used functionalised polyolefins as compatibilisers, and not as a matrix.

2.2.3 Compatibilisers

Compatibilisers are compounds that can interact with both the reinforcement and the resin matrix of a WPC. The interaction could be due to covalent bonds, secondary bonding (such as hydrogen bonding and van der Waals' forces), polymer molecular entanglement and mechanical interlocking. Compatibilisers act as a bridge to link hydrophilic wood and hydrophobic plastics, resulting in improved stress transfer and interfacial adhesion between wood and matrix [212]. Compatibilisers have two different domains: a wood-binding domain with a structure compatible to the wood, and a plastic-binding domain, with a structure compatible to the polymer matrix [182]. A careful selection of compatibilisers and optimisation is needed in order to produce a WPC with acceptable properties and performance [143]. Too high and too low concentration of compatibiliser can have undesirable effects on the properties of WPCs.

According to Lu et al. [212], Meyer was the first person who suggested using a compatibiliser for WPCs and Gaylord patented maleic anhydride (MA) as a compatibiliser to combine cellulose and PE or PVC in the presence of a free radical initiator. In the 1980s a number of patents were issued claiming the use of isocyanate and MA as compatibilisers in WPC systems. Other compatibilisers such as silane and propylene oxide were also added to the WPCs. Kokta's group in Canada investigated a number of compatibilisers such as silanes,

isocyanates, alkoxysilanes, and anhydrides [212] and subsequently patented poly(methylene [polyphenyl isocyanate]) as a compatibiliser for cellulose-PE composites. According to Lu et al. [212], Woodhams et al. successfully introduced MAPP with low MW as a compatibiliser to thermo mechanical pulp and isotactic PP composites.

Table 2.2 Compatibilisers used in WPCs [212]

Compatibilisers	
▪ *Organic compatibilisers*	
1. Acrylates	- Glycidyl methacrylate (GMA) - Hydroxyethyl methacrylate (HEMA)
2. Amides and imides	- N,N′-m-phenylene bismaleicimide (BMI)
3. Anhydrides	- Acetic anhydride (AA) - Succinic anhydride (SA) - Maleic anhydride (MA)
4. Chlorotriazines and derivatives	- 2-Diallylamino-4,6-dichloro-s-triazine (AACA) - Methacrylic acid,3-((4,6-dichloro-s-triazine-2-yl) amino)propyl ester (MAA-CAAPE)
5. Epoxides	- Butylene oxide (BO) - Propylene oxide (PO)
6. Isocyanates	- Ethyl isocyanate (EIC) - Hexamethylene diisocyanate (HMDIC) - Poly[methylene(polyphenyl isocyanate)] (PMPPIC)
7. Organic acids	- Abietic acid (ABAC) - Linoleic acid (LAC)
8. Monomers	- Acrylonitrile (AN) - Butyl acrylate (BA) - Methacrylic acid (MAA)
9. Polymers and copolymers	- Ethyl/vinyl acetate (E/VAC) - Maleated PE (MAPE) - Maleated PP (MAPP) - Polymethacrylic acid (PMAA) - Polyvinyl acetate (PVAC)
▪ *Inorganic compatibilisers*	
1. Sodium silicate (Na_2SiO_3)	
▪ *Organic-inorganic agents*	
1. Silanes	- γ -Methacryloxypropyltrimethoxy silane - γ -Glycidoxy propyltrimethoxy silane - γ -Aminopropyltriethoxy silane
2. Titanates	- Titanium di(dioctylpyrophosphate)oxyacetate

Takase and Shiraishi [213] reported glycidyl methacrylate and hydroxyethyl methacrylate as compatibilisers. More attention was given to high MW MAPP and their application by Shiraishi's group in Japan. Maleic anhydride (MA) acid and MMA were used as compatibilisers during this period. In the 1990s some attention was paid to the application of some compatibilisers, such as MAPP, in melt blending processes (e.g. IM and extrusion) in the United States and Sweden [212]. Lu et al. [212] classified compatibilisers into organic,

inorganic, and organic-inorganic groups and he listed over forty compatibilisers that have been used in WPCs. Some of these compatibilisers are shown in Table 2.2. Silanes with different functional groups [214], isocyanates and blocked isocyanates [215], ethylene-vinyl alcohol copolymer [201] and styrene maleic anhydride (SMA) [216] have been used a compatibilisers for WPCs in the last decade. More recently, new compatibilisers, such as a palm oil fatty acid additive [217], PP modified with an organosilane [150], polyethylenimine [218] and asphalt rubber [219] have been produced and used as compatibilisers for WPC systems. However, MAPE and MAPP remain the most poplar and common compatibilisers used for WPCs [7].

EVOH was used as a compatibiliser in parts of this study. EVOH contains a wood binding domain (hydroxyl groups) and a polymer binding domain (ethylene part). Furthermore, EVOH is inexpensive, harmless to handle, and environmentally friendly [201]. Degraded LLDPE was also used as a compatibiliser for wood-LLDPE systems in other parts of this study. As mentioned in Chapter 1, this may help to convert the polymer waste into useful products and reduce the production cost of WPCs.

2.3 Processing

The manufacture of WPCs is often a two-step process [7]. First, the raw materials are mixed together in a process called compounding. In the compounding process, the wood particles and additives are fed into molten polymer. Additives can be colourants, stabilisers, blowing agents, reinforcing agents, foaming agents or lubricants, which help tailor the end product to the target area of application [17]. In a second step, the compounded material is formed into the product. In this stage the compounded material is pressed or shaped into an end product or formed into pellets for future processing. The final properties of WPCs depend to a large extent on the compounding process and processing conditions. Effective mixing, for example, is crucial to achieve good dispersion of wood particles and the best properties of the composite [62]. According to Yeh and Gupta [220], better processing can be a solution for achieving better compatibility between the WPC components, besides compatibilisation. The preferred manufacturing processes for WPCs are either extrusion or IM [7, 221]. The effects of processing on the mechanical properties of WPCs manufactured by IM [222] and extrusion [221] have been investigated. Migneault et al. [222] found that the IM process resulted in WPCs with better physical and mechanical properties, while the extrusion process resulted in WPCs with higher densities. They conclude that the differences in mechanical behaviour according to processing method could be due to the composite density and fibre alignment. In the IM process fibres are aligned in the main flow direction, whereas in the

extrusion process fibres are randomly oriented. Bledzki and Faruk [223] found that IM WPCs made with 30% hardwood and PE had higher specific tensile strength than extruded WPCs, and a similar MOE and density. Migneault et al. [222] confirmed that the IM process resulted in higher tensile strength, higher MOE, higher flexure and lower WA and TS compared to extruded composites. Stark et al. [224] observed that the surface of WPCs made by the IM process were polymer-rich, while wood particles were apparent on extruded WPCs surfaces.

The mechanical properties of WPCs made with a twin-screw extruding system were found to perform better than those made with a single-screw extruding system, due to the improved dispersion of the filler [221, 225]. Different variables, including feed rate, screw speed, barrel temperature and screw geometry may affect the properties of the final WPCs. Yeh and Gupta [220] found that the change in the former variables does not significantly affect the tensile strength and modulus of WPCs, but it does affect the moisture absorption behaviour. WPCs processed using a higher screw speed have a lower rate of WA than WPCs processed using a lower screw speed. Also, a high screw speed and a long residence time are believed to result in a decrease in the size of wood particles and reduce the rate of WA. The extrusion process is generally accompanied by fibre breakage when slender fibres are used [226]. Processing conditions such as temperature, residence time, pressure, cooling rate, shear rate, and shear stress could affect the mechanical properties of the final product [220]. The effect of the amount and type of compatibilisers on the properties of WPC appears to be more pronounced than the effect of processing and processing conditions. Yeh and Gupta [220] proposed that the tensile strength of WPCs is dependent on the compatibiliser content and not on the processing conditions employed. According to Jayaraman and Halliwell [228], Miller et al. have assessed the tensile strength of wood fibre-waste plastic composites with particular emphasis on compatibilisers.

2.4 Applications and marketing

With consumption estimated at over ninety thousand million kilograms (~2 billion pounds) per year, and annual average growth rates of 10-15%, WPCs and the products and equipment associated with their manufacture comprise one of the fastest growing segments in the plastics industry. Ashori [17] reported that over 200 million kilograms (~460 million pounds) of WPCs were produced in 1999. The production of WPCs has grown four-fold between the years 1997 and 2000 [228]. The production of WPCs has increased to above 300 million kilograms (~700 million pounds) in 2001 [17]. The WPCs market is now a multibillion-dollar business [17]. WPCs have become on of the largest part of the plastic industry, with an average annual growth rate of roughly 18% in Northern America and 14% in Europe [230].

According to Jiang and Kamdem [230] the market for PVC/wood composites will be the most active, with a growth perspective of 200% expected from 2002 to 2010, in comparison with 130% for PP/wood composites, and 40% for PE/wood composites.

It is forecast that the demand for natural fibre/plastic composites will grow about 60% per year for construction products and 50% per year for automotive applications [231]. The actual forecast demand for these composites in North America and Europe between 2001 and 2010 is shown in Figure 2.7.

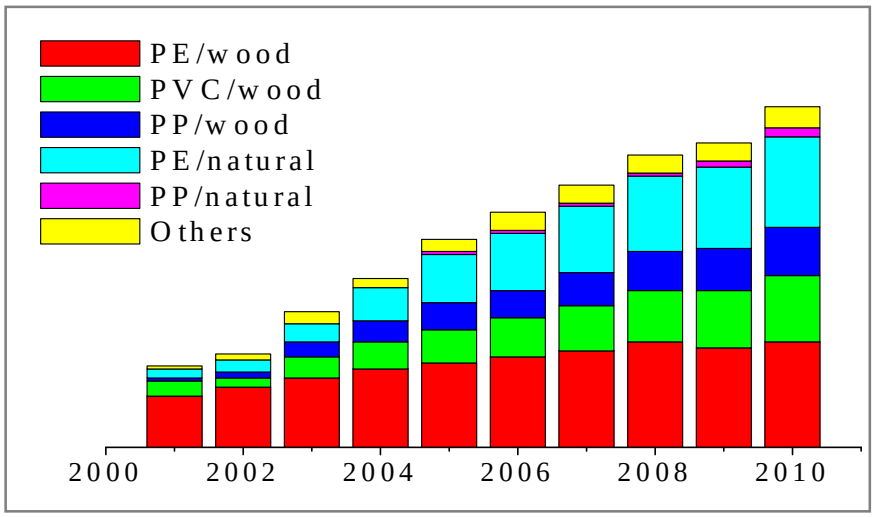

Figure 2.7 Forecast demand for WPCs in North America and Europe between 2001 and 2010 [230].

WPCs have found many applications, replacing natural wood and pure plastics [232]. WPCs are used in a large number of applications, ranging from in automotives, constructions, marine, electronic to aerospace, as shown in Figure 2.8 [17].

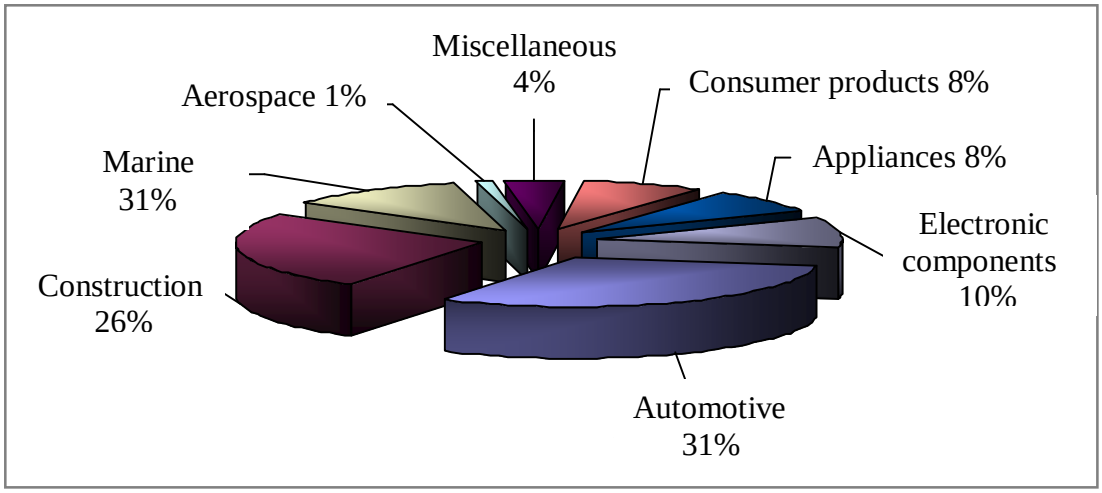

Figure 2.8 WPCs used in 2002 [17].

The aesthetic appearance and low maintenance of WPCs are continuing to drive WPCs to replace conventional and traditional materials in many applications. Conventional and traditional materials are replaced by WPCs in almost any sector, as shown in Figure 2.9. WPCs replace tropical timbers and pressure-impregnated timbers in certain decking sectors due to ecological and weight advantages. On the other hand, the non-metallic properties and energy-saving aspect are the major reasons for WPCs to replace aluminum profiles [22].

WPCs properties such as strength, stiffness, impact resistance, density and colour are important considerations in many WPC applications. This means that the WPCs applications can be based on the properties that WPCs offer. For example, WPCs are used in automotive applications due to their low specific gravity. WPCs can be used to make some household products, such as paintbrush handles, scissor handles and flowerpots. This is because of their aesthetic appearance. The product can look like wood, but it can be processed like plastic.

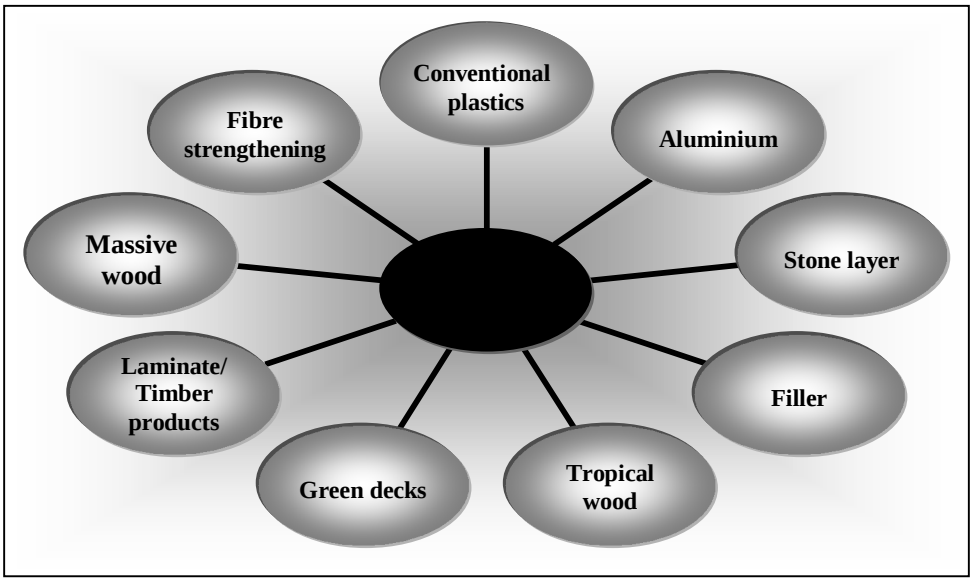

Figure 2.9 Substitution of conventional materials by WPCs [22].

WPCs are used in several building applications, such as decking, roof tiles, and window trim because they look like wood and offer improved thermal and creep performance compared with unfilled plastics.

Classic applications for WPCs are decking, fencing, industrial flooring, timbers, railing, mouldings, roofing, window and door profiles, as well as automotive applications such as rear shelf-trim panels, instrument panels, load floors and cabback panels [20]. Table 2.3 shows an extensive, but not complete list of WPC applications [15].

Table 2.3 WPC markets and applications [15]

Sector	Construction	Interiors & internal finishes	Automotive	Garden & outdoor	Industrial & Infrastructure	Others
End marketing applications	Cladding-exterior horizontal & vertical	Balustrades	Door & head liners	Decking	Handrails	Black piano keys
	Doorframes and components	Blinds & shutters	Ducting	Fencing and fence posts	Industrial packaging	Hot tubs
	Ducting	Coving	Interior panels	Garden furniture	Marine pilings & bulkheads	
	Fascias, soffits and barge boards	Dado rails	Rear shelves	Outhouses (sheds, etc)	Pallets & crates & totes	
	Pre-finished floorboards	Decorative profiles	Spare tyre covers	Park benches	Piers & docks	
	Roofline products	Interior panels	Truck floors	Playground equipment	Railings	
	Shingles (roof tiles)	Kitchen cabinets		Playground surfaces	Railway sleepers	
	Stairs	Laminate flooring			Rubbish bins	
	Timber	Office furniture			Signage	
	Window frames and components	Shelving				
		Skirting boards				
		Sound-proofing				
		Worktops				

2.4 References

1. Roger R., Advances and Challenges of Wood Polymer Composites, Proceedings of the 8th Pacific Rim Bio-Based Composites Symposium, Malaysia, 2006.
2. Manas C., Salil K., Plastics Technology Handbook, 4th edition, CRC Press, USA, 2006. 146-153.
3. Haihong J., Pascal K., Journal of Vinyl and Additive Technology, 10, 59-69, 2004.
4. Schnieder M., Wood Fibre and Science, 26, 142-151, 1994.
5. Schnieder M., Wood Science and Technology, 29, 121-127, 1995.
6. Wang S., Zhang A., Forestry Studies in China, 9, 57-62, 2007.
7. Rowell R., Handbook of Wood Chemistry and Wood Composites, 1st edition, CRC Press, UK, 2005. 10-434.
8. Bledzki A., Gassan J., Progress in Polymer Science, 24, 221-274, 1999.
9. Ismail H., Rozman H., Jaffri R., Ishak Z., European Polymer Journal, 33, 1627-1632, 1997.

10. Kuruvilla J., Romildo D., Beena J., Sabu T., Laura H., Revista B., Revista Brasileira de Engenharia Agrícola e Ambiental, 3, 367-379, 1999.
11. Young L., Qinglin W., Fei Y., Yanjun X., Composites: Part A, 38, 1664-1674, 2007.
12. Yi W., Morphological Characterisation of Wood Plastic Composite (WPC) with Advanced Imaging Tools: Developing Methodologies for Reliable Phase and Internal Damage Characterisation, Masters thesis, Oregon State University, USA, 2007. 2.
13. Andrea W., Salim H., Building and Environment, 42, 2637-2644, 2008.
14. Selke S., Wichman I., Composites: Part A, 35, 321-326, 2004.
15. Optimat Ltd and Merl Ltd, Research Report, Wood Plastic Composites Study: Technology and UK Market Opportunities, The Waste and Resources Action Programme, UK, 2003. 1-82.
16. Winandy J., Stark N., Clemons C., Considerations in Recycling of Wood Plastic Composites, Proceedings of the 5th Global Wood and Natural Fibre Composites Symposium, Germany, 2004.
17. Ashori A., Bioresource Technology, 99, 4661-4667, 2008.
18. Clemons C., Forest Products Journal, 52, 10-18, 2002.
19. Schneider M., Witt A., Forest Product Journal, 54, 19-24, 2004.
20. Kharazipour A., Schöpper C., Müller C., Euring M., Review of Forests; Wood Products and Wood Biotechnology of Iran and Germany - Part III, 1st edition, University of Gottingen, Germany, 2009. 56-69.
21. Salamone J., Polymeric Materials Encyclopedia, Volume 11, 1st edition, CRC Press, USA, 1996. 8755-8759.
22. Oksman K., Sain M., Wood Polymer Composites, 1st edition, Woodhead Publishing Limited, UK, 2008. 300-330.
23. Ellis W., Sanadi A., Expanding the Limits of Wood Polymer Composites: Studies Using Dynamic Mechanical Thermal Analysis, Proceedings of the 18th Risø International Symposium on Materials Science, Denmark, 1997.
24. Xanthos M., Functional Fillers for Plastics, 1st edition, Wiley-VCH Verlag, Germany, 2005. 249-267.
25. San H., Nee L., Meng H., ARPN Journal of Engineering and Applied Sciences, 3, 13-19, 2008.
26. Rowell R., The Chemistry of Solid Wood, 1st edition, American Chemical Society, USA, 1984. 229-446.
27. Madhoushi M., Polymer Testing, 28, 301-306, 2009.
28. Pritchard G., Reinforced Plastics, 48, 26-29, 2004.
29. Morreale M., Scaffaro R., Maio A., La Mantia F., Composites: Part A, 39, 503-513, 2008.
30. Youngquist A., Forest Products Journal, 45, 25-30, 1995.
31. Bryant B., Forest Products Journal, 16, 20-27, 1966.
32. Goldsteint I., Loos W., Special treatments, Volume 1, ed. Nicholas D., Degradation and Protection of Wood, 1st edition, Syracuse University Press, USA, 1973. 341-371.
33. Stamm A., Dimensional Changes of Wood and their Control, Chapter 8, ed. Goldstein I., Wood Technology: Chemical Aspects, American Chemical Society, USA. 1977. 115-139.
34. Kenaga D., Wood and Fibre Science, 2, 40-51, 1970.
35. Hills P., Composites, 3, 211-215, 1972.
36. Handa T., Seo I., Akimoto H., Saito M., Ikeda Y., Physical Properties of Wood-Polymer Composites Materials Prepared by I.C.T-type Electron Accelerator, Proceedings of the 15th Japan Congress on Materials Research, Japan, 1972.
37. Spindler M., Pateman R., Hills P., Composites, 4, 246-253, 1973.
38. Baas P., Journal of Microscopy-Oxford, 104, 83-90, 1975.
39. Munozescalona A., Bolsaitis P., Viela J., Journal of Materials Science, 11, 1711-1724, 1976.
40. Plessis T., Du Toit G., Radiation Physics and Chemistry, 9, 869-873, 1977.
41. Witt A., Radiation Physics and Chemistry, 9, 271-288, 1977.
42. Okumura M., Shiraishi N.; Sadoh T., Journal of the Society of Materials Science, 26, 465-471, 1977.
43. Lya V., Majali A., Radiation Physics and Chemistry, 12, 107-110, 1978.
44. Moustafa A., Kandil E., Hady B., Ghanem N., Die Angewandte Makromolekulare Chemie, 65, 121-132, 1977.
45. Coutts R., Campbell M., Composites, 10, 228-232, 1979.

46. Witt A., Henise P., Griest L., Radiation Physics and Chemistry, 18, 67-80, 1981.
47. Gouloubandi R., Radiation Physics and Chemistry, 19, 85-88, 1982.
48. Moore G., Kline D., Blankenhorn P., Wood and Fibre Science, 15, 358-375 ,1983.
49. Zadorecki P., Karnerfors H., Lindenfors S., Composites Science and Technology, 27, 291-303, 1986.
50. Rozman H., Kumar R., Abusamah A., Journal of Applied Polymer Science, 57, 1291-1297, 1995.
51. Matuana L., Park C., Balatinecz J., Polymer Engineering and Science, 38, 1962-2872, 1998.
52. Beardmore P., Johnson C., Composites Science and Technology, 26, 251-281, 1986.
53. Feldman D., Lacasse M., Beznaczuk L., Progress in Polymer Science, 12, 277-299, 1986.
54. Gauthier R., Joly C., Coupas A., Gauthier H., Escoubes M., Polymer Composites, 19, 287-300, 1998.
55. Maldas D., Kokta B., Journal of Applied Polymer Science, 41, 185-194, 1990.
56. Kokta B., Maldas D., Daneault C., Béland P., Journal of Vinyl Additive and Technology 12, 146-153, 1990.
57. Park B., Balatinecz J., Polymer Composites, 18, 425-431, 1997.
58. Elvy S., Dennis G., Ng L., Journal of Materials Processing Technology, 48, 365-371, 1995.
59. Matuana L., Park B., Balatinecz J., Polymer Engineering and Science, 37, 1137-1147, 1997.
60. Helbert W., Cavaillé J., Dufresne A., Polymer Composites, 17, 604-611, 1996.
61. Stark N., Matuana L., Polymer Degradation and Stability, 86, 1-9, 2004.
62. Bledzki A., Letman M., Viksne A., Rence L., Composites: Part A, 36, 789-797, 2005.
63. Beg M., Pickering K., Composites: Part A, 39, 1091-1100, 2008.
64. Li R., Polymer Degradation and Stability, 70, 135-145, 2000.
65. Stark N., Matuana L., Polymer Degradation and Stability, 92, 1883-1890, 2007.
66. Beg M., Pickering K., Polymer Degradation and Stability, 93, 1939-1946, 2008.
67. Doh G., Lee S., Kang I., Kong Y., Composite Structures, 68, 103-108, 2005.
68. Hristov V., Lach R., Grellmann W., Polymer Testing, 23, 581-589, 2004.
69. Sailaja R., Composites Science and Technology, 66, 2039-2048, 2006.
70. Kim H., Kim S., Kim H., Yang H., Thermochimica Acta, 451, 181-188, 2006.
71. Pritchard G., Reinforced Plastics, 51, 28-31, 2007.
72. Markarian J., Plastics, Additives and Compounding, 10, 20-25, 2008.
73. Yao F., Wu Q., Lei Y., Xu Y., Industrial Crops and Products, 28, 63-72, 2008.
74. Burgueño R., Quagliata M., Mohanty A., Mehta G., Drzal L., Misra M., Composites: Part A, 35, 645-656, 2004.
75. Srivastava V., Materials Science and Engineering, 435-436, 282-287, 2006.
76. Mansour S., El-Nashar D., Abd-El-Messieh S., Journal of Applied Polymer Science, 102, 5861-5870, 2006.
77. Lee H., Kim D., Journal of Applied Polymer Science, 111, 2769-2776, 2009.
78. Bourmaud A., Baley C., Polymer Degradation and Stability, 94, 297-305, 2009.
79. Ashori A., Nourbakhsh A., Waste Management, 29, 1291-1295, 2009.
80. Bledzki A., Faruk O., Composites Science and Technology, 64, 693-700, 2004.
81. Espert A., Vilaplana F., Karlsson S., Composites: Part A, 35, 1267-1276, 2004.
82. Morreale M., Scaffaro R., Maio A., La Mantia F., Composites: Part A, 39, 1537-1546, 2008.
83. Kretschmann D., Nature Materials, 2, 775-776, 2003.
84. Answers.com, Britannica Concise Encyclopedia: Wood. 2009. [Online]. Available: www.answers.com/topic/wood [2010, 20 July].
85. Simonaho S., Silvennoinen R., Optical Review, 11, 308-311, 2004.
86. Mark H., Gaylord N., Encyclopedia of Polymer Science and Technology, Volume 15, Ed. Bikales N., 1st edition, Interscience Publishers, USA, 1971. 1-39.
87. Shao Y., Moras S., Ulkem N., Kubes G., Canadian Journal of Civil Engineering, 27, 543-552, 2000.
88. Bond B., Hamner P., Wood Identification for Hardwood and Softwood Species Native to Tennessee, University of Tennessee, USA, 2002. 1-9.
89. Wikipedia, Hardwood. 2010. [Online]. Available: http://en.wikipedia.org/wiki/Hardwood [2010, 20 July].
90. Miller R., Encyclopedia of Science and Technology, 9th edition, McGraw-Hill, USA, 2002. 600-602.

91. Schwartz, Encyclopedia of Materials, Parts and Finishes, 2nd edition, CRC Press, USA, 2002. 869.
92. Bledzki A., Sperber V., Faruk O., Natural and Wood Fibre Reinforcement in Polymers, 1st edition, iSmithers Rapra Publishing, UK, 2002. 25-33.
93. Berger M., Stark N., Investigations of Species Effects in an Injection Moulding-Grade; Wood-Filled Polypropylene, Proceedings of the 4th International conference on Wood-Fibre Plastic composites, Madison WI, 1997.
94. Nexant Chem Systems, New Report Alert, Thermoplastic Wood Composites, Naxant Inc., USA, 2007. 1-5.
95. Qin M., Xu Q., Shao Z., Gao Y., Fu Y., Lu X., Gao P., Holmbom B., Bioresource Technology, 100, 3082-3087, 2009.
96. Nirdosha G., Setunge S., Composite Structures, 75, 520-523, 2006.
97. Almeida G. Leclerc S., Perre P., International Journal of Multiphase Flow, 34, 312-321, 2008.
98. Reiterer A., Sinn G., Tschegg S., Materials Science and Engineering A, 332: 29-36, 2002.
99. La Mantia F., Morreale M., Polymer Degradation and Stability, 93, 1252-1258, 2008.
100. Dang Z., Zhang J., Ragauskas A., Carbohydrate Polymers, 70, 310-317, 2007.
101. Rashmi R., Ali D., Maji T., Bioresource Technology, 88, 185-188, 2003.
102. Bowyer J., Shmulsky R., Haygreen J., Forest Products and Wood Science: An Introduction, 4th edition, Blackwell Publishing Company, USA, 2003. 81-98.
103. Byrne, C., Nagel, D., Carbon, 37, 259-266, 1997.
104. Cole B., Fort R., The Composition and Structure of Wood. 2008. [Online]. Available: http://chemistry.umeche.maine.edu/Fort/Cole-Fort.html [2010, 20 July].
105. Rahatekar S., Rasheed A., Gilman J., Kumar S., Jain R., Chae H., Koziol K., Windle A., Trulove P., Cellulose and Silk Nanocomposites Processing using Ionic Liquids. 2009. [Online]. Available: www.answers.com/topic/cellulose [2010, 20 July].
106. Franco P., González A., Composites: Part B, 597-608, 36, 2005.
107. Sun X., Sun R., Sun J., Journal of the Science of Food and Agriculture, 84, 800-810, 2004.
108. Sun R., Sun X., Carbohydrate Polymers, 49, 415-423, 2002.
109. Ren J., Sun R., Liu C., Lin L., He B., Carbohydrate Polymers, 67, 347-357, 2007.
110. Sun R., Bioresources, 4, 452-455, 2008.
111. Walker J., Primary Wood Processing, 2nd edition, Springer, Netherlands, 2006. 40-70.
112. Sjöholm E., Gustafsson K., Berthold F., Colmsjö A., Carbohydrate Polymers, 41, 1-7, 2000.
113. Nollet L., Boylston T., Handbook of Meat, Poultry and Seafood Quality, 1st edition, Blackwell Publishing, Australia, 2007. 202-203.
114. Tan K., Humic Matter in Soil and the Environment, 1st edition, CRC Press, USA, 2003. 77-86.
115. Marchessault R., Coulombe Z., Morikawa H., Canadian Journal of Chemistry, 60, 2372-2382, 1982.
116. Twede D., Selke S., Cartons, Crates and Corrugated Board: Handbook of Paper and Wood Packaging Technology, 1st edition, DEStech Publications, USA, 2005. 101-103.
117. Sefara N., Birkett M., Development of an Alternative Solvent to Replace Benzene in the Determination of Organic Soluble extractives in Wood, Sappi Forest Products, International conference: African Pulp and Paper Week, South Africa, 2004.
118. TAPPI test methods, T 264 om-88 and T 222 om-88, TAPPI Press, USA, 1992.
119. Zhang X., Nguyen D., Paice M., Tsang A., Renaud S., Enzyme and Microbial Technology, 40, 866-873, 2007.
120. Hillis W., Phytochemistry, 11, 1207-1218, 1972.
121. Shi-fa W., Ai-jun Z., Forestry Studies in China, 9, 57-62, 2007.
122. Várhegyi G., Granola M., Blasi C., Industrial & Engineering Chemistry Research, 43, 2356-2367, 2004.
123. Garves K., Holz als Roh- und Werkstoff, 39, 253-254, 1981.
124. Ridout B, Timber Decay in Buildings, 1st edition, English Heritage, UK, 2000. 9-10.
125. Marklund E., Varna J., Composites Science and Technology, 69, 1108-1114, 2009.
126. Bindschedler L., Tuerck J., Maunders M., Ruel K., Conil M., Danoun S., Boudet A., Joseleau J., Bolwell G., Phytochemistry, 68, 2635-2648, 2007.
127. Salmén L., Comptes Rendus Biologies, 327, 873-880, 2004.

128. Bledzki A., Gassan J., Theis S., Mechanics of Composite Materials, 34, 563-568, 1998.
129. Yang H., Kim H., Son J., Park H., Lee B., Hwang T., Composite Structures, 63, 305-312, 2004.
130. Karina M., Onggo H., Syampurwadi A., Journal of Biological Science, 7, 393-396, 2007.
131. Unger A., Schniewind A., Unger W., Conservation of Wood Artifacts; A Handbook, 1st edition, Springer, Germany, 2001. 37.
132. Bengtsson M., Oksman K., Composites: Part A, 37, 752-765, 2006.
133. Koichi G., Yong C., Journal of Solid Mechanics and Materials Engineering, 1, 1073-1084-2007.
134. Bodig J., Jayne, B., Mechanics of Wood and Wood Composites, 1st edition, Van Nostrand Reinhold Company, USA, 1982. 461-464.
135. Nygård P., Tanem B., Karlsen T., Brachet P., Leinsvang B., Composites Science and Technology, 68, 3418-3424, 2008.
136. Karmarkar A., Chauhan S., Modak J., Chanda M., Composites: Part A, 38, 227-233, 2007.
137. Bouafif H., Koubaa A., Perré P., Cloutier A., Composites: Part A, 40, 1975-1981, 2009.
138. Georgopoulos S., Tarantili P., Avgerinos E., Andreopoulos A., Koukios E., Polymer Degradation and Stability, 90, 303-312, 2005.
139. Hansson L., Antti A., Journal of Materials Processing Technology, 171, 467-470, 2006.
140. Tze W., Wang S., Rials T., Pharr G., Kelley S., Composites: Part A, 38, 945-953, 2007.
141. Nunez A., Kenny J., Reboredo M., Polymer Engineering and Science, 42, 733-742, 2002.
142. Marcovich N., Villar, M., Journal of Applied Polymer Science, 90, 2775-2784, 2003.
143. Hristov V., Krumova M., Michler G., Macromolecular Materials and Engineering, 288, 677-683, 2006.
144. Mamunya Y., Zanoaga M., Myshak V., Tanasa F., Lebedev E., Grigoras C., Semynog V., Journal of Applied Polymer Science, 101, 1700-1710, 2006.
145. Tserki V., Matzinos P., Kokkou S., Panayiotou C., Composites: Part A, 36, 965-974, 2005.
146. Wielage B., Lampke L., Marx G., Nestler K., Starke D., Thermochimica Acta, 337, 169-177, 1999.
147. Gröndahl M., Teleman A., Gatenholm P., Carbohydrate Polymers, 52, 359-366, 2003.
148. Mészáros E., Jakab E., Várhegyi G., Journal of Analytical and Applied Pyrolysis, 79, 61-70, 2007.
149. Mouritz A., Gibson A., Fire Properties of Polymer Composite Materials, 1st edition, Springer, Netherlands, 2006. 43-46.
150. Nachtigall S., Cerveira G., Rosa S., Polymer Testing, 26, 619-628, 2007.
151. Liu H., Wu Q., Han G., Yao F., Kojima Y., Suzuki S., Composites: Part A, 39, 1891-1900, 2008.
152. Oksman K., Lindberg H., Journal of Applied Polymer Science, 68, 1845-1855, 1998.
153. Brinson H., Brinson L., Polymer Engineering Science and Viscoelasticity, 1st edition, Springer-Verlag New York, 2007. 187.
154. Orozco J., Rego J., Katime I., Journal of Applied Polymer Science, 40, 2219-2230, 1990.
155. Behzad M., Tajvidi M., Ehrahimi G., Falk R., International Journal of Engineering Transactions B, 7, 95-104, 2004.
156. Gatenholm P., Bertilsson H., Mathiasson A., Journal of Applied Polymer Science, 49, 197-208, 1993.
157. Ghasemi I., Azizi H., Naeimian N., Journal of Vinyl and Additive Technology, 15, 113-119, 2009.
158. Shi S., Gardner D., Composites: Part A, 37, 1276-1285, 2006.
159. Neagu R., Gamstedt E., Lindström M., Composites: Part A, 36, 772-788, 2005.
160. Adhikary K., Pang S., Staiger M., Chemical Engineering Journal, 142, 190-198, 2008.
161. Matuana L., Kamdem D., Polymer Engineering and Science, 42, 1657-1666, 2002.
162. Lundin T., Cramer S., Falk R., Felton C., Journal of Materials Science and Engineering, 16, 547-555, 2004.
163. Ndiaye D., Fanton E, Therias S., Vidal L., Gardette A., Composites Science and Technology, 68, 2779-2784, 2008.
164. Celina M., George G., Polymer Degradation and Stability, 40, 323-335, 1993.
165. Wise J., Gillen K., Clough R., Degradation and Stability, 49, 403-418, 1995.
166. Knight J., Calvert P., Billingham N., Polymer, 26, 1713-1718, 1985.

167. Attwood J., Philip M., Hulme A., Williams G., Shipton P., Polymer Degradation and Stability, 91, 3407-3415, 2006.
168. Rabek J., Polymer Photo-degradation: Mechanisms and Experimental Methods, 1st edition, Kluwer Academic Publishers, Netherlands, 1995. 62-63.
169. Naddeo C., Guadagno L., Luca S., Vittoria V., Camino G., Polymer Degradation and Stability, 72, 239-247, 2001.
170. Ravve A., Principles of Polymer Chemistry, 1st edition, Kluwer Academic Publishers, USA, 2000. 609-611.
171. Orton C., Parkinson D., Evans P., Owen N., Society for Applied Spectroscopy, 58, 1265-1271, 2004.
172. Kutz M., Handbook of Environmental Degradation of Materials, 1st edition, William Andrew Inc., USA, 2005. 278-282.
173. Muck A., Kubát P., Oliveira A., Ferreira L., Cvačka J., Civiš S., Zelinger Z., Zima J., Journal of Hazardous Materials B, 95, 175-184, 2002.
174. Wang X., Ren H., Applied Surface Science, 254, 7029-7034, 2008.
175. Deka M., Petrič, Bioresources, 3, 346-362, 2008.
176. Prachayawarakorn J., Songklanakarin Journal of Science and Technology, 25, 595-606, 2003.
177. Raj R., Kokta B., Dembele F., Sanschagrain B., Journal of Applied Polymer Science, 38, 1987-1996, 1989.
178. Dányádi L., Janecska T., Szabo Z., Nagy G., Moczo J., Pukánszky B., Composites Science and Technology, 67, 2838-2846, 2007.
179. Anagnostopoulosa G. , Partheniosa J., Andreopoulos A., Galiotis C., Acta Materialia, 4173-4183, 2005.
180. Bengtsson M., Gatenholm P., Oksman K., Composites Science and Technology, 65, 1468-1479, 2005.
181. Sretenovic A., Müller U., Gindl W., Composites: Part A, 37, 1406-1412, 2006.
182. Zhang C., Li K., Simonsen J., Polymer Engineering and Science, 46, 108-113, 2006.
183. Min X., Zhi C., Journal of Forestry Research, 15, 77-79, 2004.
184. Mohanty A., Misra M., Drzal L., Natural Fibres, Biopolymers and Biocomposites, 1st edition, CRC Press: Taylor and Francis, USA, 2005. 188.
185. Lee S., Teramoto Y., Shiraishi N., Journal of Applied Polymer Science, 83, 1473-1481, 2002.
186. Yildiz U., Yildiz S., Gezer E., Bioresource Technology, 96, 1003-1011, 2005.
187. Schneider M., Phillips J., Journal of Forest Engineering, 11, 83-89, 2000.
188. Pu Y., Zhang J., Elder T., Deng Y., Gatenholm P., Ragauskas A., Composites: Part B, 38, 360-366, 2007.
189. Cai X., Riedl B., Zhang S., Wan H., Composites: Part A, 39, 727-737, 2008.
190. Thwe M., Liao K., Composites: Part A, 33, 43-52, 2002.
191. Brahmakumar M., Pavithran C., Pillai R., Composites Science and Technology, 65, 563-569, 2005.
192. Ichazo M., Albano C., González J., Perera R., Candal M., Composite Structures, 54, 207-217, 2001.
193. Salamone J., Concise Polymeric Materials Encyclopedia, 1st edition, CRC Press, USA, 1999. 276-280.
194. Chanda M., Roy S., Plastics Technology Handbook, Chapter 5, 4th edition, CRC Press, USA, 2007. 146-152.
195. Afrifah A., Hickok R., Matuana L., Composites Science and Technology, 70, 167-172, 2010.
196. Kim H., Yang H., Kim H., Lee B., Hwang T., Journal of Thermal Analysis and Calorimetry, 81, 299-306, 2005.
197. Araújo R., Pasa V., Progress in Organic Coatings, 51, 6-14, 2004.
198. Brydson A., Plastic materials, 7th edition, Butterworth-Heinemann, UK, 1999. 210-231.
199. Robertson G., Food Packaging: Principles and Practice, 2nd edition, CRC Press, USA, 2006. 20-21.
200. Barnetson A., Plastics Materials for Packaging, 1st edition, Rapra Technology, UK, 1996. 11-12.
201. Kim J., Yoon T., Mun S., Rhee J., Lee J., Bioresource Technology, 97, 494-499, 2006.
202. Li B., He J., Polymer Degradation and Stability, 83, 241-246, 2004.

203. Dealy J., Larson R., Structure and Rheology of Molten Polymers, 1st edition, Carl Hanser Verlag, Germany, 2006. 70-71
204. Sworen J., Wagener K., Macromolecules, 40, 4414-4423, 2007.
205. Joubert D., Ethylene and Propylene Compolymerisation Utilizing Fischer Tropsch 1-olefins, PhD thesis, University of Stellenbosch, 2000. 78-79.
206. Kricheldorf H., Nuyken O., Swift G., Handbook of Polymer Synthesis, 2nd edition, Marcel Dekker Inc., USA, 2005. 22-24.
207. Bingham E., Cohrssen B., Powell C., Patty's Toxicology, Chapter 10, 5th edition, John Willey & Sons, USA, 2001. 205-246.
208. Olabisi O., Handbook of Thermoplastics, 1st edition, Marcel Dekker Inc., USA, 1997. 20-21.
209. Abdel-Bary E., Handbook of Plastic Films, 1st edition, Rapra Technology, UK, 2003. 241-243.
210. Lu Z., Chemical Coupling in Wood-Polymer Composites, PhD thesis, Louisiana State University, 2003. 233.
211. Aaltonen, P., Fink G., Löfgren B., Seppälä J., Macromolecules, 29, 5255-5260, 1996.
212. Lu J., Wu Q., McNabb H., Wood and Fibre Science, 32, 88-104, 2000.
213. Takase S., Shiraishi N., 1989. Journal of Applied Polymer Science, 37, 645-659, 1989.
214. Kuan C., Kuan H., Ma C., Huang C., Composites: Part A, 37, 1696-1707, 2006.
215. Lee S., Wang S., Composites: Part A, 37, 80-91, 2006.
216. Yeh S., Agarwal S., Gupta R., Composites Science and Technology, 69, 2225-2230, 2009.
217. Othman N., Ismail H., Mariatti M., Polymer Degradation and Stability, 91, 1761-1774, 2006.
218. De la Orden M., Sánchez C., Quesada M., Urreaga J., Composites: Part A, 38, 2005-2012, 2007.
219. Estevez M., Journal of Cleaner Production, 17, 1359-1362, 2009.
220. Yeh S., Gupta R., Composites: Part A, 39, 1694-1699, 2008.
221. Karger-Kocsis J., Polypropylene: An A-Z reference, Ed. Czvikovszky, 1st edition, Kluwer Academic Publishers, UK, 1999. 882-889.
222. Migneault S., Koubaa A., Erchiqui F., Chaala A., Englund K., Wolcott M., Composites: Part A, 40, 80-85, 2009.
223. Bledzki AK, Faruk O. Cellular Polymer, 23, 211-227, 2004.
224. Stark N., Matuana L., Clemons C., Journal of Applied Polymer Science, 93, 1021-1030, 2004.
225. Yang H., Wolcott M., Kim H., Kim S., Kim H., Polymer Testing, 25, 668-676, 2006.
226. Sui G., Fuqua M., Ulven C., Zhong W., Bioresource Technology, 100, 1246-1251, 2009.
227. Jayaraman K., Halliwell R., Composites: Part B, 40, 645-649, 2009.
228. Li T., Wolcott M., Composites: Part A, 35, 303-311, 2004.
229. Morton J., Current and Emerging Applications for Natural & Wood Fibres Composites, Proceedings of the 7th International Conference of Wood Fibre-Plastic Composites, USA, 2003.
230. Jiang H., Kamdem D., Journal of Vinyl Additive and Technology, 10, 59-69, 2004.
231. Jiang H., Kamdem D., Bezubic B., Ruede P., Journal of Vinyl Additive and Technology, 9, 138-145, 2003.
232. Guerra A., Gaspar A., Contreras S., Lucia L., Crestini C., Argyropoulos D., Phytochemistry, 68, 2570-2583, 2007.

Chapter 3
The effect of different wood spcies on the properties of wood-LLDPE composites

Abstract

The effects of the macromolecular composition and content of different wood species on the properties of wood-LLDPE composites using EVOH as a compatibiliser were investigated. The macromolecular composition and content of three hardwood species *A. cyclops* (acacia), *E. grandis* (eucalyptus), *Q. alba* (oak) and one softwood species *P. radiata* (pine) and the morphological properties such as particle lengths were determined in order to investigate these effects. Significant differences were found between the species in terms of both macromolecular composition and content and particle lengths. Composites were prepared using 10% wood content and different amounts 0, 2, 5, 7 and 10% of EVOH. Use of *A. cyclops* resulted in a composite with superior mechanical and thermal properties compared with the other species, due to its higher cellulose and lignin contents and a favourable wood particle lengths; however, *A. cyclops* composites also showed a higher WA and TS rate, which is due to the higher number of free hydroxyl groups present in these composites. The higher number of free hydroxyl groups in *A. cyclops* composites can be attributed to the higher cellulose content. Composites containing wood species with a high lignin and extractive content, such as *A. cyclops* and *Q. alba*, exhibited higher resistance to UV degradation.

Keywords: *WPCs, mechanical properties, thermal properties, UV resistance.*

3.1 Introduction

It has been shown that the properties of WPCs depend on several factors: the physical and the mechanical characteristics of the polymer matrix, the macromolecular composition and content of the wood, and the chemical interactions between the polymer and wood [1]. Consequently, different wood species can therefore be expected to have different effects on the properties of WPCs, as they have a different macromolecular composition and content. There is evidence to prove this. Rogers and Simonsen [2] suggested that the choice of wood species could influence the surface roughness, tendency to chip, and porosity, and that these differences could affect the interfacial bonding of WPCs. Berger and Stark [3] identified the

key variables when wood is used as a filler to be the moisture content, purity, particle length, and species. Differences in the mechanical properties of WPCs made with pine and fir were confirmed by Saputra et al. [4] and Wolcott [5]. Clemons and Stark [6] reported that the mechanical properties of WPCs decreased when pine flour was replaced with wood from salt cedar and Utah juniper. The surface roughness and macromolecular composition and content of the wood surface influence the fibre-matrix interaction, leading to WPCs with different viscoelastic properties [7]. It was found that hardwood composites appeared to outperform softwood composites in terms of tensile and flexural properties, and heat deflection temperature [3]. Hence, different species could have a significant influence on the properties of WPCs [5].

Although the wood content in WPCs can be much higher in practical applications, a content of 10% was selected for use in this study, because it allows for easy preparation and charactisation of WPCs. Different quantities of EVOH (0, 2, 5, 7 and 10%) were used as compatibilisers. A careful selection of compatibilisers and optimisation is required in order to produce WPCs with acceptable properties and performance, as discussed in Section 2.2.3 [8].

3.2 Experimental

3.2.1 Materials

Woods from four different species, namely *A. cyclops* (acacia), *E. grandis* (eucalyptus), *P. radiata* (pine) and *Q. alba* (oak), were used as reinforcing filler. These species were supplied from the Department of Forest and Wood Science at Stellenbosch University.

The average particle size of these species is 180 µm. The matrix polymer LLDPE, with butene as comonomer and an average MW of 294 000, was supplied by Sasol Polymers (South Africa). EVOH with a melt index of 3.50 g/10 min and 44% ethylene content (Sigma-Aldrich) was used as a compatibiliser. Xylene (Merck Chemicals) was used for the preparation of WPCs, to melt the mixture of LLDPE and EVOH.

A mixture of Irganox 1010 and Irgafos stabilisers (Sasol) was added to inhibit thermal degradation during the preparation of WPCs. Mylar polyester film with a thickness of 125 µm (Wire System Technology, South Africa), was used to avoid any possible adhesion between the moulded composites and the press plates during film preparation.

Cyclohexane (Sigma-Aldrich) and absolute ethanol (Merck Chemicals) were used for the wood extractions. Sulphuric acid (Merck Chemicals) was used for the determination of the lignin content, and acetyl acetone (Sigma-Aldrich), dioxane, hydrochloric acid, methanol and diethyl ether (Merck Chemicals) were used for the determination of the cellulose content.

3.2.2 Preparation of the wood-LLDPE composites

Wood-LLDPE composites were prepared by mixing LLDPE with 0, 2, 5, 7 and 10% finely ground EVOH and heating in a small volume of xylene to about 160 ^{o}C. A mixture of Irganox 1010 and Irgafos stabilisers was added to the LLDPE and EVOH. The blend was removed from the flask after complete melting and 10 wt% wood particles (dried at 105 ^{o}C for 24 h) was added while stirring. The composite was then cooled to ambient temperature and dried in a vacuum oven at 50 ^{o}C.

3.2.3 Film preparation

In order to prepare films from these composites to be used in certain testing procedures, such as mechanical testing, WA and TS tests, composites were remelted before they were pressed into films by compression moulding in a heated hydraulic press (Apex Construction Ltd., UK). Wood-LLDPE samples were pressed in a mould (different types of moulds, depending on the types of test the samples were to be subjected to) at 140°C and 15 MPa for 3 min between Mylar sheets. The pressure (15 MPa) was applied again and the plates were maintained at 140 ^{o}C for 5 min to ensure complete melting. The pressure was removed and then reapplied three times at 140 ^{o}C for 1 min. Then the films were cooled to ambient temperature.

3.3 Charactisation

3.3.1 Chemical analysis of wood

Solvent (ethanol:cyclohexane 1:2) (E/C) and hot water (HW) extractive contents as well as lignin and cellulose contents were determined. E/C and HW extractions were performed according to Tappi standard T 264 om-88 [9]. The Klason lignin content was determined according to Tappi 222 om-88 [9]. The cellulose content was determined using the Seifert method [10]. Chemical analysis of wood species was measured in triplicate.

3.3.2 X-ray diffraction

X-ray diffraction (XRD) was performed at iThemba LABS (South Africa) on a Bruker AXS D8 ADVANCE diffractometer at room temperature with filtered CuKα radiation. Samples were scanned at 2θ angles (diffraction angle) ranging from 6^{o} to 50^{o}, with a sampling width of 0.02^{o}. Each tested sample had thickness of 0.82 mm and diameter of 14.80 mm.

3.3.3 Mechanical properties

The tensile strength and elongation at break were determined according to ASTM D 638, using a Lloyd LRX tensile tester (Metrology). Five samples (25 mm x 6.0 mm x 0.27 mm) were tested for each composite. The surface hardness was measured using a UHL VMHT

MOT microhardness tester with a test load of 25 g, dwell time of 15 s and an indentation speed of 50 µm/s. Ten measurements were taken from each composite (disks of 21.10 mm diameter and 3.53 mm thickness). DMA was performed using a Perkin Elmer DMA 7e analyzer. The apparatus was calibrated according to standard procedures. The extensional mode in DMA was used to obtain a stress-strain curve for each sample. MOE was determined from the linear slope of a stress-strain curve at 5% strain. The sample dimensions were 22 mm x 4 mm x 0.27 mm.

3.3.4 Thermal analysis

The thermal characteristics of the composites were determined by differential scanning calorimetry (DSC). A TA Instruments Q100 DSC system was used. It was first calibrated by measuring the melting temperature of indium metal according to a standard procedure. All measurements were conducted under a nitrogen atmosphere, and at a purge gas flow rate of 50 mL/min. The samples were heated from 25 to 220 ^{o}C at 10 ^{o}C/min, held isothermally at 220 ^{o}C for 1 min and then cooled to -50 ^{o}C at a rate of 10 ^{o}C/min, during which time the cooling crystallisation curve was recorded. At -50 ^{o}C the temperature was kept constant for 1 min, after which the melting curve was recorded between -50 and 220 ^{o}C at a heating rate of 10 ^{o}C/min. The T_m and the heat of fusion (ΔH_f) were calculated from the thermograms obtained during the second heating. The values of ΔH_f were used to estimate the degree of crystallinity (X_c) of each composite, with 288.7 J/g taken as a value of the enthalpy of fusion (ΔH_f^o) of completely crystalline PE [11].

Thermogravimetric analysis (TGA) was conducted using a Perkin Elmer TGA 7. The change in weight as a function of temperature was determined with a resolution of 0.1 mg, in a nitrogen atmosphere. Approximately 5 mg of each sample was analyzed, by heating from 20 to 900 ^{o}C at a rate of 20 ^{o}C/min.

3.3.5 Water absorption and thickness swelling

The WA was determined after immersion of samples in water at room temperature for 11, 20, 29, 34, 43 and 52 days. Three specimens from each sample were weighed before and after immersion and the WA was calculated as follows:

$$WA\ (\%) = (M_I - M_0) / M_0 \times 100$$

where M_I is the mass of the sample after immersion (g) and M_0 is the mass of the sample before immersion (g).

The TS was calculated after immersion of a film sheet from each sample in water at room temperature for 11, 20, 29, 34, 43 and 52 days. The thickness (varying from 0.25-0.29 mm) of

three films from each sample was measured before and after immersion and the TS was calculated as follows:

$TS\ (\%) = (T_{h1} - T_{h0}) / T_{h0} \times 100$

where T_{h1} is the thickness of the sample film after immersion (g) and T_{h0} is the thickness of the sample film before immersion (g). Three samples were used for determining the WA and TS.

3.3.6 Melt index

A melt flow indexer, Ceast (Wirsam Scientific and Precision Equipment), was used to obtain the melt index (MI) of each composite. The measurements were performed according to ASTM D 1238, 190 ^{o}C and 2.16 kg. Each value of MI is an average of six samples.

3.3.7 Morphological observations

A Zeiss Axiolab optical microscope (OM) with magnification of 100x and a high resolution camera CCD-IRIS (Sony) was used to determine the morphology before and after degradation, and the dispersion of wood particles in the composites. A Leica EZ4D microscope with 35x magnification and the Leica measurement software were used to measure the particle lengths and lengths distribution of the wood particles. At least 200 particles were measured for each species.

3.3.8 UV degradation

Accelerated weathering tests were performed by exposing film samples of LLDPE and wood-LLDPE composites to UV-B light (313 nm) in a QUV Weatherometer (Q-Panel Company) for 99 days, which correlates to 8 years of sun exposure. All the samples were disks 0.80 mm thick and 39.21 mm in diameter.

3.3.9 Fourier transform infrared analysis

Fourier transform infrared analysis (FTIR) spectra were acquired using a Perkin Elmer FTIR spectrometer (model Paragon 1000 PC). All spectra were recorded from 450 to 4000 cm^{-1} by using a photo-acoustic unit (PAS) at a resolution of 8 cm^{-1}. FTIR was used to determine the degree of UV degradation.

3.4 Results and discussion

3.4.1 Chemical analysis of wood

Chemical analysis of wood species are presented in Table 3.1. Standard deviations are given in parentheses. The hemicelluloses form part of the remaining percentage. There are marked differences in the values of hemicelluloses, cellulose and lignin between the four types of

wood. All hardwoods species (*A. cyclops*, *E. grandis* and *Q. alba*) had a higher cellulose content than softwood species (*P. radiata*). The E/C-soluble extractive content, comprising waxes, fats, resins and some gums [3], was the highest in *P. radiata*, followed by *A. cyclops*, *Q. alba* and *E. grandis*. The water-soluble extractive content, comprising of tannins, gums, sugars, and starches and colouring matters [9] is the highest in *A. cyclops* followed by *Q. alba*, *P. radiata* and *E. grandis*. In conclusion, the four different wood species show clear differences in terms of macromolecular composition and content. This can be expected to affect the performance and properties of the WPCs made with these species.

Table 3.1 Macromolecular composition and content of the investigated wood species

	A. cyclops (hardwood)	*E. grandis* (hardwood)	*P. radiata* (softwood)	*Q. alba* (hardwood)
Cellulose content [%]	47.4 (0.3)	37.7 (1.7)	31.8 (0.8)	38.1 (0.1)
Lignin content [%]	22.7 (1.5)	20.6 (1.8)	22.1 (1.7)	25.0 (0.9)
E/C extractives [%]	02.4 (0.4)	01.2 (0.1)	03.5 (0.1)	02.0 (0.2)
HW extractives [%]	03.6 (0.4)	01.8 (0.3)	02.4 (0.3)	03.2 (0.2)
Others [%]	23.8 (1.6)	38.7 (3.4)	40.2 (2.2)	32.7 (0.7)

Calculations of % cellulose, lignin and extractives were based on oven dry mass wood

3.4.2 X-ray diffraction

Figure 3.1 shows the XRD patterns of LLDPE, EVOH, *A. cyclops* and its composites. The XRD patterns of the other species and their composites are shown in Appendix A. In general, LLDPE and all the composites give a sharp crystalline peak and a small peak in the region of the Bragg angle (2θ) between 20° and 25°, which indicates the semicrystalline nature [12]. LLDPE has three main crystalline diffraction peaks at 2θ of 21.5°, 23.7° and 36.2°, corresponding to the 110, 200 and 020 lattice planes of the orthorhombic crystal lattice [13]. The strong diffraction peak in LLDPE is located at 2θ of 21.4°. The amorphous halo is centred on 2θ = 19.8° [12].

Although EVOH is semicrystalline, it shows a very weak crystalline structure, in the region of the 2θ between 10° and 50° [10]. The strong diffraction peaks of EVOH are located at the 2θ angles of 20.3° and 21.7°. The two peaks correspond to the (200) and (020) planes, respectively.

The diffraction patterns of the four wood species have a typical form of native cellulose I, with a monoclinic lattice, characteristic of wood structure and displaying well defined peaks at 16.4°, 22° and 34.5°, respectively. The 16.4° is probably due to the 110 plane, while the

22° reflection corresponds to the 200 crystallographic plane. The peak at 34.5° corresponds to the 023 or 004 planes. The appearance of 16.4° and 22.0° as separate peaks indicates that these wood species have a high cellulose content [14]. The strong diffraction peak in all wood species is located at 2θ of 2.02° due to the 002 lattice plane of cellulose [15].

The clear presence of characteristic LLDPE peaks in all the composites, in the same position as the peaks of neat LLDPE, indicates that there is no change in the crystalline structure of LLDPE. On the other hand, there is a decrease in the amount of crystallinity as indicated by a decrease in the intensity of these peaks. This means that the crystalline structure of LLDPE is not significantly influenced by compounding with different wood species, nor by the incorporation of a functionalised polymer such as EVOH. No evidence of co-crystallisation of the composites components was found.

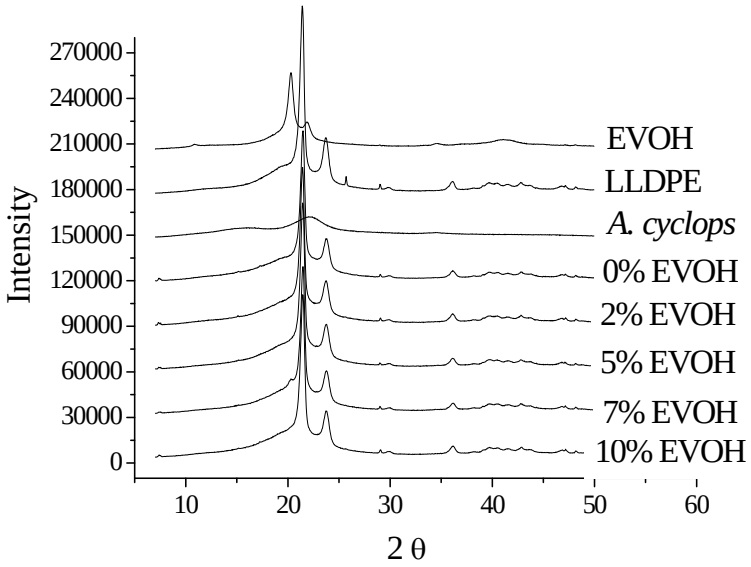

Figure 3.1 XRD spectra recorded for the EVOH, LLDPE, *A. cyclops* and its composites.

3.4.3 Mechanical properties

Table 3.2 and Figure 3.2 show the tensile strength and EAB of LLDPE and all the related wood-LLDPE composites. Standard deviations are given in parentheses. Noncompatibilised composites had the lowest strength properties. The tensile strength increased as the amount of compatibiliser increased. Composites with 7% EVOH showed higher tensile strength than others. Increasing the content of EVOH to up 10% reduced the tensile strength. The tensile strength of the *A. cyclops* composite was significantly higher than that of the *E. grandis*, *P. radiata* and *Q. alba* composites. According to literature (see Section 2.2.1.4), this could be explained by a strong interfacial adhesion between LLDPE and *A. cyclops* particles due to a higher cellulose content, since cellulose is the main component providing the wood's strength

and structural stability [16-20]. Wood with a high cellulose content contains more hydroxyl groups on the wood surface, which promote stronger interaction and better interfacial adhesion between the wood and the LLDPE matrix via the compatibiliser than wood with lower cellulose content.

The EAB of all the composites decreased, compared to LLDPE. As discussed earlier in Section 2.2.1.4, the addition of WF in the composites increases the stiffness and brittleness and reduces EAB [21]. This decrease can be related to the stiffening effect of wood species. The EAB increased with increasing amounts of EVOH. Composites with 7% EVOH showed higher EAB values, while composites with 0% EVOH had the lowest EAB value in comparison to LLDPE and other composites. With the exception of *E. grandis* composites, increasing the content of EVOH to up 10% caused a dramatic reduction in the EAB.

Table 3.2 Tensile strength and EAB of wood-LLDPE composites

Samples	Tensile strength, N/mm^2	EAB, %	Tensile strength, N/mm^2	EAB, %
LLDPE	10.2 (0.1)	> 100.0		
	A. cyclops composites with		*P. radiata* composites with	
0% EVOH	11.9 (0.3)	33.0 (0.1)	08.5 (0.2)	19.9 (0.1)
2% EVOH	14.5 (0.2)	33.5 (0.2)	12.0 (0.2)	26.4 (0.1)
5% EVOH	21.0 (0.3)	44.5 (0.2)	12.1 (0.2)	40.7 (0.1)
7% EVOH	23.5 (0.3)	88.1 (0.1)	12.6 (0.3)	32.1 (0.2)
10% EVOH	13.6 (0.2)	34.8 (0.1)	11.7 (0.2)	31.5 (0.2)
	E. grandis composites with		*Q. alba* composites with	
0% EVOH	10.2 (0.2)	24.4 (0.2)	10.8 (0.1)	19.3 (0.2)
2% EVOH	11.1 (0.1)	28.2 (0.2)	13.6 (0.1)	22.8 (0.2)
5% EVOH	12.8 (0.2)	28.6 (0.1)	14.4 (0.1)	24.4 (0.2)
7% EVOH	13.3 (0.1)	33.5 (0.1)	14.5 (0.1)	31.4 (0.2)
10% EVOH	08.6 (0.1)	49.2 (0.1)	11.8 (0.1)	22.5 (0.3)

As shown in Table 3.2 and Figure 3.2 there is no significant difference in the EAB for *E. grandis*, *P. radiata* and *Q. alba* composites, especially at 7% EVOH content, but the *A. cyclops* composite generally showed a significantly larger EAB. The lignocellulosic fibres are responsible for the decrease of the deformation capability. The better interfacial adhesion between *A. cyclops* particles and LLDPE, due to its high cellulose content, increases toughness or ductility [11]. The ratio of lignin to cellulose can also play a role. The higher it is the better is the interfacial adhesion that can be achieved, since lignin acts as a natural adhesive within the cellulose. Furthermore, hemicelluloses can play a role. This is because hemicelluloses are amorphous and more deformable than crystalline cellulose. Consequently,

species with high hemicelluloses content may have better EAB compared to species with a low hemicelluloses content.

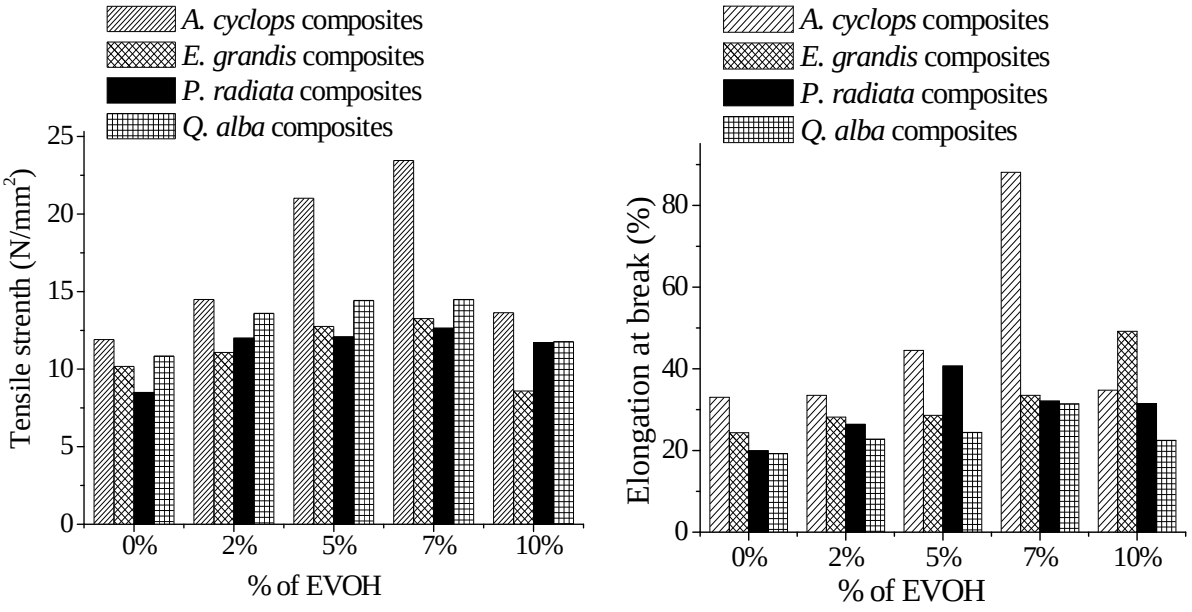

Figure 3.2 Tensile strength and EAB versus the percentage of EVOH of wood-LLDPE composites.

Table 3.3 presents a summary of all hardness measurements performed on LLDPE and wood-LLDPE composites. The average hardness increased with the addition of 10% wood and different EVOH contents, in comparison with neat LLDPE. As mentioned in Section 2.2.1.4, an increase in hardness is evident when the content of the filler increases [22]. Hardness was considerably increased with the addition of 10% wood particles and 2, 5 and 7% EVOH in comparison to neat LLDPE. Composites with 7% EVOH showed to have the highest values of hardness, while composites with 0% EVOH had the lowest values. Increasing the content of EVOH to up 10% resulted in a decrease in the hardness of these materials. The hardness values in Table 3.3 are represented graphically in Figure 3.3. As shown in Figure 3.3, the hardness of *P. radiata* composite was higher than in *A. cyclops*, *E. grandis* and *Q. alba* composites. The hardness of a WPC is generally related to the hardness of the polymer and the wood, and to polymer-wood interactions [23-24]. This means that the ultimate hardness values of these composites are dependent on the hardness of the wood [25-29], regardless to the polymer-wood interactions, since all the composites were prepared using the same polymer matrix. This means that the lignocellulosic component in *P. radiata* has a considerably higher hardness than the lignocellulosic in the other species. Investigations have shown that wood hardness is influenced by its density and moisture content [29-30]. Higher density increases the hardness, and as the moisture content level increases, the hardness decreases [29].

Table 3.3 Hardness of LLDPE and all wood-LLDPE composites

Samples	Hardness, MPa	Samples	Hardness, MPa
LLDPE	2.1 (0.3)	*P. radiata* composites with	
A. cyclops composites with			
0% EVOH	2.5 (0.7)	0% EVOH	2.3 (0.5)
2% EVOH	3.1 (1.7)	2% EVOH	2.5 (0.7)
5% EVOH	3.7 (2.5)	5% EVOH	2.9 (1.1)
7% EVOH	4.1 (2.2)	7% EVOH	3.6 (2.3)
10% EVOH	3.3 (1.5)	10% EVOH	2.8 (1.2)
E. grandis composites with		*Q. alba* composites with	
0% EVOH	2.7 (0.7)	0% EVOH	2.5 (0.7)
2% EVOH	3.9 (1.7)	2% EVOH	2.8 (0.6)
5% EVOH	4.2 (2.7)	5% EVOH	2.9 (1.1)
7% EVOH	4.7 (2.8)	7% EVOH	3.5 (1.1)
10% EVOH	3.6 (1.1)	10% EVOH	2.6 (0.7)

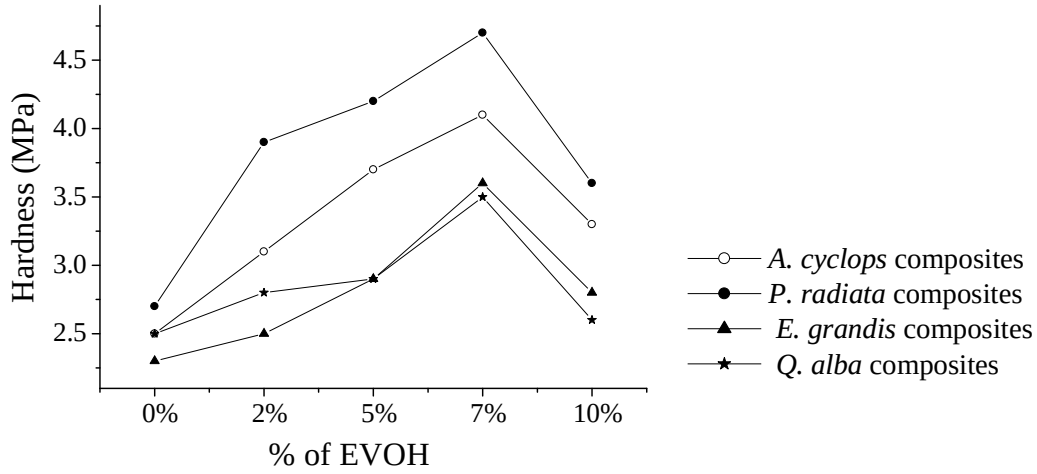

Figure 3.3 Hardness versus the percentage of EVOH in all the wood-LLDPE composites.

All the stress-strain curves of LLDPE and wood-LLDPE composites are shown in Appendix B. As it can be seen in Table 3.4, the MOE increased significantly with the addition of 10% wood particles and 2, 5 and 7% EVOH, in comparison to neat LLDPE. Composites with 7% EVOH showed the highest MOE, while composites with 0% EVOH illustrated the lowest values of MOE. Increasing the content of EVOH up to 10% affected the MOE badly in all composites. It is believed that better wood dispersion and compatibility between wood and polymer matrix is achieved via the use of a compatibilizer, and that the compatibiliser is thus responsible for the improved properties of WPC, including MOE. Hence, the addition of 7%

EVOH significantly improved the MOE or stiffness of the composites, especially in the cases of *A. cyclops* and *Q. alba* composites. Since the properties of these composites are dependent on the properties of the constituents and the interfacial interaction between wood and polymer matrix, the difference in the MOE or stiffness of these composites is related to the difference in the stiffness properties of all the composite's components. With the exception of the different wood species, all other components are the same. Thus, the difference in the stiffness properties must be related to the wood composition. It appears that *Q. alba* and *A. cyclops* are stiffer and they impart more stiffness to the composites to a larger extent than the other two species. This is propably due to the cellulose content. The higher the cellulose content, the stiffer the wood will be, as explained in Section 2.2.1.4. The MOE of cellulose is reported to be about 130 GPa, while the MOE of lignin is about 2 GPa [31-32], and that of hemicelluloses are about 8 GPa [33].

Table 3.4 MOE of LLDPE and all the wood-LLDPE composites

Samples	MOE, MPa	Samples	MOE, MPa
LLDPE	0.4	*P. radiata* composites with	
A. cyclops composites with			
0% EVOH	1.1	0% EVOH	0.5
2% EVOH	1.3	2% EVOH	1.5
5% EVOH	2.0	5% EVOH	1.4
7% EVOH	2.9	7% EVOH	2.4
10% EVOH	1.6	10% EVOH	1.6
E. grandis composites with		*Q. alba* composites with	
0% EVOH	0.9	0% EVOH	2.6
2% EVOH	1.1	2% EVOH	2.9
5% EVOH	0.9	5% EVOH	2.9
7% EVOH	2.3	7% EVOH	3.0
10% EVOH	0.9	10% EVOH	2.3

3.4.4 Thermal analysis

Table 3.5 lists the T_m, crystallisation temperature (T_c), ΔH_f and X_c values for the neat LLDPE and all the wood-LLDPE composites. The X_c was determined by using the following equation:

$$X_c(\%) = \frac{\Delta H_f}{\Delta H_f^o} \text{ x100}$$

The X_c of each composite was corrected (X_c^{corr}) taking into account the wood added to the composites. In comparison to LLDPE, all wood-LLDPE composites showed negligible

change in the T_c and T_m, and an apparent decrease in the ΔH_f and X_c. These results agreed fairly well with many results published previously [1, 15, 33-38], as shown in Section 2.2.1.4. As can be seen in Table 3.5, X_c^{corr} of each composite was higher than its X_c. The increase in the X_c of the composites, as the EVOH content increases, was due to the compatibiliser effect, which extended the predominance of the crystallisation process [35].

Table 3.5 DSC results of LLDPE and WPCs

Sample	T_m, °C	T_c, °C	ΔH_f, J/g	X_c, %	X_c^{corr}, %
LLDPE	121.4	108.1	108.4	37.7	37.7
A. cyclops composites with					
0% EVOH	120.9	109.4	88.9	30.8	34.2
2% EVOH	120.1	107.2	75.9	28.9	32.8
5% EVOH	120.7	107.9	94.8	32.8	36.6
7% EVOH	120.5	107.9	95.7	33.1	39.9
10% EVOH	121.0	107.7	106.6	36.9	46.2
E. grandis composites with					
0% EVOH	120.2	107.9	98.4	34.1	37.9
2% EVOH	121.2	109.1	99.3	34.4	39.1
5% EVOH	120.7	108.2	100.9	35.0	41.1
7% EVOH	121.4	108.5	82.6	28.6	34.9
10% EVOH	120.5	108.0	102.8	35.6	44.5
P. radiata composites with					
0% EVOH	120.9	108.4	88.9	30.8	34.2
2% EVOH	120.6	107.8	93.1	32.2	37.1
5% EVOH	121.2	107.9	97.7	33.8	39.8
7% EVOH	120.6	108.0	91.2	31.8	38.8
10% EVOH	120.8	108.3	90.9	31.2	39.0
Q. alba composites with					
0% EVOH	121.2	107.2	86.9	30.1	33.4
2% EVOH	120.9	107.7	89.5	31.0	35.2
5% EVOH	120.6	108.1	95.5	33.2	39.0
7% EVOH	121.0	107.4	91.9	31.9	38.8
10% EVOH	121.2	108.3	104.0	36.0	45.0

It has been reported before, the crystallinity of WPCs is much greater than that of the corresponding WPCs without compatibilisers [39-40]. Overall, the same trend is observed for the samples prepared in this study. It is clear that the presence of EVOH allows the wood particles to act as nucleating sites for crystallisation, thus influencing the overall crystallinity of the samples. In the absence of EVOH, the lack of compatibility between wood and the matrix causes a slight decrease in overall crystallinity, which indicates that the lack of interaction can influence the ability of the LLDPE matrix to crystallise. The slight decrease in the T_m and X_c can be used as evidence to support XRD results in Section 3.4.2. The X_c of the

matrix decreases, while T_c indicates that the crystalline structure of LLDPE is not significantly influenced by compounding with different wood species in the presence of EVOH, as indicated earlier by XRD in Section 3.4.2. Some authors relate the change in T_m to the change in the spherulites shape. Harper and Wolcott [41] believed that the addition of wood tends to push the spherulites from a spherical shape towards a truncated shape. DSC melting and crystallisation curves of LLDPE and wood-LLDPE composites are shown in Appendix C.

The thermal stability of the four wood species, LLDPE, and all wood-LLDPE composites was determined with TGA, which measures the weight loss of the sample with increasing temperature. The thermal stability of the four wood species is illustrated in Figure 3.4. All TGA curves in Figure 3.4a show a small weight loss before 100 °C, which can be attributed to the evaporation of water. The weight loss rate gradually increased above 200 °C, and a distinct weight loss appeared between 200 and 400 °C. All four wood samples exhibit a loss of about 75 wt% at 400 °C. *Q. alba* has the highest weight loss and *P. radiata* the lowest.

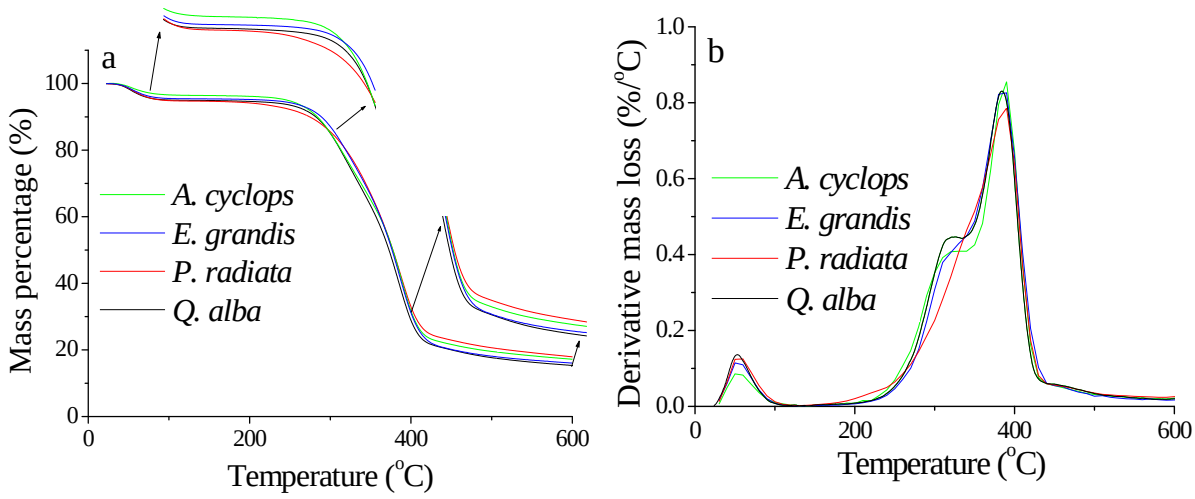

Figure 3.4 a) TGA and b) DTG curves of the four wood species.

DTG curves displayed in Figure 3.4b allow a comparison of the thermal stability between the wood species. With exception to *P. radiata*, the degradation profiles show two peaks and a shoulder, and it becomes apparent that the degradation between 200 and 400 °C is actually a two-step process. The first degradation event is observed between 218 and 260 °C, and can be attributed to the decomposition of hemicelluloses and the slower decomposition of lignin. The second degradation above 350 °C can be attributed to the degradation of cellulose. These results are consistent with previously published results [1, 11, 35, 42-43]. The onset temperature T_0 (the beginning of some extractives, hemicelluloses and lignin decomposition), the first decomposition temperature T_1 (the shoulders in Figure 3.4b), the second

decomposition temperature T_2 (the peaks in Figure 3.4b), the final decomposition temperature T_f and the residual weight at 600 °C of the investigated wood species are summarized in Table 3.6.

Table 3.6 Thermal degradation temperatures and residue weight of the investigated wood species

Wood species	T_0, °C	T_1, °C	T_2, °C	T_f, °C	Residue at 600 °C, %
Q. alba	258.4	321.7	385.7	538.0	12.0
P. radiata	218.9	-------	388.4	513.8	13.7
A. cyclops	245.2	321.2	387.5	524.8	13.5
E. grandis	234.6	324.7	385.4	507.7	13.3

Comparison of T_0 indicates that *P. radiata* and *E. grandis* started to degrade at lower temperatures than *A. cyclops* and *Q. alba*, which means that at low temperatures woods from *P. radiata* and *E. grandis* are less stable than wood from *Q. alba* and *A. cyclops*. This could be explained by the higher cellulose content of *A. cyclops* and *Q. alba*, as shown in Table 3.1. With the exception of *P. radiata*, T_1 values did not differ significantly for the four wood species; it appeared around 322 °C. T_2 values are also in a close temperature range around 386 °C. The final decomposition temperature T_f of *Q. alba* and *A. cyclops* occurred at higher temperatures than for *P. radiata* and *E. grandis*. This indicates that wood from *P. radiata* and *E. grandis* is less stable even at higher temperatures than the other two species, which could be attributed to the lower lignin content.

According to Tserki et al. [44] the lower stability of wood at low temperatures can be attributed to a high lignin and hemicelluloses content, while the high stability of wood at low temperatures is due to higher cellulose content. They demonstrated that lignin appears to be more heat resistant than hemicelluloses and cellulose at high temperatures due to its low degradation rate. This confirms that the decomposition of lignin occurs in a wider temperature range than that of hemicelluloses and cellulose. At 600 °C no significant quantitative difference in wood residue between the four wood species could be determined. The highest wood residue was determined for P. *radiata* and the lowest for *Q. alba*. It can be concluded that a higher cellulose and lignin content of wood leads to a better thermal stability over the entire temperature range.

Figure 3.5 shows the TGA curves of the LLDPE and all wood-LLDPE composites. The weight loss of LLDPE occurred in one step, between 390 and about 520 °C due to the decomposition of C-C bonds in the main chain of LLDPE. All wood-LLDPE composites showed a small weight loss below 100 °C, which can be attributed to the evaporation of water.

The weight loss rate gradually increased above 200 °C and a distinct weight loss appeared between 250 and 530 °C, in two main degradation steps. The first degradation step below 300 °C can be attributed to the decomposition of individual wood components such as hemicelluloses, the onset of the decomposition of lignin and extractives. The second degradation step between 400 and 550 °C can be attributed due to the decomposition of cellulosic materials in the wood and the C-C bonds in the main chain of LLDPE. The first degradation step occurred between T_{01} (onset temperature of the first degradation step) and T_{f1} (final temperature of the first degradation step).

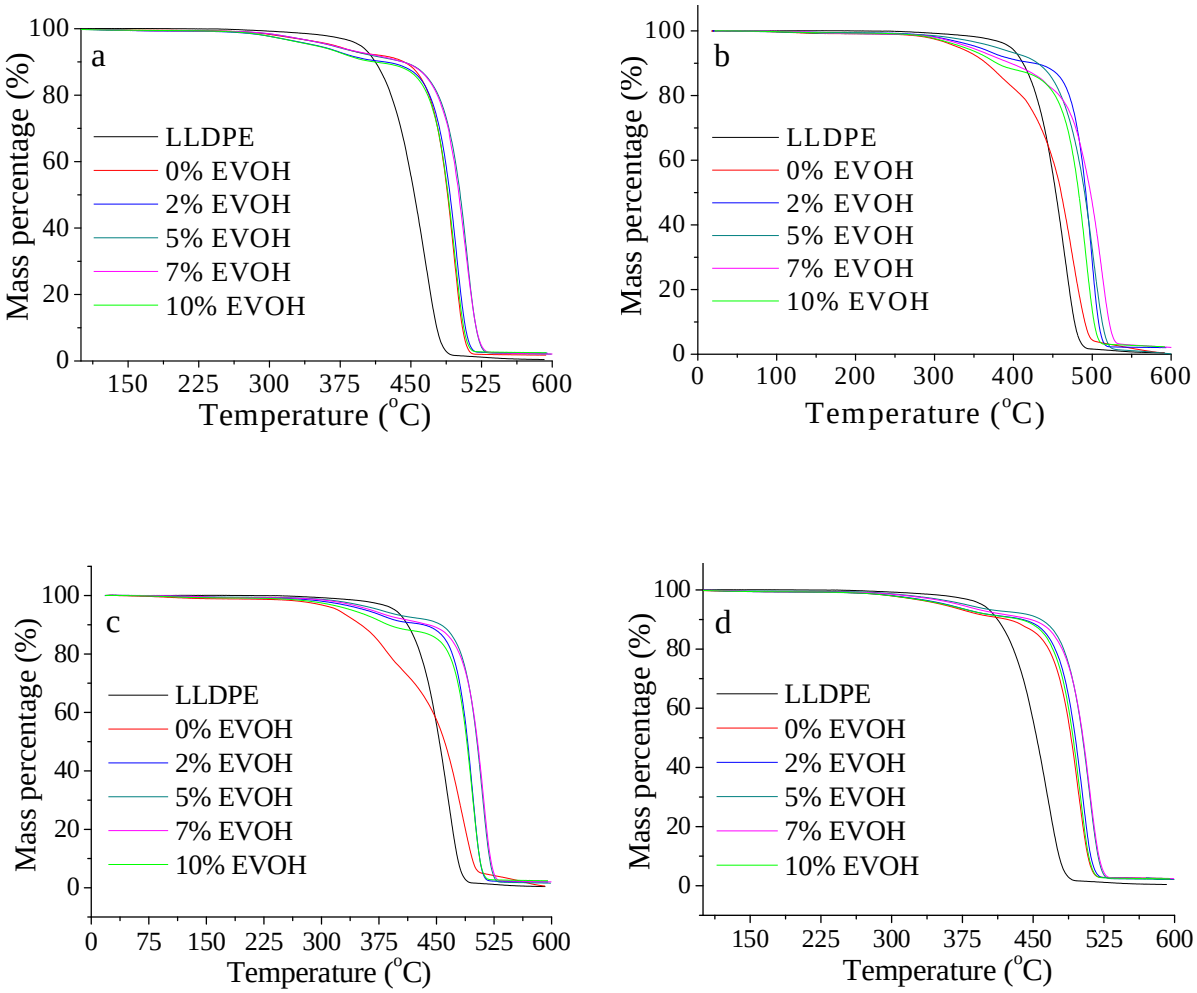

Figure 3.5 TGA curves of the LLDPE and all composites: a) *A. cyclops*, b) *E. grandis*, c) *P. radiata* and d) *Q. alba* composites.

The second degradation step occurred between T_{02} (onset temperature of the second degradation step) and T_{f2} (final temperature of the second degradation step), as shown in Table 3.7. As in the cases of neat wood samples, the differences in T_{01}-T_{f1} and T_{02}-T_{f2} in Table 3.7 indicate that *E. grandis* and *P. radiata* composites degraded before the *A. cyclops* and *Q. alba* composites at both lower and higher temperatures. This means (once again) that at low and

high temperatures wood from *E. grandis* and *P. radiata* is less stable than wood from *A. cyclops* and *Q. alba*. T_{02} and T_{f2} in the cases of *A. cyclops* and *Q. alba* composites were shifted to higher temperature in comparison to *E. grandis* and *P. radiata* composites, which means that *A. cyclops* and *Q. alba* improved the thermal stability of LLDPE more than the *E. grandis* and *P. radiata* composites. This can be attributed to a higher cellulose and lignin content of *A. cyclops* and *Q. alba*.

Table 3.7 TGA results of LLDPE and all wood-LLDPE composites

Sample	T_{01}, ^oC	T_{f1}, ^oC	T_{02}, ^oC	T_{f2}, ^oC	Residue at 600 ^oC, %
LLDPE	--------	--------	399.9	519.6	0.4
Composites with 0% EVOH of					
A. cyclops	273.4	390.6	401.3	519.5	2.5
E. grandis	259.8	381.9	397.4	500.1	2.4
P. radiata	256.9	378.0	395.4	518.5	1.8
Q. alba	274.3	392.5	399.2	519.5	0.4
Composites with 2% EVOH of					
A. cyclops	277.2	391.6	403.2	525.3	2.4
E. grandis	270.5	388.7	400.3	519.3	0.6
P. radiata	265.6	382.9	399.3	520.4	2.3
Q. alba	284.0	395.4	402.2	524.2	2.1
Composites with 5% EVOH of					
A. cyclops	293.7	395.8	406.1	528.2	2.1
E. grandis	278.0	394.2	402.3	525.0	1.6
P. radiata	266.6	394.2	400.3	527.2	2.1
Q. alba	297.6	399.3	403.2	528.2	0.1
Composites with 7% EVOH of					
A. cyclops	295.9	403.9	408.7	529.9	2.4
E. grandis	278.0	397.5	403.9	529.2	2.0
P. radiata	277.3	397.5	402.2	528.2	0.5
Q. alba	300.5	400.3	407.0	531.4	0.1
Composites with 10% EVOH of					
A. cyclops	264.6	379.9	403.2	522.4	2.4
E. grandis	261.7	378.8	394.5	513.7	2.0
P. radiata	260.8	377.0	390.6	518.5	2.5
Q. alba	272.4	388.7	402.2	519.4	2.3

The most important information that could be deduced from the above TGA results is that: (1) the thermal stability of wood-LLDPE composites with EVOH was better than the thermal stability of composites without EVOH, (2) the highest thermal stability was observed in the composites with 7% EVOH, (3) the thermal stability of the composites decreased as the amount of EVOH was increased up to 10%, (4) woods with higher cellulose and lignin contents had better thermal stability than woods with lower cellulose and lignin content, and

hence use of woods with higher cellulose and lignin contents probably lead to the production of composites with better thermal stability, and (5) *A. cyclops* species produced composites with better thermal stability

3.4.5 Water absorption and thickness swelling

As illustrated in Figure 3.6, the rate of WA in all wood-LLDPE composites increased up to 43 days and thereafter it became almost constant. *P. radiata* composites had lower WA rate than *E. grandis*, *Q. alba* and finally *A. cyclops* composites.

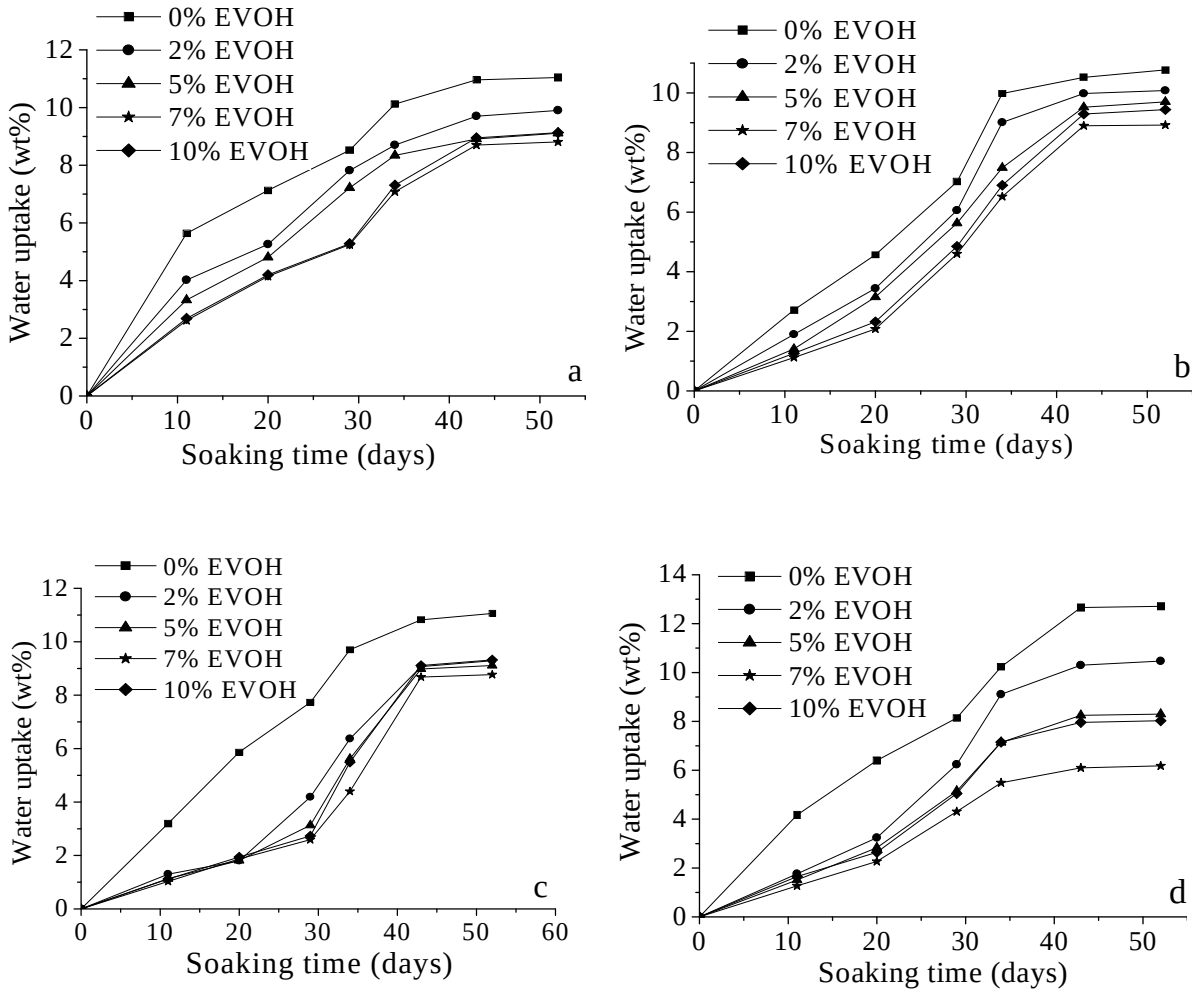

Figure 3.6 WA of a) *A. cyclops*, b) *E. grandis*, c) *P. radiata* and d) *Q. alba* composites.

WA is mainly due to the hydrogen bonding of water molecules to hydroxyl groups on the cell walls of the wood [45]. Amorphous cellulose and hemicelluloses are mostly responsible for the high WA of natural fibres, since they contain many easily accessible hydroxyl groups which offer a high level of hydrophilic character to fibres [46]. As a result, wood in noncompatibilised composites take up high amounts of water. On the other hand, using EVOH as a compatibiliser reduced WA rate of the composites. This indicates that EVOH improved the compatibility between the wood and the LLDPE matrix. This is because EVOH

interacts with the hydroxyl groups of the cellulosic wood and forms bonds that are more resistant to water penetration, thus WA is limited. The remaining free hydroxyl groups on the wood surface are responsible for the WA rate of these composites. This means that the *P. radiata* composites are compactly bonded and have fewer free hydroxyl groups than the other composites and thus they show less absorption of water [47]. The fewer free hydroxyl groups in *P. radiata* is probably due to the lower amount of cellulose in these species, as was shown in Table 3.1.

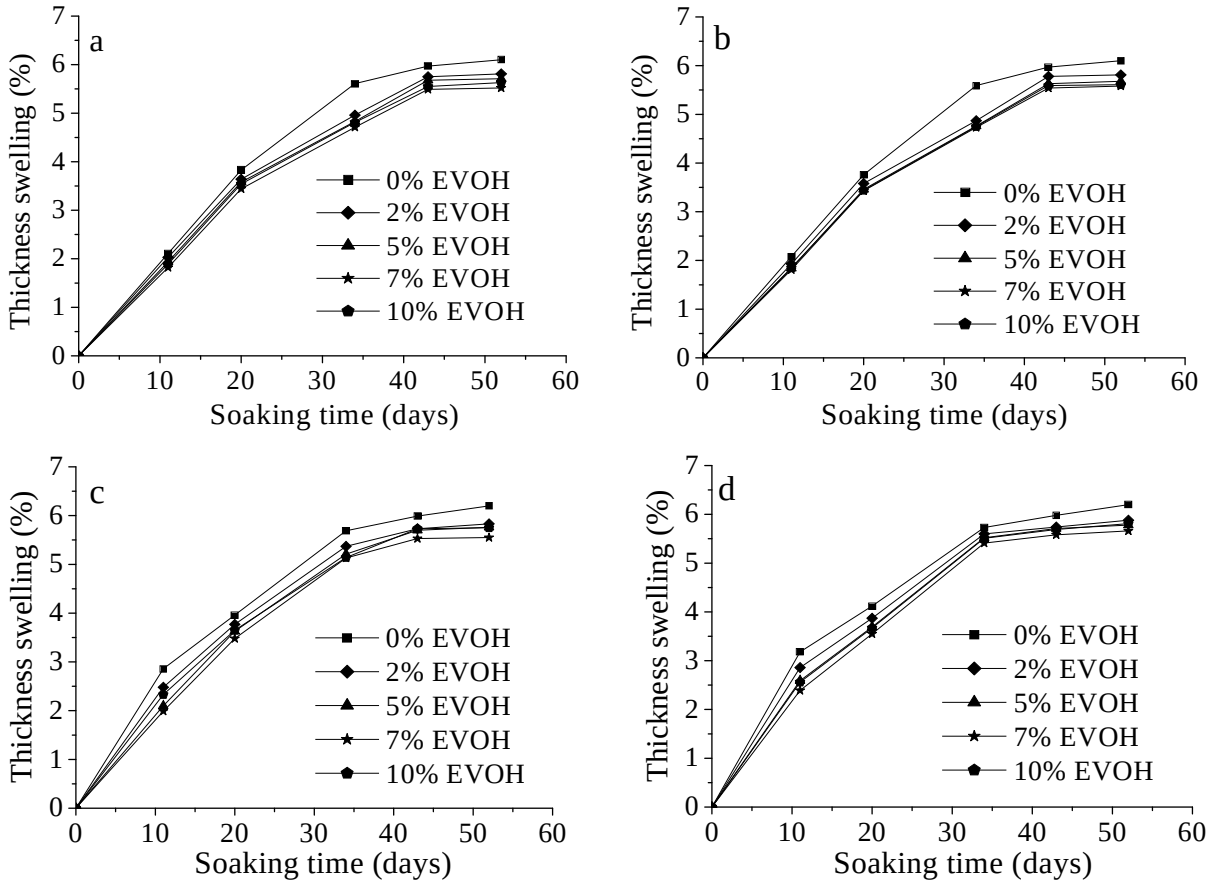

Figure 3.7 TS of a) *A. cyclops,* b) *E. grandis,* c) *P. radiata* and d) *Q. alba* composites.

As shown in Figure 3.7, the TS of all the wood-LLDPE composites increased with the WA and thus showed a similar trend (increase in the WA). This is because the thicker layer (described in Section 2.2.1.1) of the secondary wall was expanded. The TS of all the composites followed a similar trend to the WA behaviour. It increased with immersion time until an equilibrium condition was attained. It should also be noted that *P. radiata* composites had a lower TS than the other composites, which corresponded to the lowest WA rate. The WA and TS values of the composites with 0% EVOH were the highest. The WA and TS rates of the wood-LLDPE composites were also significantly reduced upon the addition of EVOH. Increasing the amount of EVOH from 2 to 5 to 7% led to a decrease in the WA and TS rates. Wood-LLDPE composites with 7% EVOH content had the lowest WA and TS rates.

Increasing the amount of EVOH to 10% resulted in an increase in the WA and TS rates. It is important to note that the rates of WA and TS cannot be ascribed only to the presence of free hydroxyl groups. WA and TS can also be affected by the concentration of the water extractives in the wood species. This is because most of these extractives are water soluble. During the WA and TS tests all or most of these extractives will be dissolved in the water. A large effect on the rate of WA and TS was observed when species with higher amounts of water extractives, such as *A. cyclops* and *Q. alba*, were used. This is because more extractives were dissolved during the WA or TS tests. This fact was confirmed by the change in the colour of water after the WA test, as shown in Figure 3.8.

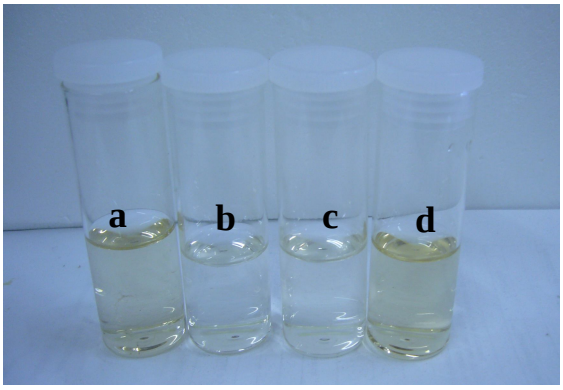

Figure 3.8 Change in the water colour after WA test: a) *A. cyclops*, b) *E. grandis*, c) *P. radiata* and d) *Q. alba* composites.

3.4.6 Melt index

As shown in Figure 3.9, *A. cyclops*, *Q. alba* and *E. grandis* composites generally showed an increase in the MI, in comparison to neat LLDPE, while *P. radiata* composites showed the opposite trend. The difference in the melt indices between these composites could be attributed to the difference in the filler-filler and polymer-filler interactions [48]. Maiti and Hassan [49] found that incorporation of WF into some polymers, such as PP, results in an increase in melt viscosity. This melt viscosity increases with an increase in filler content. This was found to be dependent on the wood loading and on the nature of wood fibre to fibre interactions. In fact, increased viscosity and shear thinning was reported for WF-filled PE and PP [49-52]. This is because wood particles are generally porous and have a very irregular shape. Incorporation of wood particles introduces discontinuity in the matrix and the extent of discontinuity increases with an increase in wood content in composites. It can be argued here that the melt viscosity of the matrix increases due to increased obstruction by the irregular-shaped WF particles [53]. The higher melt index of *A. cyclops* and *Q. alba* composites can also be due to a higher cellulose content in these wood species than in the others. The more hydroxyl groups of cellulose are bonded to the LLDPE matrix via a compatibiliser, the higher

the melt index of the composites [54]. Most importantly, the incorporation of different wood particles and EVOH into LLDPE matrix did not badly affect the MI of composites, and thereby making them suitable for processing.

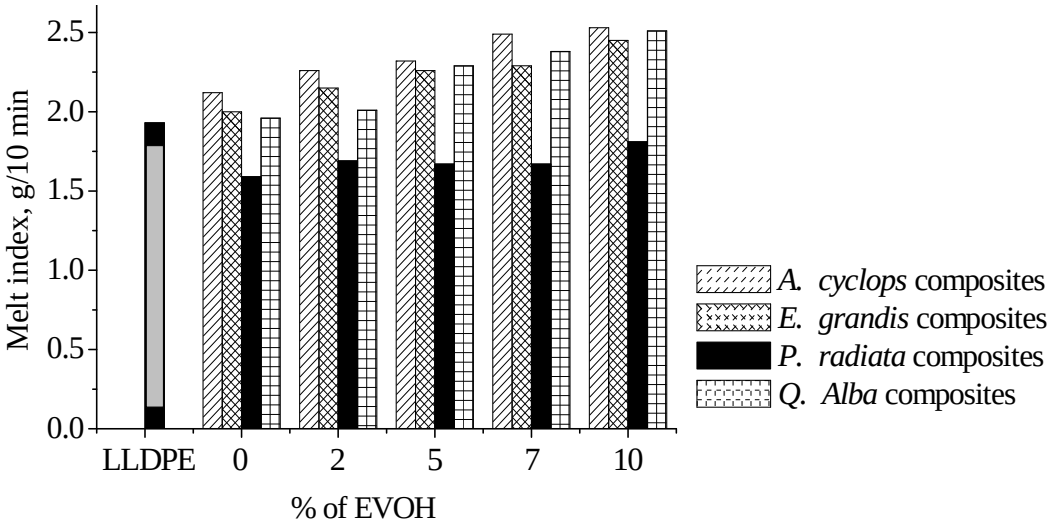

Figure 3.9 Melt index of LLDPE and all wood-LLDPE composites.

3.4.7 Morphological observations

A good and random distribution of the wood particles was achieved, especially in the case of *A. cyclops* composites, as shown in Figure 3.10.

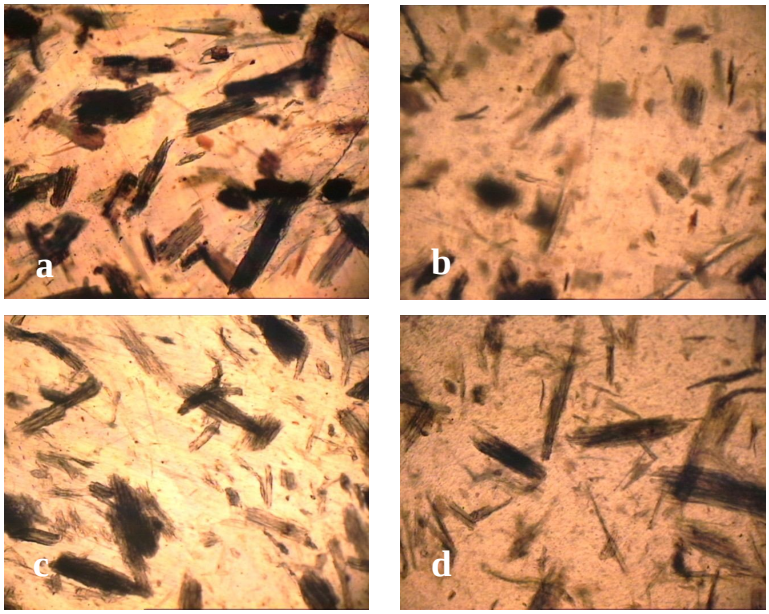

Figure 3.10 Optical micrographs of a) *A. cyclops*, b) *E. grandis*, c) *P. radiata* and d) *Q. alba* composites with 7% EVOH.

Figure 3.10 shows the morphology and distribution of the wood particles in the four wood-LLDPE composites with 7% EVOH. The morphology and distribution of the wood particles

in the wood-LLDPE composites with 0, 2, 5 and 10% EVOH is shown in Appendix D. These images show a large variation in the size, length and shape of the wood particles, and that wood particles were randomly orientated. Fewer very small wood particles are presented in the *A. cyclops* composite, as shown in Figure 3.10a. Wood particles in *A. cyclops* composites seem to be more uniform and well dispersed in the LLDPE matrix than the other wood species. These structural differences can be responsible for the difference in the mechanical and physical properties of these composites [55]. For example, tensile properties of short particles reinforced composites strongly depend on particle length, particle loading, particle dispersion, particle orientation and particle matrix interfacial bond strength [56].

Figure 3.11 shows that the average particle lengths of *A. cyclops* and *Q. Alba* were the highest, about 0.225 and 0.229 mm, respectively. The particle lengths of *E. grandis* and *P. radiata* were 0.168 mm and 0.142 mm, respectively. This is important because the length of the wood particle and its distribution affect the mechanical properties of WPCs significantly [57]. The particle lengths can be affected by the mixing method, processing conditions, nature of the polymeric matrix and its rheological properties, particle content and the resulting interactions. Short and narrow wood particles (0.24-0.50 mm) are preferable [17], because they provide a high specific surface area, which increases the adhesion between the wood and the polymer matrix, and results in a homogenous distribution and better compatibility.

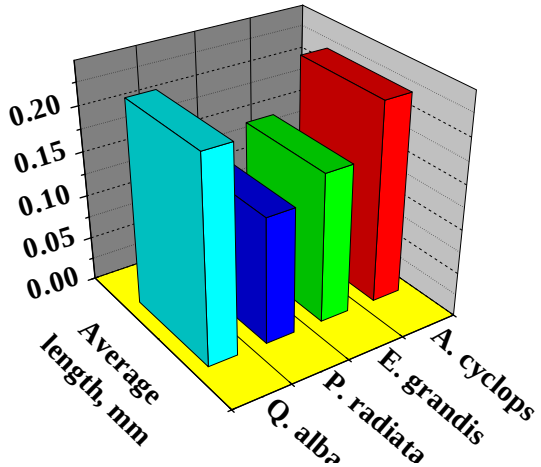

Figure 3.11 Average particle lengths of the four wood species.

In this study, it was difficult to calculate the actual values of the aspect ratios because the length of these wood species varied. This is probably due to the method of preparation of the wood samples. Because the aspect ratio is the length to diameter, *A. cyclops* and *Q. Alba* appear to have higher aspect ratios than *P. radiata* and *E. grandis* due to their higher particle lengths (during the wood preparation, wood chips were comminuted with a Retsch mill to a

particle diameter of about 180 μm). The low aspect ratios of *E. grandis* and *P. radiata* limit their reinforcing ability in comparison to *A. cyclops* and *Q. Alba* [58].

3.4.8 UV degradation

Figure 3.12 shows optical micrographs of LLDPE and all wood-LLDPE composites with 7% EVOH. LLDPE and all the wood-LLDPE composites had undergone degradation. Cracks extending in all directions were created over the entire surface of the LLDPE and all wood-composites with 7% EVOH. UV degradation was less noticeable in the composites than in LLDPE, due to the presence of wood, which absorbs UV radiation. All the composites showed colour changes towards a yellow-brown. This reflects chemical changes due to photo-degradation, and mostly due to the breakdown of lignin and wood extractives [59], as discussed in Section 2.2.1.4. The *A. cyclops* and *Q. alba* composites showed a much better UV resistance than LLDPE and the other two composites. Optical microscope micrographs of composites with 0, 2, 5 and 10% EVOH are shown in Appendix D.

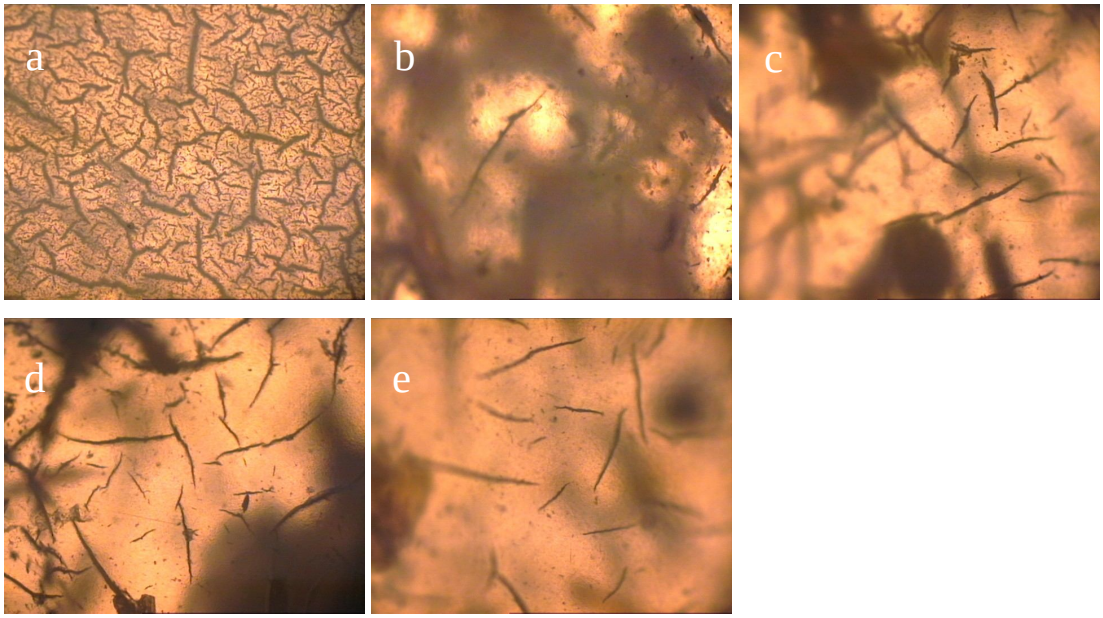

Figure 3.12 Optical micrographs of a) LLDPE, b) *A. cyclops*, c) *E. grandis*, d) *P. radiata* and e) *Q. alba* composites with 7% EVOH after exposure to UV for 99 days (Mag. 100x).

The degree of UV degradation was evaluated by infrared spectroscopy (IR), which is a very sensitive method for the detection of the degradation products [60]. IR spectra of LLDPE before and after UV exposure and all wood-LLDPE composites with 7% EVOH before and after UV exposure are presented in Figure 3.13. Most of the absorption bands have a contribution from both carbohydrates (cellulose and hemicelluloses) and lignin [61-62]. IR spectroscopy has been widely used to detect carbonyl species formed during the POD of PE

by analyzing the carbonyl stretching frequency range from 1800 to 1650 cm^{-1} [63]. As shown in Figure 3.13b, the observed IR band at 1720 cm^{-1} in LLDPE after UV radiation corresponds to the carbonyl groups. This band can be seen in all composites. The bands of the carbonyl groups in wood at 1720 and 1736 cm^{-1} increased, while the small absorption bands for lignin at 1264 and 1510 cm^{-1} decreased after UV radiation. The increase in carbonyl groups is the result of an oxidation of lignin and wood extractives, while the reduction in the lignin band is due to its degradation [60].

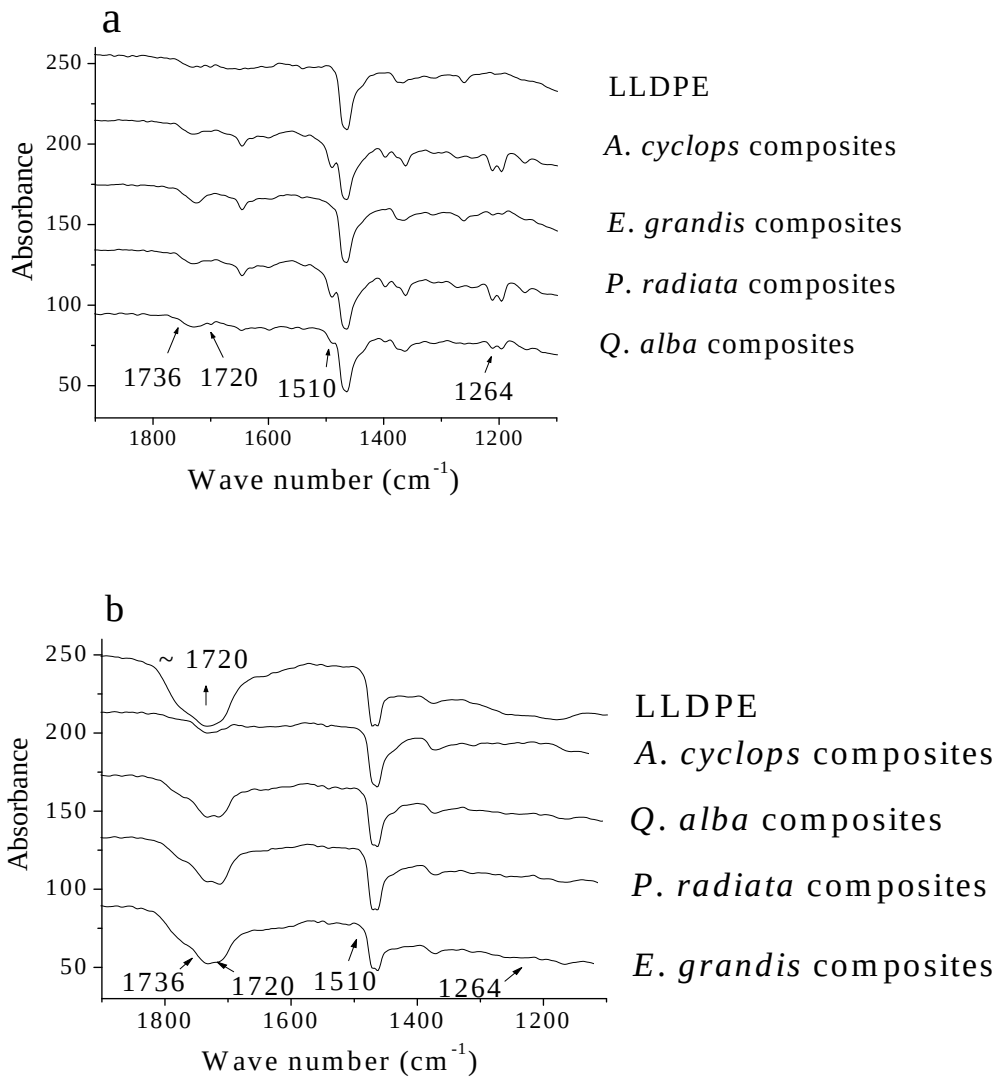

Figure 3.13 FTIR spectra of LLDPE and wood-LLDPE composites with 7% EVOH a) before and b) after exposure to UV for 99 days.

The differences in the carbonyl groups at 1720 cm^{-1} in the various wood-LLDPE composites are evidence of the presence of different degradation products. In this region, the bands associated with the different carbonyl compounds strongly overlap [64]. In the case of wood, for example, the carbonyl band is a result of the overlap of various stretching vibration bands including those of aldehydes and/or esters (1733 cm^{-1}), carboxylic acid groups (1700 cm^{-1})

and γ lactones (1780 cm^{-1}) [65]. It is, therefore, a very difficult task to charactise and quantify the various species formed during oxidation. However, these carbonyl groups are indeed produced by the degradation of LLDPE, lignin and wood extractives. It is well known that lignin and some wood extractives such as terpenes, terpenoids, phenol, lignans, tannins, flavonoids, etc. are very good light absorbers [61].

The intensities of the carbonyl bands were higher in *E. grandis* and *P. radiata* composites than in *A. cyclops* and *Q. alba* composites, indicating that the *A. cyclops* and *Q. alba* composites are more resistant to UV degradation. This is because they absorb most of the UV light due to the higher lignin and extractives content and hence most of the degradation occurs in the wood instead of the LLDPE matrix.

Figure 3.14 shows that the intensity of the carbonyl groups of the composites with 0% EVOH was higher than that of the same groups of the composites with 7% EVOH in Figure 3.13. This indicates that composites with 0% EVOH exhibited more degradation. This fact was supported by optical micrographs, as shown in Figure 3.15. It is a clear that composites with 0% EVOH in Figure 3.15 exhibited more cracks and degradation than composites with 7% EVOH in Figure 3.13.

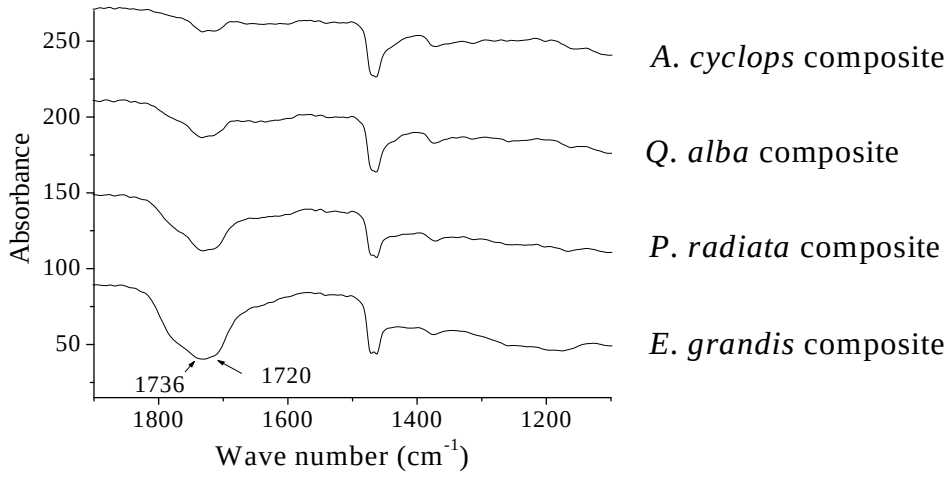

Figure 3.14 FTIR spectra of wood-LLDPE composites with 0% EVOH after exposure to UV for 99 days.

It should be noted here that the presence of wood in the polymer composites has no influence on the mechanism of POD of the host LLDPF. This, however, suggests that the presence of wood in polymer composites somehow delays or retards the photo-oxidation of the host polymer but does not change its photo-oxidation pathway. The same observation was made by Ndiaye et al. [65].

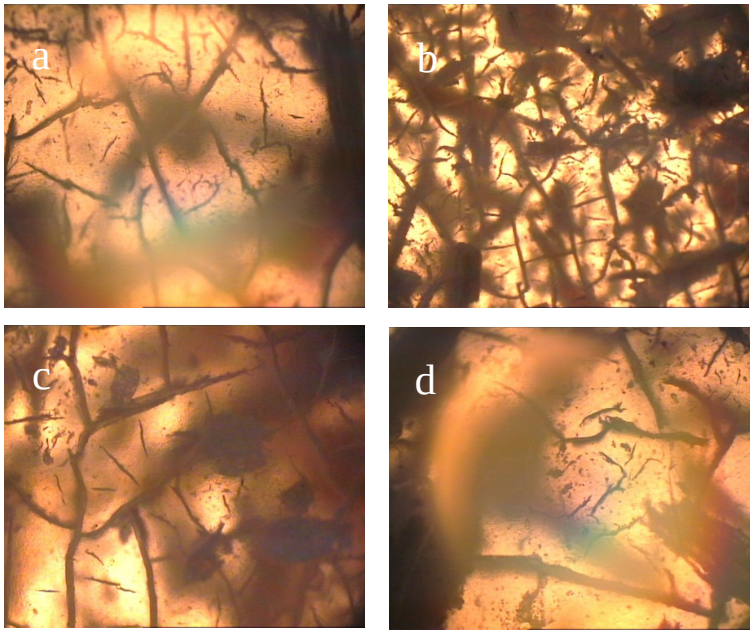

Figure 3.15 Optical micrographs of a) *A. cyclops*, b) *E. grandis*, c) *P. radiata* and d) *Q. alba* composites with 0% EVOH after exposure to UV for 99 days (Mag. 100x).

In summary, noncompatibilised composites had the poorest mechanical and thermal properties, highest WA and TS rates and lowest resistance to UV degradation compared to compatibilised composites. This is obviously due to the poor compatibility between nonpolar, hydrophobic LLDPE and the polar, hydrophilic wood particles. Most of these properties improved as the amount of compatibiliser was increased. Composites with 7% EVOH showed better properties than the other composites. *A. cyclops* composites generally exhibited better properties than *E. grandis*, *P. radiata* and *Q. alba* composites. Furthermore, although the amount of cellulose and the average particle lengths of *Q. alba* are somewhat greater than in *E. grandis* and *P. radiate* and similar to *A. cyclops*, the tensile strength properties of their composites were lower than that of *A. cyclops* composites.

All of these differences between the different wood-LLDPE composites are believed to be due to the difference in the compatibility and the adhesion at interfaces between the four species and LLDPE. Since these composites were prepared with the same types and amounts of LLDPE and EVOH, the differences in the compatibility between the four different species and LLDPE, via EVOH, are certainly due to the differences in the macromolecular composition and content of these species. Accordingly, the compatibility and interfacial adhesion between the four species and LLDPE, when using EVOH as compatibiliser were investigated. This will be discussed in the following chapter.

3.5 Conclusions

The effects of the macromolecular composition and content of the different wood species: *A. cyclops* (acacia), *E. grandis* (eucalyptus), *P. radiata* (pine) and *Q. alba* (oak) on the properties of wood-LLDPE composites when using EVOH as a compatibiliser were studied. 10% wood content and different amounts 0, 2, 5, 7 and 10% of EVOH were used. The following conclusions could be made:

1. The properties of all wood-LLDPE composites were improved when EVOH was added. This indicates that the effect of EVOH as a compatibiliser is significant.
2. Use of 7% EVOH led to composites with the most superior properties.
3. The macromolecular composition and content, particle lengths and aspect ratio of the different wood species were different and affected the WPC properties greatly.
4. In general, the hardwood species (*A. cyclops*, *E. grandis* and *Q. alba*) produce better wood-LLDPE composites than the softwood species (*P. radiata*) in terms of mechanical properties, thermal properties and resistance to UV degradation.
5. Superior mechanical properties such as tensile strength, elongation at break and MOE were achieved when wood from *A. cyclops* was used. Differences in these properties of the different woods are due to differences in the macromolecular composition and content and morphological properties between the four wood species. For example, higher cellulose and lignin contents benefit the mechanical properties of these composites.
6. Better thermal stability was achieved when wood with a higher cellulose and lignin content such as *A. cyclops* was used. The lower stability of wood at low temperatures can be attributed to a higher lignin and hemicelluloses content, while the high stability at low temperatures is due to a higher cellulose content. Lignin appears to play role even at high temperature because it is more heat resistant than cellulose and hemicelluloses.
7. A lower WA and TS rate in WPCs was achieved when wood from *P. radiata* was used. *P. radiata* is compactly bonded to the LLDPE via EVOH. It has fewer free hydroxyl groups than the other composites, due to its lower cellulose content. Higher cellulose and hemicelluloses contents, as in the case of *A. cyclops*, could lead to freer hydroxyl groups, which would affect WA and TS rate badly.
8. Water soluble extractives can have a negative effect on the WA and TS rate. This is because most of these extractives dissolve during the WA and TS tests. These extractives had a significant effect on the WA and TS rates of WPCs when *A. cyclops* and *Q. alba* were used, due to the higher amount of water extractives in these species.

9. The *A. cyclops* and *Q. Alba* composites had higher MI values than the other composites. This is also due to higher cellulose content in these species. The incorporation of different types of wood particles and the incorporation of EVOH into the LLDPE matrix did not badly affect the MI of composites and thereby making them suitable for processing.
10. *A. cyclops* species and their composites had the best resistance to UV degradation compared to other species and their composites. This is can be due to higher lignin and extractives contents. This is because lignin and some wood extractives are very good light absorbers.

A. cyclops appears to be very promising species to provide good WPC properties (with the exception of the WA) and performance (for use in the production of wood-LLDPE composites.

3.6 References

1. Mamunya Y., Zanoaga M., Myshak V., Tanasa F., Lebedev E., Grigoras C., Semynog V., Journal of Applied Polymer Science, 101, 1700-1710, 2006.
2. Rogers J., Simonsen J., Journal of Adhesion Science and Technology, 19, 975-985, 2005.
3. Berger M., Stark N., Investigations of Species Effects in an Injection-Moulding-Grade, Wood-Filled Polypropylene, Proceedings of the 4th International Conference on Woodfibre–Plastic Composites, Madison, 1997.
4. Saputra H., Simonsen J., Li K., Composite Interfaces, 11, 515-524, 2004.
5. Wolcott M., Production Methods and Platforms for Wood Plasticsm, Proceedings of the Non-Wood Substitute for Solid Wood Products Conference, Melbourne, Australia, 2003.
6. Clemons C., Stark N., Use of Salt Cedar and Utah Juniper as Fillers in Wood-Plastic Composites, Research Paper FPL-RP-641, USDA Forest Service, Forest Products Laboratory, Madison, 2007.
7. Kim J., Harper D., Taylor A., Journal of Applied Polymer Science, 112, 1378-1385, 2009.
8. Hristov V., Vasileva S., Macromolecular Materials and Engineering, 288, 798-806, 2003.
9. TAPPI test methods, T 264 om-88 and T 222 om-88, TAPPI Press, Atlanta, 1992.
10. Browning B., The Chemistry of Wood, 1st edition, Interscience Publishers, USA, 1963. 407.
11. Marcovich N., Villar, M., Journal of Applied Polymer Science, 90, 2775-2784, 2003.
12. Moly K., Radusch H., Androsh R., Bhagawan S., Thomas S., European Polymer Journal, 41, 1410-1419, 2005
13. Du W., Zhong W., Lin Y., Shen L., Du, Q., European Polymer Journal 40, 1987-1995, 2004.
14. Ha C., Ko M., Cho W., Polymer, 38, 1243-1246, 1997.
15. Lei Y., Wu Q., Yao F., Xu, Y., Composites: Part A, 38, 1664-1674, 2007.
16. Genet M., Stokes A., Salin F., Mickovski S., Thierry F., François D., Rens B., Plant and Soil, 278, 1-9, 2005.
17. Bledzki A., Gassan J., Theis S., Mechanics of Composite Materials, 34, 563-568, 1998.
18. Bledzki K., Gassan J., Progress in Polymer Science, 24: 221-274, 1999.
19. Yang H., Kim J., Park J., Lee J., Hwang S., Composite Structures, 72: 429-437, 2006.
20. Karina M., Onggo H., Syampurwadi A., Journal of Biological Science, 7, 393-396, 2007.
21. Karmarkar A., Chauhan S., Modak M., Chanda M., Composites: Part A, 38, 227-233, 2007.
22. Georgopoulos S., Tarantili P., Avgerinos E., Andreopoulos A., Koukios E., Polymer Degradation and Stability, 90, 303-312, 2005.
23. Şolpan D., Güven, O., Radiation Physics and Chemistry, 54, 583-591. 1999.

24. Caraschia J., Leãob A., Materials Research, 5, 405-409, 2002.
25. Shane B., Elvy B., Dennis G., Ng L., Journal of Materials Processing Technology, 48, 365-372, 1995.
26. Elvy B., Dennis R., Ng, T., Journal of Materials Processing Technology, 48, 365-372, 1995.
27. Yap S., Chin L., Teoh, L., Journal of Wood Chemistry and Technology, 10, 1-19, 1990.
28. Rahman R., Huque M., Islam N., Hasan M., Composites: Part A, 39, 1739-1747, 2008.
29. Tze Y., Wang S., Rials G., Pharr M., Kelley, S., Composites: Part A, 38, 945-953, 2007.
30. Hansson L., Antti A., Journal of Materials Processing Technology, 171, 467-470, 2006.
31. Kwiatkowska W., Starzycki M., Zebrowski J., Oszmiański J., Szopa, J., Journal of Biotechnology, 128, 919-934, 2007.
32. Obataya E., Norimoto M., Gril, J., Polymer, 39, 3059-3064, 1998.
33. Kim H., Kim S., Kim H., Yang H., Thermochimica Acta, 451, 181-188, 2006.
34. Doh G., Lee A., Kang I., Kong Y., Composites Structure, 68, 103-108, 2005.
35. Mengeloglu F., Kabakci, A., International Journal of Molecular Sciences, 9, 107-119, 2008.
36. Sui G., Fuqua M., Ulven C., Zhong, W., Bioresource Technology, 100, 1246-1251, 2009.
37. Espert A., Camacho W., Karlson S., Journal of Applied Polymer Science, 89, 2353-2360, 2003.
38. Sailiaja R., Composites Science and Technology, 66, 2039-2048, 2006.
39. Adhikary K., Pang S., Staiger M., Chemical Engineering Journal, 39, 190-198, 2008.
40. Sailiaja R., Composites Science and Technology, 66, 2039-2048, 2006.
41. Harper D., Wolcott, M., Composites: Part A, 35: 385-394, 2004.
42. Gröndahl M., Teleman A., Gatenholm P., Carbohydrate Polymyers, 52, 359-366, 2003.
43. Mészáros E., Jakab E., Várhegyi G., Journal of Analytical and Applied Pyrolysis, 79, 61-70, 2007.
44. Tserki V., Matzinos P., Kokkou S., Panayioyou C., Composites: Part A, 36, 965-974, 2005.
45. Ichazo M., Albano C., González J., Perera R., Candal M., Composite Structures, 54, 207-214, 2001.
46. Beg M., Pickering K., Composites: Part A, 39, 1565-1571, 2008.
47. Naik J., Mishra S., Polymer-Plastics Technology and Engineering, 45, 923-927, 2006.
48. Huang H., Zhang J., Journal of Applied Polymer Science, 111, 2806-2812, 2009.
49. Maiti S., Hassan M., Journal of Applied Polymer Science, 37, 2019-2032, 1989.
50. Mishra S., Naik J., Journal of Applied Polymer Science, 68, 681-686, 1998.
51. Maiti S., Mahapatro P., Polymer Composites, 9, 291-296, 2004.
52. Li T., Wolcott M., Composites: Part A, 35, 303-311, 2004.
53. Hristov V., Takács E., Vlachopoulos J., Polymer Engineering and Science, 46, 1204-1214, 2006.
54. Lu X., Zhang M., Rong M., Shi G., Yang, G., Composites Science and Technology, 63, 177-186, 2003.
55. Migneault S., Koubaa A., Erchiqui F., Chaala A., Englund K., Wolcott, M., Composites: Part A, 40, 80-85, 2009.
56. Joseph K., Filho R., James B., Thomas S., de Carvalho L., Revista Brasileira de Engenharia Agrícola e Ambiental, 3, 367-379, 1999.
57. Migneault S., Koubaa A., Erchiqui F., Chaala A., Englund K., Krause C., Wolcott M., Journal of Applied Polymer Science, 110, 1085-1092, 2008.
58. Xanthos M., Functional Fillers for Plastics, 1st edition, Wiley-VCH Verlag, Germany, 2005. 251.
59. Rowell R., The Chemistry of Solid Wood, 1st edition, American Chemical Society, USA, 1984. 229-446.
60. Naddeo C., Guadagno L., Vittoria, V., Polymer Degradation and Stability, 85, 1009-1013, 2004.
61. Zahri S., Belloncle C., Charrier F., Pardon P., Quideau S., Charrier, B., Applied Surface Science, 253, 4985-4989, 2007.
62. Pandey K., Polymer Degradation and Stability, 87, 375-379, 2005.

63. Salvalaggio M., Bagatin R., Fornaroli M., Fanutti S., Palmery S., Battistel, E., Polymer Degradation and Stability, 91, 2775-2785, 2006.
64. Roy P., Surekha P., Rajagopal C., Chatterjee S., Choudhary V., Polymer Degradation and Stability, 92, 1151-1160, 2007.
65. Ndiaye D., Fanton E., Therias S., Vidal L., Tidjani A., Gardette J., Composites Science and Technology, 68, 2779-2784, 2008.

Chapter 4
Compatibility of different wood species and LLDPE with EVOH as the compatibilizer

Abstract

Due to the difference in the properties of *A. cyclops*-LLDPE, *E. grandis*-LLDPE, *P. radiata*-LLDPE and *Q. alba*-LLDPE composites, as shown in Chapter 3, the compatibility and adhesion properties between the four species and LLDPE were studied. This is because any deficiency in the compatibility and interfacial adhesion can be the reason for inferior mechanical and thermal properties of WPCs. The compatibility and adhesion properties were studied with scanning electron microscopy (SEM), OM, FTIR, DMA and TGA. An EVOH content of 7% was found to be optimum; larger amounts of EVOH resulted in declining properties. *A. cyclops*-LLDPE composites generally showed better compatibility and adhesion properties compared to the other wood-LLDPE composites.

Keywords: *WPCs, compatibility, interface adhesion, fracture surface*

4.1 Introduction

In order to fully understand the main results reported in Chapter 3, namely the following: (1) the weaker properties of *E. grandis*, *P. radiata* and *Q. alba* composites in comparison to those of *A. cyclops* composites, (2) 7% EVOH being the optimum amount of compatibiliser that led to the production of wood-LLDPE composites with superior properties and (3) the weaker tensile strength properties of *Q. alba* composites in comparison to *A. cyclops* composites, although both species have higher cellulose content and almost the same average particle length (comparison to *E. grandis* and *P. radiata* composites). These composites needed to be further evaluated. The difference in the compatibility and interfacial adhesion are believed to be the reasons for inferior mechanical and thermal properties of these composites.

The first important factor in the production of acceptable WPCs is good compatibility between wood and the polymer matrix [1]. Mechanical properties [2] and thermal stability [3] of WPCs are strongly influenced by the compatibility and interfacial adhesion between the wood and polymer. For example, to improve the mechanical strength of composites, good interfacial adhesion between the matrix and wood particles is essential to transfer stress from the matrix to the wood particles [4]. On the other hand, poor compatibility and interfacial adhesion between wood and the polymer matrix can lead to the formation of voids, which in

turn causes an increase in the WA and TS rates of a WPC [5]. This, however, has a negative effect on mechanical and physical properties [6-7].

This chapter reports on the differences in compatibility and interfacial adhesion between the four wood species and LLDPE when using 0, 2, 5, 7 and 10% EVOH as a compatibiliser. It is obvious that a careful selection of compatibilisers and optimisation is needed in order to produce WPCs with acceptable properties and performance [8].

4.2 Experimental

The same materials and methods described in Chapter 3 (Section 3.2) for the preparation of the different wood-LLDPE composites and making films from these composites for use in certain testing procedures were also used in this part of the study.

4.3 Characterisation

EZ4D microscope (Section 3.3.6), FTIR (Section 3.3.8), DMA (Section 3.3.2) and TGA (Section 3.3.3) were used. A Leo® 1430VP SEM was used to study the morphology of the composites before and after quenching them in liquid nitrogen and breaking them to create a fracture surface. The samples were sputtered-coated with gold before analysis. In the case of DMA, the compression mode was used to determine the tan δ and E'. Tan δ and E′ can be used to provide information about the compatibility and interfacial adhesion in the composite systems [8-11]. Tan δ and E′ of the LLDPE and wood-LLDPE composites with 7% EVOH were determined as a function of temperature. The temperature ranges were -140 to 130 ^{o}C. A scanning rate of 5 ^{o}C/min was used.

4.4 Results and discussion

4.4.1 Morphology and compatibilisation

The four noncompatibilised composites showed poor compatibility and weak adhesion between the wood and LLDPE matrix. They displayed a rough morphology with many voids or holes, as shown in Figure 4.1 (see the circles). This can be attributed to the incompatibility and weak adhesion between the hydrophilic wood and hydrophobic LLDPE as discussed in Section 2.2.1.4. This means that the wood particles of the four wood species were not able to bond effectively with LLDPE without the use of compatibilisers, resulting in weaker interphases, the formation of voids, and consequently undesirable properties, as reported in Chapter 3. Similar findings were also reported by others [12-15]. The wood particles appear to form aggregates in the absence of EVOH in the cases of *A. cyclops, E. grandis* and *Q. alba* composites. This can be seen in Figures 4.1a, 4.1b and 4.1d (see the arrows). This is most likely due to the cellulose content. The hydroxyl groups of cellulose on the surface of *A.*

cyclops, *E. grandis* and *Q. alba* species form hydrogen bonds and attract each other [16-17]. The tendency of wood to form aggregates can be due to a high intramolecular bonding among the wood particles [16]. The *P. radiata* composite appeared not to form aggregates due to its lower cellulose content in comparison to the other species, as shown in Table 3.1 (Section 3.4.1).

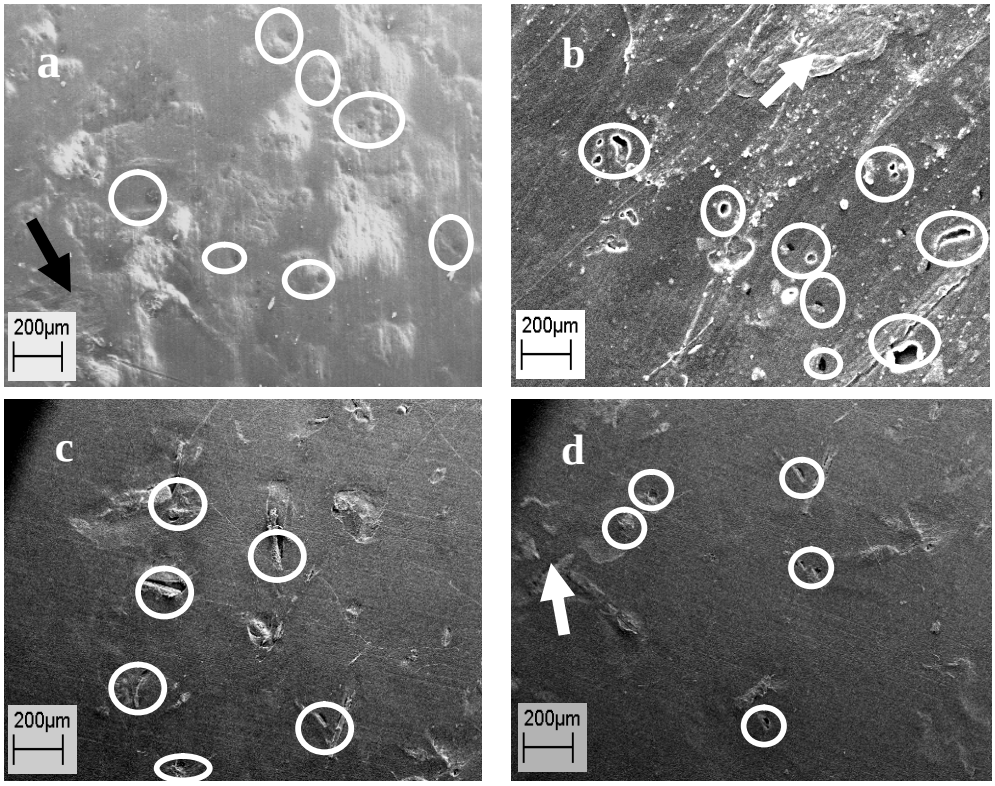

Figure 4.1 SEM images of wood-LLDPE composites with 0% EVOH of a) *A. cyclops*, b) *E. grandis*, c) *P. radiata* and d) *Q. alba* (Mag. 30x).

Fewer voids (as shown in Figures 4.2 and 4.3 (see the circles)) and aggregations (as shown in Figures 4.4 (see the circles)) were observed in all the wood-LLDPE composites with 2 and 5% EVOH, while hardly any voids were observed in composites with 7% EVOH, as shown in Figure 4.5. Hence the EVOH had significant effects on the compatibility of these composites.

Compatibility and interfacial adhesion between the four wood species and LLDPE matrix were improved by the addition of EVOH, thereby resulting in improved properties, as observed in Chapter 3. This is because EVOH forms linkages between the wood and LLDPE. WPC properties can be improved by using compatibilisers and via the enhanced adhesion between the components and the improvement of the nature of the matrix-filler interface [11, 18]. Although some authors believe that the aggregation of wood can be formed only at high filler content [19-21], others have reported the formation of wood aggregates in WPCs with 10% and 20% WF content [22-23]. It is believed that the probability for the aggregates to form increases with increasing wood content.

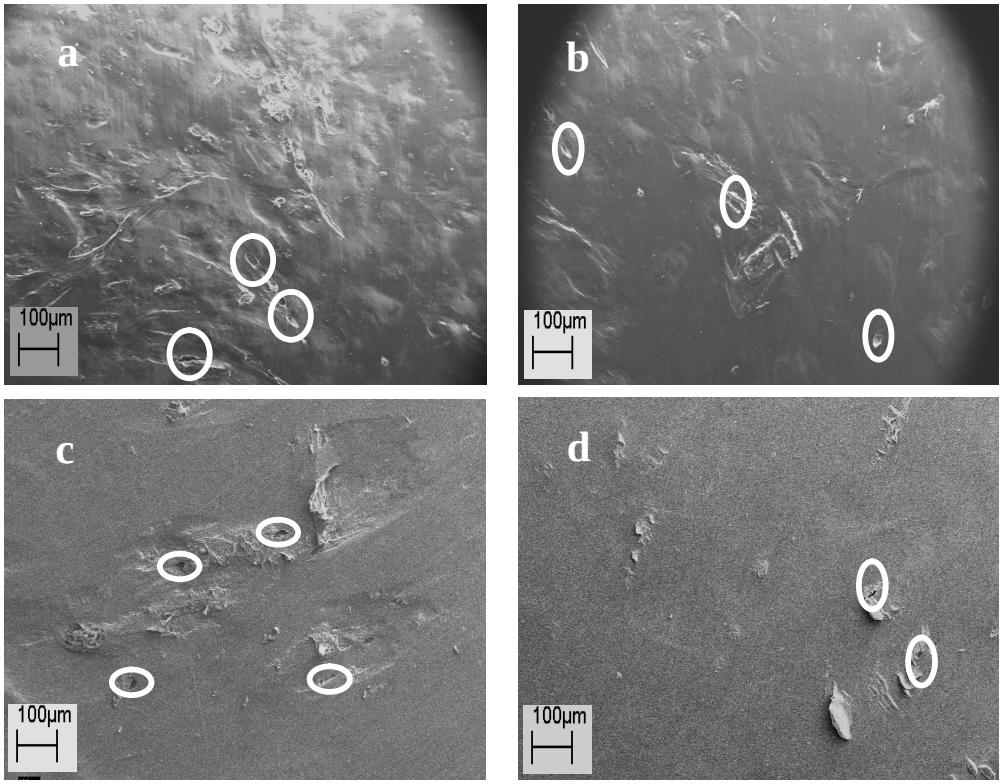

Figure 4.2 SEM images of wood-LLDPE composites with 2% EVOH of a) *A. cyclops,* b) *E. grandis,* c) *P. radiata* and d) *Q. alba* (Mag. 50x).

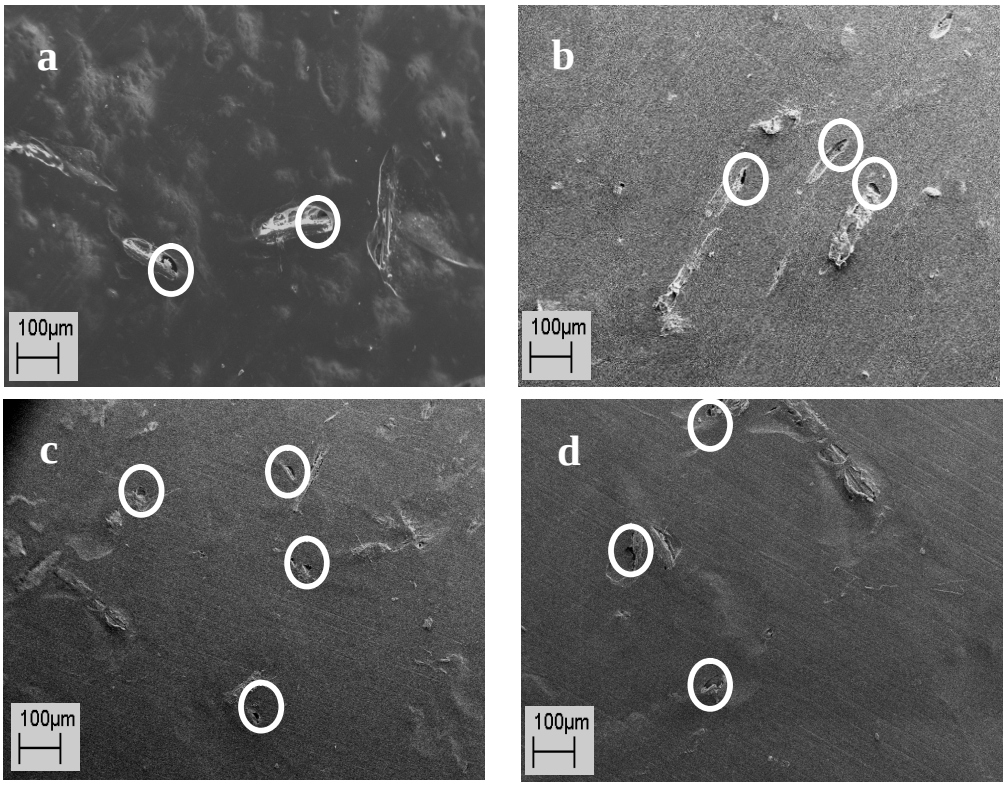

Figure 4.3 SEM images of wood-LLDPE composites with 5% EVOH of a) *A. cyclops,* b) *E. grandis,* c) *P. radiata* and d) *Q. alba* (Mag. 50x).

In this study, aggregates were formed in some composites with 2 and 5% EVOH, as shown in Figure 4.4 (see the circles). The amounts of 2 and 5% EVOH are still not adequate to impart sufficient compatibility between the wood particles and LLDPE, although some improvement in the properties of these composites are observed over noncompatibilised composites, as found in Chapter 3. Aggregates can be due to insufficient mixing. It is difficult or even impossible to determine the size and the distribution of these aggregates. These aggregates act more like a discontinuity within the matrix structure rather than as a reinforcing material. However, these aggregates can be considered as a contributing factor for weakening the mechanical properties of WPCs [24]. This may explain the weaker properties of wood-LLDPE composites with 2 and 5% EVOH content that were obtained in Chapter 3.

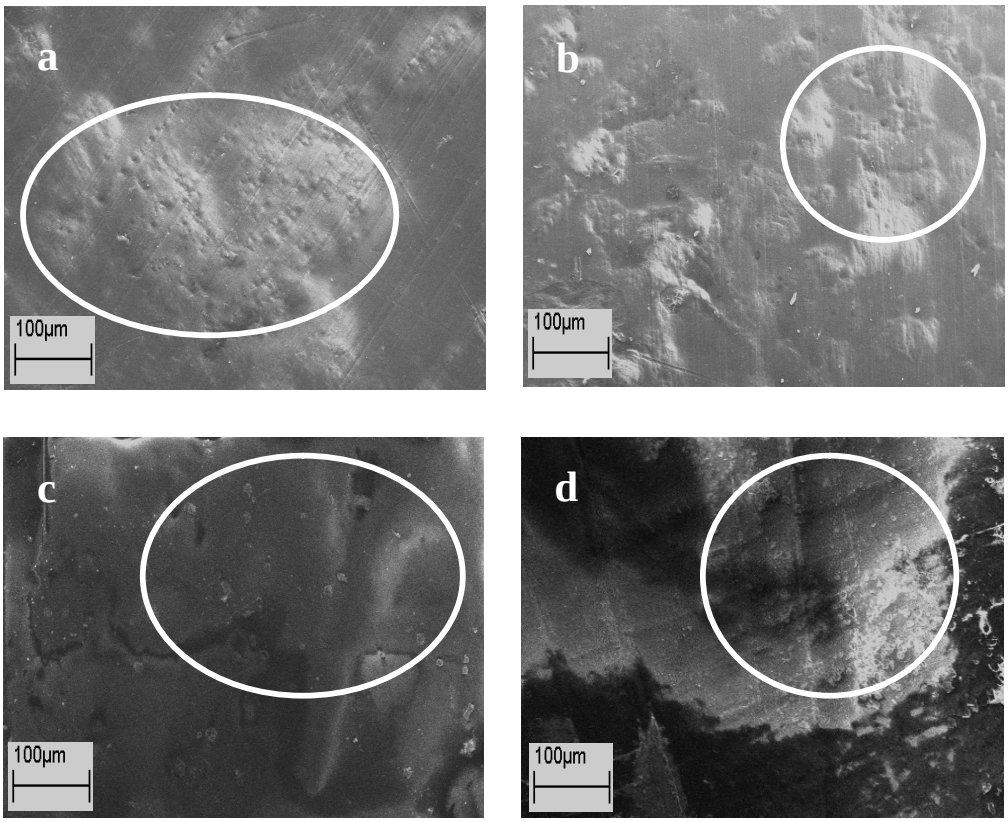

Figure 4.4 SEM images showing the aggregation of wood in composites of a) *A. cyclops* with 5% EVOH, b) *E. grandis* with 5% EVOH, c) *P. radiata* with 5% EVOH and d) *Q. alba* with 2% EVOH (Mag. 500x).

Wood-LLDPE composites with 7% EVOH displayed better morphology with no voids, as shown in Figure 4.5. This can be attributed to the better compatibility and strong adhesion between the wood and LLDPE via EVOH. The use of 7% of EVOH changed the morphology and produced a more homogenous surface with fewer or no voids. This is why the wood-LLDPE composites with 7% EVOH had better properties and performance than others, as described in Chapter 3.

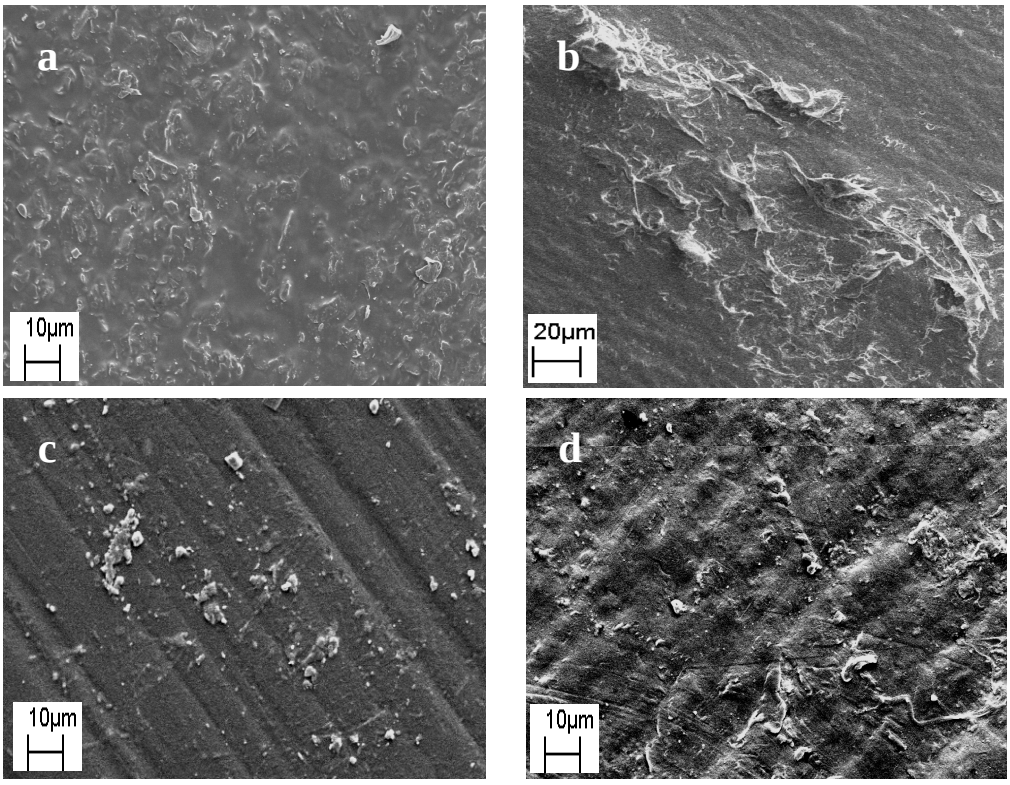

Figure 4.5 SEM images of wood-LLDPE composites with 7% EVOH of a) *A. cyclops*, b) *E. grandis*, c) *P. radiata* and d) *Q. alba* (Mag. 400x).

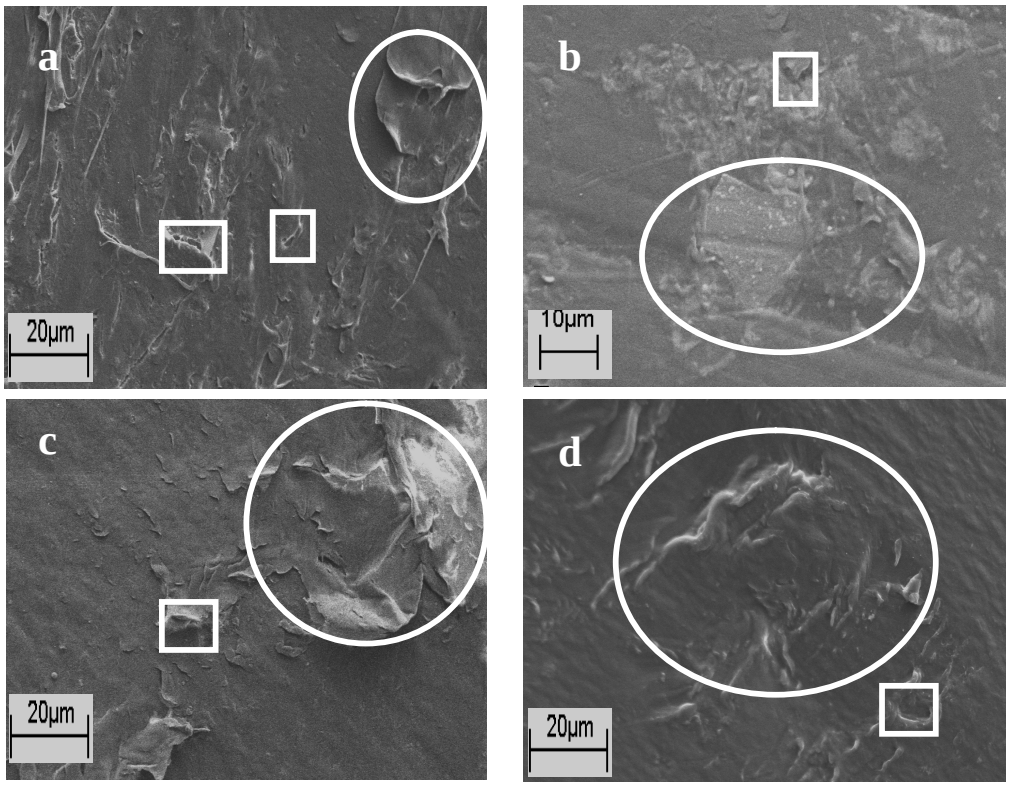

Figure 4.6 SEM micrographs of wood-LLDPE composites with 10% EVOH of a) *A. cyclops*, b) *E. grandis*, c) *P. radiata* and d) *Q. alba* (Mag. 400x).

Increasing the content of EVOH to up 10% reduced the compatibility and negatively affected the adhesion between the wood particles and LLDPE matrix. As shown in Figure 4.6, aggregation of wood (see the circles) and some voids (see the rectangles) were formed. When too high concentrations of compatibiliser are added, it not only clusters around the wood but also tends to form a separate phase within the polymer matrix. This leads to the formation of wood bundles or aggregates, which in turn leads to the formation of voids, which results in a significant deterioration of the mechanical properties of the WPCs. For this reason, the properties of wood-LLDPE composites were reduced when 10% EVOH was added, as resulted in Chapter 3. Similar observations were made by Hristov et al. [25].

While it is difficult or even impossible to draw definite conclusions or obtain full information about the difference in the compatibility between the four wood particles and LLDPE via EVOH by simply looking at the above SEM images, it is clear that the addition of EVOH as a compatibiliser is of crucial importance. As with any composite, the compatibility of the components being mixed is of key importance for dispersion of the wood particles as well as for creating strong interfaces in the composite. Hence the significant improvements in the properties of wood-LLDPE composites as reported in Chapter 3 are due to the compatibilisation effect. The compatibility and interfacial bonding between the wood particles and the LLDPE matrix were improved when EVOH was added. The optimum concentration of EVOH is 7%, which led to the production of composites with superior properties. Although the optimum concentration of EVOH was the same in the four wood-LLDPE composites, the degree of improvement in the properties was different, and it varied between these composites. It is important to emphasise once again that a careful selection of compatibiliser and optimisation of the amount is required in order to produce WPC with good compatibility, better adhesion properties and superior mechanical performance [25]. According to Klyosov [26] it is very important to understand that not simply adding the correct amount of compatibiliser will improve the properties of the WPCs. It is also important to highlight the significance of optimizing the manufacturing conditions, as well as the other additives in the formulation of the composites.

4.4.2 Fracture surface

The difference in the compatibility and adhesion between wood-LLDPE composites was investigated by looking at SEM images taken from the fractured surface after quenching the composites containing 7% EVOH in liquid nitrogen, as shown in Figure 4.7. These micrographs showed that there were no voids at the interface between the LLDPE and the *A. cyclops* and *Q. alba* particles (Figure 4.7a and 4.7d), while some voids are visible between the

matrix and the *E. grandis* and *P. radiata* particles (Figure 4.7b and 4.7c). This suggest that the adhesion between the LLDPE matrix and the *A. cyclops* and *Q. alba* particles via EVOH was better than between LLDPE and *E. grandis* and *P. radiata* particles. Furthermore, the cracks observed in the wood particle (Figures 4.7a and 4.7d) are good evidence for the strong adhesion between the LLDPE matrix and the wood [27-28].

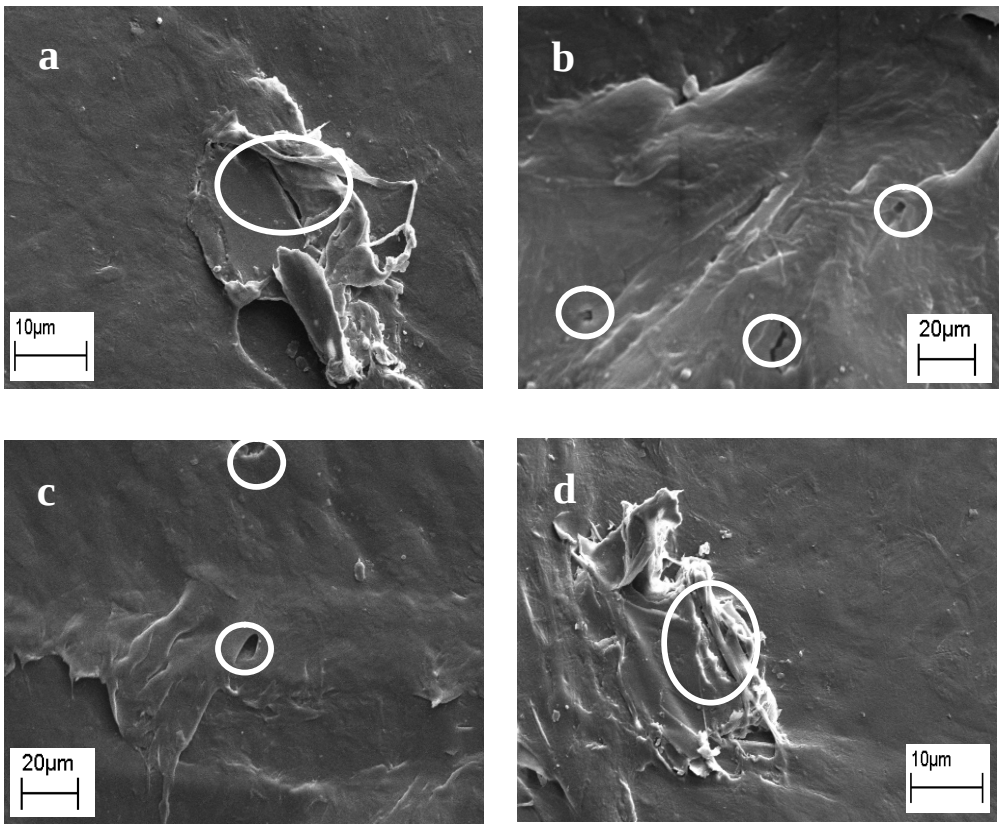

Figure 4.7 SEM micrographs of fractured surfaces of wood-LLDPE composites with 7% EVOH of a) *A. cyclops*, b) *E. grandis*, c) *P. radiata* and d) *Q. alba* (Mag. 1000x).

Good interfacial adhesion is favourable to the stress transfer across the interface [29]. For *E. grandis* and *P. radiata* composites it was difficult to see any cracks in the wood particles because the surfaces appeared to be covered by LLDPE. However, the difference in the stress transfer at the interfaces between the different wood particles and LLDPE matrix is based on the degree of adhesion [30]. On the other hand, the lignin and hemicelluloses may have hindered the efficiency of stress transfer between matrix and wood particles [31]. Lignin and hemicelluloses play an important role in binding the cellulose fibrils that allows efficient stress transfer to the cellulose molecules [32]. EVOH appears to facilitate efficient stress transfer at the interface between the wood and polymer matrix. This explanation can be supported by the general concepts and information described in literature regarding to the effect of compatibiliser on the WPC system [30, 33-37].

The difference in the adhesion between the LLDPE matrix and the four wood species can be explained by the varying cellulose content. As stated in Section 2.2.1.4, wood with a higher cellulose content contains more hydroxyl groups at the surface, which in turn promotes stronger interaction and better interfacial adhesion between the wood and the LLDPE matrix, via EVOH, than wood with a lower cellulose content. According to Qin et al. [34], a low cellulose concentration effectively prevents good stress transfer between the wood particles and matrix, and leads to inferior properties. According to Sawyer and Grubb [38] the lack of wood to polymer bonding can result in a decrease in the stress transfer from the polymer to the wood particle and limit reinforcement. According to Dányádi et al. [20] a larger number of bonds between wood and matrix can lead to better stress transfer.

In conclusion, the better compatibility and interfacial adhesion of composites with 7% EVOH in comparison with the other composites (composites with different percentage of EVOH) is due to the absence of wood aggregates. In the cases of composites with 0, 2, 5 and 10% EVOH the wood aggregates made the composites non-homogeneous (see Figures 4.1, 4.4 and 4.6), which then led to a difficulty for stress transfer from the matrix to the wood particles [39]. A similar explanation was given by Levita et al. [40].

4.4.3 Wood particle size

Information on the average particle lengths and minimum and maximum particle length of the four wood species is tabulated in Table 4.1 and showing in Figure 4.8. This is important because the effectiveness of fibre reinforcement is dependent on the particle length [41]. Although there is very little information on the effect of particle length on the physical properties of WPCs, results obtained by Migneault et al. [42] indicate that particle length has a significant effect on the properties of WPCs.

Table 4.1 Morphological properties of the wood particles

Composite	Minimum particle length, mm	Maximum particle length, mm	Average particle length, mm	SD[a] of average particle length, mm
A. cyclops	0.045	1.309	0.225	0.157
E. grandis	0.019	0.741	0.186	0.118
P. radiata	0.022	0.730	0.142	0.135
Q. alba	0.005	0.821	0.229	0.176

[a] SD standard deviation

The four wood species had markedly different average particle lengths. *A. cyclops* has a lower average particle size than the other species. The greatest variation in the particle lengths was

observed for *P. radiata* and *E. grandis*, as indicated by the cumulative counts curves in Figure 4.8. The cumulative average particle lengths are derived by software integration.

It was difficult to determine the correct wood particle size (based on the length, width and thickness) due to their method of preparation. Since these species were comminuted to a particle diameter of about 180 μm, and since particles with greater length should have a larger size, particle length will be referred here to as particle size.

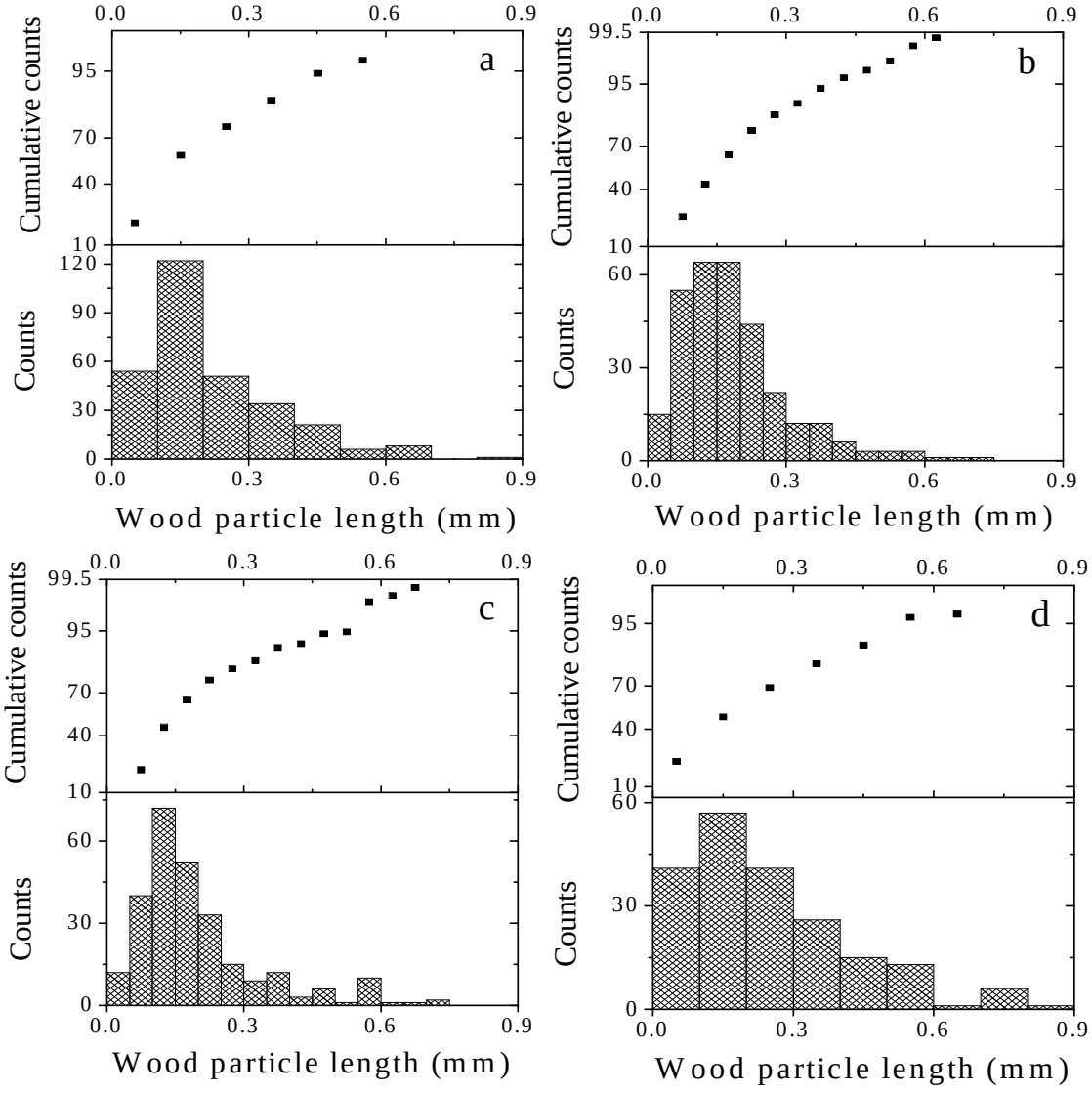

Figure 4.8 Histograms of particle lengths and cumulative average particle lengths for a) *A. cyclops*, b) *E. grandis*, c) *P. radiata* and d) *Q. alba*.

The majority (about 40%) of *A. cyclops* particles had a length or size of 0.15 mm. About 40% of *A. cyclops* particles were having size between 0.2-0.5 mm. The majority of *E. grandis* particles had a size of 0.125 (about 20%) and 0.175 mm (about 20%). About 32% of *E. grandis* particles had a size of 0.2-0.5 mm. The majority (about 27%) of *P. radiata* had a size

of 0.125 mm. Approximately 29% of *P. radiata* particles had particles with sizes varied of 0.2-0.5 mm. The majority which is about 35% of *Q. alba* particles were having size of 0.15 mm. 40% of *Q. alba* particles showed to have size between 0.2-0.5 mm. *A. cyclops*, *E. grandis* and *P. radiata* and *Q. alba* were having about 5, 3, 6 and 10% particles with size of > 0.5 mm. Hence, it is difficult to conclusions about the effect of the above differences in the particle size of the four species on the compatibility and final properties of the composites. However, wood particles with size of 0.24-0.50 mm are preferable [43].

Although the amount of cellulose and the average particle size of *Q. alba* are somewhat higher than in *E. grandis* and *P. radiata*, the tensile strength properties of the *Q. alba* composites do not differ greatly. It must be noted here that fillers with the same average particle size can have widely differing distributions, and it is the distribution that is generally more important in determining the effects in polymer composites [44]. The lower strength of *Q. alba* composites is probably due to the presence of voids. The very small particles of *Q. alba* (see the minimum particle size of *Q. alba* in Table 4.1) provide imperfect surface area, and probably imperfect edges or interfaces at the boundaries with the LLDPE matrix. This is because the size of the contact surface area between the LLDPE and the *Q. alba* particles via EVOH is not suitable.

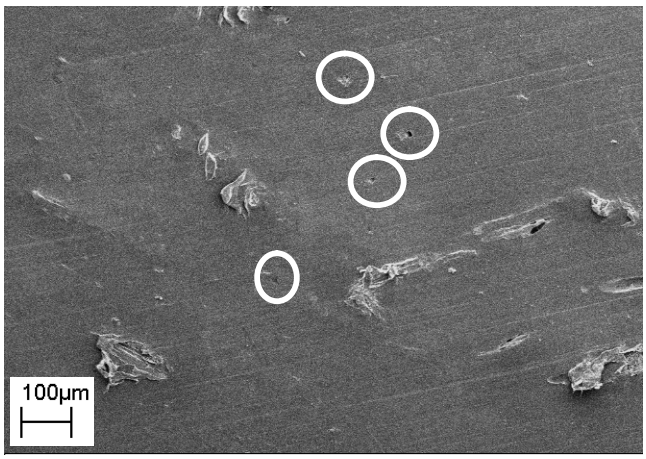

Figure 4.9 SEM micrograph of the *Q. alba* composite with 7% EVOH (Mag. 50x).

It is known that the specific surface area, which depends on the average particle size of the filler, determines the size of the contact surface between the polymer and the filler [45]. As a result, the ends of *Q. alba* particles are debonded from the matrix, leading to the formation of voids. This in turn decreases the interfacial adhesion between *Q. alba* particles and the LLDPE matrix via EVOH compared to e.g. *A. cyclops* particles. A similar finding was reported by Prachayawarakorn et al. [46]. Dányádi et al. [20] mention that very small particles induce the separation or debonding at the interfaces. However, the formation of voids in the

Q. alba composite due to the incorporation of too small particles in the LLDPE matrix could be confirmed by SEM (Figure 4.9).

4.4.4 FTIR analysis

FTIR spectra of the LLDPE, EVOH, the four wood species and the four wood-LLDPE composites with 7% EVOH content are shown in Figure 4.10. IR spectroscopy has been used particularly to investigate the formation of hydrogen bonding and predict the compatibility and miscibility of polymer blends [47-49]. Figure 4.10b shows the major changes caused by the incorporation of wood into the LLDPE matrix via 7% EVOH, changes occurred in the region 3700-3250 cm^{-1} (centred at 3344-3405 cm^{-1}). The bands in this region are all due to hydroxyl stretching motions of EVOH and cellulose. Figure 4.10a shows that these absorption bands are broad in the wood spectra, due to a wide distribution of hydrogen bonded hydroxyl groups in wood (self association) [50]. These absorption bands were slightly shifted to higher wavenumbers after blending the WPCs (centred at 3372-3508 cm^{-1}), as shown in Figure 4.10b. The small shift of these bands can be an indication of the formation of new hydrogen bonds [51-52].

According to Kim et al. [50] the shift in the hydroxyl bands can be explained by the new distribution of hydrogen bonded moieties resulting from the competition of interactions between hydroxyl groups of the wood and the compatibiliser. Besides a decrease in the intensity, these absorption bands also became broader, due to the incorporation of wood and EVOH into the LLDPE matrix.

The intensities of the absorption bands of the *A. cyclops* and *Q. alba* composites are lower and broader than those of the *E. grandis* and *P. radiata* composites. This is due to the larger number of hydrogen bonds formed in A. *cyclops* and *Q. alba* composites [21]. The absorption bands of *A. cyclops* and *Q. alba* composites have the same intensity in this region and overlap (they appear as one band in the top of the small spectra in Figure 4.10b). This may indicate that wood particles with sizes of 0.2-0.5 mm are preferable when using EVOH as a compatibiliser. Both these species had the same percentage of particles with sizes 0.2-0.5 mm. Consequently, the higher cellulose content and the presence of a higher percentage of particles with sizes 0.2-0.5 mm in *A. cyclops* and *Q. alba* provide more reactive hydroxyl groups situated on the cellulosic fibre surface, which promotes strong interactions and more hydrogen bonds between the polymer matrix and wood via the EVOH. The hydroxyl groups of EVOH promote more hydrogen bonds with the hydroxyl groups on the surface of the cellulose, while the nonpolar part (ethylene part) of the EVOH interacts with the LLDPE matrix [6].

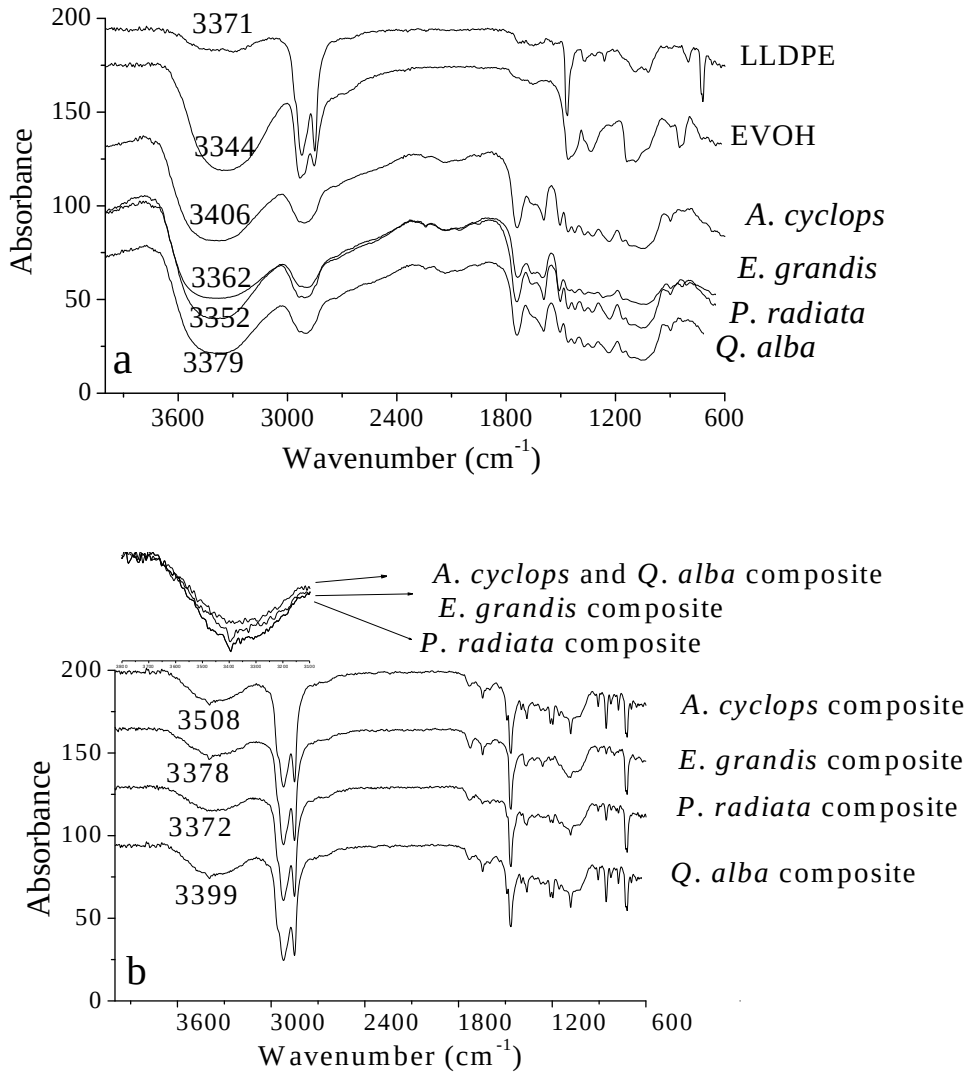

Figure 4.10 FTIR spectra of a) LLDPE, EVOH, and the four wood species, and b) the four wood-LLDPE composites with 7% EVOH.

According to the results in Sections 4.4.3 and 4.4.4 it is concluded that the inferior properties of *Q. alba* composites are due to the presence of very small particle sizes (Figure 4.9), and to oversized particles (> 0.5 mm). Larger particles debond easily under the effect of an external load [52]. A similar trend has been observed in the case of mineral fillers. It has been reported that the presence of small amounts of oversized particles in a polymer matrix can cause a significant reduction in toughness [44].

4.4.5 Dynamic mechanical properties

The temperature dependence of tan δ and E′ for LLDPE and wood-LLDPE composites with 7% EVOH is presented in Figures 4.11 and 4.12. With increasing temperature, tan δ values of LLDPE and wood-LLDPE increased due to the increased polymer chain mobility of the matrix, as shown in Figure 4.11. LLDPE and all wood-LLDPE composites with 7% EVOH

show very weak traces of α-transition between 75 to 100 °C. As shown in Table 4.2, the γ-transition and β-transition of wood-LLDPE composites with 7% EVOH were observed at slightly higher temperature in comparison to virgin LLDPE. This shift to higher temperature can be an indication of the presence of new processes that have restricted the mobility of chains in the crystalline region. Then more energy is required for these transitions to occur. This, however, indicates better interfacial interaction between wood and LLDPE via EVOH at the interface [9]. This better interfacial interaction appears to be more pronounced in *A. cyclops* composites than in *Q. alba*, *E. grandis* and *P. radiata* composites, respectively. This is because the γ-transition and β-transition of *A. cyclops* composites showed a larger shift toward higher temperature than others.

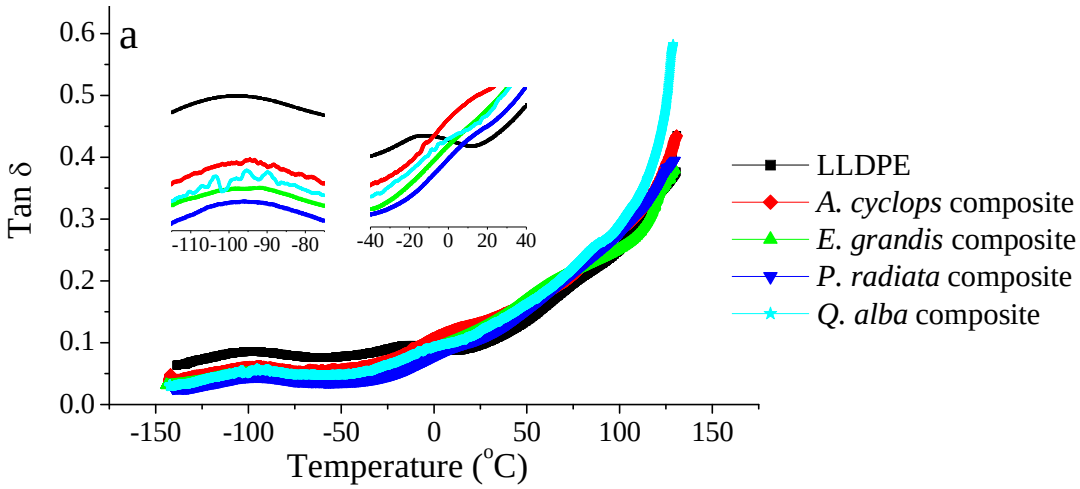

Figure 4.11 Temperature dependence of tan δ of LLDPE and different composites with 7% EVOH.

Table 4.2 Summary of tan δ peak temperature at γ- and β-transitions

Composite	Tan δ peak temperature at γ-transition or T_g, °C	Tan δ at peak temperature β-transition, °C
LLDPE	-100.3	-12.1
A. cyclops	-94.2	-01.5
E. grandis	-97.8	-07.4
P. radiata	-98.1	-08.0
Q. alba	-95.4	-04.9

The E′ values of LLDPE and the four composites significantly decreased with increasing temperature due to the increase in the polymer chain mobility of the matrix, as shown in Figure 4.12. As can be seen in this figure, the incorporation of different wood species into the LLDPE matrix in the presence of 7% EVOH resulted in a remarkable increase in the E′, especially at higher temperature. This enhanced stiffness of the composites can be attributed

to the improved compatibility between matrix and wood particle [35-36]. According to Kim et al. [9] this increase in the stiffness of LLDPE is due to the reinforcing effect imparted by different wood species. This seems to be more noticeable in the case of the *A. cyclops*. *A. cyclops* composite appears to have a higher E′, while slight difference between the E′ of the *E. grandis*, *P. radiata* and *Q. alba* composites was observed, especially at low temperature range. It can also be seen that as the composites go through higher temperature, the difference between *A. cyclops* and other composites becomes negligible. The difference in E′ values is due to the difference in the compatibility, which is due to the difference in the macromolecular composition and content of the wood species, since the amount and type of LLDPE and EVOH are the same in all these composites.

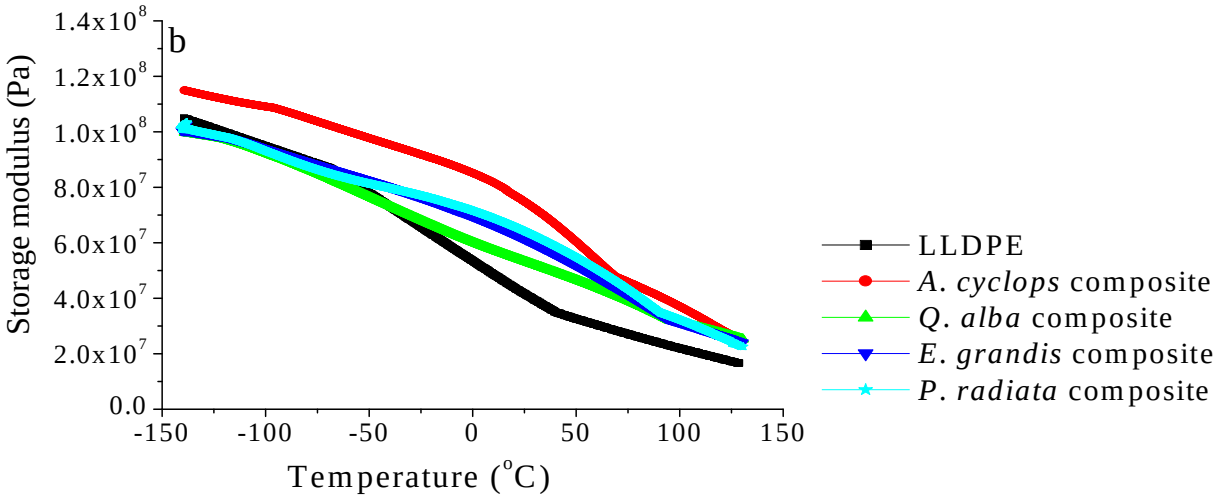

Figure 4.12 Temperature dependence of E′ of LLDPE and composites with 7% EVOH.

4.4.6 Thermal stability

Many authors [6, 9, 53] have attributed the improvement in thermal stability of WPCs to the enhanced adhesion between the polymer matrix and wood particles caused by the compatibiliser. The differences in the decomposition temperatures between the composites in Table 3.7 confirmed these findings. First, better compatibility and adhesion are achieved when a compatibiliser is added. The improved thermal stability of the composites with EVOH is due to the enhanced interfacial adhesion and additional intermolecular bonding between wood particle and polymer matrix that result from EVOH [6, 9]. For this reason, compatibilised composites showed better mechanical properties than noncompatibilised composites. Second, the highest thermal stability was observed in the composites with 7% EVOH. This results in accordance with the morphological observations. Indications are that a 7% EVOH content can be considered the optimum amount of compatibiliser for improving the compatibility and interfacial adhesion in these composites. Finally, the best compatibility

between LLDPE and wood particles was obtained in *A. cyclops* composites, as also highlighted by the better thermal stability of *A. cyclops* composites.

From data presented in Chapters 3 and 4, it can be concluded that the main factor in the production of acceptable wood-LLDPE composites is the compatibility between wood and polymer matrix. A careful compatibiliser optimisation is required in order to produce this acceptable WPC. The better compatibility of *A. cyclops* composites may be due to the macromolecular composition and content of *A. cyclops* species. They have favourable average particle size and a narrower range of average particle size. Woods, especially hardwoods, with higher cellulose, lignin and extractives content seem to produce composites with good mechanical and thermal properties and resistance to UV degradation. Softwoods such as *P. radiata* appear to produce composites with low WA and TS rates. Furthermore, wood extractives were found to have a negative effect on the WA and TS properties and positive impact on the resistance to UV degradation. As a result, we are giving more attention to the effect of these extractives on the properties of WPCs. Therefore, Chapter 5 investigates the effect of wood extractives on the properties of wood-LLDPE composites.

4.5 Conclusions

The properties of compatibility and adhesion between four different species and an LLDPE matrix with 10% wood content and different amounts of EVOH (0, 2, 5, 7 and 10%) as a compatibiliser were studied. Results of morphological observations, FTIR and thermal analysis led to the following conclusions:

1. All composites that showed higher mechanical and thermal properties (Chapter 3), exhibited better compatibility and interface adhesion. Although SEM micrographs did not show significant differences in the compatibility between the four wood species and LLDPE, they did show that the addition of EVOH as a compatibiliser is of crucial importance.
   - ❖ The compatibility and interfacial bonding between the particles from the four wood species and the LLDPE matrix were improved when EVOH was added.
   - ❖ The optimum concentration of EVOH that produces composites with better properties and performance was found to be 7%.
   - ❖ Increasing the amount of EVOH to 10% caused a dramatic reduction in the compatibility and interface adhesion between the wood and LLDPE matrix.
2. SEM micrographs of the fractured samples provided information about the compatibility and interface adhesion between the four species and LLDPE. Interfacial

stress transfer occurred along the wood particles in case of *A. cyclops* and *Q. alba* composites with 7% EVOH, indicating the good adhesion between the *A. cyclops* and *Q. alba* species and the LLDPE matrix when an optimum amount of EVOH was used.

3. The four wood species had markedly different average particle sizes. *A. cyclops* had a relatively lower average particle size than the others. Greater variations in the particle sizes were observed for *P. radiata* and *E. grandis*.
4. Although *Q. alba* has high cellulose content and the same average of preferable wood particle size as *A. cyclops*, its composite showed less compatibility and less interface adhesion between the LLDPE matrix and *Q. alba* particles, due to the presence of very small and oversized wood particles.
5. Although it is difficult to use FTIR spectra to obtain much information about the formation of hydrogen bonds, there were indications that more hydrogen bonds were formed in the cases of the *A. cyclops* and *Q. alba* composites. This confirms the better compatibility and interface adhesion between the LLDPE and these species via EVOH in comparison to *E. grandis*, *P. radiata* species.
6. Tan δ from DMA confirmed the better compatibility and interface adhesion between *A. cyclops* and *Q. alba* and LLDPE in the presence of EVOH; the γ-transition or T_g was shifted toward higher temperature, in comparison to LLDPE and the other composites.
7. The differences in the decomposition temperatures revealed by the TGA results also supported most of the findings mentioned here.

These results emphasise that controlling the interface to ensure better compatibility between the wood particles and polymer matrix is a very important aspect to take into consideration when developing WPCs.

4.5 References

1. Ndiaye D., Fanton E., Therias S., Vidal L., Gardette A., Composites Science and Technology, 68, 2779-2784, 2008.
2. Morsyleide F., Bor-sen C., Eliton S., Delilah F., Tina G., Luiz H., William J., Syed H., Bioresource Technology, 100, 5196-5202, 2009.
3. Manikandan N., Thomas S., Groeninck G., Composites Science and Technology, 61, 2519-2529, 2001.
4. Maurizio A., Aleksandra B., Maria E., Gennaro G., Anita G., Materials, 2, 911-925, 2009.
5. Yang H., Kim H., Park H., Lee B., Hwang T., Composite Structures, 72, 429-437, 2006.
6. Nachtigall S., Cerveira G., Rosa S., Polymer Testing, 26, 619-628, 2007.
7. Shi S., Gardner D., Composites: Part A, 37, 1276-1285, 2006.
8. Hristov V., Vasileva S., Macromolecular Materials and Engineering, 288, 798-806, 2003.
9. Kim S., Kim S., Kim H., Yang S., Thermochimica Acta, 45, 181-188, 2006.
10. Behzad M., Tajvidi M., Ehrahimi G., Flak R., International Journal of Engineering Transactions: Part B, 17, 95-104, 2004.

11. Liu H., Wu Q., Han G., Yao F., Kojima Y., Suzuki S., Composites: Part A, 39, 1891-1900, 2008.
12. Orden M., Sánchez C., Quesada M., Urreaga, J., Composites: Part A, 38, 2005-2012, 2007.
13. Acha B., Reboredo M., Marcovich N., Composites: Part A, 39, 1507-1516, 2007.
14. Yang H., Kim H., Park H., Lee B., Hwang, T., Composite Structures, 77, 45-55, 2007.
15. San H., Nee L., Meng H., ARPN Journal of Engineering and Applied Sciences, 3, 13-19, 2008.
16. Bledzki A., Gassen, J., Progress in Polymer Science, 24, 221-274, 1999.
17. Yeh S., Gupta, R., Composites: Part A, 39, 1694-1699, 2008.
18. Lee S., Yang H., Kim H., Jeong C., Lim B., Lee J., Composite Structures, 65, 459-469, 2004.
19. Nunez A., Sturm P., Kenny J., Aranguren M., Marcovich N., Reboredo M., Journal of Applied Polymer Science, 88, 1420-1428, 2003.
20. Dányádi L., Janecska T., Szabo Z., Nagy G., Moczo J., Pukánszky, B., Composites Science and Technology, 67, 2838-2846, 2007.
21. Dányádi L., Renner K., Moczo J., Pukánszky, B., Polymer Engineering and Science, 47, 1246-1255, 2007.
22. Kaci M., Cimmino S., Silvestre C., Duraccio D., Macromolecular Materials and Engineering, 291, 869-876, 2006.
23. Bouza R., Pardo S., Barral L., Abad M., Polymer Composites, 30, 880-886, 2008.
24. Nwabunma D., Kyu T., Polyolefin Composites, 1st edition, Wiley-Interscience, USA, 2008. 185.
25. Hristov V., Krumova M., Michler G., Macromolecular Materials and Engineering, 291, 677-683, 2006.
26. Klyosov A., Wood-plastic Composites, 1st edition, Wiley-Interscience, USA. 2007. 90-185.
27. Yang H., Wolcott M., Kim H., Kim S., Kim, H., Composite Structures, 79, 369-375, 2007.
28. Bengtsson M., Oksman K., Composites Science and Technology, 66, 2177-2186, 2006.
29. Cheremisinoff N., Handbook of Engineering Polymeric Materials, 1st edition, CRC Press, USA, 1997. 591-681.
30. Mohanty A., Misra M., Drzal L., Natural Fibres; Biopolymers and Biocomposites, 1st edition, CRC Press, USA, 2005. 186-418.
31. Kelly A., Concise Encyclopedia of Composite Materials, 1st edition, MIT Press, USA, 1990. 267.
32. Zhong J., Wei, J., E Xpress Polymer Letters, 1, 681-687, 2007.
33. Rahman M., Huque M., Islam N., Hasan, M., Composites: Part A, 40, 511-517, 2009.
34. Qin C., Soykeabkaew N., Xiuyuan N., Peijs T., Carbohydrate Polymers, 71, 458-467, 2008.
35. Araŭjo J., Waldman W., De Paoli M., Polymer Degradation and Stability, 93, 1770-1775, 2008.
36. Beg M., Pickering, K., Polymer Degradation and Stability, 93, 1939-1946, 2008.
37. Dominkovics Z., Dányádi L., Pukánszky B., Composites: Part A, 38, 1893-1901, 2007.
38. Sawyer L., Grubb D., Polymer Microscopy, 2nd edition, Springer, Netherlands, 1996. 248.
39. Chotirat L., Chaochanchaikul K., Sombatsompop N., International Journal of Adhesion and Adhesives, 27, 669-678, 2007.
40. Levita G., Marchetti A., Lazzeri A., Polymer Composites, 10, 39-43, 1989.
41. Sufyan G., Pekka K., Lippo V., The Open Dentistry Journal, 3, 36-41, 2009.
42. Migneault S., Koubaa A., Erchiqui F., Chaala A., Englund K., Krause C., Wolcott M., Journal of Applied Polymer Science, 110, 1085-1092, 2008.
43. Bledzki A., Gassan J., Theis S., Mechanics of Composite Materials, 34, 563-568, 1998.
44. Rothon R., Advances in Polymer Science, volume 139, Mineral Fillers in Thermoplastics I Raw Materials and Processing, Springer, Germany, 1999. 74-91.
45. Prachayawarakorn J., Anggulalat K., Songklanakarin Journal of Science and Technology, 25, 595-606, 2003.
46. Pukánszky B., Fekete E., Advances in Polymer Science, Volume 139, Mineral Fillers in Thermoplastics I Raw Materials and Processing, Springer, Germany, 1999. 114-120.
47. Dong J., Ozaki Y., Macromolecules, 30, 286-292, 1997.
48. Colemman M., Moskala E., Polymer, 24, 251-257, 1983.
49. Moskala E., Varnell D., Coleman M., Polymer, 26, 228-232, 1985.
50. Kim J., Yoon T., Mun S., Rhee J., Lee, J., Bioresource Technology, 97, 494-499, 2006.

51. White W., American Mineralogist, 56, 46-53, 1971.
52. Adhikary K., Pang S., Staiger, M., Composites: Part B, 39, 807-815, 2008.
53. Wilkes C., Summers J., Daniels C., Berard M., PVC Handbook, 1st edition, Hanser Verlag, USA, 2005. 260.

Chapter 5
The effect of wood extractives on the properties of wood-LLDPE composites

Abstract

The effect of wood extractives on the properties of wood-LLDPE composite system was studied. Hot water (HW) extractives, solvent extractives and both HW and solvent extractives were removed from the woods via Soxhlet extraction using the Tappi standard T 264 om-88 method. Wood-LLDPE composites were prepared using 10% unextracted and extracted wood from four wood species and 7% EVOH as a compatibiliser. The mechanical properties, crystallinity and melting behaviour, thermal stability, water absorption (WA) behaviour and resistance to UV radiation of composites filled with unextracted wood species and composites filled with the same wood species but without the above extractives were determined, and then compared. The results illustrated that there are several distinct advantages and disadvantages associated with the use of woods without extractives as a filler. Unextracted wood flour produced composites with better mechanical properties and better resistance to UV radiation, while the extracted woods produced composites with lower WA rates and better thermal stability.

Keywords: *WPCs, wood extractives, mechanical properties, thermal properties*

5.1 Introduction

The chapter applies to the investigation of the effect of the wood extractives on the properties of wood-LLDPE composites in order to gain more knowledge about the effect of wood's macromolecular composition and content on the properties of WPCs. This is important because wood extractives contribute strongly to the wood properties, although they only contribute a few percent to the entire wood composition [1]. These extractives have a strong negative impact on the wettability of the wood surface [2], they can be toxic and harmful to the environment [3], some extractives with an unpleasant odour can be emitted during the production of WPCs and cause pollution in the work environment which may impair the health of workers [4], the oxidation of extractives tends to increase the acidity of wood and promote degradation [5], and their use may create an unfavourable effect on the thermal stability of the final product [6]. It is therefore necessary to investigate what the impact of removing these extractives has on the final properties of wood-LLDPE composites.

A comparison between the mechanical properties, thermal properties, WA rate and resistance to UV radiation between composites filled with extracted wood species and composites filled with the original species (unextracted species) was carried out using 7% EVOH as a compatibiliser.

As found in Chapters 3 and 4, 7% EVOH was found to be the optimum concentration of EVOH produced wood-LLDPE composites with better compatibility and superior properties when using 10% wood content as a filler.

5.2 Experimental

5.2.1 Extraction processes

Cyclohexane (Sigma-Aldrich), absolute ethanol (Merck Chemicals) and hot distilled water were used for the extractions. The extractives were removed from the wood via Soxhlet extraction according to Tappi standard methods T 264 om-88 [7]. HW was applied to remove the polar extractives, while solvent (ethanol:cyclohexane 1:2, E/C) extraction was applied to remove the nonpolar extractives. There is no single solvent is able to remove all of these extractives [8]. Hence, in order to achieve complete extraction, E/C and HW extractions were performed consecutively. Although the solvent extraction process is tedious, and leads to insufficient recovery of wood extractives from wood samples [9], it is the only available way to extract these extractives from wood in order to determine their affect on the properties of wood-LLDPE composites. The extraction procedures were identical for all wood samples.

A sample of about 5 g of air dry wood of each species with particle size 180 μm was placed in a paper extraction thimble. Filter paper was placed on the top of the thimble to prevent any loss of the species. The extraction thimble was placed in position in the Soxhlet apparatus on the top of a clean, dry and weighed 500 mL around bottom flask containing 250 mL of distilled water or a mixture of 1:2 E/C (73 mL:147 mL). The Soxhlet extraction was carried out by boiling water reflux for 4 h. After refluxing, wood species was transferred from the thimble to the Büchner funnel to remove the excess solvent. The wood species and thimble were then washed three times with distilled water in the case of HW extraction and with ethanol and distilled water in the case of E/C extraction. Each wood species was air-dried (for about one week) before using it in the preparation of wood-LLDPE composites. In order to determine the amount of extractives, water or E/C was evaporated from the 250 mL flask. After drying the flask in an oven at 103 ^{o}C for 30 min, it was weighed and the percentage of extractives determined based on the weight of the oven dry flask. All the measurements were carried out in triplicate.

5.2.2 Preparation of the wood-LLDPE composites

The same materials and preparation method as described in Section 3.2 were used here. Due to supply shortage, a new LLDPE matrix was used as matrix in the WPC systems (and in further studies). The LLDPE matrix was also supplied by Sasol (South Africa). The comonomer was butene and the average MW was 137 000. The previously used LLDPE had a MW of 294 000. Coincidentally, this may serve as an indication of the effect of the MW of the polymer matrix on the properties of the composites.

5.3 Characterisation

Characterisation of LLDPE and all the wood-LLDPE composites were carried out by using various techniques: XRD, DSC, TGA, FTIR, DMA, OM and SEM. The following determinations were also carried out: tensile strength, EAB, hardness, WA behaviour and resistance to UV degradation. The same procedures were performed and the same sample dimensions were used, as shown in Chapters 3 (Section 3.3) and 4 (Section 4.3). Impact properties were determined using a Ceast impact pendulum tester. The specimens were tested using a 15 J pendulum and a 150^{o} release angle. These samples (5 mm x 50 mm x 1.5 mm) were injection moulded. At least three specimens were tested for each sample.

5.4 Results and discussion

5.4.1 Removed extractives

As is shown in Figure 5.1, the colour and the amount of the extracted materials varied from species to species. The highest amount of total extractives was extracted from *A. cyclops*, while the lowest amount of extractives was extracted from *E. grandis*.

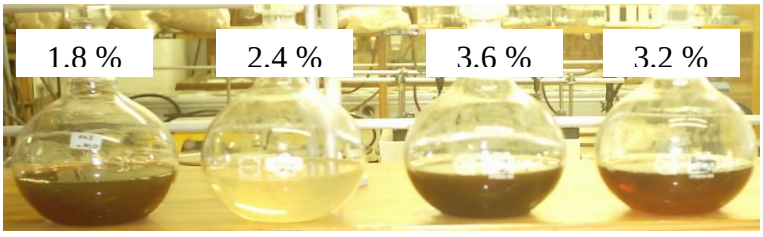

a)

E. grandis *P. radiata* *A. cyclops* *Q. alba*

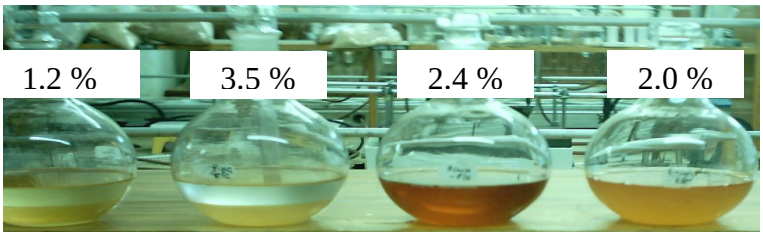

b)

Figure 5.1 Extractive content of the four species after a) HW and b) E/C extractions.

The highest amount of polar extractives (waxes, fats, resins and some gums) was removed from *P. radiata*, followed by *A. cyclops*, *Q. alba* and *E. grandis*, while the highest amount of HW extractives (tannins, gums, sugars, starches and colouring matter) was removed from *A. cyclops*, followed by from *Q. alba*, *P. radiata* and *E. grandis* [7]. The quantity and type of these extractives therefore differ from species to species.

5.4.2 XRD results

As shown in Figure 5.2 and Appendix A, there is no difference in the XRD patterns between the composites with unextracted woods and composites with extracted woods. All the diffraction peaks of LLDPE, *A. cyclops* and EVOH discussed earlier in Section 3.4.2 were observed. This indicates that the extractives do not have any effect on the crystallinity of *A. cyclops* or any *A. cyclops* composites. This is expected, as these extractives are deposited in the wood without strong bonds to other wood components, as discussed in Sections 2.2.1.1 and 2.2.1.3. Once again, the crystalline structure of LLDPE was not affected by compounding with wood and compatibiliser.

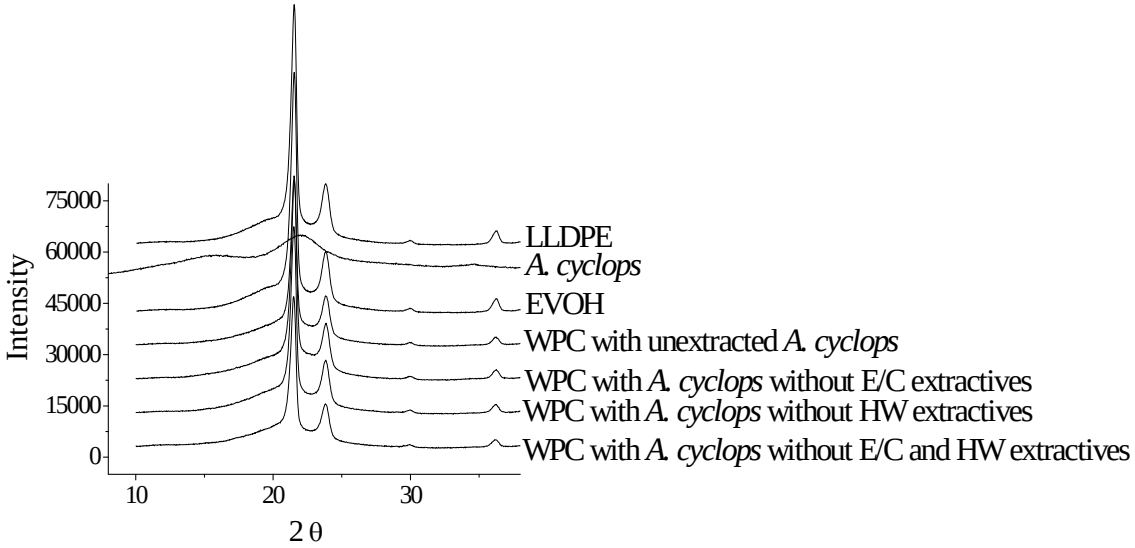

Figure 5.2 XRD spectra recorded for the LLDPE, *A. cyclops*, EVOH and all *A. cyclops* composites with and without extractives.

5.4.3 Mechanical properties

The tensile strength, EAB, impact strength and hardness of LLDPE and the composites with woods with and without extractives are shown in Table 5.1. The differences in mechanical properties between wood-LLDPE composites prepared using different unextracted wood species were explained and discussed in Chapters 3 and 4. Use of extracted wood (all species) as filler in a LLDPE matrix resulted in a dramatic decrease in the tensile strength, EAB and impact strength, as illustrated in Table 5.1 and Figure 5.3. On the other hand, wood-LLDPE composites made with extracted wood showed an increase in hardness. The decreases in

tensile strength, EAB and impact strength in different wood-LLDPE composites are more pronounced for wood without both E/C and HW extractives than for wood without HW extractives or E/C extractives, respectively. HW extraction is known to change the composition of wood significantly. HW extraction eliminates more materials than solvent extraction. Beside water-soluble extractives, HW removes a portion of the cell wall material of wood (some low MW polysaccharides, such as hemicelluloses) and extracts some inorganic extractives [8, 10-12]. The removal of some low MW hemicelluloses most likely causes changes of the fibre surface and accessibility [13-14].

Table 5.1 Mechanical properties of LLDPE and composites with and without extractives

Composite	Tensile strength, N/mm^2	EAB, %	Impact strength, J/m^2	Hardness, MPa
LLDPE	11.8 (0.7)	> 100.0	2983.0 (1.0)	2.4 (0.5)
Composites with unextracted wood of				
A. cyclops	17.5 (0.7)	15.0 (0.7)	852.3 (0.1)	2.8 (0.4)
E. grandis	14.4 (0.5)	06.7 (0.9)	710.2 (0.1)	2.8 (0.4)
P. radiata	13.7 (0.4)	14.8 (0.7)	781.3 (0.1)	3.1 (0.7)
Q. alba	16.5 (0.5)	12.1 (0.4)	852.3 (0.1)	2.6 (0.5)
A. cyclops composites with wood without				
E/C extractives	16.5 (0.2)	13.3 (0.3)	852.3 (0.1)	3.1 (0.7)
HW extractives	14.7 (0.3)	13.2 (0.3)	781.3 (0.1)	3.0 (0.0)
HW & E/C extractives	07.9 (0.3)	12.3 (0.2)	781.3 (0.1)	3.0 (0.7)
E. grandis composites with wood without				
E/C extractives	14.1 (0.3)	06.3 (0.2)	710.2 (0.1)	3.0 (0.0)
HW extractives	12.4 (0.3)	06.1 (0.2)	639.2 (0.1)	3.7 (1.5)
HW & E/C extractives	10.6 (0.3)	07.0 (0.3)	639.2 (0.1)	3.8 (0.6)
P. radiata composites with wood without				
E/C extractives	12.2 (0.2)	13.0 (0.3)	710.2 (0.1)	4.2 (1.1)
HW extractives	12.1 (0.3)	10.7 (0.3)	710.2 (0.1)	3.2 (1.1)
HW & E/C extractives	10.6 (0.3)	09.1 (0.2)	710.2 (0.1)	3.5 (1.0)
Q. alba composites with wood without				
E/C extractives	13.5 (0.3)	11.2 (0.2)	852.3 (0.1)	2.3 (1.0)
HW extractives	12.2 (0.3)	04.8 (0.2)	781.3 (0.1)	3.3 (1.1)
HW & E/C extractives	11.1 (0.3)	06.1 (0.3)	781.3 (0.1)	3.3 (0.7)

With the exception of *A. cyclops* and *Q. alba* composites without E/C extractives, the hardness increases for all composites containing wood without extractives. No significant difference was detected between wood-LLDPE composites without HW extractives and wood-LLDPE composites without both E/C and HW extractives, especially in the cases of *A. cyclops*-LLDPE, *E. grandis*-LLDPE and *P. radiata*-LLDPE composites. This is because the HW extraction eliminates a greater quantity of materials than E/C extraction, as stated above.

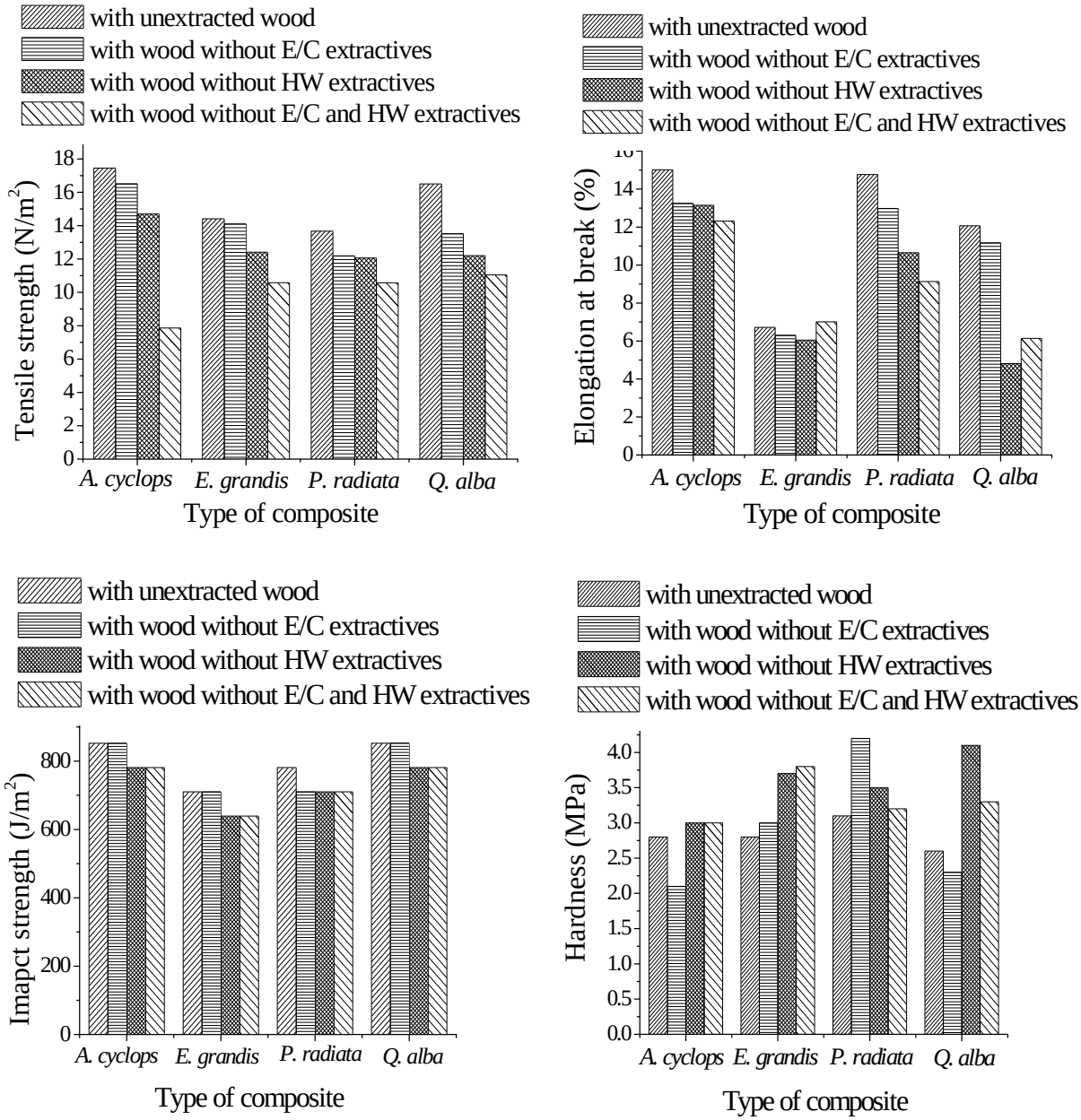

Figure 5.3 Mechanical properties of all composites with unextracted and extracted wood.

The difference in the hardness between these composites, as shown in Table 5.1 and Figure 5.3, can be due to several factors, as these extractives are known to contribute to, and affect, the wood's surface hardness [15-16]. This difference in the hardness can be explained by the effect the extractives have on the wood permeability, density, hardness, and compressive strength. The change in the wood hardness and density after removing these extractives is believed to be the major reason for the increased hardness of all the composites. Cragg et al. [17] found that the hardness correlates positively with density. Hirata et al. [18] concluded that the hardness distribution reflects the distribution of density of the wood surface. We, however, agree with Tze et al. [15], that further investigations are needed to verify the extractives effects on the wood hardness.

5.4.4 Thermal properties

5.4.4.1 Crystallisation and melting behaviour

Table 5.2 tabulates the T_c, T_m, ΔH_f, X_c and X_c^{corr} values of neat LLDPE and the composites with woods with and without extractives. There was no significant difference between composites made with extracted woods and composites made with unextracted woods.

Table 5.2 DSC results of WPCs with woods with and without extractives

Composites	T_c, °C	T_m, °C	ΔH_f, J/g	X_c, %	X_c^{corr}, %
LLDPE	105.7	124.1	108.2	37.5	37.5
Composites with extracted wood of					
A. cyclops	107.4	121.0	98.8	34.2	41.2
E. grandis	107.3	121.4	101.8	35.3	42.5
P. radiata	108.4	121.7	96.6	33.5	40.3
Q. alba	107.3	121.1	95.5	33.1	39.8
Composites with wood without E/C extractives of					
A. cyclops	106.4	123.5	101.0	35.0	42.1
E. grandis	106.7	123.4	103.6	35.9	43.2
P. radiata	108.4	123.0	102.3	35.4	42.7
Q. alba	109.5	121.3	106.8	37.0	44.6
Composites with wood without HW extractives of					
A. cyclops	107.7	120.4	100.7	34.9	42.0
E. grandis	107.4	120.9	100.7	34.9	42.0
P. radiata	110.1	121.4	98.8	34.2	41.2
Q. alba	110.0	121.0	100.9	35.0	42.1
Composites with wood without both E/C and HW extractives of					
A. cyclops	107.7	121.3	102.1	35.4	42.6
E. grandis	107.0	124.4	102.0	35.3	42.6
P. radiata	108.3	122.4	102.0	35.3	42.6
Q. alba	110.3	121.7	102.2	35.4	42.6

There are no significant differences in the X_c (~33 to ~36 %) and X_c^{corr} (~39 to ~44 %) between the composites made with extracted woods and composites made with unextracted woods. In comparison to LLDPE, all composites showed negligible change in the T_c and T_m. They showed a very small decrease in the ΔH_f and X_c. X_c^{corr} of each composite was higher than its X_c. All the possible reasons for the change in the crystallisation and melting behaviour of these composites were discussed in Section 2.2.1.4. Melting and crystallisation curves of all composites are shown in Appendix C.

5.4.4.2 Thermal stability

The removal of extractives had a positive impact on the thermal stability of wood and wood-LLDPE composites. As shown in Tables 5.3 and 5.4, the removal of wood extractives

generally improved the thermal stability of the four wood species and all the wood-LLDPE composites. T_0, T_1, T_2, T_f and the residual weight at 600 ^oC of the four species before and after extractions are summarised in Table 5.3. DTG curves are shown in Figures 5.4, 5.5 and 5.6; the degradation profiles of all species changed after E/C, HW, and both E/C and HW extractions.

Table 5.3 Thermal degradation temperatures and residual weight of the investigated wood species

Species	T_0, ^oC	T_1, ^oC	T_2, ^oC	T_f , ^oC	Residue at 600 ^oC, %
Original wood species					
A. cyclops	245.2	321.2	387.5	524.8	13.5
E. grandis	234.6	324.7	385.4	507.7	13.3
P. radiata	218.9	-------	388.4	513.8	13.7
Q. alba	258.4	321.7	385.7	538.0	12.0
After E/C extraction					
A. cyclops	256.0	318.7	392.6	538.5	11.4
E. grandis	238.3	315.6	391.5	526.7	11.2
P. radiata	235.5	------	399.1	530.1	09.5
Q. alba	259.5	322.1	385.3	547.1	08.8
After HW extraction					
A. cyclops	254.7	316.7	391.0	530.4	12.0
E. grandis	251.8	316.7	392.6	515.3	08.6
P. radiata	235.4	------	399.1	521.9	09.3
Q. alba	268.5	328.0	389.4	542.6	09.2
After HW and E/C extractions					
A. cyclops	266.6	321.7	396.0	526.5	09.6
E. grandis	250.6	317.2	394.5	512.9	09.4
P. radiata	240.9	------	399.1	515.3	08.2
Q. alba	268.0	324.7	391.5	542.6	07.4

The effects of E/C extraction on the thermal stability of wood appear to be less pronounced compared to HW extraction and both E/C and HW, as illustrated in Table 5.3. Figure 5.4 shows the derivative thermogravimetric (DTG) curves of LLDPE and the four species with and without E/C extractives. The DTG curves of *Q. alba* before and after E/C extraction are nearly identical and the changes are negligible. In most cases, T_0, T_2 and T_f shifted to significantly higher temperatures. T_1 of *P. radiata*, *A. cyclops* and *E. grandis* showed a small shift towards lower temperature. The effect of E/C extraction on the thermal stability of *P. radiata* and *E. grandis* was more distinct than for *Q. alba* and *A. cyclops*. For *P. radiata* the area under the peak became smaller and the peak narrower and the effect of E/C extraction were most significant. For *E. grandis* the height of the shoulder was decreased and the peak intensity increased, which results in a net decrease of the area under the shoulder and the

peak. T_1 of *E. grandis* showed a shift towards lower temperature. The quantity of wood residue decreases for all four wood species after E/C extraction and is more significant for *P. radiata* and *Q. alba*, than for *A. cyclops* and *E. grandis*.

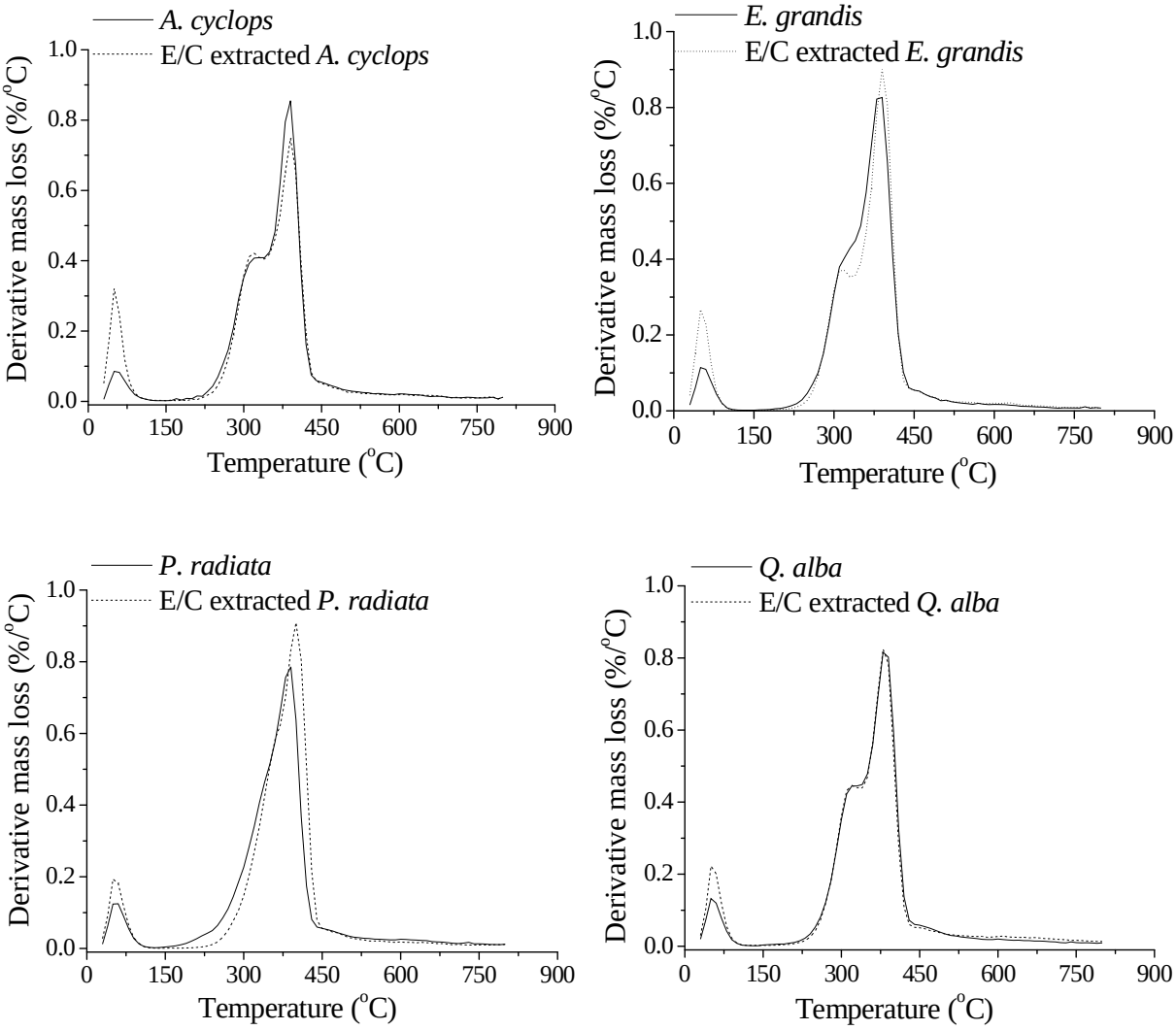

Figure 5.4 DTG curves of the four wood species before and after E/C extraction.

As it can be seen in Figure 5.5, the differences occur in the width and height of the shoulders and the peaks in the DTG curves after HW extraction. In the cases of *Q. alba* and *E. grandis*, the areas under the shoulders and peaks become smaller after extraction and the peaks are narrower. For *A. cyclops* the shoulder is higher and the peak is smaller and narrower after extraction, whereas for *P. radiata* no shoulder can be detected and the peak becomes more pronounced after extraction.

The most significant changes observed are the changes in the position of T_0, which are increased for all four wood species after HW extraction. This indicates that the thermal decomposition of some HW extractives takes place in this temperature range and that these compounds have been partly removed from the wood samples by the HW extraction.

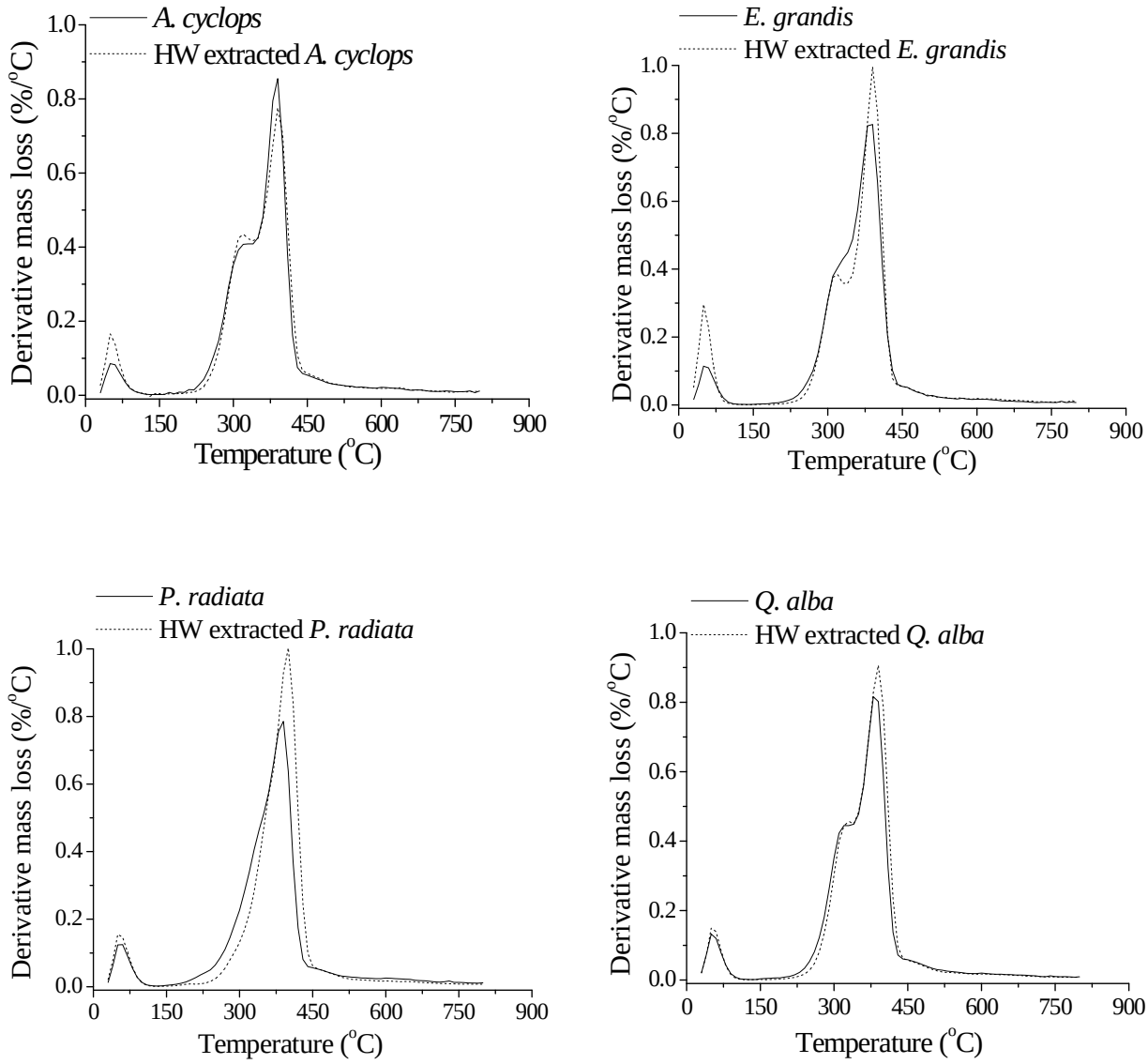

Figure 5.5 DTG curves of the four wood species before and after HW extraction.

Shi-fa and Ai-jun [19] subjected wood sawdust and PP powder to heat treatment at about 290 °C for 8 min, similar to conditions used on an industrial scale. They found that an unpleasant odour was emitted when the inner temperature of the wood sawdust reached 130 °C. They concluded that phenols, acids, aldehydes, ketones, furan derivatives and nitrogen containing compounds were most likely responsible for this and that most of these compounds are HW extractives. Ohtani et al. [20] assumed that HW extractives suppress the decomposition and loss of hemicelluloses by acting as a protector for hemicelluloses during the alkaline cooking. T_1 (the shoulder) was shifted to a higher temperature for *Q. alba* and to lower temperatures for *A. cyclops* and *E. grandis*. This is probably due to the extraction of low MW polysaccharides and some hemicelluloses from the wood samples, especially in the cases of *A. cyclops* and *E. grandis* [8, 10-12].

As was the case before the extraction, no shoulder was observed for *P. radiata*. T_2 and T_f were shifted to higher temperatures for the four wood species. The deviations in the T_0, T_1, T_2, T_f and the shape and the position of the peaks in DTG curves indicate, that the degradation of HW extracted wood occurs at higher temperatures and over a slightly narrower temperature range. This is in agreement with results reported by Várhegyi et al. [11], who found that HW extraction causes a displacement of TGA curves to higher temperatures. Finally, there is a significant decrease in the quantity of wood residue for the four wood species.

The wood residue after E/C extraction is comparable to the residue after HW extraction. In agreement with previously published results, HW washing and extraction causes a significant decrease in the char yield of some wood species [11, 21], and removes a portion of the cell wall material of wood and eliminates some inorganic matter or extractives [8, 10-12], which may catalyze the decomposition of natural polymers resulting in a lower decomposition temperature and a higher amount of char [6, 11, 21]. However, the differences in the thermal stability of wood before and after HW extraction proves that some extractives, which have an influence on the thermal stability of wood were indeed removed and also that the thermal decomposition of these extractives occurs over a wide temperature range, between ±200 and 500 ^{o}C. The thermal decomposition of the E/C extractives occurs over a narrower temperature range.

The effects of the removal of the complete extractives on the wood species, on the thermal stability are displayed in Table 5.3 and Figure 5.6. The area under the shoulders and the peaks decreased and the peaks became narrower. T_0, T_2 and T_f of all wood samples showed a clear shift to higher temperatures. T_1 of *Q. alba* was shifted to a higher temperature, while T_1 of *A. cyclops* and *E. grandis* shifted to lower temperatures. A significant decrease in the quantity of wood residue could be observed in all four wood species. These changes prove again, that the elimination of extractives increases the thermal stability of wood.

The changes after both HW and E/C extractions were more pronounced than for HW or E/C extraction alone, which could be expected, as each individual process affects different extractives, which all have an impact on the thermal stability of wood. This indicates that the more complete the removal of these extractives the better the thermal stability will be. When comparing the thermal stability of the wood species, the order remains the same as for the unextracted or original wood species (as described in Section 3.4.4): *A. cyclops* and *Q. alba* wood have better thermal stability at low and high temperature than *E. grandis* and *P. radiata*.

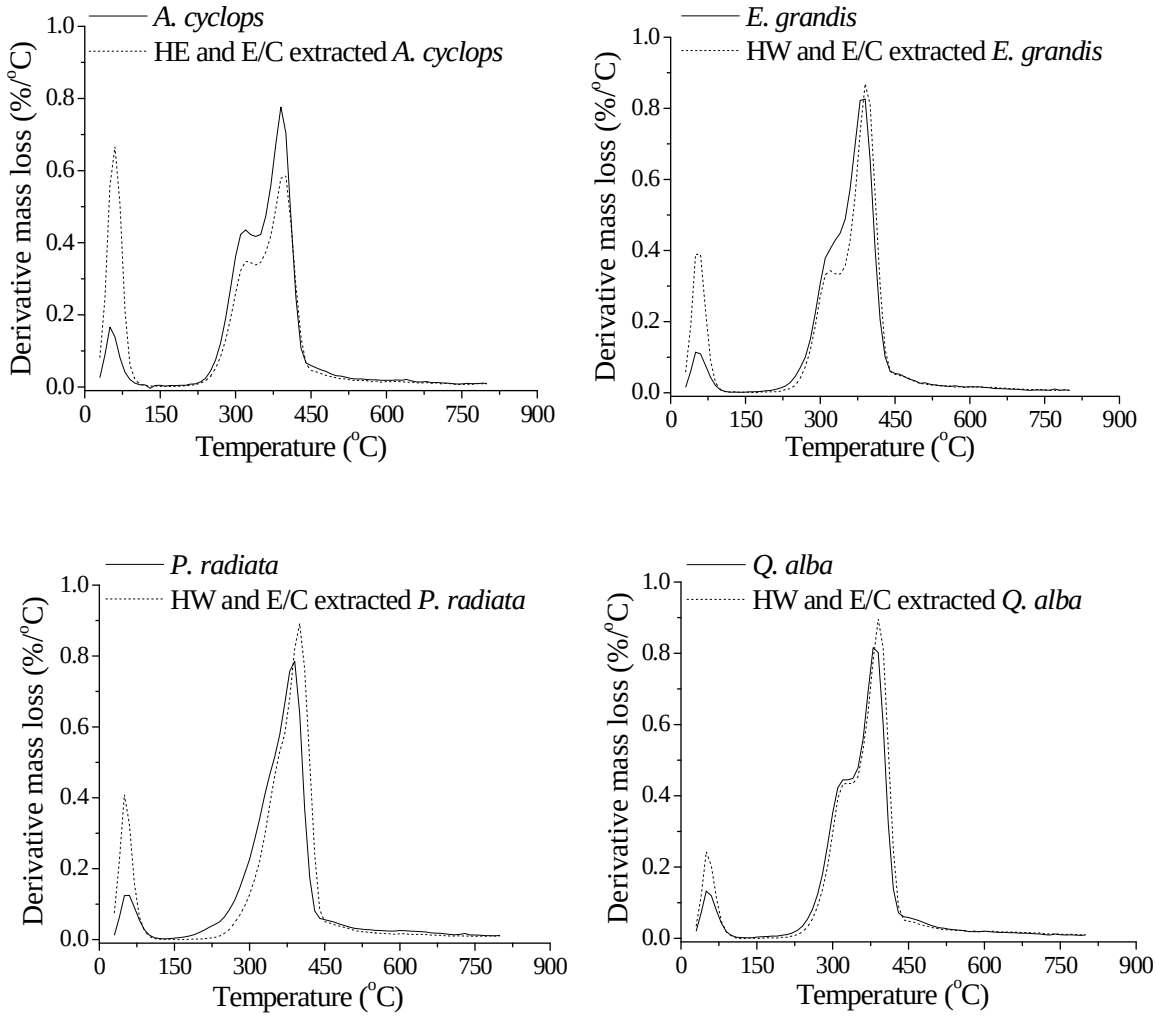

Figure 5.6 DTG curves of the four species before and after HW and E/C extractions.

As shown in Table 5.4, the removal of wood extractives generally improved the thermal stability of the wood-LLDPE composites. The two main degradation steps (T_{01} - T_{f1} and T_{02} - T_{f2}) were shifted to higher temperature when the wood without extractives was used as a filler.

As in the cases of composites with extracted woods, as discussed in Section 3.4.6, the composites with extracted wood showed a small weight loss before 100 °C, which can be attributed to the evaporation of water. The weight loss rate gradually increased above 200 °C and a distinct weight loss appeared between 250 and 560 °C, in two main degradation steps. Woods without E/C extractives showed less improvement in the thermal stability of wood-LLDPE composites than woods without HW extractives.

As shown in Figure 5.4, removal of the E/C extractives caused positive changes in the DTG curves, which can be seen in the position, width and height of the shoulders (the first degradation step in the wood-LLDPE composites) and the peaks (the second degradation step

in the wood-LLDPE composites). The peaks became broader and their intensity decreased in the case of *A. cyclops*, *E. grandis* and *Q. alba* composites. The peak in the case of *P. radiata* composite became narrower and its intensity increased. The most important changes are the changes in the position of first degradation step (between T_{01} and T_{f1}) and second degradation step (between T_{02} and T_{f2}), as shown in Table 5.4. These changes in the thermal degradation temperatures (T_{01}, T_{f1}, T_{02} and T_{f2}) between the four WPCs containing wood with and without E/C extractives show clearly that the elimination of E/C extractives has a positive effect on the thermal stability of wood-LLDPE composites.

Table 5.4 TGA results of LLDPE and wood-LLDPE composites

Composites	T_1, °C	T_{f1}, °C	T_2, °C	T_{f2}, °C
LLDPE	--------	--------	351.6	537.4
Composites with extracted woods of				
A. cyclops	254.1	391.5	403.9	548.0
E. grandis	248.4	380.1	389.6	540.5
P. radiata	235.1	380.1	395.3	542.4
Q. alba	266.4	389.6	401.0	552.2
Composites with woods without E/C extractives of				
A. cyclops	263.6	400.0	406.7	549.4
E. grandis	253.0	388.7	394.9	544.1
P. radiata	251.3	389.6	393.4	545.7
Q. alba	268.3	398.1	403.8	550.1
Composites with woods without HW extractives of				
A. cyclops	266.4	402.9	408.6	552.3
E. grandis	258.8	401.9	406.7	547.4
P. radiata	254.1	402.9	405.7	549.4
Q. alba	272.1	403.8	406.7	553.8
Composites with woods without both E/C and HW extractives of				
A. cyclops	271.2	410.5	420.9	559.6
E. grandis	261.7	403.8	411.4	548.9
P. radiata	258.8	403.8	410.5	550.5
Q. alba	275.9	413.3	419.0	556.4

On the other hand, woods without HW extractives showed further improvement in the thermal stability of wood-LLDPE composites than wood without E/C extractives. As shown in Figure 5.7, the intensities of the main peaks (second degradation steps) increased in the case of *A. cyclops* and *P. radiata* composites, while they decreased for *E. grandis* and *Q. alba* composites. The peaks became broader for all four composites. All DTG curves of wood-LLDPE composites containing woods without HW extractives were shifted to higher temperatures compared to the curves obtained from wood-LLDPE composites containing

extracted wood or wood without E/C extractives. So, differences exist in the thermal degradation temperatures between the wood-LLDPE composites containing woods without HW extractives, woods without E/C extractives, and unextracted woods.

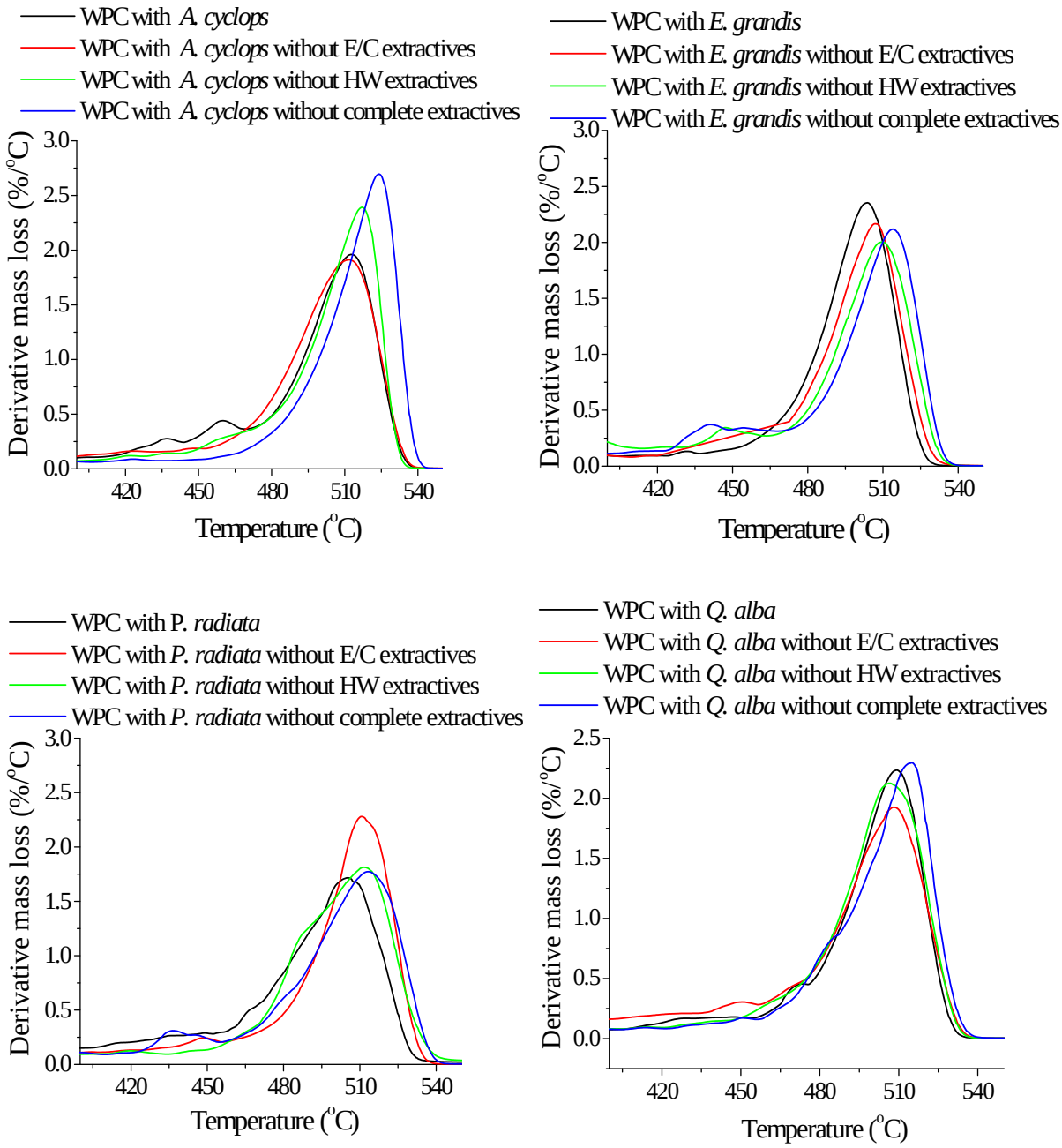

Figure 5.7 DTG curves of wood-LLDPE composites with and without extractives (400-550 °C temperature range).

The greatest improvement in the thermal stability was achieved when both types of extractives were removed, as illustrated in Figure 5.7. Woods without both E/C and HW extractives was used in order to determine the effect of the complete removal of all extractives on the thermal stability of wood-LLDPE composites. The results are displayed in Table 5.4 and Figure 5.7. The intensities of the main peaks (second degradation steps) increased in the

case of *A. cyclops*, *P. radiata* and *Q. alba* composites, while it decreased for the *E. grandis* composite. As shown in Table 5.4, all the degradation temperatures (T_1, T_{f1}, T_2 and T_{f2}) of the WPCs containing woods without both E/C and HW extractives were shifted to higher temperatures compared to other composites. This shift proves that the complete elimination of extractives affects the thermal stability of wood-LLDPE composites positively and leads to an improvement of in the thermal stability compared to the effect of these extractives individually. This signifies that the more complete the removal of these extractives is the better the improvement in the thermal stability will be.

Four *A. cyclops* composites with wood with and without the above extractives were prepared without EVOH in order to investigate whether the effect of the extractives on the thermal stability remains the same. As expected, these composite materials showed lower thermal stability than LLDPE alone or wood-LLDPE composites made with EVOH, due to the incompatibility and weak adhesion between the hydrophilic wood and hydrophobic LLDPE. But even without EVOH, wood-LLDPE composites containing woods without both E/C and HW extractives exhibited a larger improvement in the thermal stability compared to wood-LLDPE composites containing woods without HW extractives only, without E/C extractives only and wood-LLDPE composites made with extracted wood, as shown in Figure 5.8.

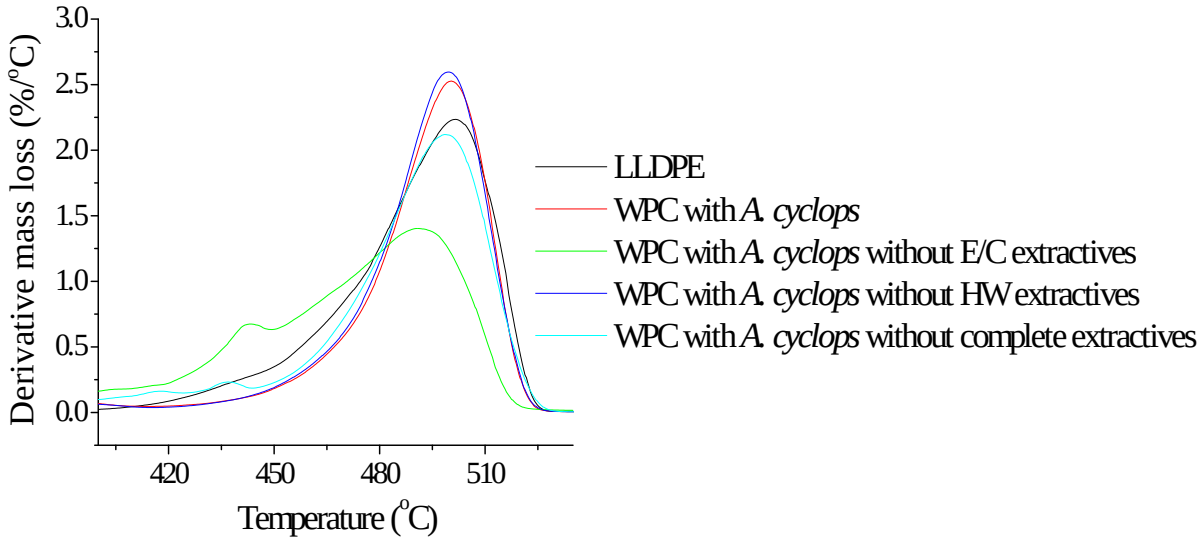

Figure 5.8 TGA curves of LLDPE and noncompatibilised *A. cyclops* composites with woods with and without extractives (400-550 °C temperature range).

It should be noted that the degree of the thermal stability of the four wood species remains the same after extractions as for the extracted wood and the same is true for the composites. After the removal of the extractives, wood-LLDPE composites containing wood from *A. cyclops* and *Q. alba* are more stable at low and high temperature than WPCs containing wood from *E.*

grandis or *P. radiata*. Both degradation steps occurred at higher temperatures in the cases of wood-LLDPE composites containing wood from *A. cyclops* and *Q. alba* than in the cases of wood-LLDPE composites containing wood from *E. grandis* and *P. radiata*. All extraction processes resulted in an improvement of the thermal stability of wood, independent of the species. The effect of combined extractions was more pronounced than that of individual extractions, and E/C-extraction caused less improvement in the thermal stability of wood than HW extraction.

Briefly, the effect of extractives on the first degradation step (between T_1 and T_{f1}) can be explained by the fact that most extractives degrade at low temperatures, and subsequently their removal should shift T_1 to higher temperatures. This in turn will shift the entire first degradation step to higher temperatures, as these extractives are deposited in the wood without strong bonds to other wood components. The effect of extractives on the second degradation step (between T_2 and T_{f2}) can be similarly explained: extraction removes a portion of the cell wall material of wood (low MW polysaccharides, such as some hemicelluloses, e.g. arabinogalactan, and eliminates some inorganic matter or extractives [8, 11], which may catalyse the decomposition of natural polymers resulting in a lower decomposition temperature [12, 22]. This effect is more pronounced for HW extraction, because a larger quantity of material is removed compared to in E/C extraction.

Overall, the effect of extractives on both degradation temperatures confirms that the decomposition of extractives occurs over a broad temperature range and in two main stages: the first stage takes place below ±200 ^{o}C and the second stage between ±250 ^{o}C, and 550 ^{o}C as indicated by Mészáros et al. [22].

5.4.5 Water absorption

As shown in Figure 5.9, the WA rates of the composites with extracted woods were lower than those in the composites with unextracted woods. This confirms the assumption made in Section 3.4.5 about the effect of wood extractives on the rate of WA of wood. This is probably because some of the wood extractives are soluble in water.

The effect of wood extractives on the WA rate of wood-LLDPE composites was less pronounced in the case of *E. grandis* due to the lowest amount of wood extractives compared with other species, as shown in Table 3.1 and Figure 5.1. This effect was more pronounced in the cases of *A. cyclops* and *Q. alba*, as indicated by the change in the water colour after the WA test, as shown before in Figure 3.8. These species contained a higher amount of water soluble extractives than the other species.

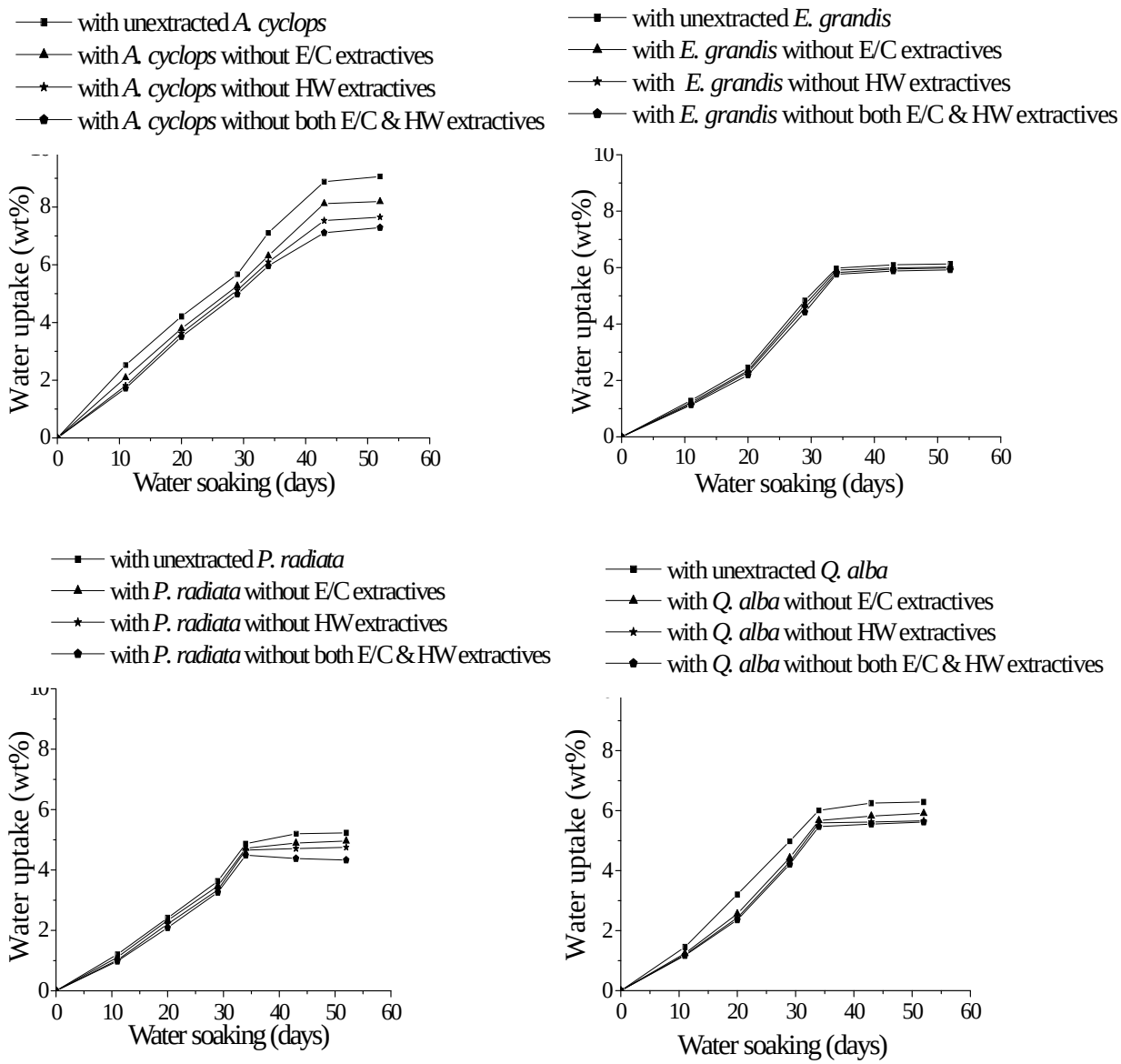

Figure 5.9 WA rates of four composites with extracted woods.

Composites with woods without both E/C and HW extractives showed the lowest WA rates due to the complete removal of the water soluble extractives. Composites made with woods without E/C extractives showed the highest WA rates but the WA was still less than for the composites made with unextracted woods. This indicates that some of water soluble extractives were removed by E/C extraction. The composites made with woods without HW extractives illustrated lower WA rates than the composites made with extracted woods and composites made with woods without E/C extractives, respectively. The photographs in Figure 5.10 confirm the effect of these extractives on the WA rate of wood-LLDPE composites. During the WA test a change in the colour of water in the cases of extracted *A. cyclops* and *Q. Alba* composites (samples 1 and 4 in Figure 5.10a) occurred, while the change in the colour after WA test did not occur in the cases of *A. cyclops* and *Q. Alba* composites without E/C and HW extractives (samples 1 and 4 in Figure 5.10d).

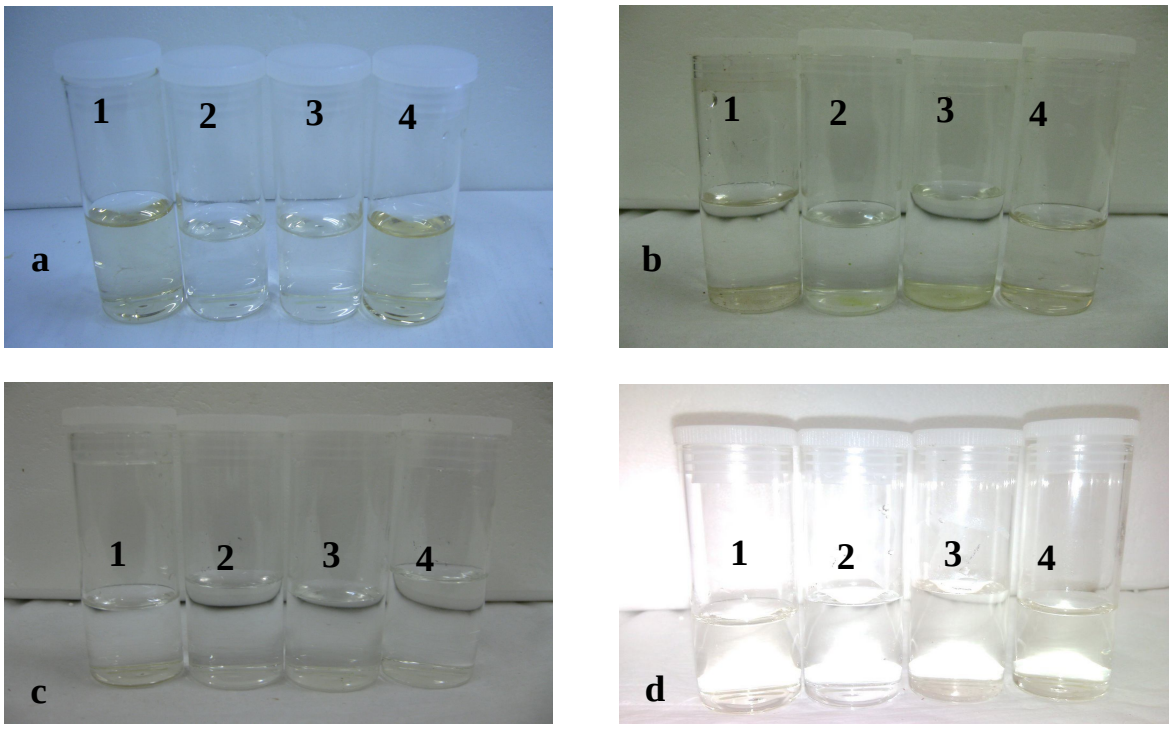

Figure 5.10 Change in the water colour after water absorption test: a) composites with extracted woods, b) composites with woods without E/C, c) composites with woods without HW extractives and d) composites with woods without both E/C and HW extractives.

The change in the colour was less pronounced in the cases of *A. cyclops* and *Q. Alba* composites with woods without E/C extractives (samples 1 and 4 in Figure 5.10b)., while the change in the colour did not seem to occur in the cases of *A. cyclops* and *Q. Alba* composites with woods without HW extractives (samples 1 and 4 in Figure 5.10c). *E. grandis* and *P. radiata* composites did not show any change in the colour of water after WA tests (samples 2 and 3 in Figure 5.10).

5.4.6 UV degradation

All samples were exposed to UV radiation for 60 days. Woods without extractives had reduced the resistance to UV radiation of wood-LLDPE composites. This was indicated by an increase in the intensities of the carbonyl bands in the FTIR spectra, as shown in Figure 5.11. This is because some of the extractives are capable of absorbing light, as mentioned in Sections 2.2.1.4 and 3.4.5.

Woods without only HW extractives appeared to produce composites with weaker resistance to UV radiation than woods without E/C extractives. Once again, this is because a larger quantity of material is removed by HW extraction compared to E/C extraction. This means that more extractives capable of absorbing light were probably be removed in the case of HW extraction than in the case of E/C extraction.

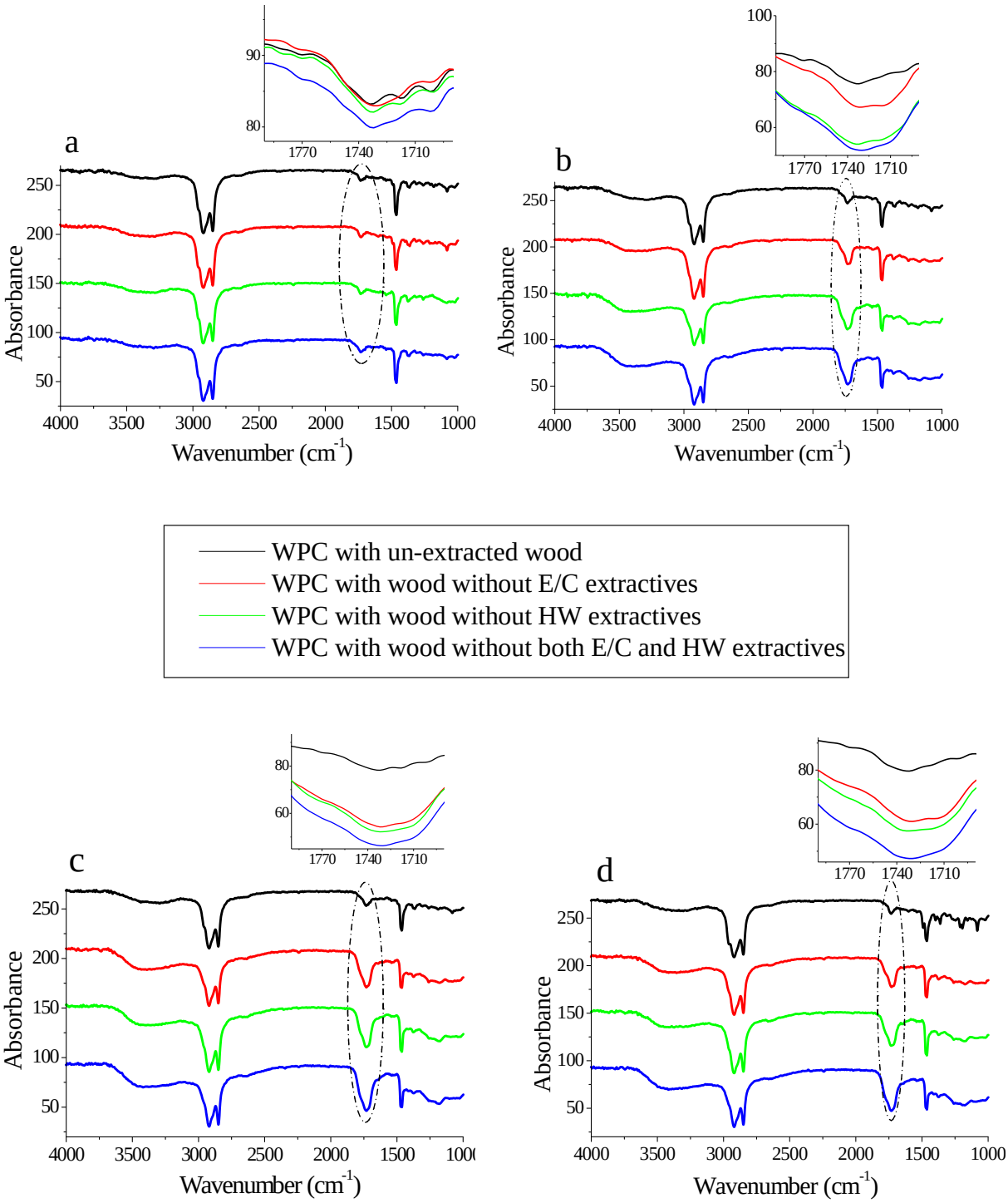

Figure 5.11 The IR bands at 1710-1780 cm^{-1} of composites with and without extractives of a) *A. cyclops*, b) *E. grandis*, c) *P. radiata* and d) *Q. alba*.

These results were confirmed by OM images, as shown in Figure 5.12. OM images were recorded only for LLDPE and *A. cyclops* composites. More cracks are present in composites with *A. cyclops* without both E/C and HW extractives than in composites with *A. cyclops* without HW extractives and composites with *A. cyclops* without E/C extractives, respectively. Similar to WPC with unextracted woods, as shown in Section 3.4.8, UV degradation was less noticeable in all the composites with extracted woods than in LLDPE.

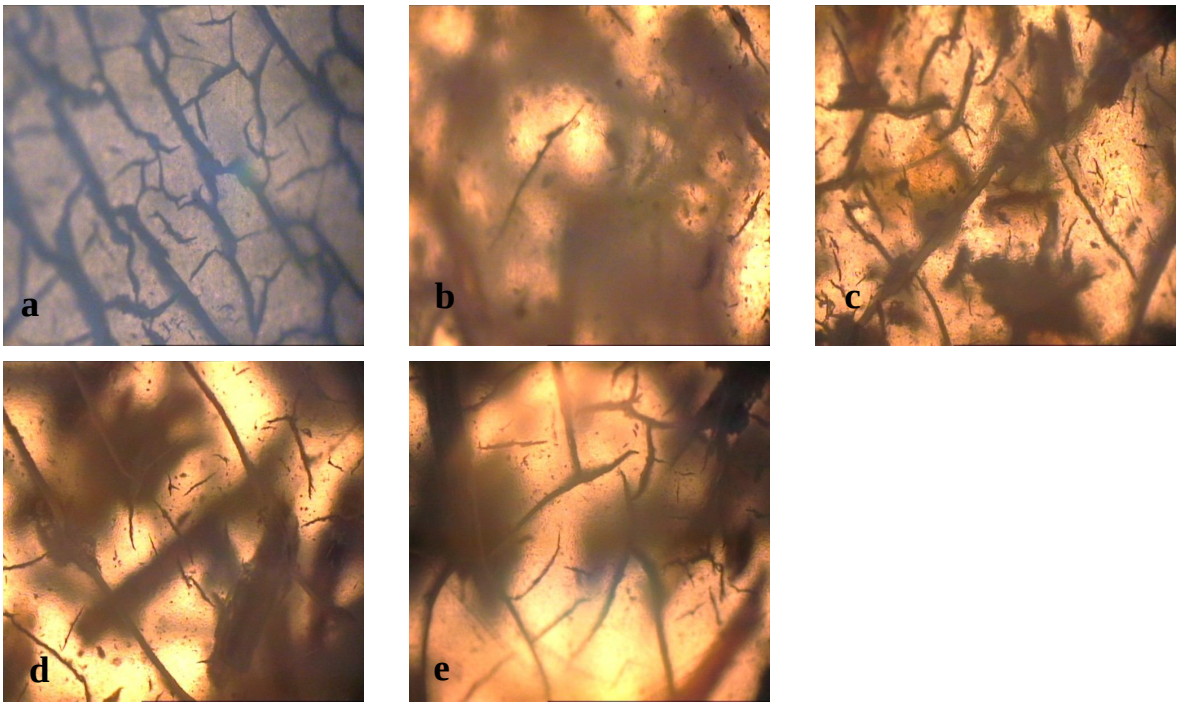

Figure 5.12 Optical microscope micrographs of a) LLDPE, b) unextracted *A. cyclops* composite, c) *A. cyclops* composite with *A. cyclops* without E/C extractives, d) *A. cyclops* composite with *A. cyclops* without HW extractives and e) *A. cyclops* composite with *A. cyclops* without both E/C and HW extractives after 60 days exposure to UV (Mag. 100x).

In short, woods with extractives resulted in composites with superior mechanical properties and better resistance to UV degradation, while woods without extractives resulted in composites with better thermal stability and low WA rate. The improvement in thermal stability and WA behaviour of composites made with woods without extractives over the composites made with unextracted woods was found to be not due to the improvement in the compatibility and interfacial adhesion between the wood and LLDPE matrix via EVOH. This is because these composites showed reduced mechanical properties than composites with unextracted woods. As concluded in Chapter 4, the better the compatibility and the interfacial adhesion the better the mechanical properties will be [23]. In order to observe the difference in the compatibility interfacial adhesion between composites made with unextracted wood and composites made with extracted wood, FTIR, DMA OM and SEM analyses were used to determine the difference in the compatibility and interfacial adhesion in composites made with unextracted *A. cyclops* and composites made with *A. cyclops* without extractives. This is described in Section 5.4.7.

5.4.7 Compatibility and interfacial adhesion

Figure 5.13a shows the FTIR spectra of LLDPE and all the *A. cyclops* composites (with and without extractives). FTIR results showed that there is a small shift in the hydroxyl stretching

bands at 3200 to 3600 cm^{-1}. This band is centred at 3362 cm^{-1} in the case of pure *A. cyclops*, and at 3368 to 3382 cm^{-1} in the cases of composites. It is attributed to the presence and distribution of new hydrogen bonds.

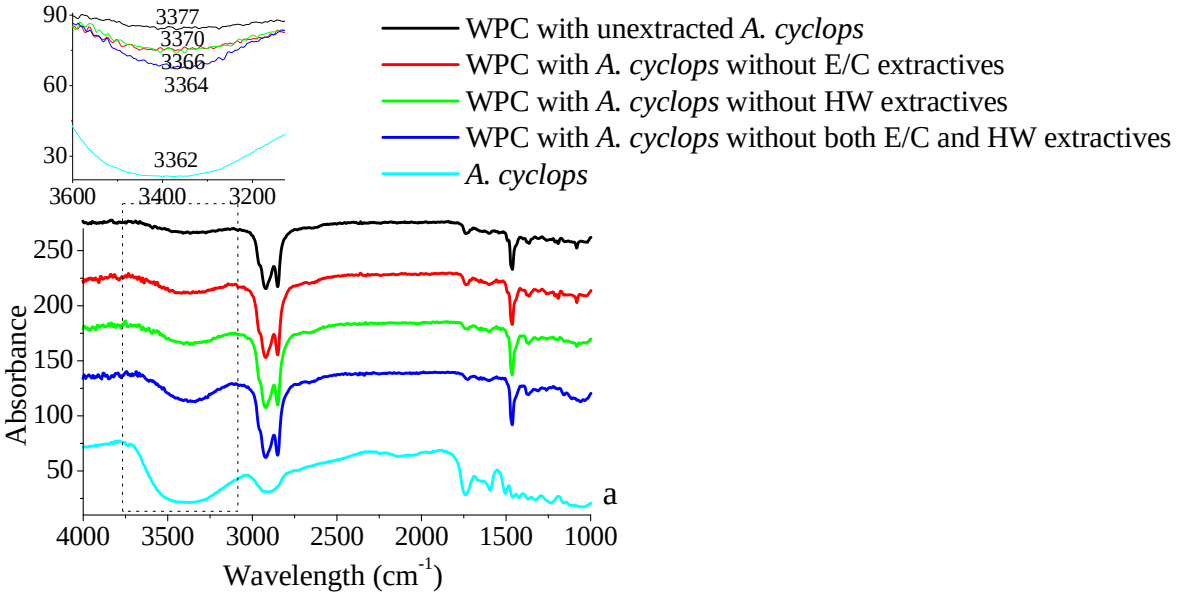

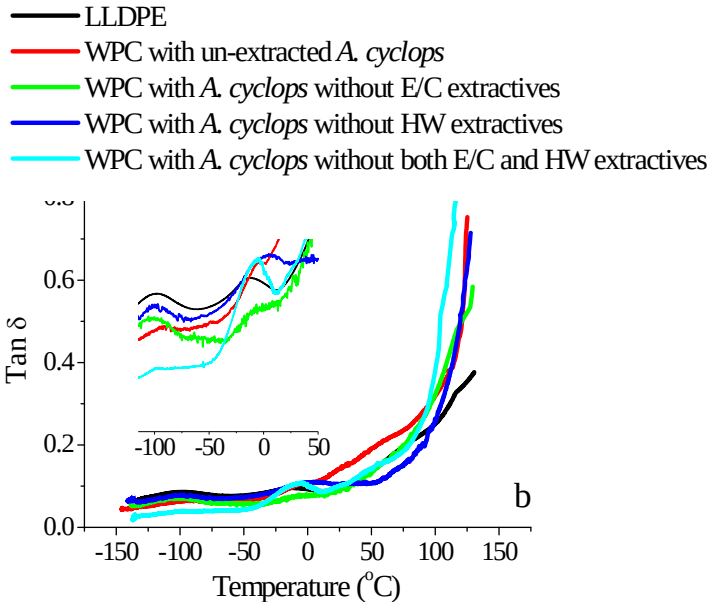

Figure 5.13 a) FTIR and b) DMA results of LLDPE and composites with unextracted *A. cyclops* and composites with *A. cyclops* without extractives.

The intensity and appearance of this band in the composite with unextracted *A. cyclops* is lower and broader than in the composites with *A. cyclops* without extractives. This means that

fewer hydrogen bonds are formed between wood and EVOH in the case of the composites with *A. cyclops* without extractives than in the case of the composite with unextracted *A. cyclops* [24-25].

DMA results exhibited that with increasing temperature, the tan δ values of composites with unextracted *A. cyclops* increased toward high temperature in comparison to composites with *A. cyclops* without extractives. As illustrated in Figure 5.13b and Table 5.5, the γ-transition (T_g) and β-transition of the composites were shifted to higher temperature in comparison to pure LLDPE. Also, the γ-transition or T_g and β-transition of the composite with extracted *A. cyclops* were observed at slightly higher temperature in comparison to composites with *A. cyclops* without extractives. This indicates better interfacial interaction between unextracted *A. cyclops* particles and LLDPE at the interface than in the case of extracted *A. cyclops* particles and LLDPE via EVOH [26-27].

Table 5.5 Summary of tan δ peak temperature at γ-transition and β-transition of LLDPE and *A. cyclops* composite with and without extractives

Composite with	Tan δ peak temperature at γ-transition or T_g, ^oC	Tan δ peak temperature at β-transition, ^oC
LLDPE	-100.2	-10.2
Unextracted *A. cyclops*	-93.8	-01.9
A. cyclops without E/C extractives	-96.9	-05.0
A. cyclops without HW extractives	-97.4	-03.4
A. cyclops without both E/C and HW extractives	-98.0	-06.6

Typical OM micrographs of composites made with *A. cyclops* with and without extractives are shown in Figure 5.14. Composite made with unextracted *A. cyclops* revealed better morphology and distribution of *A. cyclops* particles in LLDPE matrix than the composites made with *A. cyclops* without extractives. This is because wood extractives affect the polarity of the wood surface [28]. The micrographs of the composites with extracted *A. cyclops* (Figure 1b, 1c and 1d) showed less uniform distribution of particles in the matrix and more randomly and more twisted particles in comparison to the composite with extracted *A. cyclops* (Figure 1a).

Each extraction step seemed to cause shrinkage of the wood particles as reported by Choong and Achmadi [28]. Similar morphology differences were observed for *E. grandis, P. radiata* and *Q. alba* composites, as presented in Appendix D.

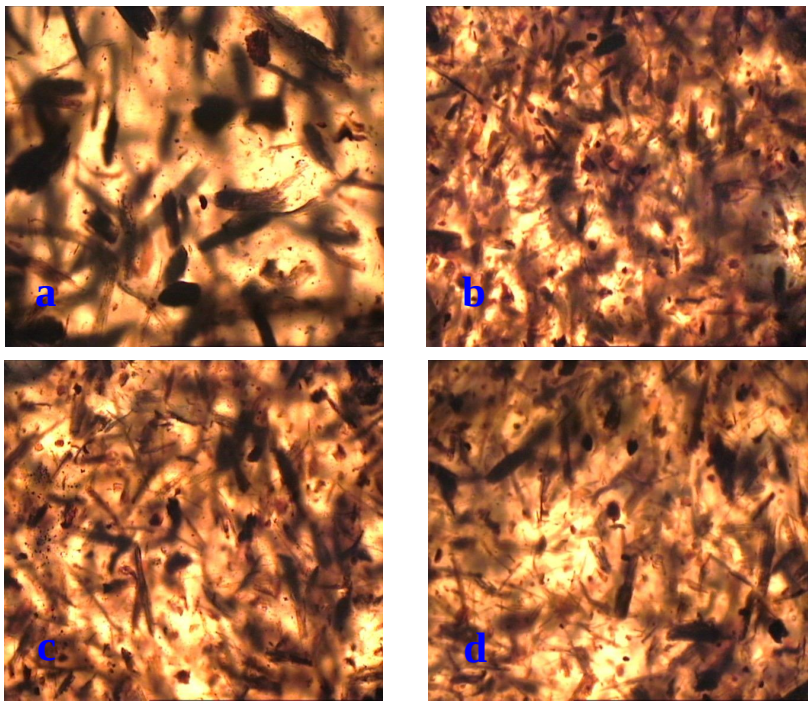

Figure 5.14 Optical microscope micrographs of a) composites with unextracted *A. cyclops*, b) composite with *A. cyclops* without E/C extractives, c) composite with *A. cyclops* without HW extractives, and d) composite with *A. cyclops* without both E/C and HW extractives (Mag. 100x).

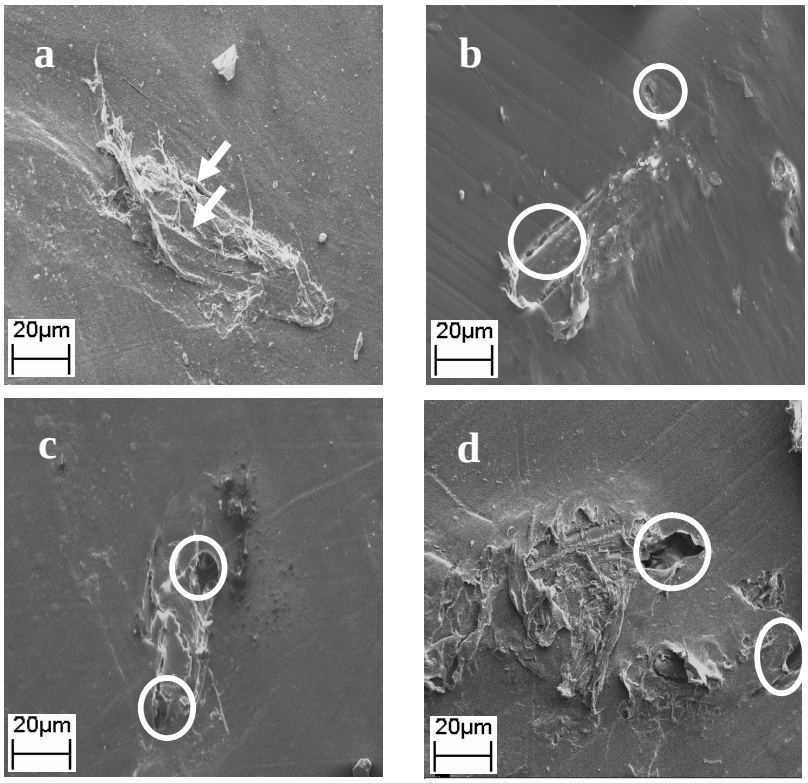

Figure 5.15 SEM micrographs of fractured surfaces of a) composite with unextracted *A. cyclops*, b) composite with *A. cyclops* without E/C extractives, c) composite with *A. cyclops* without HW extractives, and d) composite with *A. cyclops* without both E/C and HW extractives (Mag. 600x).

On the other hand, the lack of adhesion between extracted *A. cyclops* and LLDPE via EVOH resulted poor distribution and prevented the efficient stress transfer to take place during the fractured time, as shown in Figure 5.15b, 6.15c and 6.15d. The micrographs in Figure 5.15a show that there are no voids at the interface between the LLDPE and the unextracted *A. cyclops*, while particles pullout and some voids are visible between the matrix and the all extracted *A. cyclops* (see the circles in Figure 5.15b, 5.15c and 5.15d). The cracks through the wood were observed in the unextracted *A. cyclops* (see the arrows in Figure 5.15a) are good evidence for the strong adhesion between the LLDPE matrix and the *A. cyclops* particles, because stress transmission from the matrix to the wood particles was successful [29-30]. As acknowledged in Sections 2.2.1.4 and 4.4.2, good interfacial adhesion is favourable to the stress transfer across the interface [31].

The most obvious information that could be gleaned from chapters 2 to 5 is that superior properties and better compatibility and interfacial adhesion were found when 7% EVOH and extracted woods were used in wood-LLDPE composite systems. LLDPE with MW 294 000 (used in Chapter 3) was better than LLDPE with MW 137 000 (used in Chapter 5) as a matrix. This is because the properties of composites made with LLDPE with MW 294 000, with exception to the EAB, were better than that of LLDPE with MW 137 000 when using 7% of EVOH as a compatibiliser. For comparison see Tables 3.2, 3.3, 3.7, 5.1 and 5.3.

Furthermore, wood such as *A. cyclops* with a higher cellulose content, an average particle size of 180 µm, a relatively narrow particle size distribution and a lower number of very tiny and oversized particles produced wood-LLDPE composites with superior properties when using EVOH compared to *E. grandis*, *P. radiata* and *Q. alba*. When the hydroxyl groups in EVOH interacts with the hydroxyl groups of the cellulose and the nonpolar part (ethylene) in EVOH interacts with the LLDPE matrix, the resulting contact area between wood particle and LLDPE matrix, via EVOH, plays an enormous and vital role. Optimum particle length and optimum amount of cellulose available in this particular length are expected to obtain a strong adhesion at the contact area with EVOH, while presence of very tiny and oversized particle length affect badly the interaction at the interfaces. Very tiny particles provide imperfect surface area and probably imperfect edges or interfaces at the boundaries with the LLDPE matrix. Also, it has been reported that presences of small amounts of oversized particles in the polymer matrix can cause a significant reduction in toughness [32]. As found in Chapter 3 and 4, that is why the tensile strength properties *Q. alba* composites did not differ greatly from *E. grandis* and *P. radiata*, although the amount of cellulose and the average particle size of *Q. alba* were somehow higher and similar to *A. cyclops* composites. According to all of these,

the effect of the contact area at the interfaces between extracted *A. cyclops* and LLDPE is investigated in the following Chapter (Chapter 6) using different *A. cyclops* particle size with different average particle sizes and different types of EVOH with different alcohol contents.

5.5 Conclusion

The effect of wood extractives on the properties of wood-LLDPE composite systems was studied using 10% wood and 7% EVOH as a compatibiliser. Wood extractives were successfully removed from the four different wood species via Soxhlet extraction and following the Tappi standard T 264 om-88 method. The results illustrated that there are several distinct advantages and drawbacks when using woods without extractives as a filler. The major findings and conclusions of this part can be summarized as follows:

1. The properties of composites made with LLDPE with MW 294 000 (Chapter 3), with exception of the EAB, were better than those made with LLDPE with MW 137 000 when using 7% of EVOH as a compatibiliser.
2. The two extraction methods seem to affect the wood composition by removing greater amount of materials, especially the HW extraction method.
3. Unextracted woods produced composites with better mechanical properties and better resistance to UV radiation, while the extracted woods produced composites with lower WA rates and better thermal stability.
4. The improvement in thermal stability and WA behaviour of composites made with woods without extractives over the composites made with unextracted woods was found to be not due to the improvement in the compatibility and interfacial adhesion between the wood and the LLDPE matrix via EVOH.
    - ❖ The effect of extractives on the thermal stability can be explained by the range in the decomposition temperatures of the wood extractives as also found by Mészáros et al. [22]. The decomposition of extractives occurs over a broad temperature range and in two main stages: the first stage takes place below ±200 ^{o}C and the second stage between ±250 ^{o}C and 550 ^{o}C. Removing some of the cell structure (low MW polysaccharides) and eliminating some inorganic extractives seems to enhance the thermal stability, especially HW extraction method.
    - ❖ The improvement in the WA behaviour is due to the absence of the extractives that dissolve in water.

It can be concluded that using wood without extractives as filler in WPCs cannot be recommended, although they did result in improved thermal properties and a reduced WA rate. Furthermore, from an economic point of view, the reason for reinforcing the polymer

with wood is the low cost of wood, which will definitely be affected by the extraction process. Consequently, use of unextracted wood as a reinforcement in WPC systems is more favourable in terms of mechanical properties, economic aspects and weatherability.

5.6 References

1. Hillis W., Photochemistry, 11, 1207-1218, 1972.
2. De Meijer M., Haemers S., Cobben W., Militz H., Langmuir, 16, 9352-9359, 2000.
3. Kallioinen A., Vaari A., Ratto M., Konn J., Siika-aho M., Viikari L., Journal of Biotechnology, 103, 67-76, 2003.
4. Unger A., Schniewind A., Unger W., Conservation of Wood Artifacts; A Handbook, 1st edition, Springer, Germany, 2001. 37.
5. Hse C., Kuo M., Forest Product Journal, 38, 52-56, 1988.
6. Nachtigall S., Cerveira G., Rosa, S., Polymer Testing, 26, 619-628, 2007.
7. Rowell R., The Chemistry of Solid Wood, 1st edition, American Chemical Society, USA, 1984. 73.
8. Yokoi H., Nakase T., Goto K., Ishida Y., Ohtani H., Tsuge S., Sonoda T., Ona T., Journal of Analytical and Applied Pyrolysis, 67, 191-200, 2003.
9. TAPPI test methods, T 264 om-88 and T 222 om-88, TAPPI Press, Atlanta, 1992.
10. Couhert C., Commandre J., Salvador S., Fuel, 88, 408-417, 2009.
11. Várhegyi G., Granola M., Blasi C., Industrial and Engineering Chemistry Research, 43, 2356-2367, 2004.
12. Mark H., Gaylord N., Encyclopedia of Polymer Science and Technology, Volume 15, Ed. Bikales N., 1st edition, Interscience Publishers, USA, 1971. 1-39.
13. Pejic B., Kosti M., Skundric P., Praskalo J., Bioresource Technology, 99, 7152-7159, 2008.
14. Wan J., Wang X., Li F., Li H., Wang Y., Bioresource Technology, 101, 4577-4583, 2010.
15. Tze W., Wang S., Rials T., Pharr G., Kelley S., Composites: Part A, 38, 945-953, 2007.
16. Hoadley B., Understanding Wood, 1st edition, The Taunton Press, USA, 2000. 12.
17. Cragg S., Danjon C., Williams H., Holzforschung, 61, 201-206, 2007.
18. Hirata S., Ohta M., Homna Y., Journal of Wood Science, 47, 1-7, 2001.
19. Shi-fa W., Ai-jun Z, Forestry Studies in China, 9, 57-62, 2007.
20. Ohtani Y., Mazumder B., Sameshima K., Journal of Wood Science, 47, 30-35, 2001.
21. Di Blasi C., Branca C., Santoro A., Bermudez R., Journal of Analytical and Applied Pyrolysis, 57, 77-90, 2001.
22. Mészáros E., Jakab E., Várhegyi G., Journal of Analytical and Applied Pyrolysis, 79, 61-70, 2007.
23. Ndiaye D., Fanton E., Morlat-Therias S., Vidal L,, Tidjani A., Gardette J., Composites Science and Technology, 68, 2779-2784, 2008.
24. White W., American Mineralogist, 56, 46-53, 1971.
25. Kim J., Yoon T., Mun S., Rhee J., Lee, J., Bioresource Technology, 97, 494-499, 2006.
26. Kim S., Kim S., Kim H., Yang S., Thermochimica Acta, 45, 181-188, 2006.
27. Hristov V., Vasileva S., Macromolecular Materials and Engineering, 288, 798-806, 2003.
28. Choong E., Achmadi S., Wood Fiber and Science. 23, 185-196, 1991.
29. Yang H., Wolcott M., Kim H., Kim S., Kim, H., Composite Structures, 79, 369-375, 2007.
30. Bengtsson M., Oksman K., Composites Science and Technology, 66, 2177-2186, 2006.
31. Cheremisinoff N., Handbook of Engineering Polymeric Materials, 1st edition, CRC Press, USA, 1997. 591-681.
32. Rothon R., Advances in Polymer Science, Volume 139, Mineral Fillers in Thermoplastics I Raw Materials and Processing, Springer, Germany, 1999. 74-91.

Chapter 6
The effect of contact area on the morphogical, mechanical and thermal properties of wood-LLDPE composites

Abstract

The effect of contact area between the wood particles and polymer matrix achieved via the use of compatibilisers on the mechanical and thermal properties of wood-LLDPE composites was studied using different EVOHs with different hydroxyl groups content as compatibilisers and different *A. cyclops* species with different particle sizes and average particle lengths. EVOH with different ethylene contents (27, 32, 38 and 44%) and *A. cyclops* with different particle sizes (180, 250 and 450 µm) were used in this study to prepare *A. cyclops*-LLDPE composites with 10% *A. cyclops* content. The results showed that as the particle size and average particle length of the wood particle increases, EVOH with greater functionality or hydroxyl content is required. The best improvements in the mechanical and thermal properties of composites made with *A. cyclops* with particle size 180 µm were obtained when EVOH with 44% ethylene content was used. The best improvements for the composites made with *A. cyclops* with particle size 250 µm were obtained when EVOH with 38% ethylene content was used. Composites made with *A. cyclops* with particle size 450 µm had superior properties when EVOH with 27% ethylene content was used. Composites made with *A. cyclops* with particle size 180 µm had better properties than composites made with *A. cyclops* with particle sizes of 250 and 450 µm. This is due to the better compatibility and interfacial adhesion in these composites, as shown by FTIR, DMA, fracture surface (SEM), and TGA.

Keywords: *WPCs, EVOH, mechanical properties, thermal properties*

6.1 Introduction

A typical feature of any composite system is the presence of an area of contact or interface between compounds contained in the system [1]. The contact area or interfaces plays a critical role in ensuring that the properties of each component contribute optimally to the bulk properties of the final WPCs [2]. For example, the interaction at the contact area between two solids plays a major role in a large number of physical properties and engineering applications [3]. It is well known that the presence of compatibilisers leads to the creation of new structure at an interface, which subsequently influences morphology, crystallisation, rheology, mechanical, thermal, and other properties of WPCs [4-5].

It is very important to study the contact area or interfaces and their effect on the properties of composites. This becomes more important when compatibilisers with a high number of attached functional groups, such as EVOH, are used with woods with a broad particle size or higher average particle length. Wood is a heterogeneous material, and surface irregularities can affect the interaction in the contact area between the wood particles and polymer matrix when a compatibilizer is used.

As stated in Section 4.4.3, the presence of very small or short particles of *Q. alba* provides imperfect surface area and probably imperfect edges or interfaces at the boundaries with a LLDPE matrix. This is because the size of the contact surface area between the LLDPE and the *Q. alba* particles, via EVOH, is not optimised. It is known that the specific surface area, which depends on the average particle size and/or length of the filler, determines the size of the contact surface between the polymer and the filler [6]. Increasing the surface area leads to an increase in the hydroxyl groups availability. The availability of more hydroxyl groups on the surface of the wood can promote better bonding between the compatibilisers and the wood particles. Promoting better bonding between the compatibilisers and the wood particles could be dependent on the structure of the compatibilisers, the size and/or length of wood particles, and on the number of functional groups of both the wood and the compatibilizer. Wood particles with different length and size would have different interactions at interfaces with EVOH. Most importantly, long particles with a specific diameter interact better than short particles with the same diameter.

Thus, in this part of the study, an attempt was made to investigate the effect of the contact area or interface on the properties of wood-LLDPE composite systems when EVOH was used as compatibilizer and *A. cyclops* as a filler. EVOHs with different hydroxyl group contents and *A. cyclops* with different particle sizes and different particle lengths were used in this part. Each wood-LLDPE composite system was prepared with 7% EVOH and 10% wood content. IM was used to achieve optimal dispersion of wood species and optimises the properties of the composites, as discussed in Section 2.3.

6.2 Experimental

6.2.1 Materials

A. cyclops with different particle sizes (180, 250 and 450 µm) was used here as a reinforcing filler (supplied by the Department of Forest and Wood Science at Stellenbosch University). The matrix polymer LLDPE, with butene as comonomer and average MW 137 000, was supplied by Sasol Polymers (South Africa). EVOHs (Sigma-Aldrich) with different ethylene

content were used as compatibilizers: (a) EVOH with a melt index of 3.90 g/10 min and 27% ethylene content (EVOH27), (b) EVOH with a melt index of 3.80 g/10 min and 32% ethylene content (EVOH32), (c) EVOH with a melt index of 3.80 g/10 min and 38% ethylene content (EVOH38), and (d) EVOH with a melt index of 3.50 g/10 min and 44% ethylene content (EVOH44). A mixture of Irganox 1010 and Irgafos stabilisers (Sasol Polymers) was used to inhibit degradation during the preparation of the WPCs.

Table 6.1 Abbreviations and compositions of the composites used in this study

Composite	LLDPE, %	EVOH, %	*A. cyclops*, %	Type of EVOH	*A. cyclops* particle size, µm
LLDPE	100	0	0	---	---
27E180	83	7	10	EVOH27	180
32E180	83	7	10	EVOH32	180
38E180	83	7	10	EVOH38	180
44E180	83	7	10	EVOH44	180
27E250	83	7	10	EVOH27	250
32E250	83	7	10	EVOH32	250
38E250	83	7	10	EVOH38	250
44E250	83	7	10	EVOH44	250
27E450	83	7	10	EVOH27	450
32E450	83	7	10	EVOH32	450
38E450	83	7	10	EVOH38	450
44E450	83	7	10	EVOH44	450

The composite preparation method was described earlier in Section 3.2.2. Abbreviation as assigned to the different composites and their compositions are given in Table 6.1. Specimens for mechanical and thermal properties were prepared using injection moulding (Haake MiniJet Piston Injection Moulding, Germany). The processing conditions for the injection moulding were as follows: (1) injection temperature: 170-200 °C, (2) mould temperature: 60-90 °C, (3) injection pressure: 450-650 bar, and 4) cooling time: 30 s.

6.2.2 Characterisation

The following analytical equipment were used in this study: EZ4D microscope, tensile tester, microhardness tester, and DMA, DSC, TGA, OM and FTIR apparatus (as described in Section 3.3); SEM (as described in Section 4.3); and impact tester (as described in Section 5.3). Three injection moulding specimens (5 mm x 50 mm x 1.5 mm) of each composite were tested for their tensile strength, elongation at break and impact strength. Ten hardness measurements were taken from the surface of the injection moulding specimens (20 mm diameter and 1.5 mm thickness) of each composite. Specimens for morphological and fracture surface studies were pressed films as described in Section 3.3.6 and Section 4.3.

6.3 Results and discussion

6.3.1 Wood particle size

Table 6.2 lists the average, minimum and maximum particle lengths of the *A. cyclops* species of 180, 250 and 450 µm particle sizes. Standard deviations are given in parentheses. Each particle size of *A. cyclops* showed clear variation in the length.

Table 6.2 Morphological properties of the *A. cyclops* particles

A. cyclops with particle size, µm	Minimum particle length, mm	Maximum particle length, mm	Average particle length, mm
180	0.045	1.309	0.225 (0.2)
250	0.078	3.140	1.220 (0.6)
450	0.600	9.060	3.240 (1.6)

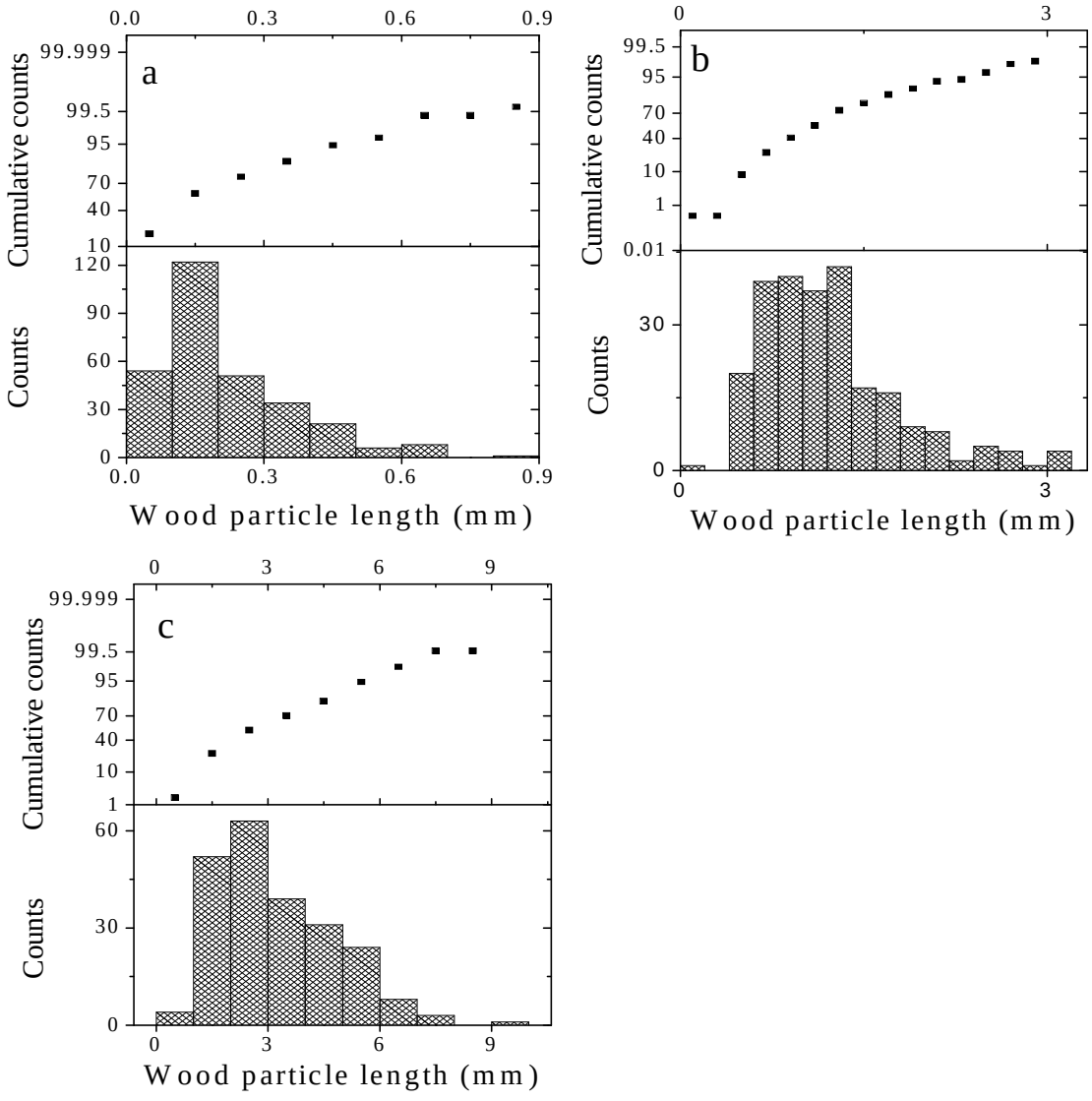

Figure 6.1 Histograms of average particle lengths and cumulative length distribution for *A. cyclops* with particle sizes of a) 180 µm, b) 250 µm and c) 450 µm.

Greater variation in the particle lengths was observed for the *A. cyclops*, with a particle size of 250 µm, as indicated by the cumulative counts curves in Figure 6.1. As it can be seen in Figure 6.1, more cumulative event counts were observed in the *A. cyclops* with particle size of 250 µm than in others. The cumulative distribution is derived by software integration. *A. cyclops* particles with particle size 180 µm comprised 55, 40, 4 and 1% of particles with lengths of 0.05-0.2, 0.2-0.5, 0.5-0.7 and > 0.7 mm, respectively. *A. cyclops* particles with particle size 250 µm contained about 36, 54, 8 and 2% wood particles with lengths of 0.08-0.9, 1-2, 2-3 and 3.1-3.2 mm, respectively. The majority (29%) of the *A. cyclops* particles with particle size 450 µm had a length of 2-3 mm. About 2, 23, 17, 0.5, 13, 11, 3.5 and 1% of *A. cyclops* particles with particle size 450 µm had lengths of 0.6-0.9, 1-2, 3-4, 4-5, 5-6, 6-7, 7-8 and 9-10 mm, respectively.

6.3.2 Distribution of wood particles

The OM images in Figures 6.2, 6.3 and 6.4 show that wood particles were randomly oriented and twisted in the LLDPE matrix in all the composites. These figures also illustrate the difference in the particle lengths in these composites. Wood particles in Figure 6.4 are longer than those in Figures 6.3 and 6.2. This supports the results reported in Section 6.3.1. 44E180 in Figure 6.2 appears to have better distribution of wood than 27E180, 32E180 and 38E180 in the cases of composites made with *A. cyclops* with particle size of 180 µm.

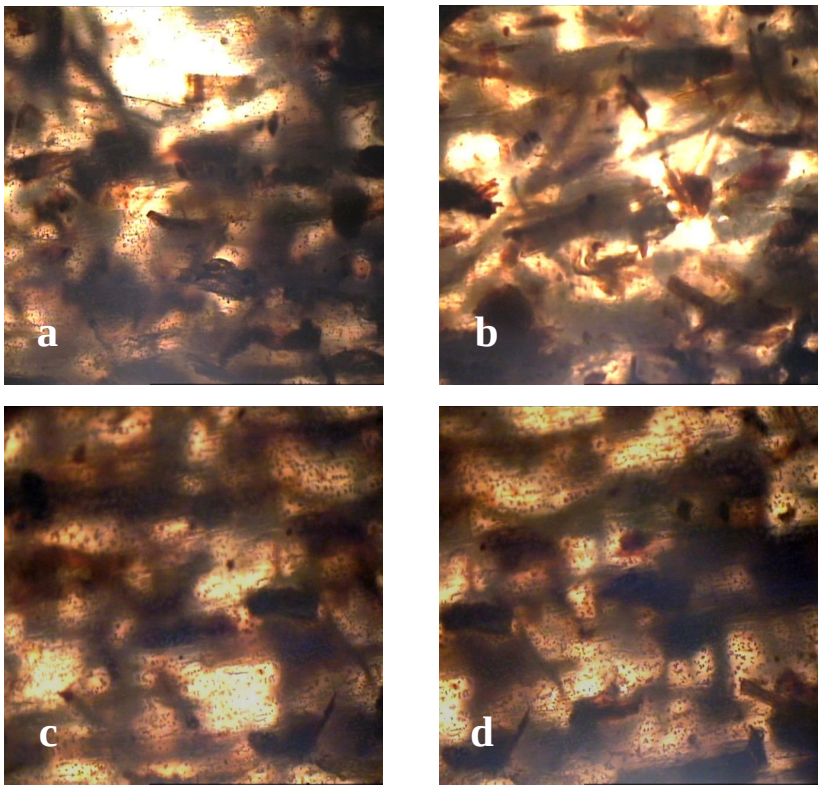

Figure 6.2 Optical micrographs of a) 27E180, b) 32E180, c) 38E180 and d) 44E180 (500X).

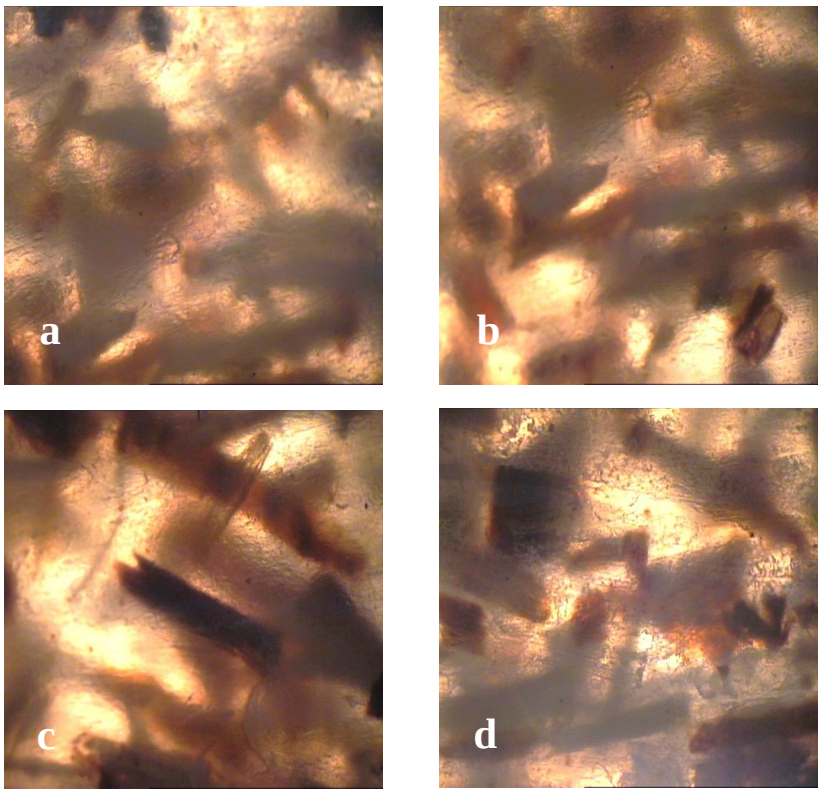

Figure 6.3 Optical micrographs of a) 27E250, b) 32E250, c) 38E250 and d) 44E250 composites (500X).

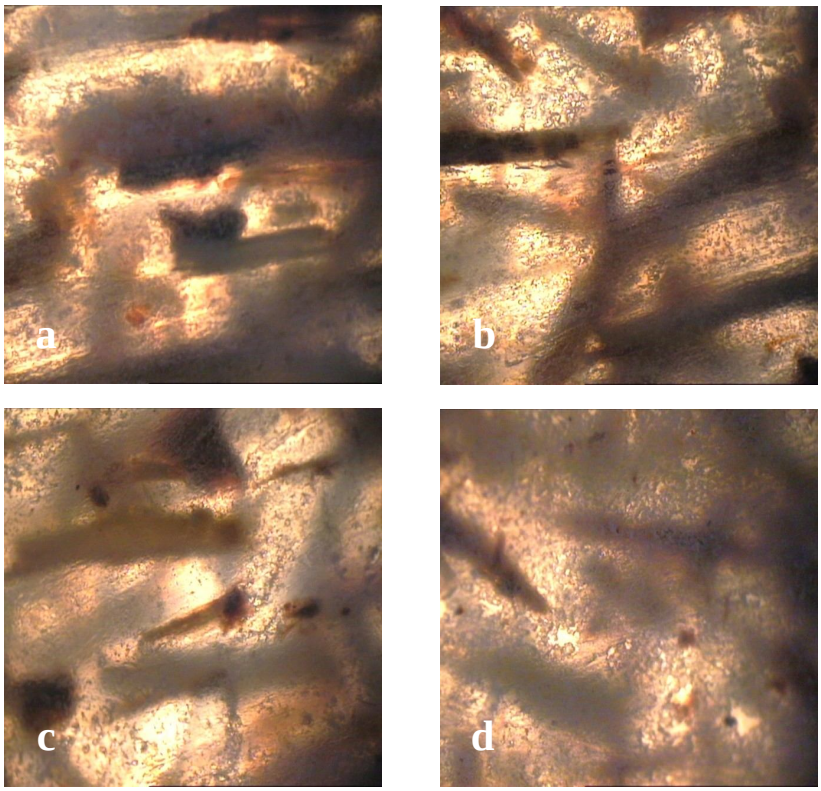

Figure 6.4 Optical micrographs of a) 27E450, b) 32E450, c) 38E450 and d) 44E450 composites (500X).

The OM images in Figure 6.3 indicate that 38E250 has better particle size than 27E250, 32E250 and 44E250 in the cases of composites made with *A. cyclops* with particle size 250 µm, and 27E450 has the best distribution of wood in comparison to 32E450, 38E450 and 44E450 in the cases of composites made with *A. cyclops* with particle size 450 µm. These morphological observations demonstrated the following. The presence of EVOH44 enhanced the compatibility and interfacial adhesion more than the other EVOHs in the in the cases of composites made with *A. cyclops* with particle size of 180 µm. EVOH38 was the best choice for enhancing the compatibility and interfacial adhesion in the cases of composites made with *A. cyclops* with particle size of 250 µm. EVOH27 has the ability to impart more compatibility and stronger interfacial adhesion than other EVOHs in the cases of composites made with *A. cyclops* with particle size of 450 µm. These morphological differences are responsible for the difference in the mechanical and physical properties of these composites.

6.3.3 Mechanical properties

Table 6.3 lists the mechanical properties, such as tensile strength, EAB, hardness and impact strength, of the LLDPE and wood-LLDPE composites. These properties provide an excellent measure of the degree of reinforcement provided by the wood particles to the composite [7].

Table 6.3 Tensile strength, EAB, hardness and impact strength of the LLDPE and wood-LLDPE composites

Composite	Tensile strength, MPa	EAB, %	Hardness, MPa	Impact strength, J/m^2
LLDPE	11.8 (0.7)	> 100.0	2.1 (0.7)	2983.0 (1.0)
27E180	11.6 (0.2)	11.5 (0.4)	3.2 (0.4)	710.2 (0.1)
32E180	13.9 (0.1)	11.8 (0.3)	2.4 (0.5)	757.6 (0.1)
38E180	16.2 (0.5)	14.9 (0.2)	2.6 (0.5)	807.9 (0.1)
44E180	18.2 (0.3)	15.9 (0.4)	2.6 (0.8)	852.3 (0.0)
27E250	11.3 (0.5)	12.3 (0.3)	2.3 (0.7)	804.9 (0.1)
32E250	12.6 (0.5)	12.1 (0.2)	2.4 (1.0)	710.2 (0.1)
38E250	13.9 (1.3)	13.1 (0.7)	2.7 (1.3)	852.3 (0.2)
44E250	13.0 (0.7)	12.1 (0.2)	2.5 (0.5)	757.6 (0.2)
27E450	17.0 (0.2)	14.9 (0.2)	2.7 (1.0)	899.6 (0.1)
32E450	11.2 (0.2)	11.1 (0.1)	2.6 (0.8)	662.9 (0.1)
38E450	12.2 (0.2)	11.8 (0.2)	2.8 (1.3)	757.6 (0.1)
44E450	13.1 (0.7)	12.2 (0.2)	2.8 (1.3)	804.9 (0.1)

Standard deviations are given in parentheses

Overall, 44E180, 38E250 and 27E450 exhibited better mechanical properties than the others. The higher tensile strength of 44E180, 27E250 and 44E450 is an indication of interaction between *A. cyclops* and LLDPE with accompanied transfer of stress from the weaker LLDPE to the *A. cyclops* through the interface [8]. Composites made with *A. cyclops* with particle size

180 µm showed an increase in the tensile properties as the content of hydroxyl groups in EVOH decreases from 27E180 to 44E180. Composites made with *A. cyclops* with particle size 250 µm showed an increase in the tensile values as the number of hydroxyl groups in EVOH decreases from 27E250 to 32E250 to 38E250 and then decrease in the case of 44E250. In the cases of composites made with *A. cyclops* with particle size 450 µm, the tensile values of 27E450 were higher than those of 32E450, 38E450 and 44E450. Indications are therefore that the tensile strength depends on the shape of the wood particle [9] and the chemical structure of the compatibilizer.

Table 6.3 also shows the expected decrease in the EAB of the composites in comparison to pure LLDPE. This behaviour is typical of reinforced thermoplastics and has been reported by many researchers [7, 10-11]. EAB and tensile strength trends of the composites (see Figure 6.5) were similar, especially in the cases of composites made with *A. cyclops* with particle sizes 180 and 450 µm. 44E180 exhibited higher EAB in the case of composites made with *A. cyclops* with particle size 180 µm, while 27E450 showed to have higher EAB in the case of composites made with *A. cyclops* with particle size 450 µm. There is not significant difference in EAB for 27E180 and 32E180. The composites made with *A. cyclops* with particle size 250 µm did not follow the trend of their tensile strength, 38E250 has the highest EAB. There is no significant difference in EAB between 27E250, 32E250 and 44E250. Also, there is no much difference in EAB between 32E450, 38E450 and 44E450. The higher EAB values of 44E180, 38E250 and 27E450 may be due to improved dispersion and good interfacial adhesion between filler and matrix in these composites [12-13].

Most of the composites were harder than pure LLDPE. As shown in Table 6.3, there is a little increase in the hardness values of the composites with increasing wood content. Similar to the EAB, the impact properties of these composites showed an inverse relationship to the tensile strength and hardness, as shown in Figure 6.5. Impact properties decreased drastically upon the addition of wood. This is because fillers and reinforcements reduce the polymer chain mobility and thereby reduce the ability to absorb energy during fracture propagation [14]. Impact results followed a similar trend as the EAB results (see Figure 6.5), as expected, as a high fibre elongation capability leads to high impact strength [15]. The impact value of 44E180 was higher than those of 27E180, 32E180 and 38E180. In the case of composites made with *A. cyclops* with particle size 250 µm, the impact value of 38E250 was higher than those of 27E250, 32E250 and 44E250, while the impact value of 27E450 was higher than those of 32E450, 38E450 and 44E450 in the case of composites made with *A. cyclops* with particle size 450 µm.

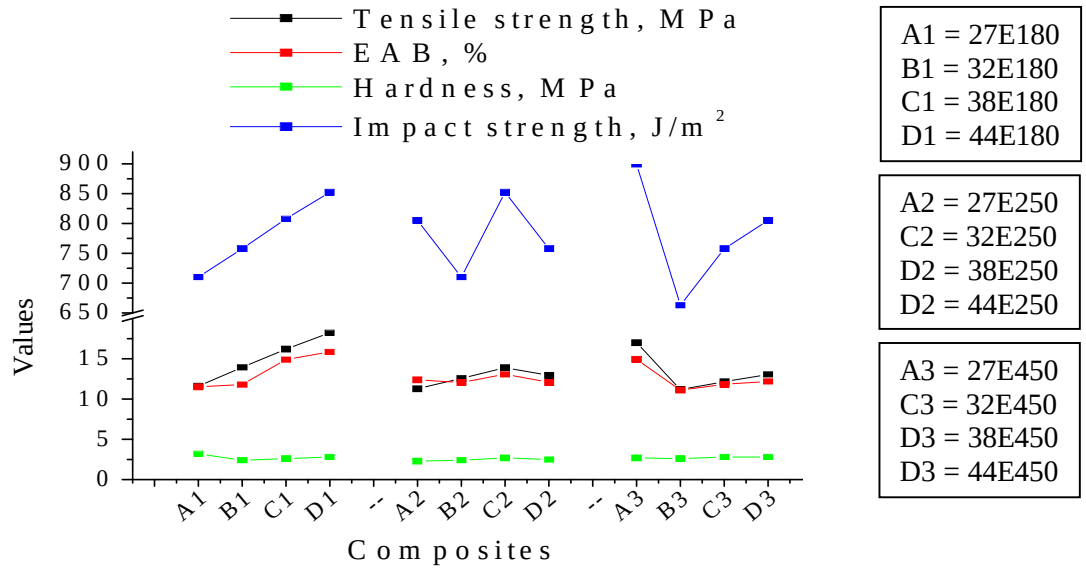

Figure 6.5 Comparison of mechanical properties of wood-LLDPE composites.

6.3.4 Stress-strain curves

A comparison of the stress-strain curves of LLDPE and the wood-LLDPE composites, obtained by extension DMA, is shown in Figure 6.6. In comparison to the tensile strength results, the values in the respective figures seem to be different to the tensile strength values tabulated in Table 6.3, but the trends remain similar. Figure 6.6 shows that LLDPE behaves as a ductile polymer, with a yield point and higher EAB. The addition of *A. cyclops* to LLDPE in the presence of all types of EVOH changed the manner of failure and decreased the ductility. Rowell [16] mentioned that increasing the toughness of wood with polymer increases the crack resistance and brittleness. Addition of fillers into a polymer matrix reduces the ductility [17-18]. Composites became stiffer with the addition of *A. cyclops* species and EVOH, but the corresponding strain at failure decreased. 38E180, 32E180 and 27E180 were stiff and strong but not tough, while 27E180 can be considered strong, stiff and tough. This is because the area under the stress-strain curve of 44E180 is larger than the area under the stress-strain curves of 38E180, 32E180 and 27E180. This indicates that 44E180 can absorb much more energy than 38E180, 32E180 and 27E180 before breakdown. As a result, 44E180 elongated more before breaking than 38E180, 32E180 and 27E180 did. More elongation or deformation indicates more ductility.

The same concepts and explanation can be applied in the cases of composites made with *A. cyclops* with particle size 250 µm between 38E250 and other composites (27E250, 32E250 and 44E250) and between 27E450 and 32E450, 38E450 and 44E450 in cases of composites made with *A. cyclops* with particle size 450 µm. This is very important because the most preferred compatibilizer is that which considerably increases both toughness and ductility

through enhanced particle to matrix adhesion and the formation of a distinct tough interface. Conversely, these composites can be weak and brittle if the compatibilizer is not effective [19].

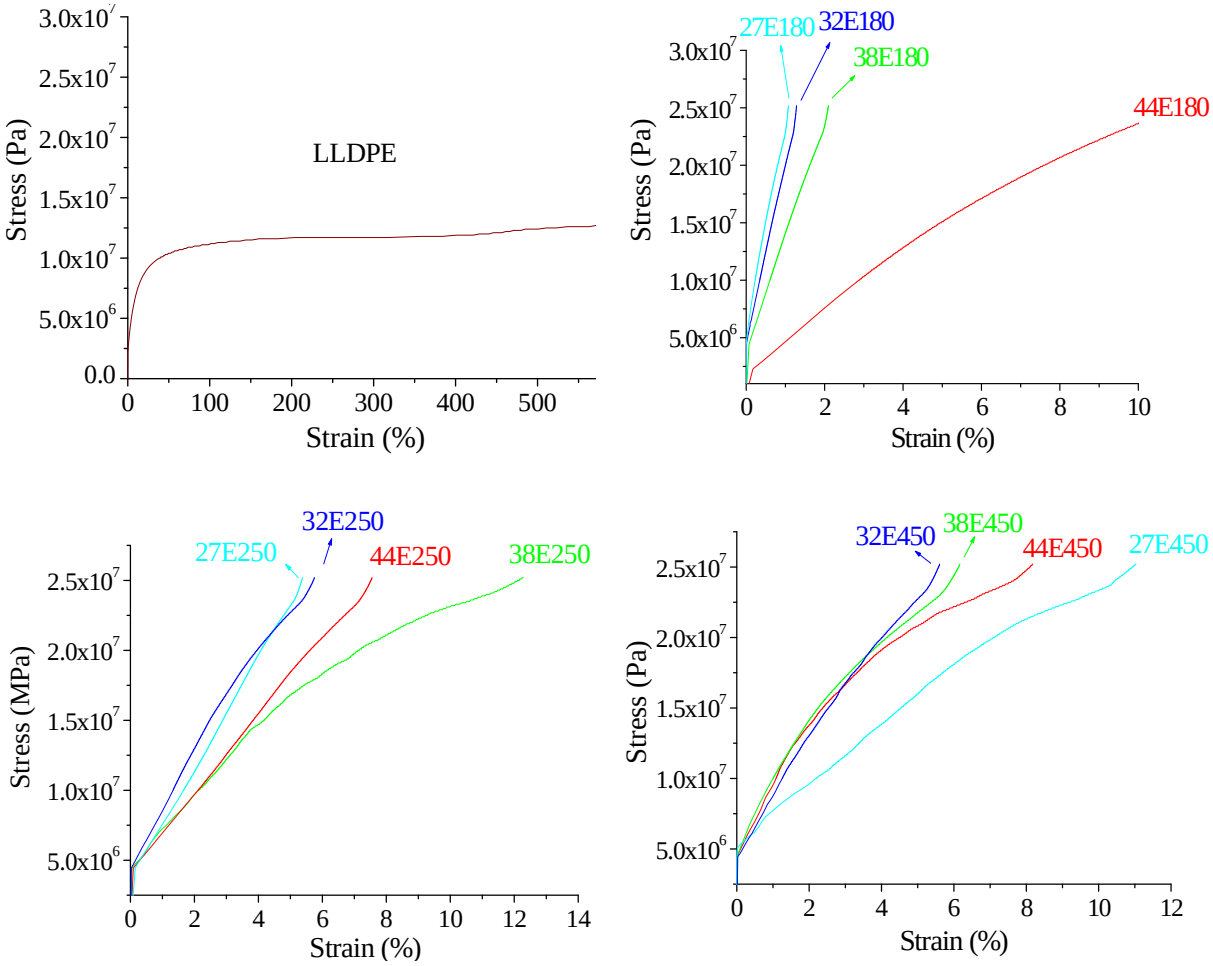

Figure 6.6 Stress-strain curves of LLDPE and the wood-LLDPE composites obtained from extension DMA.

6.3.5 Thermal behaviour

6.3.5.1 DSC results

Table 6.4 lists the T_m, T_c, ΔH_f, X_c and X_c^{corr} values for neat LLDPE and the wood-LLDPE composites. The value of 288.7 J/g was taken as a value of the ΔH_f^o of completely crystalline PE [20]. Crystallisation and melting curves of LLDPE and wood-LLDPE composites are shown in Appendix C.

As reported in Chapters 3 and 5, wood-LLDPE composites showed lower X_c than the neat LLDPE. There is no significant difference in the X_c of these composites. Composites made with *A. cyclops* with the same particle size (180 μm) showed no tendency, and a negligible difference, in the X_c, as the EVOH changes from EVOH27 to EVOH32 to EVOH38 to

EVOH44. In other words, using different EVOHs as compatibilizers and changing the wood particle size seems to have little or no influence on the melting and crystallisation behaviour of the obtained composites. A slight increase in the T_c and an insignificant decrease in the T_m in all the composites were observed.

The X_c^{corr} was generally slightly higher than X_c and X_c^{corr} of LLDPE. The X_c^{corr} of each composite was somehow higher than its X_c. Similar findings have been reported by Marcovich and Villar [20]. They related this slight increment to the nucleation effect of the wood species, as mentioned in Section 2.2.1.4. This increment was exhibited by all the composites. It is considered to be independent of the degree of compatibility between the filler and the matrix.

Table 6.4 DSC results of LLDPE and wood-LLDPE composites

Composite	T_c, °C	T_m, °C	ΔH_f, J/g	X_c, %	X_c^{corr}, %
LLDPE	105.7	124.1	108.2	37.5	37.5
27E180	109.1	122.0	92.0	31.9	38.4
32E180	110.7	122.9	94.2	32.6	39.3
38E180	109.8	121.8	92.4	32.0	38.5
44E180	107.9	120.5	95.7	33.1	39.9
27E250	107.7	121.6	91.4	31.7	38.1
32E250	107.9	121.7	96.1	32.5	39.1
38E250	110.6	122.5	93.7	33.3	40.1
44E250	109.1	122.0	90.5	31.4	37.8
27E450	110.4	122.4	90.8	32.4	39.1
32E450	107.5	120.6	87.4	30.3	36.5
38E450	110.7	122.7	93.6	31.4	37.9
44E450	109.9	123.5	90.3	31.3	37.7

The X_c values of 44E180, 38E250 and 27E450 were slightly higher than the others, suggesting that the proper compatibilizer to enhance the interfacial adhesion of the composites made with particle size 180 μm is EVOH44, while EVOH38 is the best in the cases of composites made with particle size 250 μm. Finally, EVOH27 can be considered the best in the cases of composites made with particle size 450 μm. A similar explanation was proposed by Kim at al. [21] about the increase in the X_c values of the composites.

6.3.5.2 TGA results

Figures 6.7 and 6.8 show the TGA and DTG curves of the LLDPE and wood-LLDPE composites. Typical degradation steps were observed: one degradation step for LLDPE and two degradation steps for each composite.

The TGA spectra of the composites were shifted to higher temperature, in comparison to neat LLDPE (Figure 6.7). This indicates that the thermal stability and degradation temperatures of the composites were higher than that of neat LLDPE.

Table 6.5 Thermal degradation temperatures of the composites

Composite	First degradation step, ^{o}C	Second degradation step, ^{o}C
LLDPE	--------	464.9
27E180	237.5	512.1
32E180	239.0	517.2
38E180	241.8	522.2
44E180	248.4	526.0
27E250	231.4	510.6
32E250	234.0	512.7
38E250	241.5	517.8
44E250	234.3	513.8
27E450	236.1	516.1
32E450	236.5	514.7
38E450	233.1	508.0
44E450	229.9	507.6

In Figure 6.8, LLDPE had a large and board DTG peak at 465 ^{o}C. This confirms the presence of only one degradation step, due the decomposition of the C-C bonds in the main chain of LLDPE. In all the composites, very small and broad peaks occurred before 100 ^{o}C due to the evaporation of water. Small peaks occurred at about 229-248 ^{o}C (first degradation step, middle of this peak), and large and rather sharp peaks at 500-525 ^{o}C (second degradation step, middle of this peak).

The first degradation step below 300 ^{o}C is due to the decomposition of individual wood components, such as hemicelluloses and the onset of lignin and extractives. The second degradation step between 400 and 550 ^{o}C is due to the decomposition of cellulosic materials in the wood and the C-C bonds in the main chain of LLDPE. The first and second degradation temperatures of LLDPE and each composite are shown in Table 6.5.

Results indicate that using different EVOHs with different hydroxyl content as a compatibiliser in the *A. cyclops*-LLDPE composite system improved the thermal stability of the composites. Furthermore, 44E180, 38E250 and 27E450 showed improved thermal stability than others due to the enhanced interfacial adhesion in these composites. Finally, composites with particle size 180 µm were somehow more stable than composites with particle sizes 250 and 450 µm.

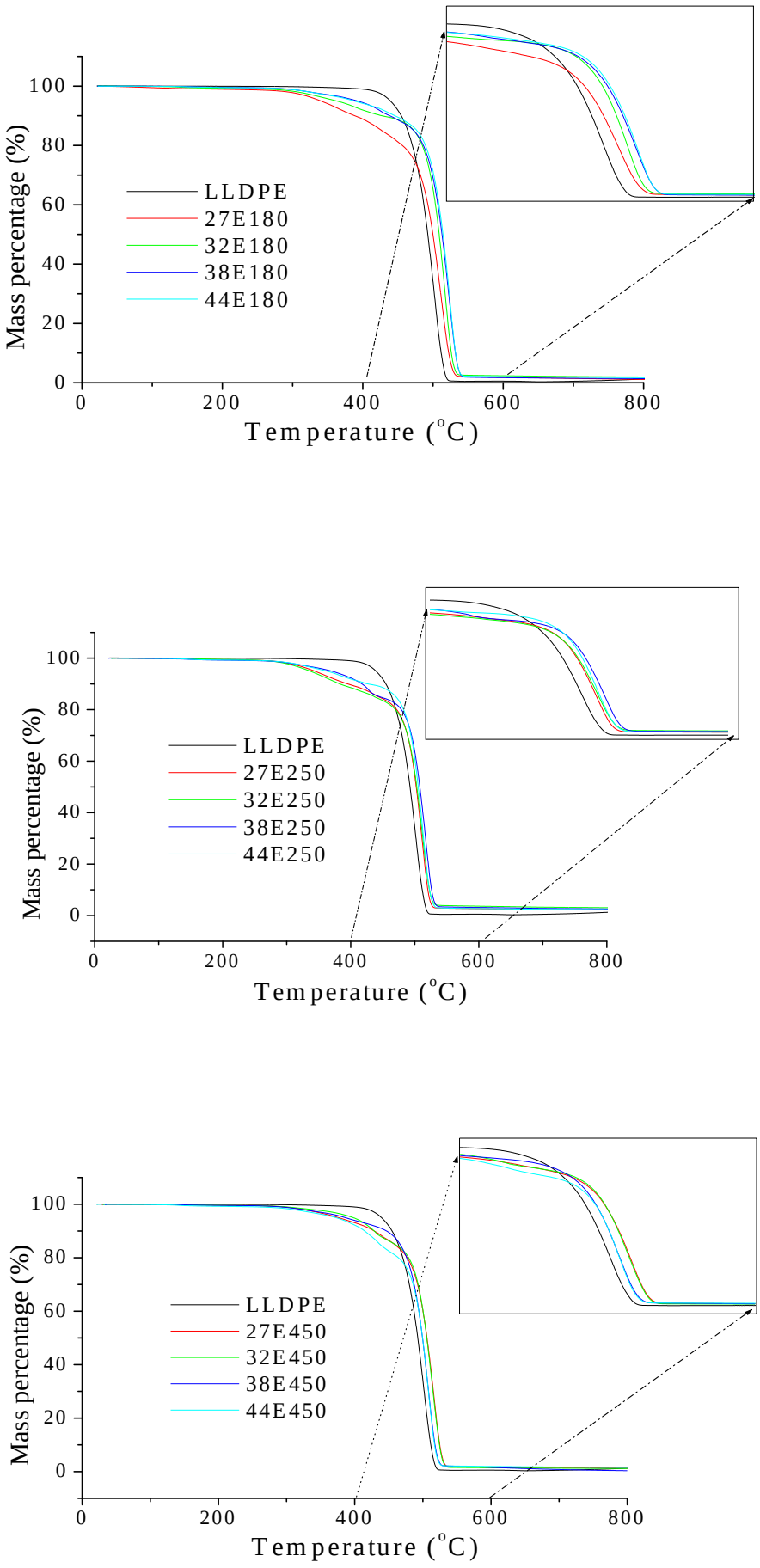

Figure 6.7 TGA curves of LLDPE and the composites.

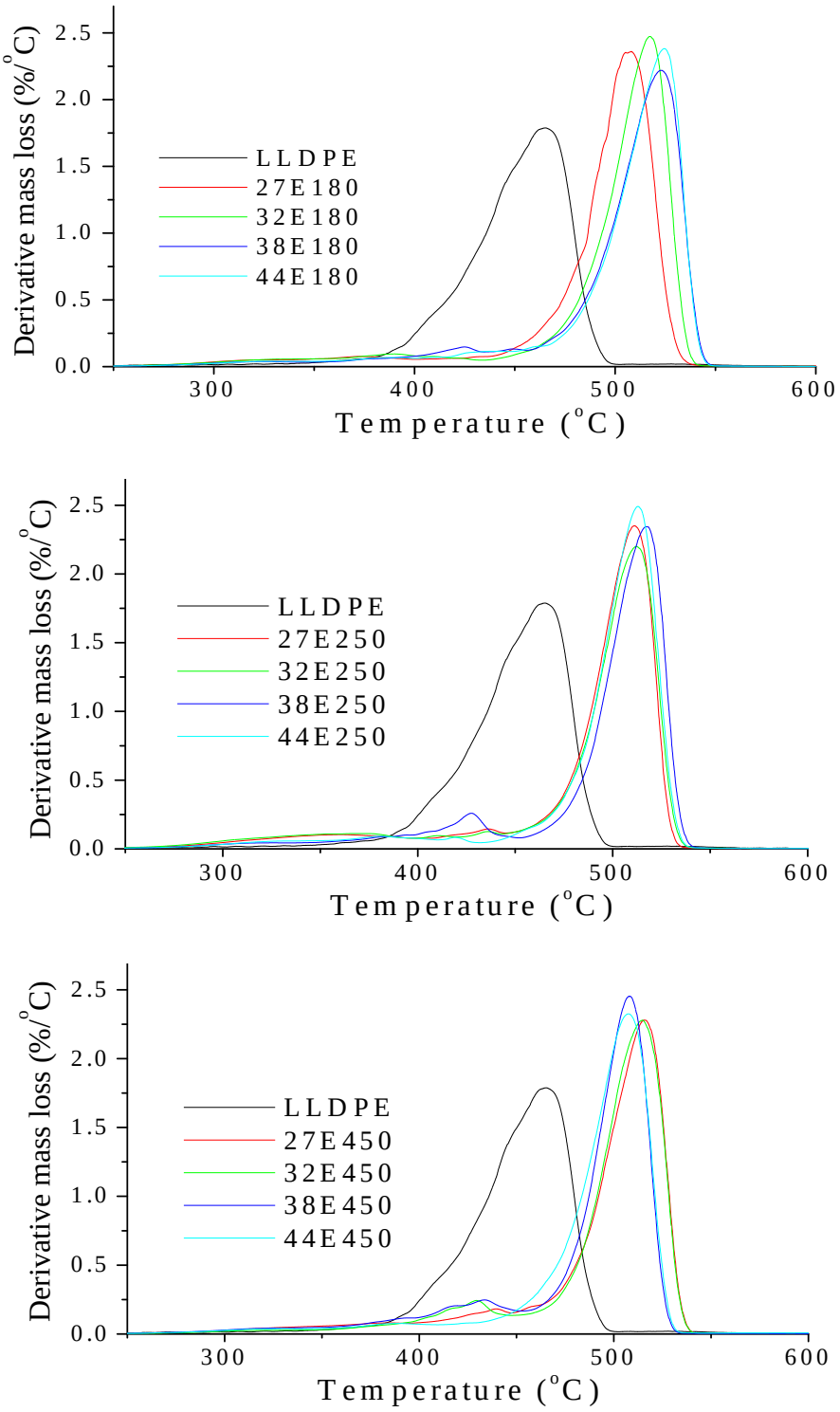

Figure 6.8 DTG curves of LLDPE and the composites.

All the results above indicate that the size and length of *A. cyclops* particles, and their distribution, play a dominant role in the ultimate mechanical and thermal properties of the composites, since the amounts of LLDPE matrix and compatibiliser used were the same. The differences in each case were the size and length of *A. cyclops* particles and the number of hydroxyl group on EVOH. The best mechanical and thermal properties were obtained when EVOH44 was used as a compatibiliser in the cases of composites made with *A. cyclops* with

particle size 180 µm and average particle length of 0.225 mm, when EVOH38 was used as a compatibiliser in the cases of composites made with *A. cyclops* with particle size 250 µm and average particle length of 1.220 mm and when EVOH27 was used as a compatibiliser in the cases of composites made with *A. cyclops* with particle size 450 µm and average particle length of 3.24 mm. This is because EVOH44 and *A. cyclops* particles with particle size 180 µm had more possible interaction sites, which means that a larger number of bonds could form on a unit surface of the wood. This in turn led to better improvement in the compatibility, a strong contact area at interfaces and better stress transfer. The same explanation can be given for EVOH38 in the cases of composites made with *A. cyclops* with particle size 250 µm and for EVOH27 in the cases of composites made with *A. cyclops* with particle size 450 µm. According to Dányádi et al. [22], functionalised polymer or compatibiliser, such as MAPP, should have an optimum number of functional groups in order to improve the interfacial adhesion. They also claimed that the availability of the hydroxyl groups of cellulose can depend on the wood particle size.

It should be emphasised here that the pressed 44E180 (composites with EVOH with 44% ethylene content and *A. cyclops* with particle size of 180 µm) that was used in Chapter 5 had different properties to similar composites made by IM. Pressed 44E180 (see Table 5.1) had lower tensile strength (17.5 MPa) and EAB (15.0%) than IM 44E180 (tensile strength 18.2 MPa and EAB 15.9%), as shown above in Table 6.3. IM 44E180 exhibited better thermal stability than pressed 44E180. According to the main peak in the DTG spectra in Figure 5.7 and 6.9, the second degradation step occurred at 525 ^{o}C for the IM composite, but at 519 ^{o}C for the pressed composite. The better properties of the IM composites can be due to density, variation in the structure (wood particles alignment) and surface quality [23]. In WPCs, mechanical properties generally increase with increasing density. The higher density of IM samples resulted in more intimate contact between the components in the composite [24]. The difference in the strength and EAB between pressed 44E180 and IM 44E180 seem to be influenced also by the difference in the sample dimensions. On the other hand, the pressed composite was harder (2.8 MPa, see Table 5.1) than the IM composite (2.6 MPa, see Table 6.3). This is because IM composites are smooth and have polymer-rich surfaces, while pressed composites have fibre-rich surfaces [23].

There were distinctive differences between the results for composites containing *A. cyclops* with different particle sizes. Use of *A. cyclops* with small particles (180 µm) yielded composites with improved mechanical and thermal properties, more so than *A. cyclops* with larger particle sizes (250 and 450 µm). According to Salemane and Luyt [25], fine or small

filler particles improve the mechanical properties of polymer composites more than large ones. The only drawback to the use of finer particles is their tendency to agglomerate. It is known that the specific surface area, which depends on the average particle size/length of the filler, determines the size of the contact surface between the polymer and the filler [6]. So, the behaviour of the small particles provides a suitable surface or contact area and enhances compatibility and interfacial adhesion between the wood and polymer matrix. This is essential to transfer stress from the matrix to the wood particles and thus improve the mechanical strength of composites. The effect of small particles can be true to some extent. This is because very small or tiny particles induce the separation or debonding at the interfaces [22], as found in Chapter 4. Differences in the compatibility and interfacial adhesion between 44E180, 38E250 and 27E450 were then studied using FTIR, DMA and SEM analysis for fractured surface composites.

6.3.6 Compatibility and interface adhesion

As was described in Chapter 3 and illustrated below in Figure 6.9a, the hydroxyl stretching band of pure *A. cyclops* was centred at 3362 cm^{-1}. According to the FTIR spectra (Figure 6.9), hydroxyl stretching bands were shifted and centred at higher frequency, which is attributed to the distribution and presence of hydrogen bonds.

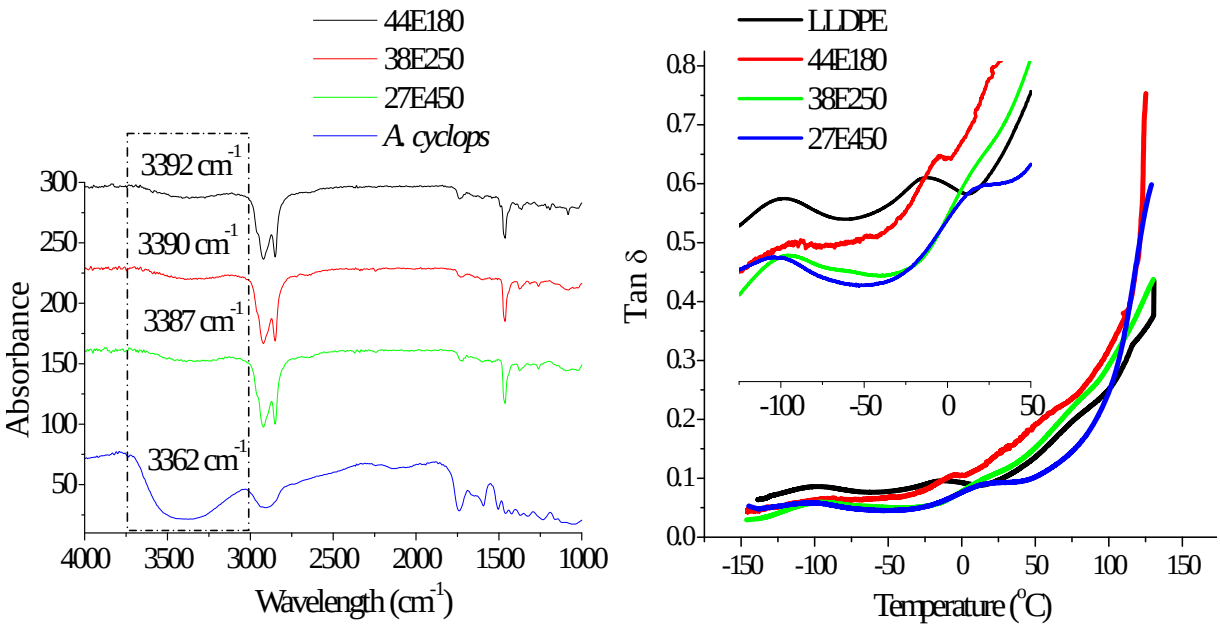

Figure 6.9 a) FTIR results of *A. cyclops* and composites and b) DMA results of LLDPE and composites.

These bands were centred at 3392, 3390 and 3387 cm^{-1} for 44E180, 38E250 and 27E450, respectively. This indicates that the formation of hydrogen bonds between wood and EVOH are higher in 44E180 than in 38E250 than in 27E450, respectively. This explains the relatively

better properties and performance of 44E180 in comparison to the others (38E250 and 27E450). It should be noted here that the hydroxyl stretching band of the pressed 44E180 was centred at 3377 cm^{-1}, as shown in Figure 5.13a, while the hydroxyl stretching band of the IM 44E180 was centred at 3392 cm^{-1}, as shown in Figure 6.10a. This is most likely due to the difference in density [24].

DMA results confirmed the FTIR results about the compatibility of the three composites (see Figure 6.9b and Table 6.6). Table 6.6 shows that the γ-transition or T_g and β-transition of the composites were shifted to higher temperatures in comparison to pure LLDPE. The γ-transition and β-transition of 44E180 were shifted to higher temperature more than 38E250 and 27E450. This is due to the better compatibility and strong adhesion between wood and the LLDPE matrix of 44E180.

Table 6.6 Summary of tan δ peak temperature at γ-transition and β-transition of LLDPE and composites

Composite with	Tan δ peak temperature at γ-transition or T_g, ^oC	Tan δ peak temperature at β-transition, ^oC
LLDPE	-104.8	-12.0
27E180	-89.5	-05.0
38E250	-98.4	-06.2
27E450	-97.3	-07.8

SEM micrographs of fractured surfaces of these composites are shown Figure 6.10. Cracks were observed through the wood particles for 44E180 and 38E250, indicating that stress were successfully transferred from the weaker LLDPE matrix to the stronger wood particles. Once again, this proof of the good compatibility and strong adhesion between the LLDPE matrix and the *A. cyclops* particles in these composites. 27E450 seemed to exhibit less compatibility, and lower adhesion between the LLDPE matrix and the *A. cyclops* particles than the 44E180 and 38E250. Although no voids were observed, pull out damage was dominant on the fractured surfaces of the 27E450. Figure 6.10c shows that particles pull out occurred in the case of 27E450 (indicated by arrows) and debonded from one end of the wood particle (see the circle). Debonding stress depends on the particle size, on the stiffness of the matrix, and interfacial adhesion. Large particles can be debonding easily under the effect of external load [22]. Therefore, the reduced properties of the 27E450 in comparison to 44E180 and 38E250 can be caused by the easy debonding of the large particles. This may form voids. These voids will subsequently merge to form catastrophic cracks. SEM micrographs of fractured surfaces

of 27E180, 32E180, 38E180, 27E250, 32E250, 44E250, 32E450, 38E450 and 44E450 are shown in Appendix E.

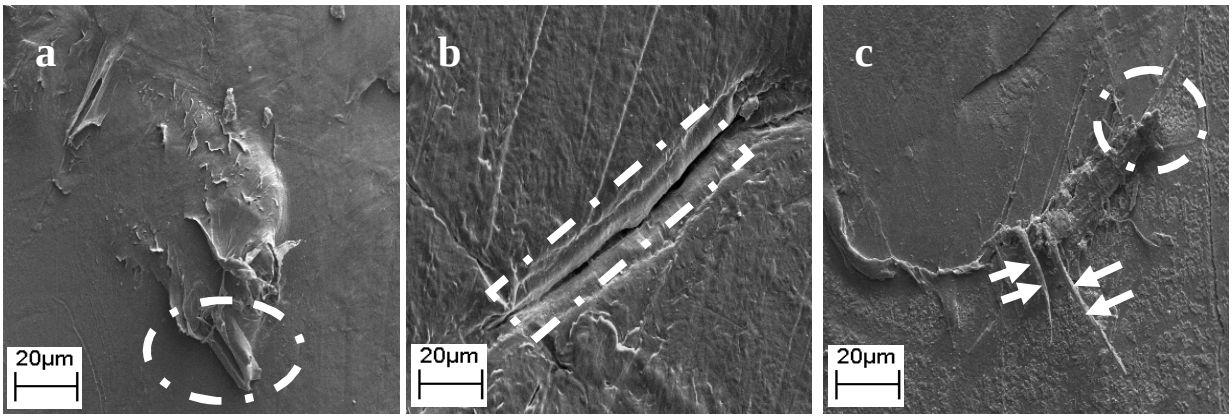

Figure 6.10 SEM micrographs of fractured surfaces of a) 44E180 b) 38E250 and c) 27E450 (Mag. 300x).

The differences in the thermal stability and decomposition temperatures (first degradation step and second degradation step), from the TGA results, as illustrated in Section 6.3.5.2, also supported the findings regarding to the better compatibility of 44E180 in comparison to 38E250 and 27E450. This is because the improvements in the thermal stability of the WPCs can be attributed to improved interfacial adhesion and compatibility between the wood and the polymer matrix due to the effects of the compatibiliser [21, 26-27]. Results indicate that the compatibility and interfacial adhesion are determined by the presence or absence of EVOH, and its functionality. It is not always the higher functionality compatibiliser that can lead to better compatibility and stronger interaction in a WPC system, as is claimed by many researchers and workers [28-29]. According to the results of this study, the effect of the functionality of functionalised polymers such as EVOH is based on the availability and number of hydroxyl groups of the functionalised polymers and the hydroxyl groups on the wood surface. Concurrently, the availability of the hydroxyl groups on the wood surface depends on the wood particle size and/or length.

Many aspects still need to be studied in order to understand more about the effect of different wood species with different macromolecular composition and contents on the properties and performance of WPC systems. The effect of the compatibiliser is addressed in the following Chapter. The possibility of using degraded LLDPE as a new compatibiliser was studied in *A. cyclops*-LLDPE composite system using 10, 30 and 50% *A. cyclops* with particle size 180 µm. To our knowledge, researchers in the field of WPCs tend always to develop and create new compatibilisers and they have not tried to use recycled or degraded materials as compatibilisers. Should the latter prove to be successful, it will impart economic and environmental advantages to these materials.

6.4 Conclusion

The effect of the contact area between the wood and polymer matrix achieved via the use of compatibilisers, on the mechanical and thermal properties of *A. cyclops*-LLDPE composites was studied using different EVOHs with different hydroxyl contents and different *A. cyclops* species with different particle sizes and average particle lengths. The effects of the particle size and average particle length were significant. The compatibility and interfacial adhesion in these composites was found to be based on the functionality or hydroxyl content of the EVOH and the hydroxyl content available on the wood surface. The availability of hydroxyl groups on the wood surface is dependent on the wood particle length and size. Hence, particle size and average particle length of wood particles, and functionality or hydroxyl contents on EVOH play the dominate role in creating a strong contact area or interfaces between wood and the polymer matrix, to afford composites with superior properties. The main conclusions of this part of the study are the following:

1. Generally, use of all the EVOHs considered in this study resulted in an improvement in all the investigated properties (mechanical and thermal properties), which indicates the improved interaction between *A. cyclops* and LLDPE in the presence of EVOH.
2. The functionality or hydroxyl content of the EVOH was proportional to the particle size and average particle length of the wood particles. It seems that as the particle size and average particle length of the wood particle increases, an EVOH with higher hydroxyl content is required. The reasons for this are the following:
   - ❖ The lower hydroxyl content of the EVOH44 afforded a greater improvement in the properties of the composites than the other EVOHs in the cases of composites made with *A. cyclops* with particle size 180 µm and average particle length 0.23 mm.
   - ❖ Composites made with *A. cyclops* with particle size 250 µm and average particle length 1.22 mm exhibited the best improvements when EVOH38 was used.
   - ❖ The best improvements in the properties of the composites made with *A. cyclops* with particle size 450 µm and average particle length 3.24 mm were achieved when EVOH27 with higher hydroxyl content was used.
3. *A. cyclops* with small particle size (180 µm) and average particle length (0.225 mm) offered better improvements in the properties of *A. cyclops*-LLDPE composites than *A. cyclops* with larger particle size (250 and 450 µm) and average particle length (1.220 and 3.240 mm).

4. IM composites showed better tensile strength, EAB and thermal stability than the pressed composites. On the other hand, pressed composites exhibited higher hardness than IM composites.

6.5 References

1. Kayuk Y., Seredenko V., Strength of Materials, 16, 1142-1148, 1984.
2. Georgopoulos S., Tarantili P., Avgerinos E., Andreopoulos A., Koukios E., Polymer Degradation and Stability, 90, 303-312, 2005.
3. Carbone G., Bottiglione F., Journal of the Mechanics and Physics of Solids, 56, 2555-2572, 2008.
4. Lu J., Wu Q., Negulescu I., Wood Fibre and Science, 36, 500-510, 2004.
5. Xanthos M., Functional Fillers for Plastics, 1st edition, Wiley-VCH Verlag, Germany, 2005. 18-23.
6. Prachayawarakorn J., Anggulalat, K., Songklanakarin Journal of Science and Technology, 25, 595-606, 2003.
7. Karmarkar A., Chauhan S., Modak J., Chanda M, Composites: Part A, 38, 227-233, 2007.
8. Bengtsson M., Gatenholm P., Oksman K., Composites Science and Technology, 65, 1468-1479, 2005.
9. Ichazo M., Albano C., González J., Perera R., Candal M., Composites Structures 54, 207-214, 2001.
10. Bledzki A., Gassan J., Progress in Polymer Science, 24, 221-274, 1999.
11. Felix J., Gatenholm P., Journal of Applied Polymer Science, 42, 609-620, 1991.
12. Djidjelli H., Benachour D., Boukerrou A., Zefouni O., Martinez-Véga J., Farenc J., Kaci M., eXPRESS Polymer Letters, 1, 846-852, 2007.
13. Bengtsson M., Stark N., Oksman K., Composites Science and Technology, 2728-2738, 2007.
14. Nygård P., Tanem B., Karlsen T., Brachet P., Leinsvang B., Composites Science and Technology, 68, 3418-3424, 2008.
15. Hristov V., Vlachopoulos J., Rheologica Acta, 46, 733-783, 2007.
16. Rowell R., Handbook of Wood Chemistry and Wood Composites, 1st edition, CRC Press, UK, 2005. 434.
17. Mueller D., International Nonwovens Journal, 12, 31-38, 2004.
18. Zhang S., Rodrigue D., Riedl B., Polymer Composites, 26, 731-738, 2005.
19. Olabisi O., Handbook of thermoplastics, 1st edition, Marcel Dekker, USA, 1997. 30.
20. Marcovich N., Villar M., Journal of Applied Polymer Science, 90, 2775-2784, 2003.
21. Kim H., Kim S., Kim H., Yang H., Thermochimica Acta, 451, 181-188, 2006.
22. Dányádi L., Janecska T., Szabo Z., Nagy G., Moczo J., Pukánszky B., Composites Science and technology, 67, 2838-2846, 2007.
23. Migneault S., Koubaa A., Erchiqui F., Chaala A., Englund K., Wolcott, M., Composites: Part A, 40, 80-85, 2009.
24. Stark N., Matuana L., Clemons C., Journal of Applied Polymer Science, 93, 1021-1030, 2004.
25. Salemane M., Luyt A., Journal of Applied Polymer Science, 100, 4173-4180, 2006.
26. Wilkes C., Summers J., Daniels C., Berard M., PVC Handbook, 1st edition, Hanser Verlag, USA, 2005. 260.
27. Nachtigall S., Cerveira G., Rosa, S., Polymer Testing, 26, 619-628, 2007.
28. Bledzki A., Faruk O., Huque M., Polymer-Plastics Technology and Engineering, 41, 435-451, 2002.
29. Hristov V., Krumova M., Vasileva S., Michler G., Journal of Applied Polymer Science, 92, 1286-1292, 2004.

Chapter 7

The use of degraded LLDPE as a compatibilizer in wood-LLDPE composite system

Abstract

LLDPE was degraded in an air oven for a period of 55 days at 114 °C and the degradation process monitored with respect to decrease in MW and the formation of functional groups. It was believed that formation of these new functional groups should allow LLDPE to be used as a compatibiliser in wood-LLDPE composites. Degraded LLDPE was used as a compatibiliser (2-7%) in wood-LLDPE composites systems (10, 30 and 50% wood content). The results show that the mechanical and thermal properties of compatibilised composites were improved over the noncompatibilised composites. These improvements were attributed to the better compatibility and adhesion between wood and the LLDPE matrix in the compatibilised composites. The optimal amount of degraded LLDPE varied according to the wood content incorporated in the composites.

Keywords: *WPCs, LLDPE, Compatibiliser, Degraded LLDPE, Fracture surface*

7.1 Introduction

Traditionally, PE is regarded as quite stable and not readily degradable at ambient temperature and in the absence of light. The degradation of PE can occur by different molecular mechanisms: thermal degradation, photo-degradation and biological degradation. PE contains only nonpolar C–C and C–H bonds which do not provide centres for nucleophilic or electrophilic attack, and the possibilities for its chemical reactivity are strongly limited to radical reactions [1]. Amorphous areas degrade first because they are more accessible [2]. The hierarchy in the oxidation susceptibility of PEs is reported to be as follows: LDPE > LLDPE > HDPE [3].

PE can undergo thermo-oxidative degradation (TOD) in the presence of oxygen. TOD occurs when the PE is subjected to sufficient heat. TOD is often a complex process involving combinations of different mechanisms [4]. Mechanisms of the TOD process of PE are well documented in the literature [5-11]. The TOD of PE is believed to proceed by a free radical mechanism. In the absence of oxygen, PE often degrades to a lower MW material, although

crosslinking may also occur, while in the presence of oxygen, different reactions take place [4]. Chain scission and macromolecular oxidation are the predominant reactions [3]. When PE is subjected to high temperatures, alkyl macro radicals are formed, which react with oxygen to form peroxy radicals. These can further react by abstracting hydrogen from elsewhere on the formed polymer, forming a hydroperoxide and recreating the macro alkyl radical. The decomposition of the hydroperoxides results in the production of ketones, alcohol, carboxylic acids, lactones, etc. [10-11]. TOD processes can be tracked by carbonyl index measurements, gravimetry, oxygen absorption, MW changes, changes in mechanical properties, etc. [12]. Changes that include bond scission, chemical transformation and formation of new functional groups have been categorized as polymer degradation [10]. Other changes such as a decrease in average MW, discolouration, and embrittlement can also be detected [13].

The hydroxyl and carbonyl species usually account for most of the oxidation products on the TOD of PE [14-15]. With respect to hydroxyl species, carbonyl species are often used to monitor the TOD of polyolefins [14]. However, the number of the various types of carbonyl group depends upon the chemical and physical structure of the polymer and on experimental conditions (e.g. temperature, oxygen concentration, etc.) [8]. Furthermore, the TOD process in PE is often accompanied by an increase in the X_c [16-17].

The TOD seems to be a very useful approach to attain polymers with improved adhesive properties and better compatibility with other materials. Mantia and Mongiov [8] found that the compatibility of a blend can be affected by the presence of species produced during TOD (e.g. carbonyl groups). According to this, Camacho and Karlsson [18] claimed that in some cases these species may act as a compatibiliser. The functional groups in degraded PE can interact with the hydroxyl groups of cellulose, while the non-polar part of degraded LLDPE interacts with the LLDPE matrix. Hence, the idea of using degraded PE as a compatibiliser for wood-LLDPE composite system is quite appealing, providing attractive economic and environmental advantages.

7.2 Experimental

7.2.1 Materials

WF from an Acacia (*A. cyclops*) with particle size of 180 μm was used as a reinforcing filler. LLDPE, with an average MW of 137 000, was used as a matrix. Degraded LLDPE was used as a compatibiliser. Degraded LLDPE was obtained by exposing LLDPE (in the form of pellets) in an air oven for a period of 55 days at 114 °C. Xylene and a mixture of Irganox were used as explained in Chapter 3 (Section 3.2.1). Composites were prepared as shown in

Chapter 3 (Section 3.2.2). The only difference is that the LLDPE, degraded LLDPE or compatibiliser and mixture of Irganox xylene were heated with a small amount of xylene to about 130 ^{o}C. The prepared composites and their abbreviations are shown in Table 7.1. Specimens for tests were prepared by injection moulding, as described in Section 6.2.1.

Table 7.1 Abbreviations and compositions of the composites used in this study

Composite	LLDPE, %	Wood, %	Degraded LLDPE, %
WPC 0-10	90	10	0
WPC 2-10	88	10	2
WPC 5-10	85	10	5
WPC 7-10	83	10	7
WPC 0-30	70	30	0
WPC 2-30	68	30	2
WPC 5-30	65	30	5
WPC 7-30	63	30	7
WPC 0-50	50	50	0
WPC 2-50	48	50	2
WPC 5-50	45	50	5
WPC 7-50	43	50	7

7.2.2 Characterisation

FTIR and DSC, as shown in Section 3.3.8 were used to monitor and determine the creation of the new functional groups and the change in the X_c in LLDPE after TOD. DSC was also used to determine the effect of using degraded LLDPE as a compatibiliser on the thermal behaviour of the composites obtained. High temperature gel permeation chromatography (HT-GPC) was used in this part to detect the change in the MW and MWD of LLDPE after TOD, MWs and MWDs of LLDPE and degraded LLDPE were measured using a Polymer Labs PL 220 GPC with a differential refractive index detector. The flow rate was 1 mL/min and measurements were done at a temperature of 140 °C. 1,2,4 Trichlorobenzene, stabilised with 2,6-di-tert-butyl-4-methylphenol was used as mobile phase.

The tensile strength and EAB were determined using the same instrument as described in Section 3.3.2. At least three injected moulding specimens were tested for each composite. The size of each specimen was 5 mm × 50 mm × 1.5 mm. The surface hardness was measured with the same microhardness tester that described in Section 3.3.2. The size of the injection moulded test specimen was a disk of 20 mm diameter and 1.5 mm thickness. The results quoted are the average of ten measurements. Impact testing was performed as described in Section 5.3. At least three injection moulded samples were tested for each composite. The size of each specimen was 5 mm × 50 mm × 1.5 mm. DMA as described in Section 3.3.2, was

used here to determine E′, E″ and tan δ. Thermal stability measurements were conducted using the same procedure and instrumentation as described in Section 3.3.3. OM (Section 3.3.6) was used here to determine the morphology and dispersion of wood particles in the composites. The SEM instrument as described in Section 4.3, was used here to study the morphology of the composites, after quenching them in liquid nitrogen (fracture surface).

7.3 Results and discussion

7.3.1 Characterisation of degraded LLDPE

As can be seen in Figure 7.1, the most significant changes in IR absorption spectra are the carbonyl (1700-1785 cm^{-1}), amorphous (1300 cm^{-1}) and hydroxyl (3400 cm^{-1}) regions [19].

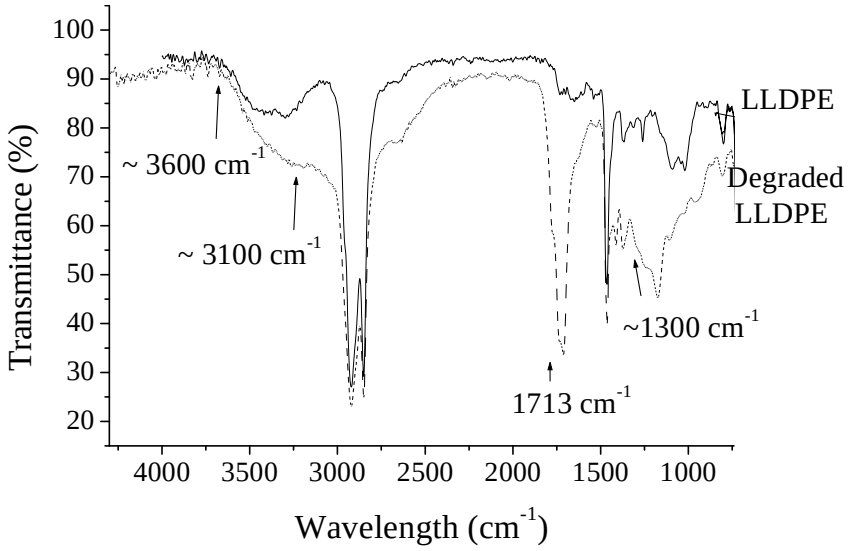

Figure 7.1 FTIR spectra of the original LLDPE and degraded LLDPE.

The IR band at 1713 cm^{-1} for the degraded LLDPE (dashed spectrum in Figure 7.1) is due to the formation of carbonyl groups, while the broad peak between 3100-3600 cm^{-1} could be assigned to the formation of hydroxyl and hydroperoxide groups. Various carbonyl species are known to form [20]. As a result, the characteristic bands of these species overlap each other, making it difficult to distinguish them, with the carbonyl band a result of overlap of various stretching vibration bands including those of aldehydes and/or esters (1733 cm^{-1}), carboxylic acid groups (1700 cm^{-1}) and γ lactones (1780 cm^{-1}) [19].

Table 7.2 presents the MW and X_c of the original and degraded LLDPE. The TOD of LLDPE caused a decrease in MW to 16 700 g/mole (MWD = 4.5) compared to the original 136 800 g/mole (MWD = 3.8). It also caused a slight increase in the X_c (37% to 40%), while the T_m (124 °C) and T_c (106 °C) remained constant. The significant reduction of MW after thermal degradation of PE is well-documented [3, 19] Oxidation of PE decreases MW due to chain scission [21]. The increase in X_c of PE upon TOD is also well known [22-23].

Table 7.2 MW and crystallinity of the original and degraded LLDPE

Sample	$\overline{M_n}$	$\overline{M_w}$	MWD	T_c, °C	T_m, °C	ΔH_f, J/g	X_c, %
LLDPE	37561	136804	3.6	105.7	124.1	108.2	37.5
Degraded LLDPE	3752	16711	4.5	105.6	123.2	117.3	40.6

7.3.2 Mechanical properties

The mechanical properties of the composites are shown in Figures 7.2-7.7. It is important to note that the standard deviations are given in parentheses next to the values of the mechanical properties. As shown in Figure 7.2, composites with no compatibilisers had the lowest values of tensile strength (6.7 (0.5)-11.5 (0.3) N/mm^2). In all the WPC systems (10, 30 and 50 % wood) the incorporation of degraded LLDPE resulted in an increase in tensile strength of the composites compared to that of the composites containing no compatibiliser. These results, in general, indicate that the effect of degraded LLDPE as a compatibiliser is significant. The improvement in the tensile properties could be attributed to improved compatibility and interfacial adhesion between wood and the LLDPE matrix. This is because the degraded LLDPE or the compatibiliser enhances the quality of the interface and in turn improves the stress transfer and eventually the tensile strength [24].

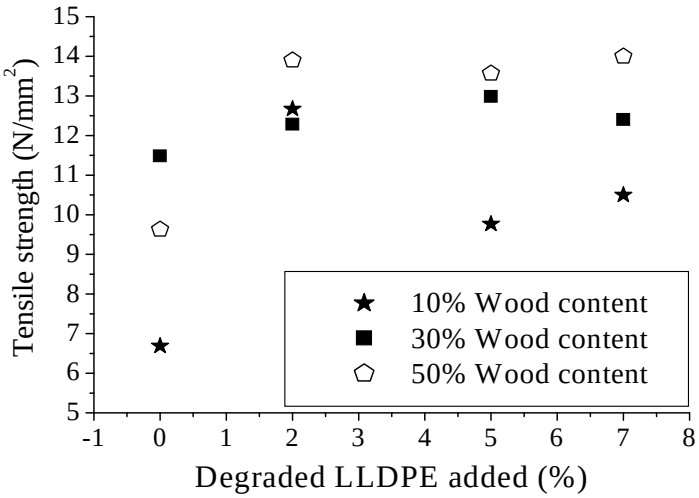

Figure 7.2 Tensile strength of WPCs as a function of the amount of degraded LLDPE added as compatibiliser. (The negative value on the x-axis is to allow for clear representation of the data).

Interesting here is that for the 10% wood composite the optimum amount of degraded LLDPE is 2%, while it is 5% for the 30% wood composite and the increase in tensile strength is steady for the 50% wood composite for the entire range of degraded LLDPE added. All the composites showed a dramatic decrease in the EAB (between 4.2 (0.6) and 14.5 (0.1)%) in comparison to virgin LLDPE (>300%), as shown in Figure 7.3, as would be expected [24-26]. There are two aspects of interest here. In the cases of the 10 and 30% wood content, the

adding of degraded LLDPE initially decreases the EAB, but adding more degraded LLDPE results in an increase in EAB. For the 50% wood content samples, however, increasing the amount of degraded LLDPE results in a steady decrease in the EAB, clearly indicating that addition of the degraded LLDPE increases the dispersion of the wood particles as well as the interaction between the wood particles and the polymer matrix. For the 10 and 30% wood composites it is possible that the addition of too much compatibiliser could result in a weakening of the LLDPE matrix.

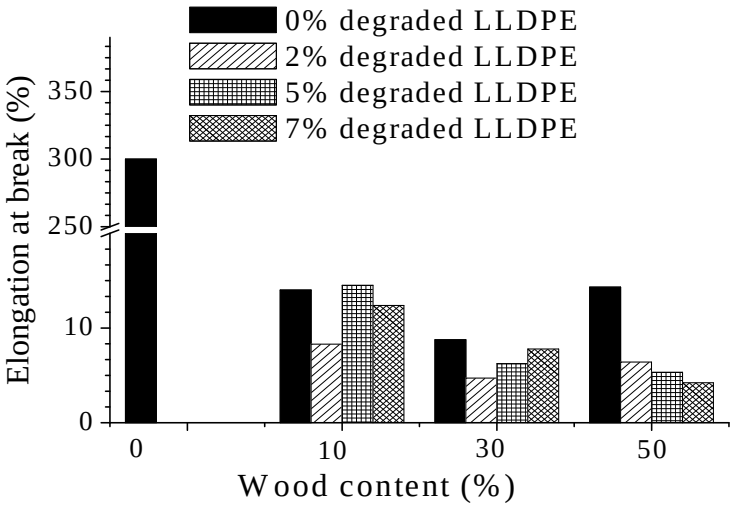

Figure 7.3 EAB for LLDPE and WPCs as a function of wood content.

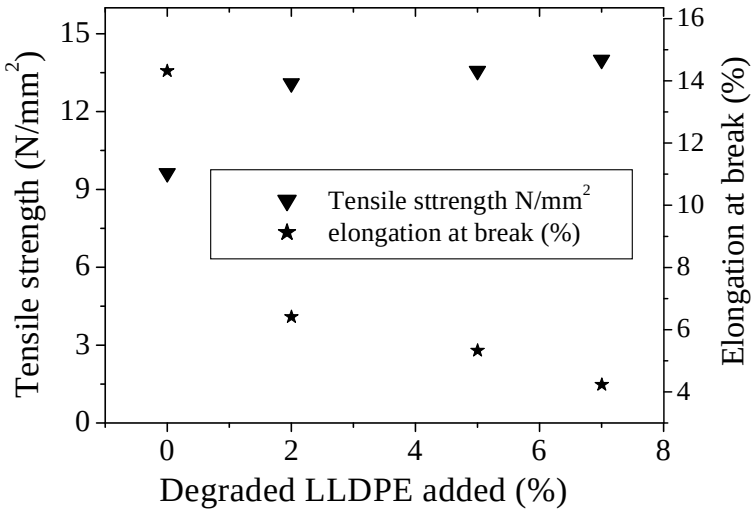

Figure 7.4 Tensile strength and elongation at break of composites with 50% wood content as a function of degraded LLDPE added.

In Figure 7.4, both the tensile strength and the EAB as a function of degraded LLDPE for the composites with 50% wood content is plotted, further illustrating the points discussed above. It is quite clear that the addition of degraded LLDPE leads to better interaction between the wood particles and the LLDPE matrix, leading to a higher tensile strength and a lower EAB.

Once again it is clear that the amount of compatibiliser need for maximum effect is determined by the amount of wood added, as shown in Figure 7.3.

Figure 7.5 shows that the reinforced LLDPE are harder than unreinforced LLDPE, as would be expected. What is also clear is that the presence of the degraded LLDPE increases the hardness of the composite compared to those composites without compatibiliser (albeit a very small increase). The hardness of WPC is generally related to the hardness of the polymer but might also be affected by polymer-wood interactions [27].

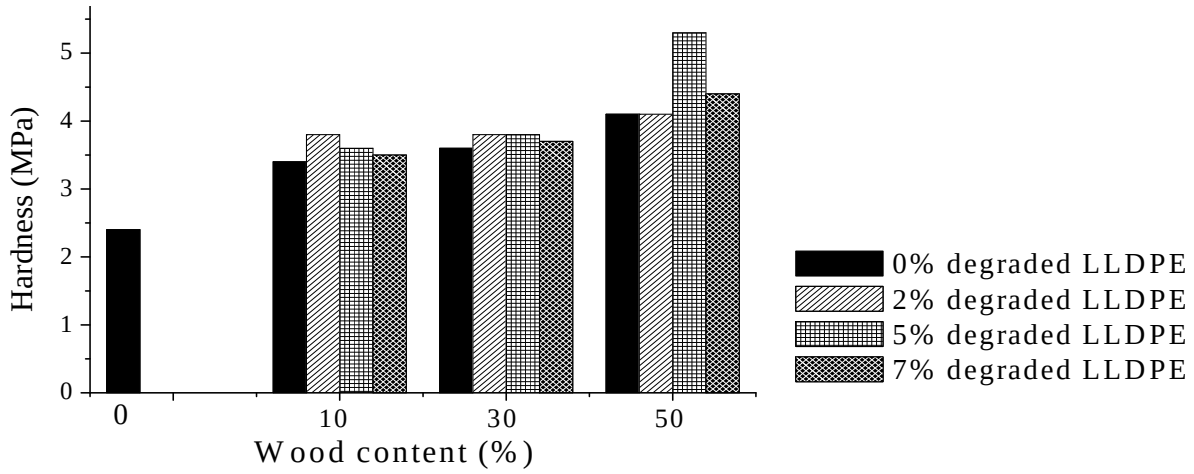

Figure 7.5 Hardness of LLDPE and WPCs as a function of wood content.

In general it is believed that the hardness of the WPCs are affected by the hardness of the wood particles [28], density and moisture content of the wood [29-30], the amount of polymer and the hardness of the polymer [31]. From Figure 7.5 it is quite clear that the hardness increases as the wood content increases.

The drop in the impact strength of WPCs (710.0 (0.2) to 1633.0 (0.1) J/m^2) in comparison to virgin LLDPE (2983.0 (0.1) J/m^2) is shown in Figure 7.6, and once again this is expected [32]. Karmarkar et al. [26] suggested two reasons for the decrease in the impact strength. The first one is that the presence of wood particles in the polymer matrix provides points of stress concentrations, thus providing sites for crack initiation, and the second being the stiffening of polymer chains due to bonding between wood particles and the matrix. In general, the composites with compatibilisers (852.0 (0.1) -1633.0 (0.1) J/m^2) have a higher impact strength than composites with no compatibiliser (710.0 (0.2) -1231.0 (0.1) J/m^2). The enhanced impact properties of the WPCs prepared with compatibiliser is probably due to better dispersion of the particles. Degraded LLDPE thus seems to improve dispersion at the wood particles as well as increasing the interaction at the wood-matrix interface. From Figure 7.6, it is also clear that composites with high wood content possess low impact strength.

Furthermore, the optimum amount of compatibiliser added is dependent on the amount of wood in the composite. For the 50% wood composites, the increase in impact strength is almost linear as the amount of degraded LLDPE added is increased.

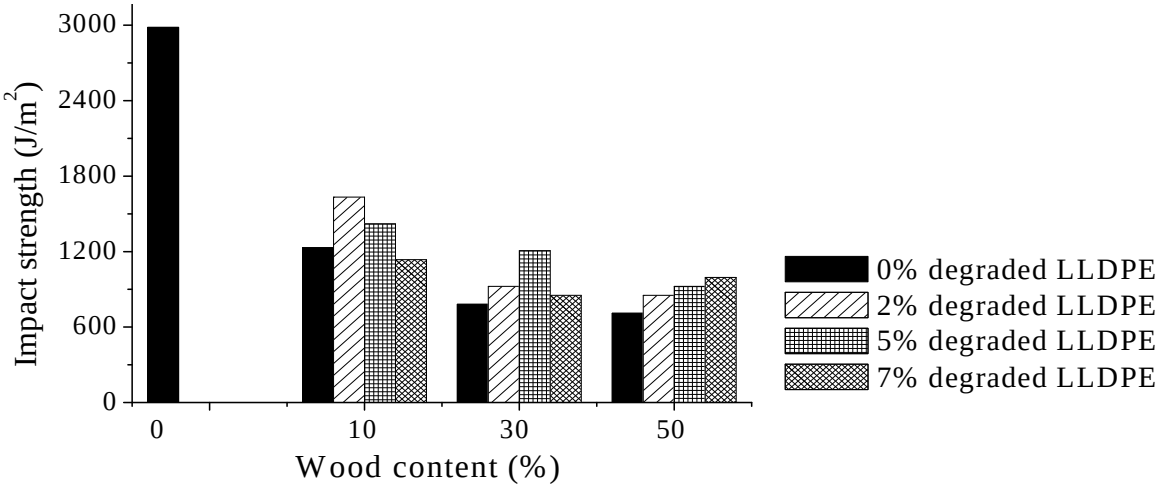

Figure 7.6 Impact strength of LLDPE and as WPCs a function of wood content.

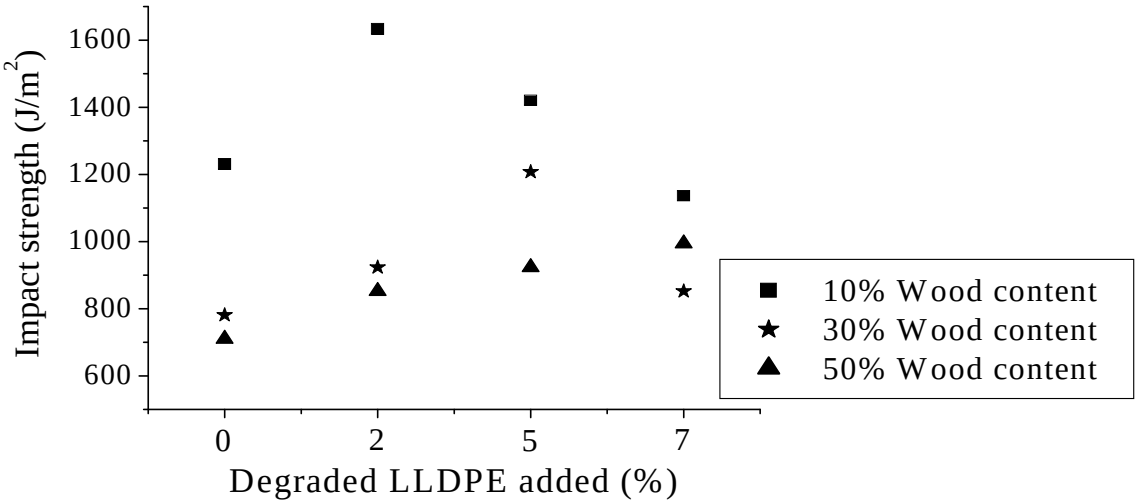

Figure 7.7 Impact strength of LLDPE and WPCs as a function of degraded LLDPE added as compatibiliser.

In Figure 7.7, a comparison between the impact properties of the WPCs as a function of degraded LLDPE added, indicates that the degraded LLDPE does influence the impact properties, and that the effect of the amount of degraded LLDPE added is dependent on the amount of wood added. As the amount of wood increased, the amount of degraded LLDPE that has a positive effect on the impact properties increased. 2% degraded LLDPE is the

optimal amount for composites with 10% wood content, while 5% seems to be the optimal amount for composites with 30%. For the 50% wood composites, the effect of adding degraded LLDPE is linear. The optimal amount could be 7% or higher. Furthermore, as indicated by many authors [33-36], increasing the wood content reduces the mechanical properties of WPC, with the exception of hardness.

7.3.3 Thermal behaviour

The results for T_c, T_m, ΔH_f, X_c and X_c^{corr} are reported in Table 7.3. Value of 288.7 J/g was taken as a value of the ΔH_f^o of completely crystalline PE [37]. Crystallisation and melting curves of LLDPE and wood-LLDPE composites made with 10% wood content are shown in Figures 7.8 and 7.9. On the other hand, crystallisation and melting curves of wood-LLDPE composites made with 30% and 50% wood content are shown in Appendix C.

Table 7.3 DSC results of LLDPE and composites

Composite	T_c, °C	T_m, °C	ΔH_f, J/g	X_c, %	X_c^{corr}, %
LLDPE	105.7	124.1	108.2	37.5	37.5
WPC 0-10	107.7	122.1	57.9	20.0	22.2
WPC 2-10	107.7	120.7	88.8	30.8	34.2
WPC 5-10	107.3	121.2	89.4	31.0	34.4
WPC 7-10	107.1	124.1	87.0	30.1	33.5
WPC 0-30	108.5	121.4	85.4	29.6	42.2
WPC 2-30	108.5	121.6	94.4	32.7	46.7
WPC 5-30	107.5	121.1	93.5	32.4	46.2
WPC 7-30	108.1	121.2	93.3	32.3	46.1
WPC 0-50	106.3	123.5	104.7	36.3	72.5
WPC 2-50	108.0	121.2	108.9	37.7	75.4
WPC 5-50	106.1	120.9	136.7	47.4	94.7
WPC 7-50	110.2	122.3	123.5	42.8	85.6

With exception to WPC 7-50, no much difference in the T_c and T_m between the composites and neat LLDPE. X_c of the composites with 50% wood content was higher than other composites and LLDPE. X_c^{corr} of the composites with 30% and 50% wood content were higher than that of neat LLDPE. As shown in Table 7.3, X_c and X_c^{corr} increased with increasing the wood content. According to Jiang and Kamdem [38], increased crystallinity of PE can be observed with increase in wood content up to 50%. The improvements in the X_c and X_c^{corr} of the compatibilised composites over the noncompatibilised composites were due to the compatibilisation effect of degraded LLDPE which extends the predominance of the crystallisation process.

The DSC heating curves of all the composites show one broad melting peak. All these curves are second heating curves. These curves exhibit one endothermic peak with two maximum points. The maximum point at lower temperature seems to correspond to the melting point of degrade LLDPE, and the upper maximum point to the melting point of the original LLDPE.

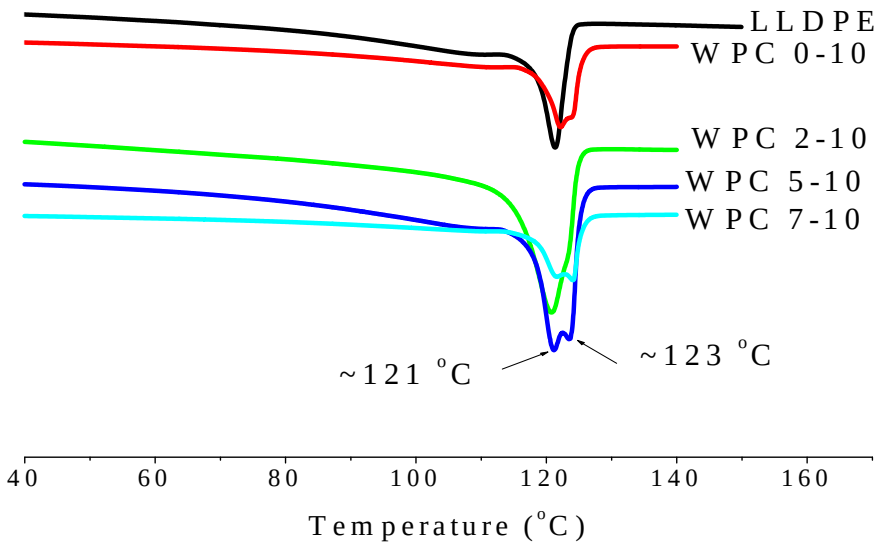

Figure 7.8 DSC heating curves of LLDPE and all the composites with 10% wood content.

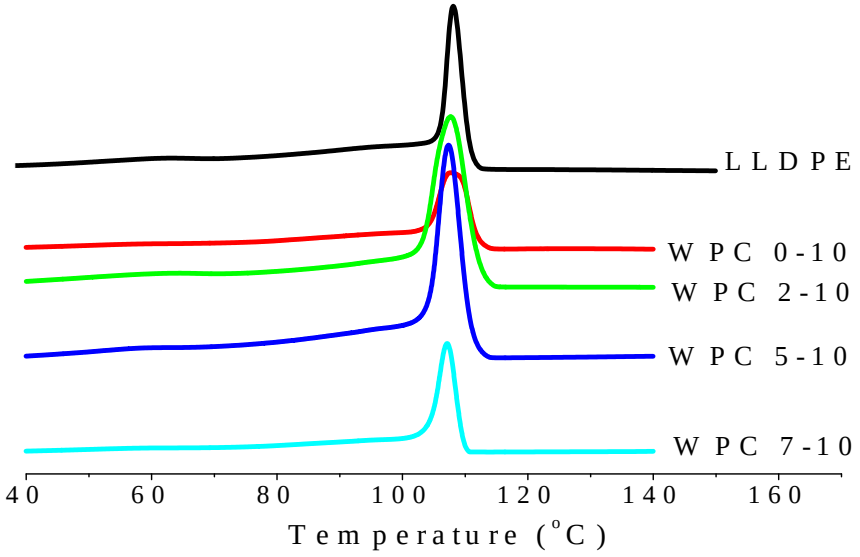

Figure 7.9 DSC cooling curves of LLDPE and all the composites with 10% wood content.

As shown in Figure 7.8, WPC 7-10 shows two maximum points at ~121 °C and ~123 °C. The first maximum point is due to presence of the degraded LLDPE which was used as a compatibiliser, while the second one is due to the presence of original LLDPE which was

used as a matrix. This is because melting point of the degraded LLDPE showed to be lower that that of original LLDPE, as shown in Table 7.2. Thermal ageing of semi-crystalline polymer above 100 °C may causes broadening and shifting the maximum melting peak towards lower temperatures [39]. It is normally accepted that the degradation, though taking place mainly in the amorphous phase, may also occur at the lamellar fold surfaces, and causes an increase in the surface free energy of the crystals resulting in reduced T_m [40]. On the other hand, there was only one crystallisation peak in the DSC curves of was observed for the LLDPE and all the composites, as shown in (Figure 7.9 and Figures in Appendix C). Figure 7.9 shows the cooling curves of LLDPE and all the composites with 10% wood content.

The dynamic TGA curves of LLDPE and WPCs are shown in Figure 7.10. As shown in the previous chapters, one degradation step for LLDPE and two degradation steps for WPCs were observed. LLDPE had one degradation step at 465 ^{o}C due to the decomposition of the C-C bonds in the main chain of LLDPE. In the cases of composites, the first degradation step below 300 ^{o}C can be attributed to the decomposition of individual wood components such as, hemicelluloses, the onset of lignin and extractives, while the second degradation step between 400 and 550 ^{o}C is due to the decomposition of cellulosic materials in the wood and the C-C bonds in the main chain of LLDPE.

As can be seen, at 10, 30 and 50% wood content, composites with 0% degraded LLDPE exhibited lower thermal stability and degraded before virgin LLDPE and the other composites. It is important to emphasise here that at 10, 30 and 50% wood content, thermal stability or degradation temperatures of composites with 2, 5 and 7% degraded LLDPE were higher than that of LLDPE. These results indicate that the use of degraded LLDPE as a compatibiliser in the WPC system improved the thermal stability of the composite. This improved thermal stability of the compatibilised composites was due to the enhanced interfacial adhesion and additional intermolecular bonding produced by the compatibilisers [41]. This is in accordance with the results found with EVOH as a compatibiliser.

These results are in agreement with the results of the mechanical properties. They confirm the efficiency of degraded LLDPE as a compatibiliser. They also confirm that the 2% degraded LLDPE is the optimal amount for composites with 10% wood content, while 5% seems to be the optimal amount for 30% wood content. On the other hand, 7% degraded LLDPE or more is expected to be the optimal amount for composites with 50% wood content.

As revealed before, this is important because for producing WPCs with acceptable mechanical performance, a careful selection of compatibilisers and optimization is needed [42].

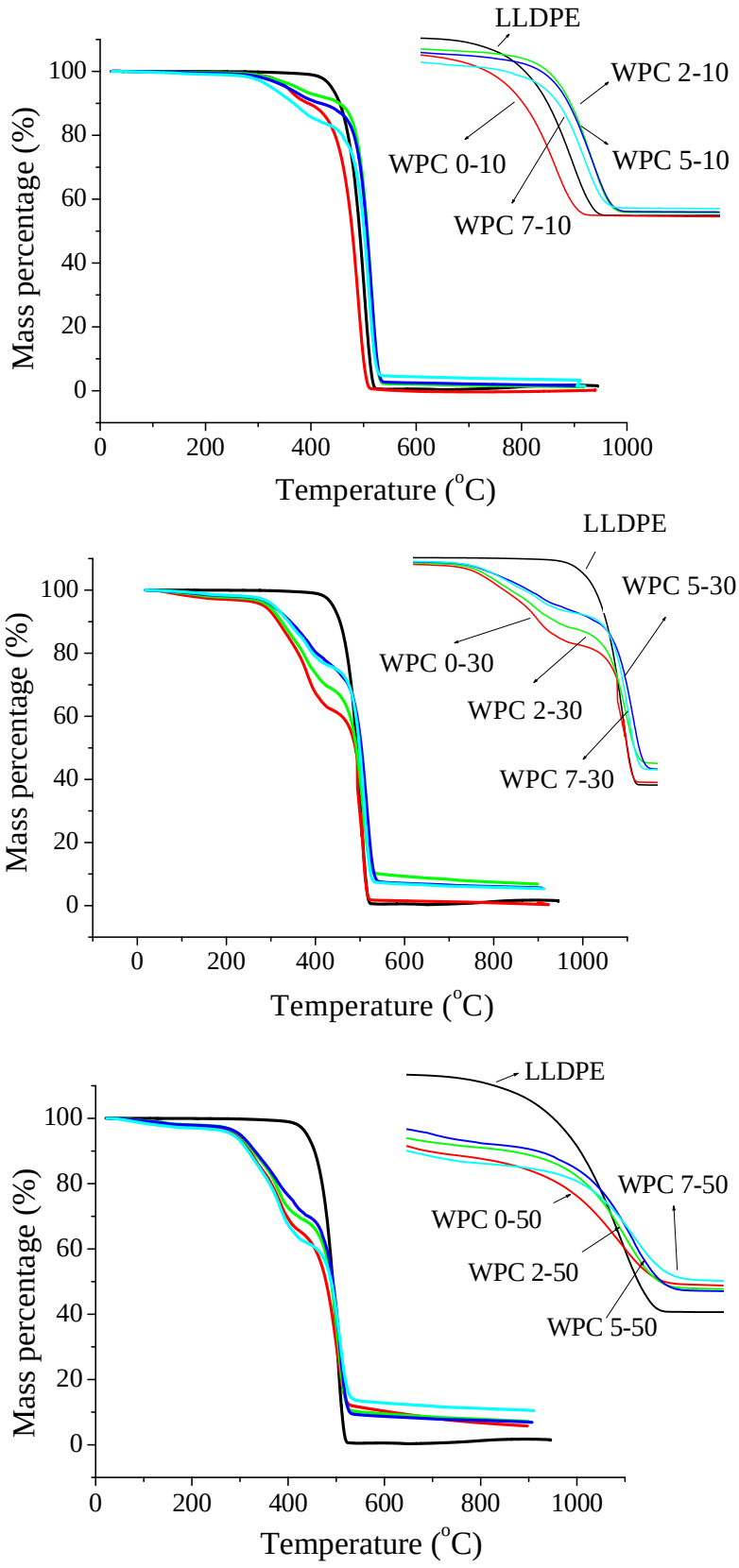

Figure 7.10 TGA curves of LLDPE and WPCs.

7.3.4 Dynamic mechanical properties

According to the above properties, DMA was performed to determine the E′, E″ and tan δ for LLDPE, WPC 2-10, WPC 5-30 and WPC 7-50 composites. Figure 7.11 presents plots of E′,

E″ and tan δ against temperature for the LLDPE, WPC 2-10, WPC 5-30 and WPC 7-50. As observed by Jiang and Kamdem [38] and Huang and Zhang [43], increasing wood content resulted an increase in the E′ and E″ and a decrease in the tan δ of the composites.

A general declining trend for all the E′ curves (Figure 7.11a) are observed when the materials go through higher temperature. The reduction in E′ with increasing temperature was due to the softening of matrix and initiation of relaxation process [41, 44-46]. At temperatures above T_g, the molecular mobility and thermal expansion increases thus reducing the interfacial interaction and as a result E′ decreased sharply. As expected, the magnitudes of E′ increased with the incorporation of rigid wood into the LLDPE matrix due to the enhanced stiffness. A general trend of increasing of E′ with the increasing wood content was observed due to the mechanical limitation posed by increasing wood concentration embedded in the viscoelastic matrix, thereby reducing the mobility and the deformation of the matrix with increasing temperature [47]. It is also interesting to note the dramatic increase in E′ of LLDPE was observed in the range between -90 to 20 ^oC.

Figure 7.11b depicts a plot of the E″ of LLDPE, WPC 2-10, WPC 5-30 and WPC 7-50 as a function of temperature. It is evident that the α- relaxation peak (~-112 ^oC) is significantly shifted to higher temperature by the addition of wood particles. This means that an increase in the T_g of LLDPE was occurred in the three composites. This is because the peak position of the E″ was used to indicate the T_g of the composite [48]. This shift to higher temperature can be an indication of an interaction between wood and polymer and a restriction in the matrix mobility [41, 44-45]. The E″ at γ- relaxation temperature was markedly increased with addition of wood particles. This is because wood particles reduce the flexibility by introducing constrained on the segmental mobility of the polymer molecule at this relaxation temperature [48]. The composite (WPC 7-51) with high E′ also had high E″ in the entire range of temperature.

Figure 7.11c displays plots of the tan δ of LLDPE, WPC 2-10, WPC 5-30 and WPC 7-50 as a function of temperature. Tan δ was obtained from the ratio of E″ (viscous phase) to E′ (elastic phase). As shown in Figure 7.11c, with increasing the temperature, the tan δ of LLDPE and composites increased due to the increased polymer chain mobility of the LLDPE. In actual fact, the addition of wood leads to the increase in both elastic and viscous abilities of the composites under dynamic load [38]. Aforementioned, tan δ is known to provide information on the T_g and energy dissipation of composite materials [41, 44-45].

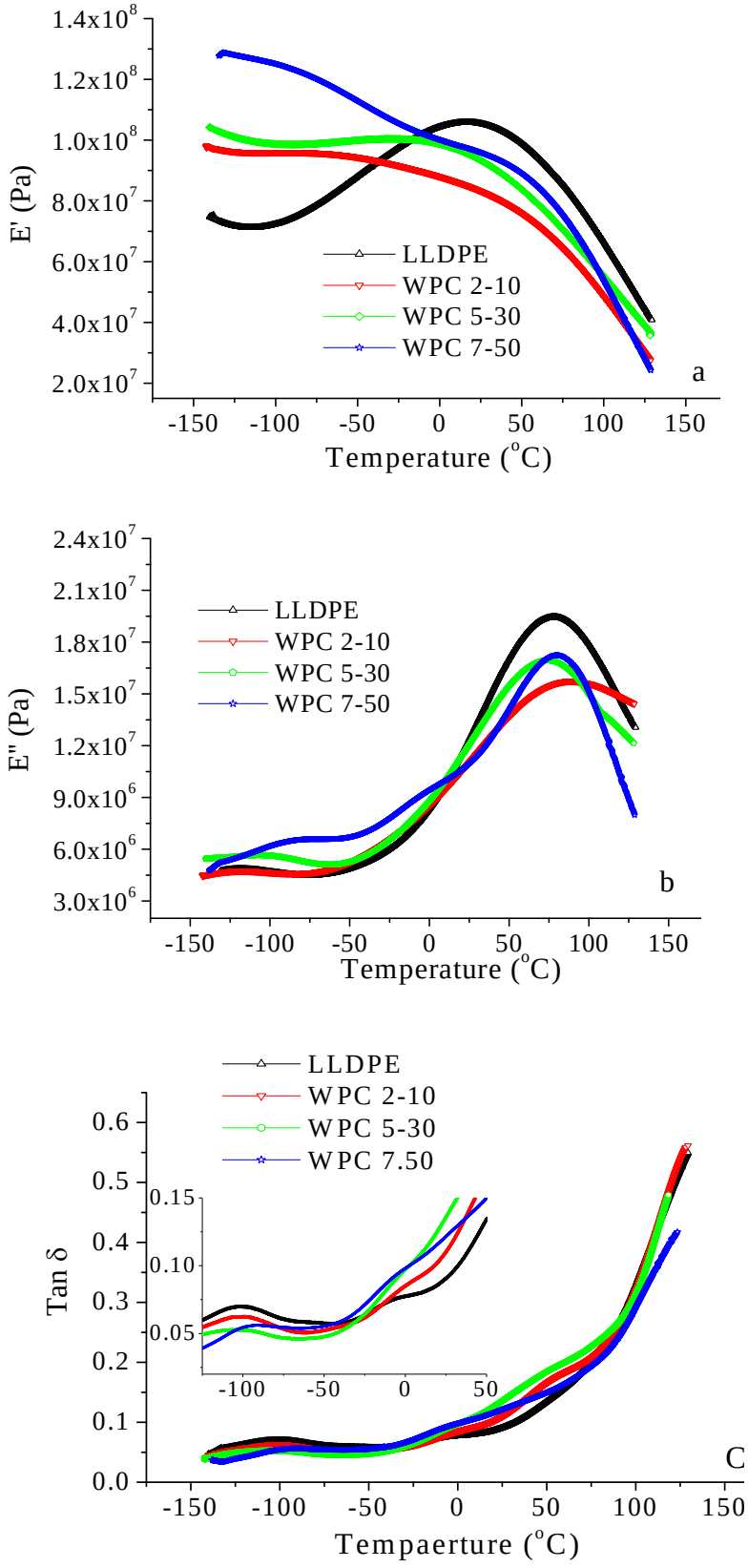

Figure 7.11 DMA results of LLDPE, WPC 2-10, WPC 5-30 and WPC 7-50 composites.

As it is seen in Figure 7.11c, γ- relaxation or T_g of the composites were shifted to higher temperature in comparison to neat LLDPE. It occurred at -106.0 °C for LLDPE, -98.6 °C for WPC 2-10, -100.7 °C for WPC 5-30 and -102.8 °C for WPC 7-50. This confirms the E″

results and indicates the good quality interfacial interaction between *A. cyclops* and LLDPE in these composites. However, all the above DMA results are in agreement with the classical observations on WPC behaviour [44-51].

7.3.5 Wood distribution

Figure 7.12 demonstrates the distribution of wood particles in the LLDPE matrix of the WPC 2-10, WPC 5-30 and WPC 7-50. As can seen in Figure 7.12a, wood particles were well dispersed in the LLDPE matrix of WPC 2-10. A 10% wood content dispersed in the LLDPE matrix without any aggregation. According to the SEM images in Figures 7.12b and 7.12c we may assume the occurrence of aggregation in the cases of composites with 30 and 50% wood particles. As shown in these figures, it is difficult to attain any information about the distribution of wood particles in the LLDPE matrix of WPC 5-30 and WPC 7-50 due to the higher wood content. Optical micrographs of the other composites are shown Appendix D.

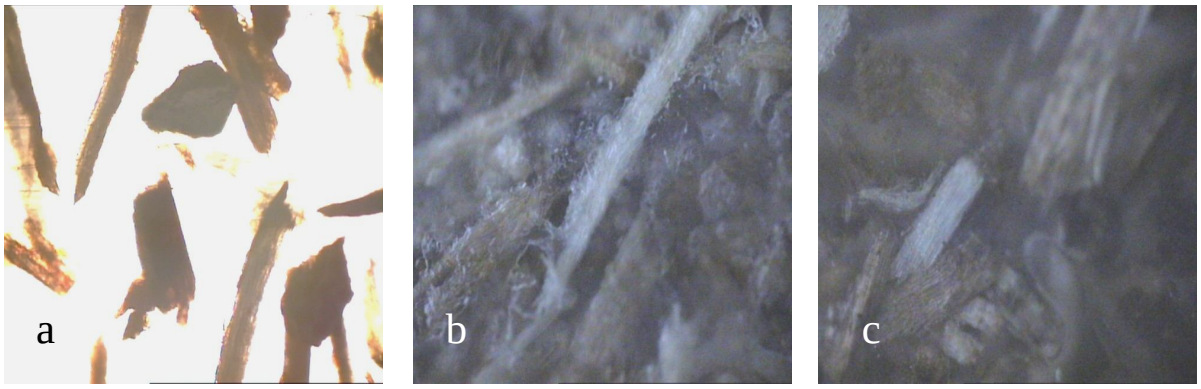

Figure 7.12 Optical micrographs of a) WPC 2-10, b) WPC 5-30 and c) WPC 7-50 (Mag. 100x).

7.3.6 Fracture surface morphology

Figure 7.13 shows the morphologies of the fracture surfaces of WPC 0-10, WPC 2-10, WPC 0-30, while figure 4.14 shows the morphologies of the fracture surfaces of WPC 5-30, WPC 0-50 and WPC 7-50. It can be seen in the cases of composites with no compatibilisers that particles were pulled out (see the arrows in Figure 7.13) and debonded (see the dashed circles in Figure 7.13) from the LLDPE matrix during the fracture of these composites. As shown in Figure 7.13, these composites show that there is no attachment between wood particle and the LLDPE matrix, indicating that there is no bonding between them. These indicate poor adhesion between hydrophilic wood and hydrophobic LLDPE. On the other hand, there are no gaps between the wood particles and LLDPE matrix in the cases of the compatibilised composites (Figures 7.14). Cracks in these composites occurred through the wood particles.

As shown in Figures 7.14a, 7.14b and 7.14c (see the dashed rectangles in Figure 7.14) it is possible to observe cracks through the wood particles when fracturing the WPCs [52], which can be an indication of stress transfer from the weaker matrix to the stronger wood particle. This is, however, only possible in the case of good compatibility and strong interfacial adhesion.

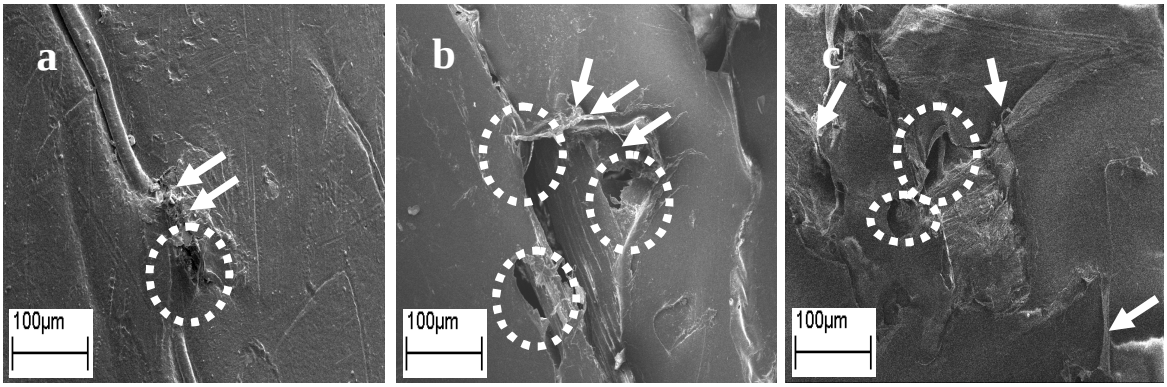

Figure 7.13 SEM micrographs of the fracture surface of a) WPC 0-10, b) WPC 0-30 and c) WPC 0-50 (Mag. 100x).

Literature reports that the stress transfer occurs not only along the wood particle length, but possibly also at the particle ends [53], as shown in Figure 7.14a (see the dashed circle in this figure). This may indicate that the combination of materials in the WPC 2-10 participated more actively and effectively in transferring stress than others. This may be the main reason for the better properties of WPC 2-10 over the others. On the other hand, the lower strength of WPC 7-50 in comparison to WPC 2-10 and WPC 5-30 may result from the lack of matrix (see the dashed circle in Figure 7.14c) due to the higher wood content..

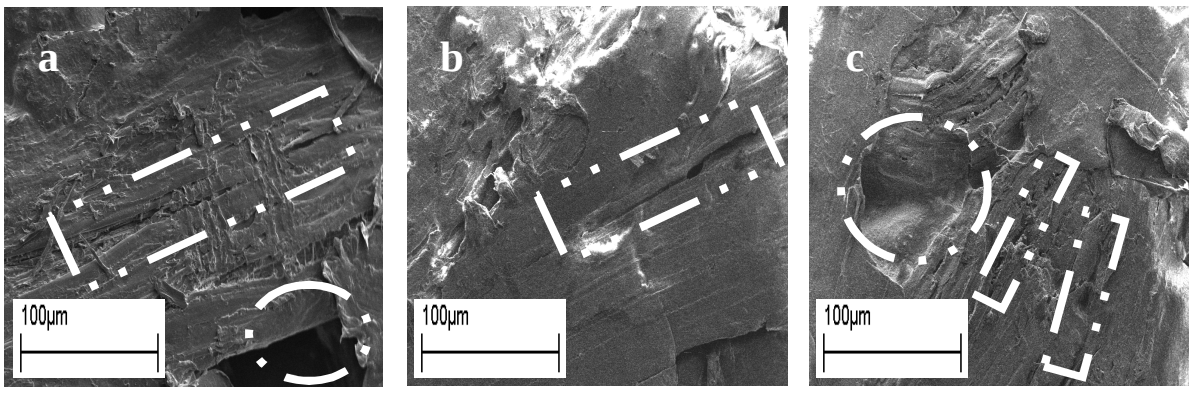

Figure 7.14 SEM micrographs of the fracture surface of a) WPC 2-10, b) WPC 5-30 and c) WPC 7-50 (Mag. 200x).

In composite materials, improved adhesion usually changes the failure mode from particle pull-out (as shown by the noncompatibilised composites) to particle breakage (as shown by

the compatibilised composites), which usually requires less energy [54]. This improved adhesion between the wood and the polymer plays an important role in the transmission of stress from the matrix to the wood particle and thus contributes toward the performance of the composite [55].

Good interfacial adhesion between the matrix and wood is essential and favourable to transfer stress across the interface [56]. It is well known that the improvement in the stress transfer will give rise to improvement in mechanical properties [57-58]. The stress transfer from the matrix to the wood particle depends on fiber-fiber and fiber-matrix interactions [59]. However, these findings suggest that the compatibility and interfacial adhesion between the wood and LLDPE matrix is very good. Hence, degraded LLDPE enhanced the quality of the interface and in turn improves the stress transfer and eventually the tensile strength.

7.4 Conclusion

The possibility of using degraded LLDPE as a compatibiliser in wood-LLDPE composite systems was investigated. The results indicate that degraded LLDPE played an important role in improving interfacial adhesion and compatibility between wood and the LLDPE matrix in wood-LLDPE composite systems at levels of 10, 30 and 50% wood content. Mechanical properties such as tensile strength and hardness, thermal and morphological properties of the compatibilised composites were somehow better than those of the noncompatibilised composites and virgin LLDPE. EAB and impact properties of the compatibilised composites were worse than that of virgin LLDPE, but better than those of the noncompatibilised composites. 2% degraded LLDPE was the optimal amount for the composites with 10% wood content, while 5% seems to be the optimal amount for the composites with 30% wood content. 7% degraded LLDPE or more is expected to be the optimal amount for the composites with 50% wood content. Fracture surface morphology confirmed this optimization by the occurrence of efficient stress transfer from LLDPE to wood particle.

7.5 References

1. Koutny M., Lemaire J., Delort A., Chemosphere, 64, 1243-1252, 2006.
2. Trifonov S., Sosnov E., Malygin A., Russian Journal of Applied Chemistry, 77, 1854-1858, 2004.
3. Chiellini E., Corti A., Antone S., Baciu R., Polymer Degradation and Stability, 91, 2739-2747, 2006.
4. Chen G., Davies A., Effect of Thermo-oxidative Ageing on Electrical Performance of Low Density Polyethylene, Proceedings of the IEEE 5th International Conference on Conduction and Breakdown in Solid Dielectrics, UK, 1995.
5. Goldberg V., Kolesnikova N., Paverman N., Kavun S., Stott P., Gelbin M., Polymer Degradation and Stability, 74, 370-385, 2001.
6. Sharma N., Chang L., Chu Y., Ismail H., Ishiaku U., Ishak Z., Polymer Degradation and Stability, 71, 381-393, 2001.

7. Hoáng E., Allen N., Liauw C., Fontán E., Lafuente P., Polymer Degradation and Stability, 91, 1356-1362, 2006.
8. Mantia F., Mongiov C., Polymer Degradation and Stability, 66, 337-342, 1999.
9. Trofimchuk E., Yablokova M., Polymer Degradation and Stability, 74, 291-295, 2001.
10. Wang Z., Wu G., Hu Y., Ding Y., Hu K., Fan W., Polymer Degradation and Stability, 77, 427-434, 2002.
11. Shah A., Hasan F., Hameed A., Ahmed S., Biotechnology Advances, 26, 246-265, 2008.
12. Bikiaris D., Prinos J., Perrier C., Panayiotou C., Polymer Degradation and Stability, 57, 313-324, 1997.
13. Schmiederer D., Gardocki A., Kühnert I., Schmachtenberg E., Polymer Engineering and Science, 48, 717-722, 2008.
14. Gugumus F., Polymer Degradation and Stability, 52, 131-144, 1996.
15. Kaci M., Remili C., Khima R., Sadoun T., Macromolecular Materials and Engineering, 288, 724-729, 2003.
16. Hamid S., Qureshi F., Amin M., Maadhah A., Polymer-Plastics Technology and Engineering, 28, 475-492, 1989.
17. Billingham N., Prentice P., Walker T., Journal of Polymer Science: Polymer Symposia, 57, 287-297, 2007.
18. Camacho W., Karlsson S., Polymer Degradation and Stability, 78, 385-391, 2002.
19. Roy P., Surekha P., Rajagopal C., Chatterjee S., Choudhary V., Polymer Degradation and Stability, 92, 1151-1160, 2007.
20. Yang R., Liu Y., Yu J., Wang K., Polymer Degradation and Stability, 91, 1651-1657, 2006.
21. Kurtz S., Rimnac C., Bartel D., Journal of Orthopaedic Research, 15, 57-61, 1997.
22. Salem M., Farouk H., Kashif I., Macromolecular Research, 10, 168-173, 2002.
23. Roy P., Surekha P., Raman R., Rajagopal C., Polymer Degradation and Stability, 94, 1033-1039, 2009.
24. Nygård P., Tanem B., Karlsen T., Brachet P., Leinsvang B., Composite Science and Technology, 68, 3418-3424, 2008.
25. Bledzki A., Gassan J., Progress in Polymer Science, 24, 221-274, 1999.
26. Karmarkar A., Chauhan S., Modak J., Chanda M., Composites: Part A, 38, 227-233, 2007.
27. Ellis W., Molecular Crystals and Liquid Crystals, 3535, 75-84, 2000.
28. Elvy S., Dennis G., Ng L., Journal of Materials Processing Technology, 48, 365-372, 1995.
29. Hansson L., Antti A., Journal of Materials Processing Technology, 171, 467-470, 2006.
30. Tze W., Wang S., Rials T., Pharr G., Kelley S., Composites: Part A, 38, 945-953, 2007.
31. Rowell R., Handbook of Wood Chemistry and Wood Composites, 1st edition, CRC Press, UK, 2005. 427.
32. Nourbakhsh A., Ashori A., Polymer Composites, 29, 569-573, 2008.
33. Stark N., Rowlands R., Wood Fiber and Science, 35, 167-174, 2003.
34. Selke S., Wichman I., Composites: Part A, 35, 321-326, 2004.
35. Lee S., Yang H., Kim H., Jeong C., Lim B., Lee J., Composite Structures, 65, 459-469, 2004.
36. Kuan H., Huang J., Ma C., Wang F., Plastics, Rubber and Composites, 32, 122-126, 2003.
37. Marcovich N., Villar M., Journal of Applied Polymer Science, 90, 2775-2784, 2003.
38. Jiang H., Kamdem D., Journal of Applied Polymer Science, 107, 951-957, 2008.
39. Boukezzi1 L., Boubakeur A., Laurent C., Lallouani M., Iranian Polymer Journal, 17, 611-624, 2008.
40. Rabello M., White J., Polymer Degradation and Stability, 56, 55-73, 1997.
41. Kim H., Kim S., Kim H., Yang H., Thermochimica Acta, 451, 181-188, 2006.
42. Hristov V., Krumova M., Michler G., Macromolecular Materials and Engineering, 291, 677-683, 2006.
43. Huang H., Zhang J., Journal of Applied Polymer Science, 111, 2806-2812, 2009.
44. Hristov V., Vasileva S., Macromolecular Materials and Engineering, 288, 798-806, 2003.
45. Behzad M., Tajvidi M., Ehrahimi G., Flak R., International Journal of Engineering Transactions: Part B, 17, 95-104, 2004.
46. Liu H., Wu Q., Han G., Yao F., Kojima Y., Suzuki S., Composites: Part A, 39, 1891-1900, 2008.
47. Pothana L., Oommenb Z., Thomas S., Composites Science and Technology, 63, 283-293, 2003.

48. Jubsilp C., Takeichi T., Hiziroglu S., Rimdusit S., Bioresource Technology, 99, 8880-8886, 2008.
49. Mohanty S., Verma S., Nayak S., Composites Science and Technology, 66, 538-547, 2006.
50. Godard E., Vincent M., Agassant J., Vergnes B., Journal of Applied Polymer Science, 112, 2559-2566, 2009.
51. Menard K., Dynamic Mechanical Analysis: A Practical Introduction, 2ed edition, CRC Press, USA, 1999. 610.
52. Bengtsson M., Gatenholm P., Oksman K., Composites Science and Technology, 65, 1468-1479, 2005.
53. Sretenovic A., Müller U., Gindl W., Composites: Part A, 37, 1406-1412, 2003.
54. Mengeloglu F., Kabakci A., International Journal of Molecular Sciences, 9, 107-119, 2008.
55. Saheb D., Jog A., Advances in Polymer Technology, 18, 351-363, 1999.
56. Cheremisinoff N., Handbook of Engineering Polymeric Materials, 1st edition, CRC Press, USA, 1997. 591-681.
57. Duchemin B., Newman R., Staiger, M., Composites Science and Technology, 69, 1225-1230, 2009.
58. Araŭjo J., Waldman W., De Paoli M., Polymer Degradation and Stability, 93, 1770-1775, 2008.
59. Dominkovics Z., Dányádi L., Pukánszky B., Composites: Part A, 38, 1893-1901, 2007.

Chapter 8

Use of functionlized PE, synthesized using a metallocene/methylalumionxane catalyst, in wood-LLDPE composites without using compatibilizers

Abstract

PE and different functionalised PEs were synthesised by copolymerising ethylene and 10-undecen-1-ol with a soluble metallocene/MAO catalyst, bis(tert-butyl-cyclopentadienyl)zirconium dichioride/MAO (bis(tert-buCp)$_2$ZrCl$_2$/MAO) at room temperature, using a 2000 mole ratio of aluminum/zirconium (Al/Zr). The copolymerisation products were characterisated by nuclear magnetic resonance spectroscopy (NMR), HT-GPC, FTIR and DSC. The incorporation of functional groups increased with increasing comonomer content. The PE and all the functionalised PEs had high MWs in order to be used as a matrix and compatibiliser, simultaneously, in WPC systems. The broadness in MWD and crystallinity decreased with increasing comonomer content. WPCs with 10 and 30% *A. cyclops* wood content of particle size 180 μm were prepared. Composites that were prepared with functionalised PE exhibited better mechanical, thermal and morphological properties than composites prepared with neat PE. Composites made with functionalised PE that contained more polar or hydroxyl groups had better mechanical, thermal and morphological properties than composites made with functionalised PE with fewer polar or hydroxyl groups. Composites with 10% wood content exhibited better properties and performance than composites with 30% wood content. The difference was found to be due to structural effects, possibly due to particles aggregation and the presence of gaps or voids.

Keywords: *Metallocene, Functionalised PE, WPCs, Aggregation.*

8.1 Background

8.1.1 General information

The functionalisation of polyolefins to enhance their properties is an area of keen interest [1]. This is because the hydrophilicity and low surface energy of polyolefins has limited their applications, especially in the areas of coatings, blends and composites, in which adhesion, compatibility, and paintability are paramount [2]. Incorporation of functional groups into polyolefins has created the opportunity to address these limitations. The functionalisation of

polyolefins can provide polymers with improved adhesion, thermal, rheological, morphological and optical properties, better affinity for dyes, and improved compatibility with other materials [1, 3]. Improvement in these properties largely depends on the number and nature of the attached functional groups [2]. It is believe that these functionalised polyolefins can be used, without the requirement for compatibilisers, in WPC systems to achieve the benefits that are otherwise offered by the filler, while still retaining most of the original properties of the polyolefin.

There are two approaches to functionalise polyolefins; chemical modification of preformed polymers, e.g. post-polymerisation, and direct copolymerisation with a functional monomer [3-6], as shown in Figure 8.1. The modification or post-polymerisation approach involves activation of the prepolymer by either exposure to high energy radiation or heating in the presence of a suitable free radical initiator, followed by initiation of the second monomer [6, 8]. The functionalisation efficiency using the post-polymerisation approach is quite low because there is no obvious reaction site in polyolefins [6]. The unreactive nature of hydrocarbon polymers lead to difficult chemical modifications, involving potentially harsh reaction conditions, and with a general lack of selectivity during the functionalisation process [4]. The obtained functionalised polyolefins usually possess a complex molecular structure coupled with a non-uniform distribution of functional groups [6]. Furthermore, this approach is normally accompanied by undesirable side reactions, such as crosslinking and degradation [3-4, 6, 8], which lead to significant deterioration in the otherwise superior mechanical and processing properties of polyolefins [6]. Although direct copolymerisation suffers from limitations, such as catalyst deactivation and comonomer homopolymerisation [3-6, 8, 9], it is a direct access route to desired polymers under mild and controlled conditions [6].

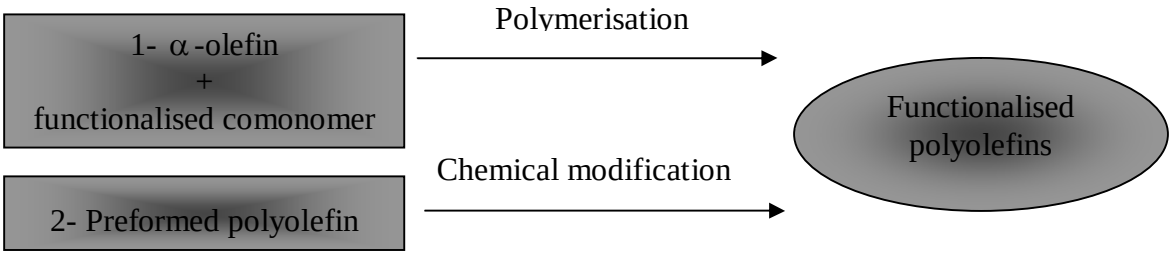

Figure 8.1 Pathways for polyolefin functionalisation.

Although Ziegler Natta catalysts are incapable of polymerizing monomers containing polar groups, metallocene catalysts have been successfully used in copolymerizing ethylene and

propylene with some functionalised monomers [6]. The functionalisation of polyolefins has been reviewed in the literature [5-6].

8.1.2 Metallocene catalysts

The term "metallocene" traditionally refers to organometallic compounds having two cyclopentadienyl (Cp) ligands and, optionally, one or more additional ligands such as an alkyl or halide. Figure 8.2a shows general molecular structures of metallocene catalysts: Cp_2MX_2 (Cp = cyclopentadienyl; M = titanium (Ti), zirconium (Zr), hafnium (Hf); X = halide, alkyl), also referred to as bis(Cp_2)MX_2. The metallocenes generally used in the synthesis of ethylene copolymers are bridged, un-bridged (as shown in Figure 8.2), substituted, and half-sandwich complexes.

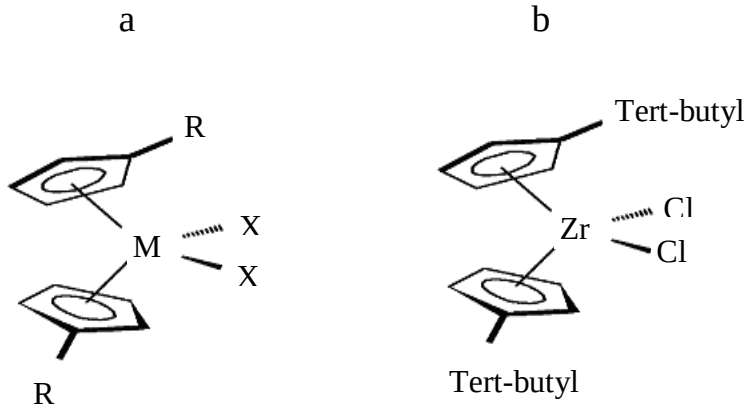

Figure 8.2 General molecular structures of a) metallocene and b) bis(tert-butCp_2)$ZrCl_2$.

The main features of metallocene complexes that affect olefin reactivity are the type transition metal in the complex, the type and number of substituents in the Cp rings, and the presence of bridges between the two Cp rings [10]. Of the three metals, Zr is the most active, followed by Hf and Ti [11]. As a result, most of these catalytic systems are based on Zr, with methylaluminoxane (MAO) as the co-catalyst [6]. MAO is the most widely used co-catalyst able to activate the largest number of metallocene catalysts [11]. The major advantage of metallocene catalysts is based on their Cp type ligands which can be broadly modified to provide the best combination of catalytic activity, MW, stereo- and regiospecificity and comonomer uptake. The ligands attached to the metal play a role in determining the effective charge on the metal atom. Ligands are used to stabilise the metal centre, to turn the electronic properties and steric crowding around the metal and to prevent dimerization of the complex. An increase in the catalytic activity of the catalyst and MW of the polymer when alkyl

substituents are introduced into the ring has been mentioned by several researchers. The size of substituents can also affect the chain transfer reaction and regeneration of the active centre. Steric factors can affect the conformation mobility of metallocene complexes, especially when several bulky substituents are introduced in the ring, and in this case it is difficult to predict their effect on all stages of the polymerisation reaction [12].

There are many different types of catalysts such as stereorigid $Et[Ind]_2ZrCl_2$, $Me_2Si[Ind]_2ZrCl_2$, $Me_2Si[2\text{-}MeInd]_2ZrCl_2$, $Me_2Si[2\text{-}Me\text{-}4,5\text{-}BenzoInd]_2ZrCl_2$ and $(n\text{-}BuCp)_2ZrCl_2$ activated with MAO used for the copolymerisation of ethylene or propylene with functional comonomers [1, 4, 6, 13]. In the copolymerisation of ethylene or propylene with functional comonomers using $(n\text{-}BuCp)_2ZrCl_2$ activated with MAO, it seems necessary that the functional group is remote from the olefinic double bond by the presence of a relatively long $(CH_2)_n$ spacer as in functional undecenes [6]. The increase in the number of carbon atoms between the functional group and double bond results in an increase in the comonomer incorporation [3].

In this part of the study, bis(tert-butyl-cyclopentadienyl)zirconium dichloride (bis(tert-$buCp)_2ZrCl_2$) (see Figure 8.2b), with MAO was chosen, for the first time, for the copolymerisation of ethylene with 10-undecen-1-ol. Catalytic data obtained by Talsi et al. [14] showed that the bulky substituent tert-butyl prevents tight cation anion contact in the $(t\text{-}BuCp)_2ZrCl_2$/MAO system, and the formation of a Zr-III species with the outer-sphere coordination of the anion becomes preferable. Thus, the Zr-III heterodinuclear pairs can initiate ethylene polymerisation and are precursors of active species in polymerisation. Aatlonen and Löfgren [1] found that a high MW functionalised PE was obtained at a Al/Zr mole ratio of 2000 when using $(n\text{-}BuCp)_2ZrCl_2$ for the copolymerisation of ethylene and 10-undecen-1-ol. Al/Zr mole ratios of 3000, 4000 and 5000 led to lower MW and narrow MWD values. This is considered very important because we believe that functionalised PE with a high MW can be used in WPC systems as a matrix and compatibiliser simultaneously. On the other hand, a narrow MWD means that it will be difficult to process these materials because their melt flow indices will be low [1]. So, the Al/Zr mole ratio was kept at 2000 for all the copolymerisation that carried out in this part. Information details including; synthesis and characterisation of this type of catalyst are presented in literature [15-18]. Some functionalised polyolefins such as MAPE, MAPP, maleated styrene-ethylene/butylene-styrene copolymer, copolymer of propylene and 10-undecenol and copolymer of ethylene and 10-undecenol were evaluated as compatibilisers in WPC system [19-20]. The ideas behind using functionalised polyolefins as a matrix and compatibiliser simultaneously in WPC system are:

❖ As far as the influence of compatibilisers on the melt flow behaviour of WPCs is concerned, the available literature data are rather controversial [21].

❖ Contradictory information is available about the effect of the number of functional groups and MW of functionalised polymer on WPC properties [21-22].

❖ Minimise the raw materials. Therefore, the mixture of polymer matrix and filler "two-phase system" would probably be less complicated than a mixture of polymer, filler and compatibiliser "three-phase system" in terms of compatibilisation and processing.

❖ Impart more environmental and economic benefits.

8.2 Experimental

8.2.1 Materials

All copolymerisation reactions of ethylene and 10-undecen-1-ol were carried out in nitrogen atmosphere, using standard Schlenk techniques. Glassware, including syringes, were kept in an oven at about 100 ^{o}C prior to use. The catalyst, bis(tert-buCp)$_2$ZrCl$_2$, was obtained from Sigma Aldrich and was used as received. Analytical grade toluene, obtained from BDH, was used as a solvent in the polymerisation of ethylene, and copolymerisation of ethylene and 10-undecen-1-ol. Toluene was dried by refluxing over sodium/benzophenone and then distilled under a nitrogen atmosphere, and stored over molecular sieves. MAO was purchased from Sigma Aldrich and used as received (10% solution in toluene). Ethylene (polymerisation grade, > 99%) was obtained from Fedgas and was used without further purification in the copolymerisation of ethylene and 10-undecen-1-ol. 10-undecen-1-ol (98%) was purchased from Sigma Aldrich. Hydrochloric acid (32%) and methanol (99.5%) from Saarchem were used to terminate the copolymerisation of ethylene and 10-undecen-1-ol. Xylene, A. *cyclops* (180 μm), and a mixture of Irganox 1010 and Irgafos stabilisers were used as described in Section 3.2.1, for the preparation of the composites. LLDPE as described in Section 5.2.2 was used as a matrix.

8.2.2 Preparation of catalyst

About 18 mg of bis(tert-buCp)$_2$ZrCl$_2$ was weighed in a Schlenk tube and dissolved in 20 mL toluene. All catalyst preparation work was performed in a glove box under a nitrogen atmosphere.

8.2.3 Method of polymerisation

Polymerisation was performed at room temperature in a 300 mL stainless steel (Parr autoclave) pressure reactor fitted with a magnetic stirring bar. The stainless steel reactor was

equipped with a pressure gauge, gas inlet and sample introduction port. The system was first evacuated and flushed with nitrogen, using Schlenk line techniques. A new Schlenk tube was sealed and transferred to a Schlenk line adjacent to the reactor. Then 1 mL (~ 0.55 μmol/L) of the catalyst and 2 mL (2 mol/L) of MAO were introduced to the Schlenk tube. About 10 and 20 mL of toluene were added to the Schlenk tube and the reactor, respectively. The Schlenk tube was allowed to stand for 5 min under stirring to preactivate the catalyst. The catalyst mixture or solution was then introduced to the reactor. The reactor was charged with 3-8 g ethylene and allowed to stand for 1-3 min under stirring to start the polymerisation. The comonomer, 10-undecen-1-ol, was then added to the reactor. After about 1-2 min, 6-8 g ethylene was added. All reactions were left to take place over 2 h, after which they were terminated via the addition of a 10% solution of hydrochloric acid and methanol for 24 h. The resulting polymer or copolymer was filtered off, then washed several times with methanol, and subsequently dried at 80 ^{o}C for at least 12 h. The same procedure and conditions were used for the polymerisation of ethylene.

The Abbreviations of each polymer or copolymer, the amount of each component used in each polymerisation process and the yields of the final products are presented in Table 8.1. It is important to note that the reactor was open before each addition and weighed after each addition mentioned above. Hence, not all the ethylene participated in all the polymerisations.

Table 8.1 Abbreviations of each prepared polymer, the amounts of the ethylene and 10-undecen-1-ol used in each polymerisation, and the yields of the final products

Polymer or compolymer	First addition of ethylene, g	Addition of 10-undecen-1-ol, mL	Second addition of ethylene, g	Yield, g
PE	8.0	---	---	1.3
PEOH1	3.0	0.5	8.0	1.6
PEOH2	3.0	1.0	6.0	1.0
PEOH3	5.0	1.5	8.0	2.0

8.2.4 Preparation of the composites

The prepared polymers (PE, PEOH1, PEOH2 and PEOH3) were melted at 130 ^{o}C with a small volume of xylene. A mixture of Irganox 1010 and Irgafos stabilisers was added to inhibit any possible degradation that may occur during the preparation of the composites. After complete melting, the melted polymer was removed from the flask and 10 and 30 wt% wood particles (dried at 105 ^{o}C for 24 h) were added rapidly, while stirring. The composite was then cooled to ambient temperature and dried in a vacuum oven overnight at 50 ^{o}C. The abbreviated names and the compositions of each of the composites used in this study are

listed in Table 8.2. Specimens to be used in various tests to determine the mechanical and thermal properties were prepared by IM, as described in Section 6.2.1.

Table 8.2 Abbreviations and the compositions of each composite used in this part of the study

Abbreviation	Type of polymer or copolymer	Polymer or copolymer, %	*A. cyclops*, %
PEW10	PE	90	10
PEOH1W10	PEOH1	90	10
PEOH2W10	PEOH2	90	10
PEOH3W10	PEOH3	90	10
PEW30	PE	70	30
PEOH1W30	PEOH1	70	30
PEOH2W30	PEOH2	70	30
PEOH3W30	PEOH3	70	30

8.2.5 Characterisation

Nuclear magnetic resonance (NMR) spectra (^{13}C and ^{1}H NMR) were recorded at 120 ^{o}C on a Varian VXR 300 MHz spectrometer. Typical conditions were: a pulse angle of 45^{o} and 0.82 s acquisition time The samples (~80 mg) were dissolved in a 9:1 mixture of 1,2,4-trichlorobenzene-C_6D_6. C_6D_6 at δ = 128.02 ppm was used as an internal secondary reference. FTIR, as described in Section 3.3.8 was used to confirm the presence of hydroxyl groups in the functionalised PEs. FTIR was also used to determine the compatibility between these polymers and wood particles by monitoring the formation of hydrogen bonding. DSC, as described in Section 3.3.3 was used to record the T_m, T_c and X_c values of the prepared functionalised PEs and their composites. The MW and MWD of the functionalised PEs were determined using high-temperature gel permeation chromatography (HT-GPC). HT-GPC analyses were conducted on a PL-GPC 220 high-temperature chromatograph equipped with a differential refractive index detector and three PL gel MIXED-B columns (Polymer Laboratories). The concentration of the samples was 2 mg/ml in 1,2,4-trichlorobenzene solvent, stabilised with 0.0125% 2,6- di-tert-butyl-4-methylphenol. A flow rate of 1 ml/min and temperature of 160 ^{o}C was maintained for all experiments. The MW calibration was carried out with monodisperse polystyrene standards (EasiCal from Polymer Laboratories).

At least three samples of each functionalised PE and composite were tested for their tensile strength, EAB and hardness, as described in Section 3.3.2. Sample sizes used for tensile strength and EAB tests were 5 mm × 50 mm × 1.5 mm, and the size of the sample used for the hardness test was 20 mm diameter x 1.5 mm thickness. The hardness results quoted are the average of ten measurements. Impact testing was performed as described in Section 5.3. At

least three IM specimens were tested for each composite. The size of each specimen was 5 mm × 50 mm × 1.5 mm. DMA, as described in Section 3.3.2 was used here to determine E′, E″ and tan δ. Thermal stability measurements were conducted using the same procedure and instrumentation as described in Section 3.3.3. The morphologies of the composites, after quenching in liquid nitrogen (fracture surface), were studied using SEM, as described in Section 4.3.

8.3 Results and discussion

8.3.1 Characterisation of the PE and copolymers

The chemical structures of PE and functionalised PEs were characterised by ^{13}C NMR spectroscopy. The formation of PE and functionalised PEs was clearly evident from the ^{13}C NMR spectra of the PE, PEOH1, PEOH2 and PEOH3. As shown in Figure 8.3a, the methylene signals appeared at about 30.5 ppm in all the spectra. The signal due to the branching carbon appeared at 38.2 ppm (labeled as * in the scheme of Figure 8.3a) and the resonances of the α (labeled number 1 in the scheme of Figure 8.3a), β (labeled number 2 in the scheme of Figure 8.3a) and γ (labeled number 3 in the scheme of Figure 8.3a) carbons at 34.6, 27.4 and 30.6 ppm, respectively. PE did not show these signals. The ^{13}C NMR spectra of the PEOH1, PEOH2 and PEOH3 also showed signals at about 62.9 ppm (labeled number 6 in the scheme of Figure 8.3a), these originate from the chain end carbon of the alcohol branch and indicates the presences of a hydroxyl group at the chain end. ^{13}C NMR spectra in Figure 8.3a reveal that the concentration of the polar groups in PEOH3 was greater than in PEOH2 and PEOH1, as indicated by the intensities of the signals at 62.9 ppm.

^{1}H NMR spectroscopy was used to determine the comonomer content of the copolymer and confirm the presence of the hydroxyl group at the chain end. The ^{1}H NMR spectra of PE, PEOH1, PEOH2 and PEOH3 are shown in Figure 8.3b. The signals of the methylene protons were located between 1.35 and 1.67 ppm. The signals at about 3.65 (labeled as * in the scheme of Figure 8.3b) ppm are a clear indication of the presence of hydroxyl group, which was used to determine the comonomer incorporations. The comonomer incorporations were calculated based on the integration of characteristic peaks of the methylene protons and hydroxyl groups. ^{1}H NMR spectroscopy is a much more convenient method by the integration of signals [23]. ^{1}H NMR spectra in Figure 8.3b also confirms the greater concentration of the polar groups in PEOH3 in comparison to PEOH2 and PEOH1, as indicated by the intensities of the signals at 3.65 ppm. PE did not show this signal. These results are similar to results obtained by Aaltonen and coworkers [1, 3-4]. For more information about the structure of these polymers see the FTIR spectra in Appendix F.

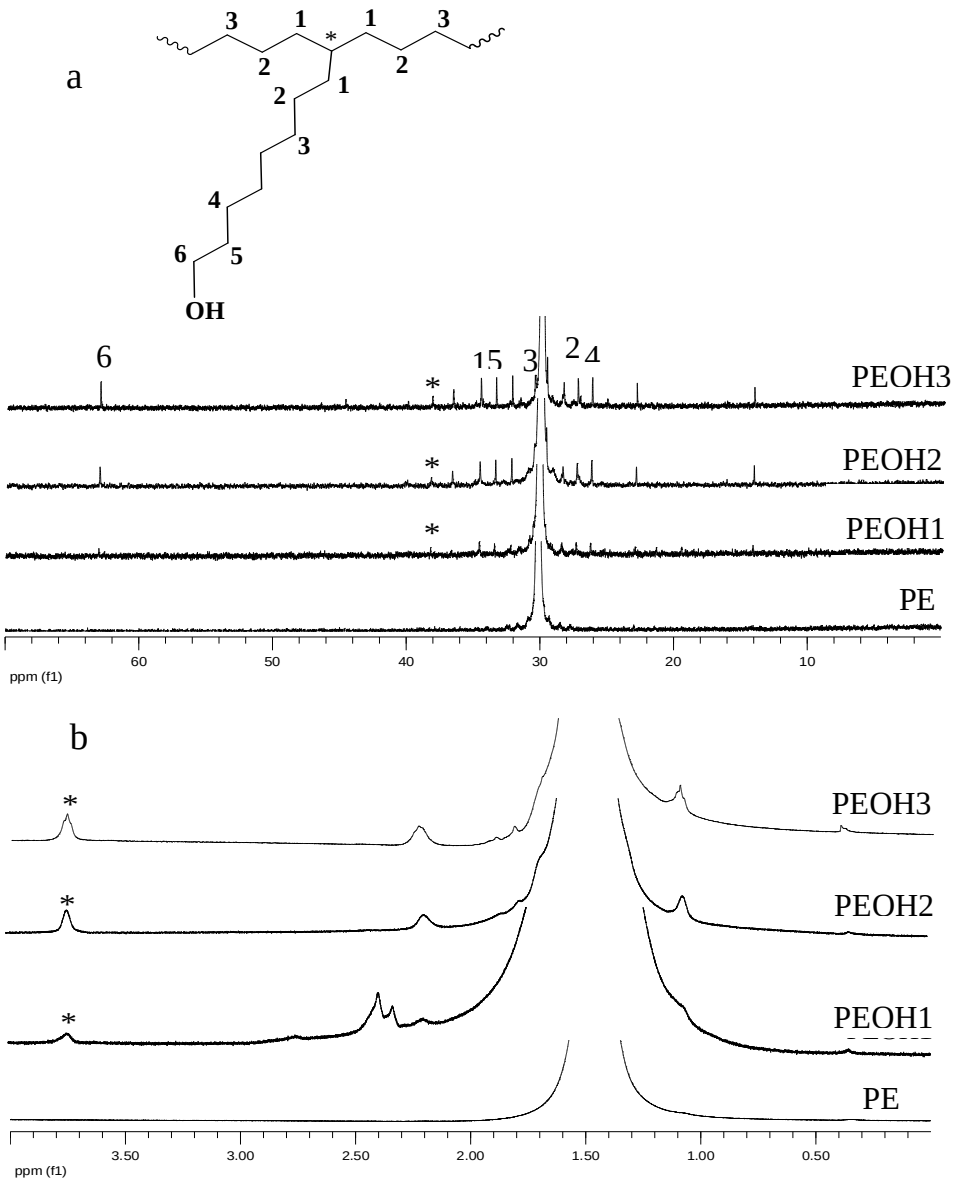

Figure 8.3 a) ^{13}C NMR and b) ^{1}H NMR spectra of PE, PEOH1, PEOH2 and PEOH3 (solvent 1,2,4 trichlorobenzene).

Table 8.3 Properties of the prepared PE, PEOH1, PEOH2 and PEOH3

Polymer or copolymer	Comonomer content, %	$\overline{M_n}$	$\overline{M_w}$	MWD	T_c, °C	T_m, °C	ΔH_f, J/g	X_c, %
PE	0.0	149215	1026280	6.9	115.7	133.0	180.1	62.4
PEOH1	0.2	116018	758782	6.5	115.9	133.4	164.3	56.9
PEOH2	0.3	35135	161770	4.6	115.7	131.5	163.9	56.8
PEOH3	0.8	444340	1473217	3.3	114.0	130.1	160.5	59.8

The comonomer content values, MW, MWD, T_m, T_c, ΔH_f and X_c of PE, PEOH1, PEOH2 and PEOH3 are given in Table 8.3. The value of 288.7 J/g was taken as a value of ΔH_f^o of completely crystalline PE [24]. Because the most important factors influencing the properties of the obtained PE and functionalised PEs are MW and X_c, the relationship between these factors and comonomer content are illustrated in Figure 8.4.

The three-dimensional plot in Figure 8.4 shows the projections of data points in three dimensional spaces on the surface of each plane. The X_c decreased with incorporation of hydroxyl groups and increased with increasing MW.

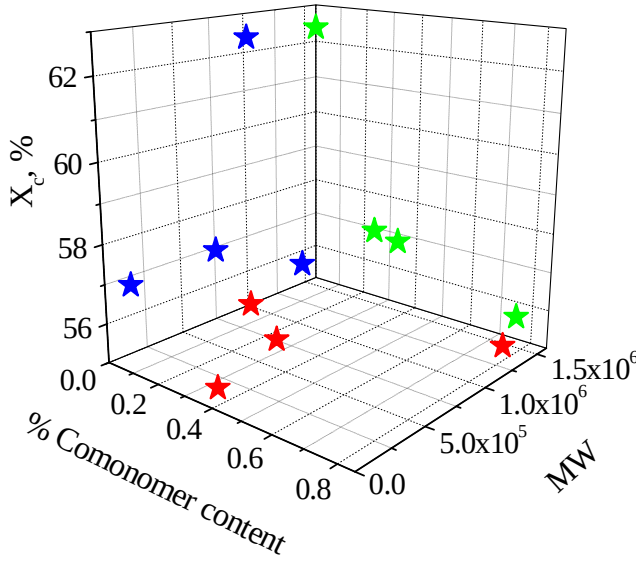

Figure 8.4 The relationship between comonomer content and the MW and X_c of the obtained PE and functionalised PEs.

8.3.2 Mechanical properties of PE, functionalised PEs and composites

The mechanical properties of PE, PEOH1, PEOH2, PEOH3 and their composites are presented in Table 8.4 and Figure 8.5. Calculated standard deviations are given in parentheses. PE exhibited higher tensile strength and EAB than the functionalised PEs. PEOH3 had the highest values of hardness and impact strength compared to PE and the other functionalised PEs. The better properties of PE and PEOH3 in comparison to the other functionalised PEs are due to their higher MW, as shown in Table 8.3.

PE exhibited better mechanical properties than its composites (PEW10 and PEW30). This is due the incompatibility and weak adhesion between the hydrophilic wood and hydrophobic PE, as has been frequently discussed. On the other hand, the functionalised polymers (PEOH1, PEOH2 and PEOH3) exhibited lower mechanical properties, with the exception to the EAB and impact properties, than their composites. Fillers generally cause a dramatic

decrease in the EAB and impact properties [25]. This is because fillers and reinforcements reduce the polymer chain mobility and thereby reduce the ability to absorb energy during fracture propagation [24]. These results, however, implied that some adhesion was promoted in these composites due to the presence of hydroxyl groups in their matrices.

Table 8.4 Mechanical properties of PE, PEOH1, PEOH2, PEOH3 and their composites

Composite	Tensile strength, MPa	EAB, %	Hardness, MPa	Impact strength, J/m^2
PE	27.8 (1.9)	16.8 (1.3)	04.3 (0.5)	1893.9 (0.1)
PEOH1	16.8 (0.3)	08.9 (1.4)	04.3 (0.5)	1799.2 (0.1)
PEOH2	19.4 (0.2)	10.3 (0.4)	05.3 (0.5)	1751.9 (0.1)
PEOH3	27.3 (0.5)	12.9 (0.9)	06.2 (0.4)	2036.0 (0.1)
PEW10	10.1 (1.0)	05.7 (1.0)	05.7 (1.0)	1231.1 (0.1)
PEOH1W10	20.6 (1.1)	12.2 (0.8)	07.3 (1.0)	1420.5 (0.1)
PEOH2W10	23.2 (0.4)	09.9 (1.8)	07.5 (1.1)	1373.1 (0.1)
PEOH3W10	29.5 (0.4)	14.2 (0.8)	06.3 (0.8)	1515.2 (0.1)
PEW30	15.2 (0.1)	11.5 (0.6)	06.8 (0.8)	852.3 (0.1)
PEOH1W30	18.6 (1.4)	08.4 (1.3)	07.5 (1.1)	947.0 (0.1)
PEOH2W30	21.5 (0.5)	09.4 (0.3)	07.7 (1.2)	1136.4 (0.1)
PEOH3W30	28.8 (0.2)	10.9 (1.1)	06.5 (0.8)	1231.1 (0.1)

Figure 8.5 shows the mechanical properties of PE, PEOH1, PEOH2, PEOH3 and their composites. Composites with 10% wood content had superior mechanical properties, with the exception of the hardness. This is to be expected, because the hardness of the WPCs increases with an increase in the wood particle loading [26]. Better improvements could be achieved if more comonomer was incorporated in the functionalised PEs. This is why PEOH3W10 demonstrated better mechanical properties than PEOH1W10 and PEOH2W10. Increasing the wood content from 10 to 30% caused a small reduction in the mechanical properties. The number of hydroxyl groups on the wood surface and the number of hydroxyl groups in the functionalised PEs in the cases of the composites made with 30% wood content form less adequate bonding between the wood and the functionalised PE matrices than in the cases of the composites made with 10% wood content, probably due to aggregation.

The probability of the formation of aggregates increases with increasing wood content, and the strength decreased with increasing number and size of aggregates [22]. The strength decreased drastically at higher filler contents (30%) because of aggregation lack of matrix continuity [27]. The aggregation and orientation of the anisotropic wood particles are the most important structural phenomena that determine the properties of WPCs [22]. Most importantly, even in the cases of composites made with 30% wood content, a composite made

with functionalised PE containing more hydroxyl groups (PEOH3W30) demonstrated better mechanical properties than composites made with functionalised PEs with fewer hydroxyl groups, as in PEOH1W30 and PEOH2W30.

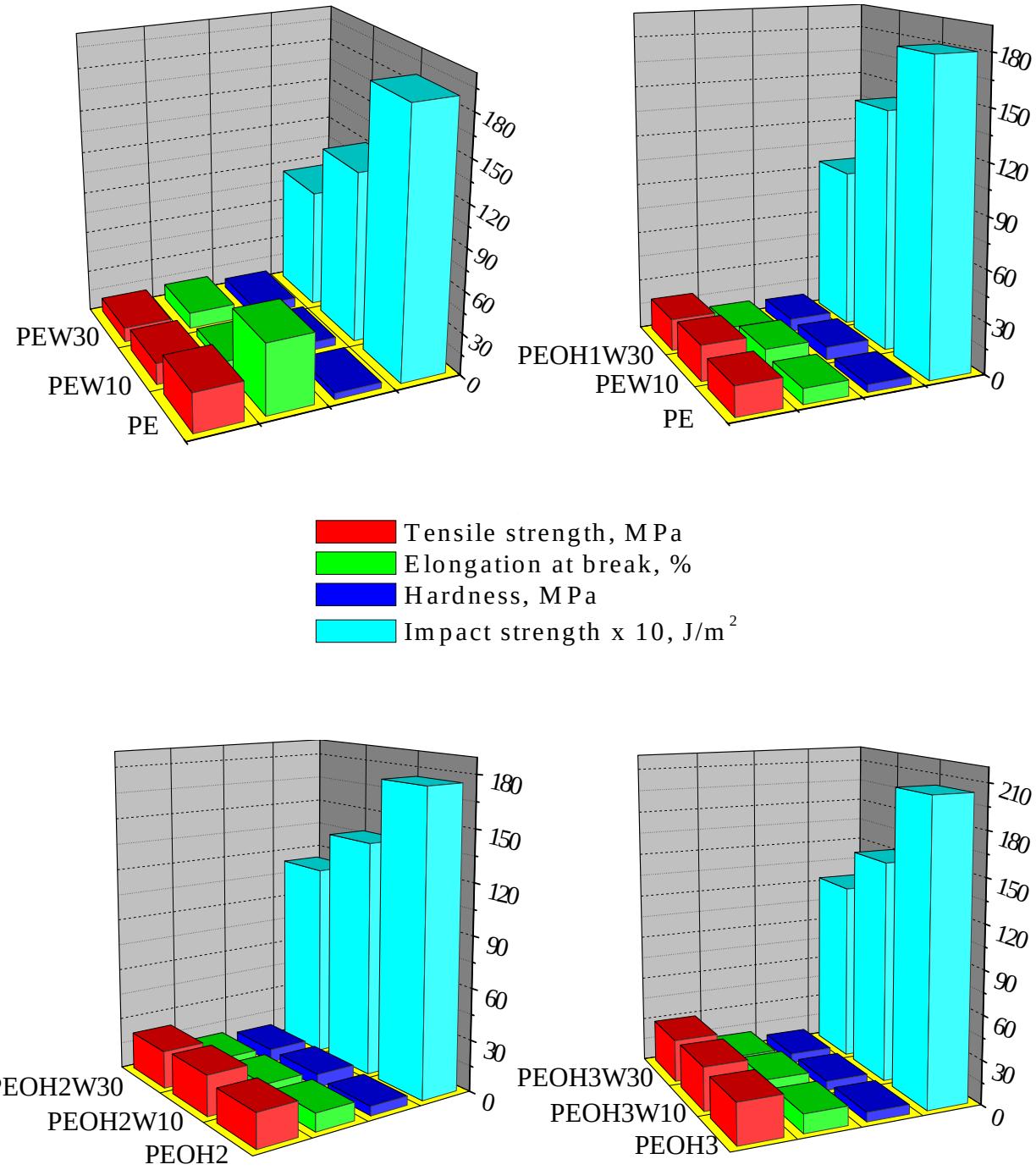

Figure 8.5 Mechanical properties of PE, PEOH1, PEOH2, PEOH3 and their composites.

8.3.3 Dynamic mechanical properties

The curves of E′, E″ and tan δ dependence on temperature of PE, PEOH1, PEOH2, PEOH3 and their composites are shown in Figure 8.6, 8.7 and 8.8, respectively. Figure 8.6 shows the E′ of PE, PEOH1, PEOH2, PEOH3 and their composites. A general declining trend was

observed with increasing temperature. This is due to the softening of the matrix and the initiation of a relaxation process [28].

At temperatures above T_g the molecular mobility and thermal expansion increased thus reducing the interfacial interaction, and hence E′ decreased sharply. The E′ increased remarkably upon the addition of wood into PE or the functionalised PE matrix, due to the enhanced stiffness [28-30]. The enhanced stiffness of the composites can be primarily attributed to the improved compatibility between filler and matrix [31]. The E′ increased with an increasing amount of wood, from 10 to 30%. This is because of the mechanical limitation posed by increasing the wood concentration embedded in the viscoelastic matrix, thereby reducing the mobility and the deformation of the matrix with increasing temperature [28].

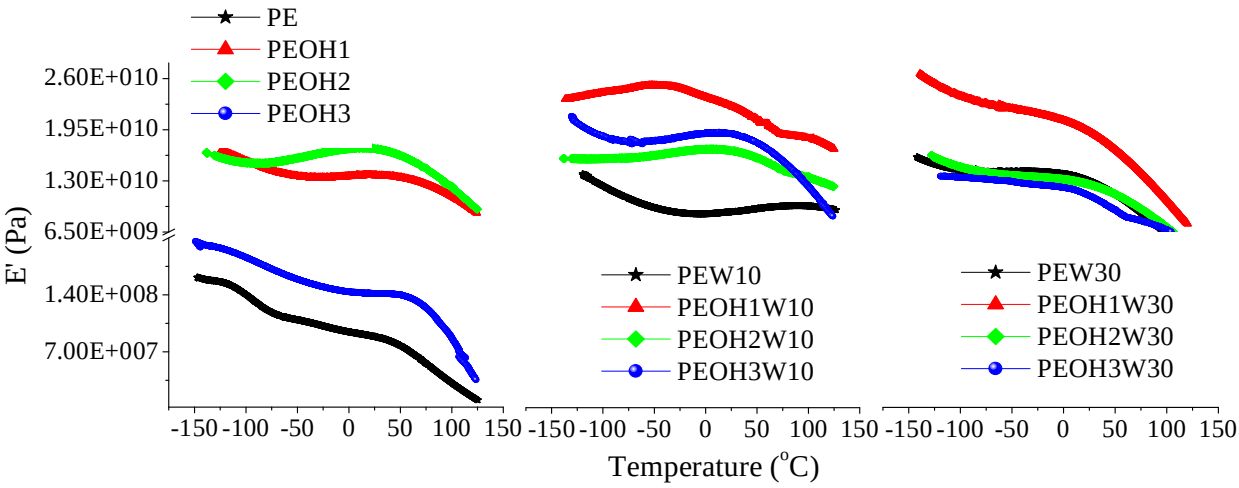

Figure 8.6 E′ of PE, PEOH1, PEOH2, PEOH3 and their composites.

Among these composites, PEOH1W30 exhibited the maximum E′ value at low temperature, while PEOH1W10 displayed the maximum E′ value at high temperature. The lowest E′ value was observed for PE over the entire temperature range. There was no significant difference between PEW30, PEOH2W30 and PEOH3W30. These differences in E′ can be due to the distribution of wood in the tested specimens, since the E′ of composites is dependent on the type of wood species [32]. This is because a uniform dispersion of wood particle in a matrix can lead to an increase the E' [28].

Figure 8.7 shows the E″ of PE, PEOH1, PEOH2, PEOH3 and their composites. Two noticeable transitions or relaxations were detected in all the curves, with the exception of PEOH1W10 and PEOH2W10 curves. The first transition (γ-transition or T_g) was observed at -104.4, -103.4, -102.4 and -100.4 °C for PE, PEOH1, PEOH2 and PEOH3, respectively. This

transition was observed at -104.1, -100.7, -99.7 and -96.8 °C for PEW10, PEOH1W10, PEOH2W10 and PEOH3W10, respectively. In the cases of composites with 30% wood content, this transition was detected at -105.5, -102.8, -102.5 and -98.4 °C for PEW30, PEOH1W30, PEOH2W30 and PEOH3W30, respectively. On the other hand, the second transition (β-transition) was observed at 61.9, 81.7, 83.0 and 87.0 °C for PE, PEOH1, PEOH2 and PEOH3, respectively. In the cases of composites with 10% wood content, β-transition was observed at 91.6, 92.7, 93.6 and 95.6 °C for PEW10, PEOH1W10, PEOH2W10 and PEOH3W10, respectively. This transition was observed at 67.2, 70.2, 72.2 and 69.3 °C for PEW30, PEOH1W30, PEOH2W30 and PEOH3W30, respectively.

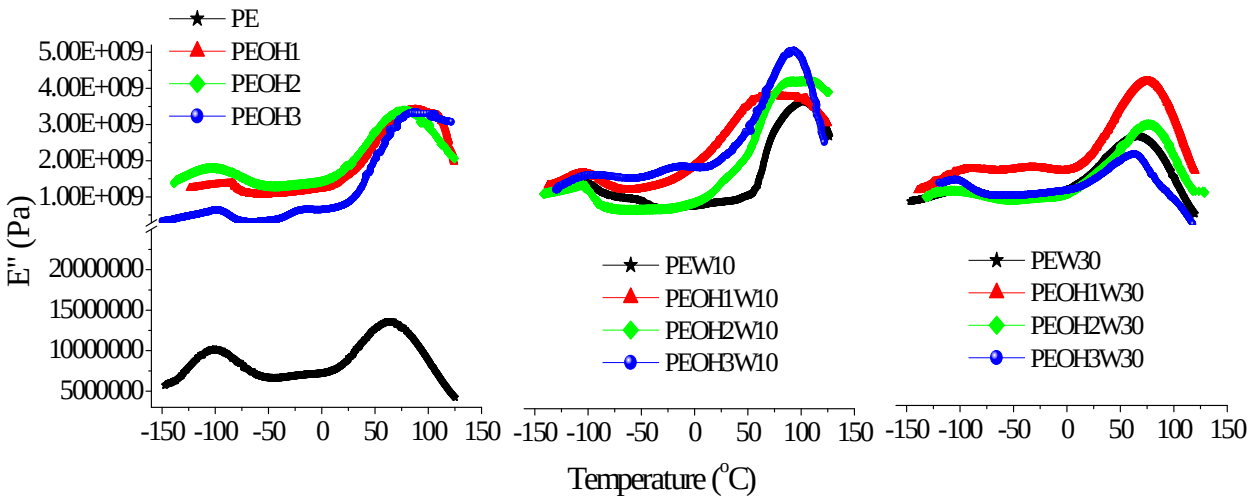

Figure 8.7 E″ of PE, PEOH1, PEOH2, PEOH3 and their composites.

As has been frequently mentioned, the shift of the γ-transition or T_g and the β-transition of the composites to higher temperature indicate better interfacial interaction between the wood particle and the functionalised PE matrix. The PE composites (PEW10 and PEW30) showed the opposite trend. Most of these transitions of the PE composites were shifted to lower temperatures, indicating lower compatibility and weak adhesion between the hydrophilic wood and hydrophobic PE.

The temperature dependence of tan δ of PE, PEOH1, PEOH2, PEOH3 and their composites is shown in Figure 8.8. The tan δ values of PE, PEOH1, PEOH2, PEOH3 and their composites increased with increasing temperature due to the increased PE chain mobility. Although tan δ is less distinctive than E″ with regards to the γ-transition process [33], most of the tan δ curves show two maxima, at around –100 °C and 125 °C, corresponding to the two transitions mentioned in the case of E″. The addition of 10 and 30% of wood into PEOH1, PEOH2 and PEOH3 matrices led to a shift in the γ-transition to higher temperatures, resulting in higher T_g

values than those of the pure functionalised PEs, with the exception of PEOH2W10. This shift was more pronounced in the composites with 10% wood content than in the composites with 30% wood content. This shift, once again, indicates the better interfacial interaction between the wood particle and the functionalised PE matrix. As in the case of E″, PE and its composites did not follow the same trend due to the lower compatibility and weak adhesion between the hydrophilic wood and the hydrophobic PE. The addition of wood also led to a decrease in the height of the tan δ peak, which suggests that, some degree of interfacial bonding existed between the wood particles and the functionalised PE matrices [28].

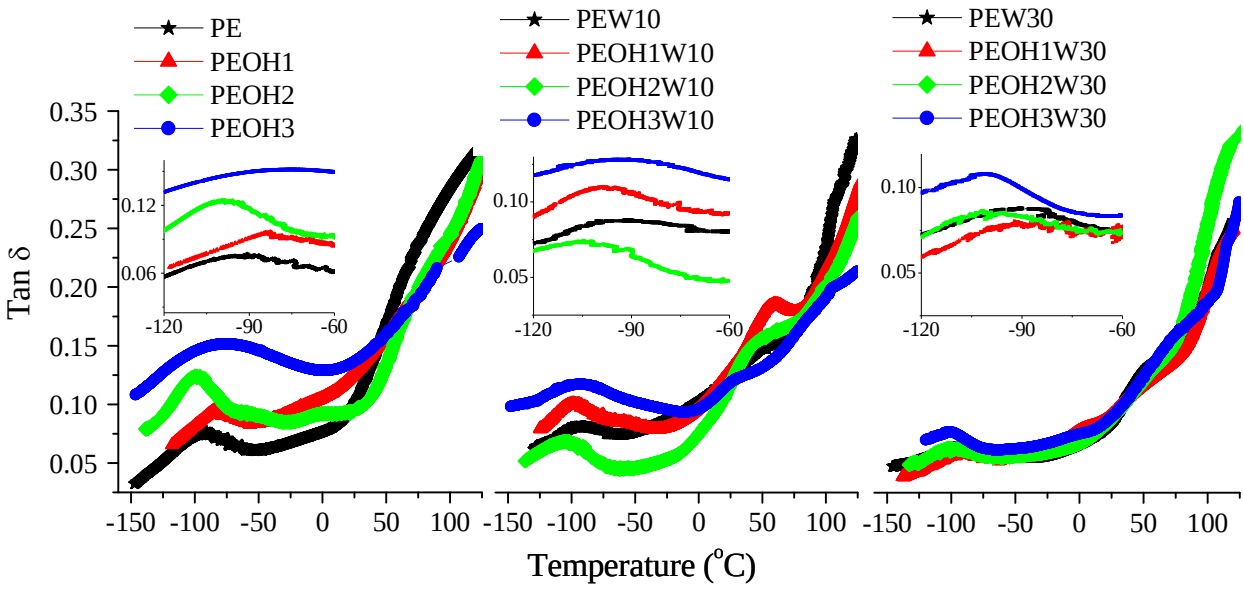

Figure 8.8 Tan δ of PE, PEOH1, PEOH2, PEOH3 and their composites.

On the other hand, the difference in the tan δ peaks amplitude can be related to chain mobility and the number of amorphous polymer matrix chains involved in the transition [34]. The tan δ curves of the composites made with 30% wood content almost overlapped. Consequently, no clear difference can be seen in the behaviour of these composites at temperatures above the γ-transition or T_g, this could be attributed to problems of particle agglomeration due to the high proportions of wood used. The wood particles introduced a high degree of restraint, reducing the mobility and deformability of the matrix.

8.3.4 Thermal properties

Table 8.5 lists the T_m, T_c, ΔH_f, X_c and X_c^{corr} values, and Figure 8.10 presents the DSC heating and cooling curves for the PE, PEOH1, PEOH2, PEOH3 and their composites. A ΔH_f^o value of 288.7 J/g for completely crystalline PE [24] was used to calculate the X_c of PE, PEOH1, PEOH2, PEOH3 and their composites.

Figure 8.9 shows the DSC cooling curves of PE, PEOH1, PEOH2, PEOH3 and their composites. There was one exothermic peak for the crystallisation between 114 and 120 ^{o}C. Only a single peak was detected in the melting endotherms for each sample at about 130 and 135 ^{o}C.

In the case of PE and functionalised PEs, the single melting peak moves to lower temperature with an increase in the hydroxyl group concentration as we move from PE to PEOH1 to PEOH2 to PEOH3.

Table 8.5 Melting and crystallisation data for PE, PEOH1, PEOH2, PEOH3 and their composites

Sample	T_c, ^{o}C	T_m, ^{o}C	ΔH_f, J/g	X_c, %	X_c^{corr}, %
PE	115.7	133.0	180.1	62.4	62.4
PEOH1	115.9	133.4	164.3	56.9	56.9
PEOH2	115.7	131.5	163.9	56.8	56.8
PEOH3	114.0	130.1	160.5	55.6	55.6
PEW10	117.0	133.6	148.1	51.3	57.0
PEOH1W10	117.2	132.9	154.2	53.4	59.3
PEOH2W10	116.8	130.6	157.6	54.6	60.7
PEOH3W10	120.0	131.8	152.3	52.8	58.6
PEW30	116.6	134.4	119.6	41.4	59.2
PEOH1W30	116.9	134.6	141.2	48.9	69.9
PEOH2W30	116.1	132.7	150.3	52.1	74.4
PEOH3W30	117.5	133.0	122.1	42.3	60.4

The slight change in the T_c (~1 to ~6 ^{o}C) of the composites in comparison to the neat PE or functionalised PEs indicates that the crystallisation of the composites become a bit rapid. Based on peak temperature changes, PEOH3W10 showed the best improvement (5.94 ^{o}C).

ΔH_f of PE was higher than those of all the functionalised PEs. ΔH_f of each composite was lower than that of its pure PE or functionalised PEs. As a result, X_c of each composite was lower than X_c of its pure PE or functionalised PE matrix. However, the X_c decreased as the wood content increased. With the exception of PE and its composites, X_c^{corr} of each composite was higher than its X_c.

Addition of wood into PE or functionalised PE caused only a minor change in the T_m (1-2 ^{o}C). It has been suggested [34] that this may not be a real effect but merely a result of the difference in the heat capacity between the filled and unfilled composites, resulting in an apparent temperature lag during the measurement.

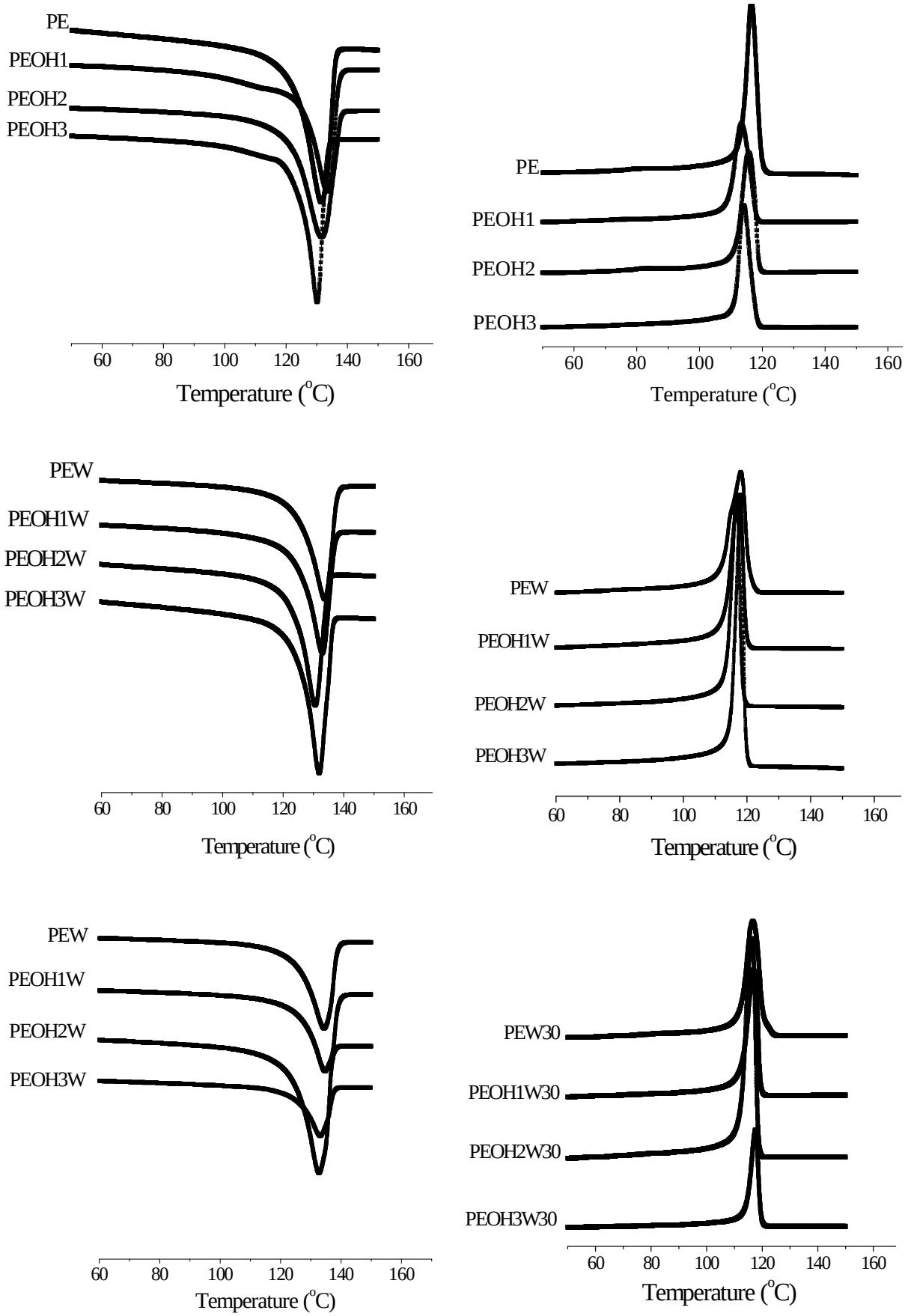

Figure 8.9 DSC heating and cooling curves of PE, PEOH1, PEOH2, PEOH3 and their composites.

Thermal properties of PE, PEOH1, PEOH2, PEOH3 and their composites based on TGA results are presented in Figure 8.10.

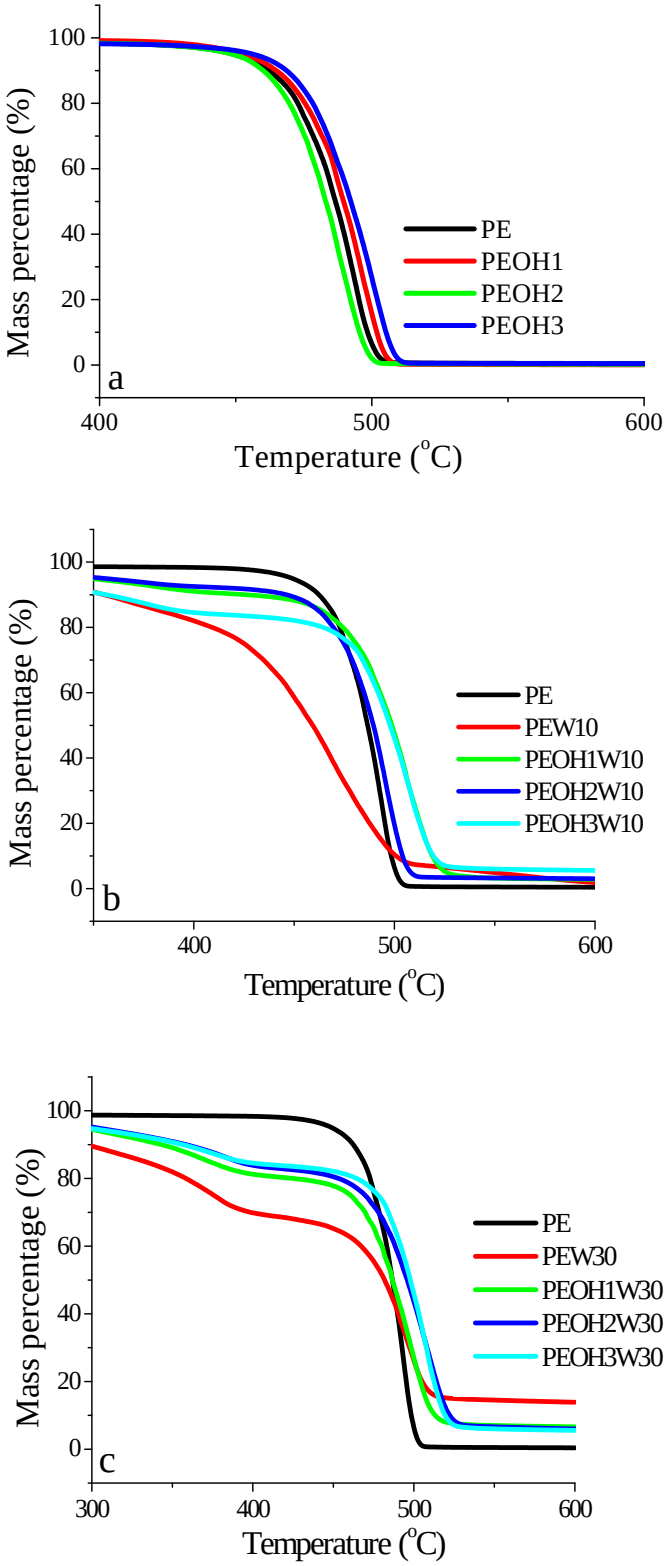

Figure 8.10 TGA curves of PE, PEOH1, PEOH2, PEOH3 and their composites.

From Figure 8.10a, it can be seen that the weight loss of PE, PEOH1, PEOH2 and PEOH3 occurred in a one step degradation process from above 400 to less than 550 ºC. The quantity

of these materials' residue is very low (~ 0.1-0.4%). The highest residue was determined for PE (0.4%) and the lowest for PEOH1 (0.1%). The residues of PEOH2 and PEOH3 were (0.2%) and (0.4%), respectively. As shown in Figure 8.10a, the highest thermal stability was observed for PEOH3 and the lowest stability was exhibited by PEOH2. The lower stability of PEOH2 in comparison to PE, PEOH1 and PEOH3 may be attributed to its lower MW, as shown in Table 8.3. It is occasionally observed that increasing MW produces increased thermal stability [35].

As shown in Figure 8.10b and 8.10c, the TGA curves of the composite materials show one initial and two main stages of weight loss. The initial weight loss was observed at about 100 ^{o}C (not shown in Figure 8.10), due to the evaporation of moisture in the wood. The first main weight loss stage started from approximately 200 to about 380 ^{o}C, due to the decomposition of hemicelluloses and lignin. The second weight loss stage observed above 400 ^{o}C, due to the cellulosic materials of wood and to the PE or functionalised PE matrix. As shown in Figure 8.10b, PEOH3W10 showed to be more stable than PEOH2W10, PEOH1W10, PE and PEW10, respectively. The highest residue was determined for PEOH3W10 (5.6%) and the lowest for PEW10 (1.8%). The residue of PEOH1W10 and PEOH2W10 were (2.9%) and (3.1%), respectively.

The quantity of residue decreased as the amount of wood increased. As shown in Figure 10c, the quantity of residue in the cases of the composites with 30% wood content was approximately between (5.7-14.1%). The highest residue was determined for PEW30 (14.1%) and the lowest for PEOH3W30 (5.7%). The residue of PEOH1W30 and PEOH2W30 were (6.7%) and (6.2%), respectively. PEOH3W30 was more stable than PEOH2W30 PEOH1W30, PE and PEW30, respectively. However, in both cases (composites with 10 and 30% wood content), the thermal stability of the composites increased with increasing the hydroxyl groups incorporated into PE. The improved thermal stability of the WPC is due to the enhanced adhesion between the polymer matrix and the wood particles, resulting in enhanced overall mechanical properties of the composites [36]. This indicates that the more functional groups incorporated into PE, the better compatibility and adhesion between the wood and the functionalised PE would be.

PEOH3W10 showed to be more stable than PEOH3W30, as shown in Figure 8.11. This is because the number of hydroxyl groups in functionalised PE is too small in comparison to hydroxyl of wood in the composites with 30% wood content. The hydroxyl groups on the surface of wood form hydrogen bonding and attract each other and form aggregates.

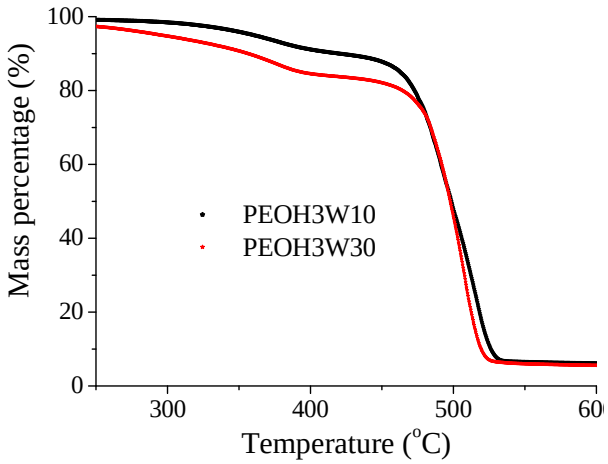

Figure 8.11 Difference in the thermal stability between PEOH3W10 and PEOH3W30.

8.3.5 Wood distribution

Figures 8.12 and 8.13 represent the morphology and distribution of the wood particles in the composites with 10 and 30% wood content. Composites with 10% wood content (Figure 8.12) seem to be more uniform and somehow well dispersed in the functionalised PE matrices than in the composites with 30% wood content (Figure 8.13).

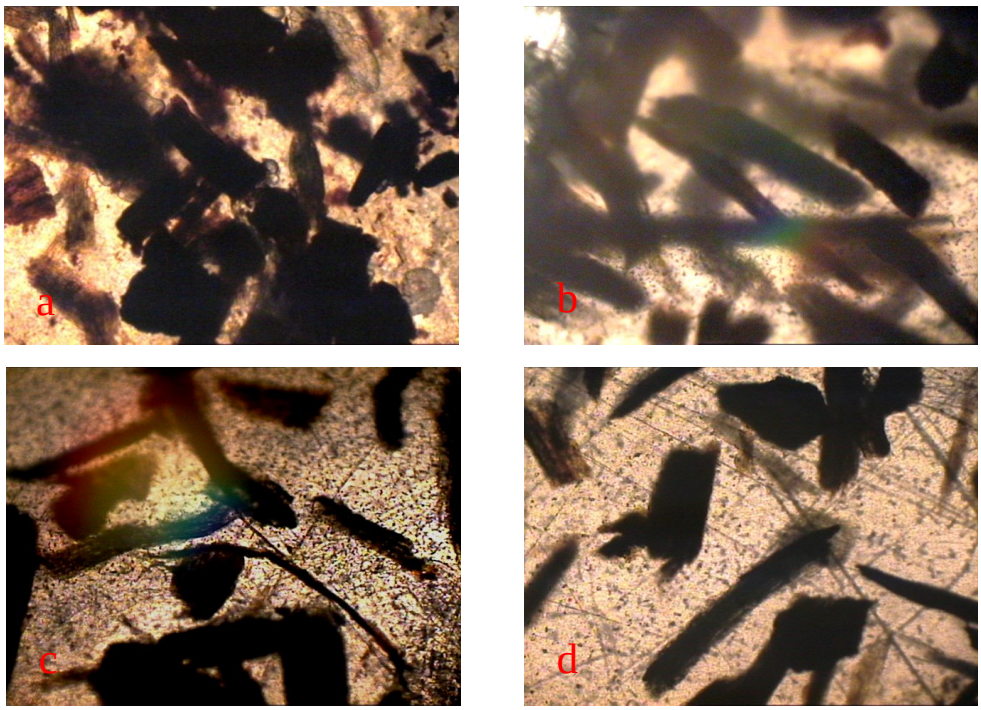

Figure 8.12 Optical micrographs of a) PEW10, b) PEOH1W10, c) PEOH2W10 and d) PEOH3W10 (Mag. 100x).

According to the optical images in Figure 8.12, wood particles show better dispersion in the PEOH3 matrix in comparison to the PE, PEOH1 and PEOH2 matrices, respectively. As shown in Figure 8.13, aggregates were formed in the cases of composites with 30% wood content. A slightly better dispersion of wood particles is shown in the PEOH3 matrix in

comparison to the PE, PEOH1 and PEOH2 matrices. In both cases (composites with 10 and 30% wood content), the worst morphology was observed when PE was used as a matrix. These structural differences, however, can be responsible somehow for the differences in the mechanical and physical properties of these composites [37].

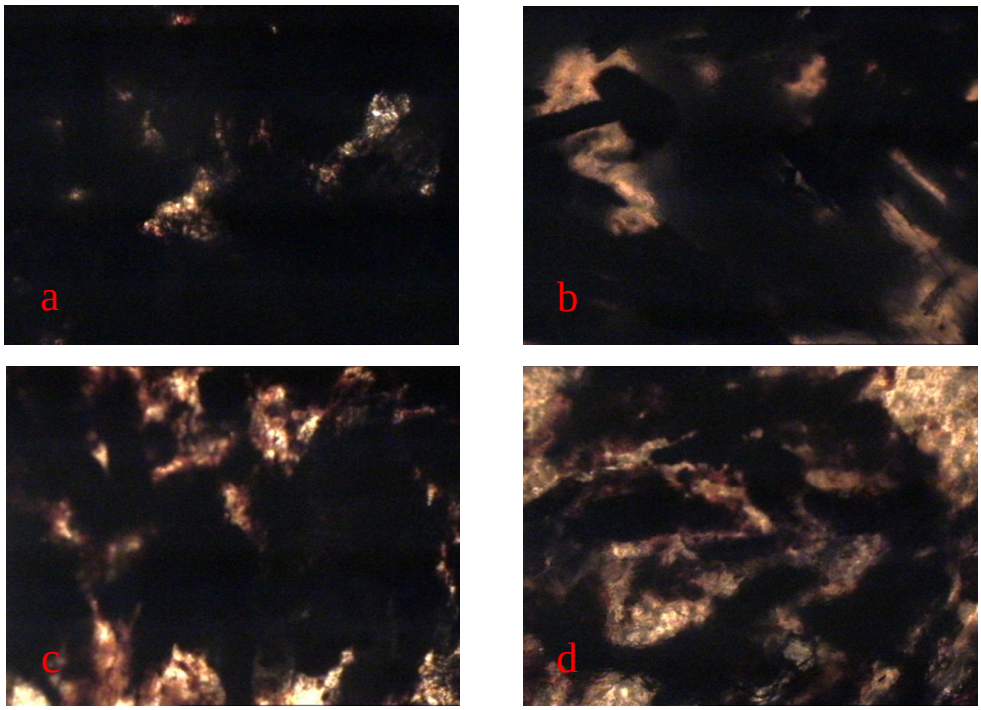

Figure 8.13 Optical micrographs of a) PEW30, b) PEOH1W30, c) PEOH2W30 and d) PEOH3W30 (Mag. 100x).

The worst mechanical and thermal properties PEW10 and PEW30 as shown above can be due to the incompatibility and weak interfacial adhesion between the hydrophilic wood and the hydrophobic PE matrix, as illustrated in Figures 8.12 and 8.13. The deviation in the mechanical and thermal properties at large wood contents (30%) in comparison to low wood content (10%) can be due to structural effects, which is possibly due to the particles aggregation, as show in Figure 5.13. Properties of WPCs often deteriorate at high filler contents [38]. For example, the probability of the formation of aggregates increases with increasing wood content and the strength decreases with increasing number and size of the aggregates [22]. In actual fact, strength decreases drastically at the largest filler contents obviously because of the lack of matrix continuity and aggregation [27]. Optical micrographs of PE, PEOH1, PEOH2 and PEOH3 are shown Appendix D.

8.3.6 Fracture surface

SEM micrographs of the fractured surfaces of the composites are shown in Figure 8.14 and 8.15. These micrographs confirm most of the findings discussed above. In both cases (composites with 10 and 30% wood content), the worst compatibility and interfacial adhesion

were observed when PE was used as a matrix (PEW10 and PEW30), as shown in Figures 8.14a and 8.15a. As can be seen in these figures, frequent surface defects and distinct gaps between the wood particles and the PE matrix are visible. This is, however, due to the incompatibility and weak interfacial adhesion between the hydrophilic wood and the hydrophobic PE matrix, as mentioned many times before.

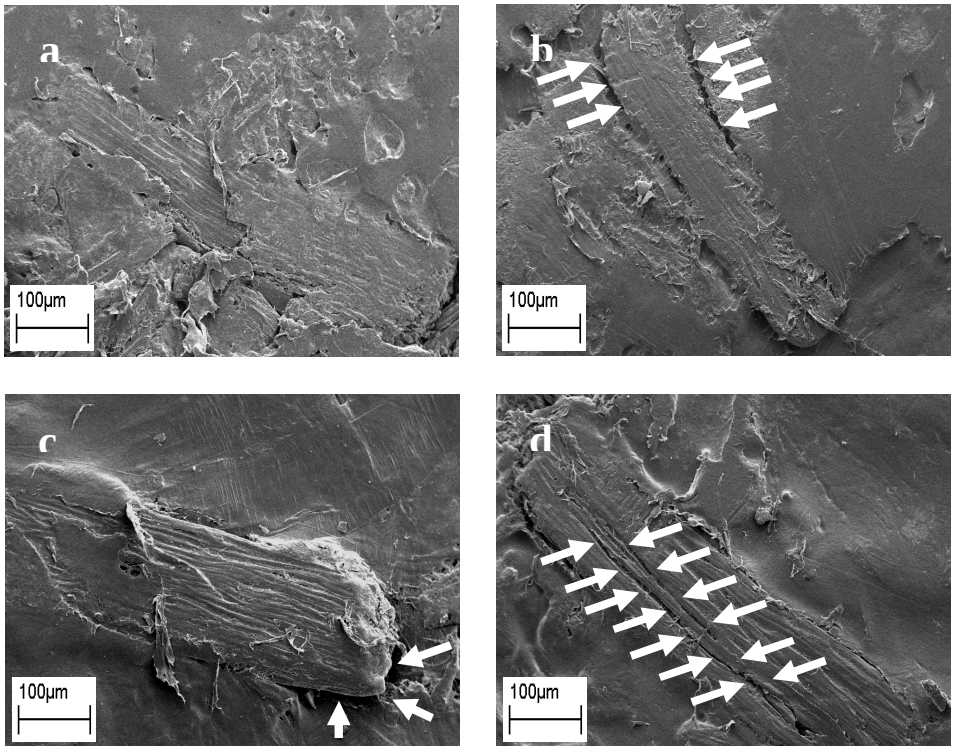

Figure 8.14 SEM micrographs of the fractured surfaces of a) PEW10, b) PEOH1W10, c) PEOH2W10 and d) PEOH3W10 (Mag. 100x).

Using functionalised PE as a matrix imparted a positive effect on the compatibility and interfacial adhesion of these composites. This positive effect increased with increasing the number of incorporated hydroxyl groups into the PE matrix. Better compatibility and interfacial adhesion was observed in the case of PEOH3W10, as shown in Figure 8.14d. This is because the cracks (see the arrows in Figure 8.14d) occurred through the wood particles, which indicates that there is good adhesion and better compatibility between the wood particles and the PEOH3 matrix. It is reported [39] that being able to observe cracks through the wood particles when fracturing the WPCs can be seen as an indication of stress transfer from the weaker matrix to the stronger wood particle. This is only possible in the case of good compatibility and strong interfacial adhesion. Literature reports that the stress transfer occurs not only along the wood particle length, but possibly also at the particle ends [40], as shown in Figure 8.14c (see the arrows in this figure). It can be seen in Figure 6.14b, that debonding from one end of the wood particle (see the arrows in this figure) was observed in the case of PEOH1W10.

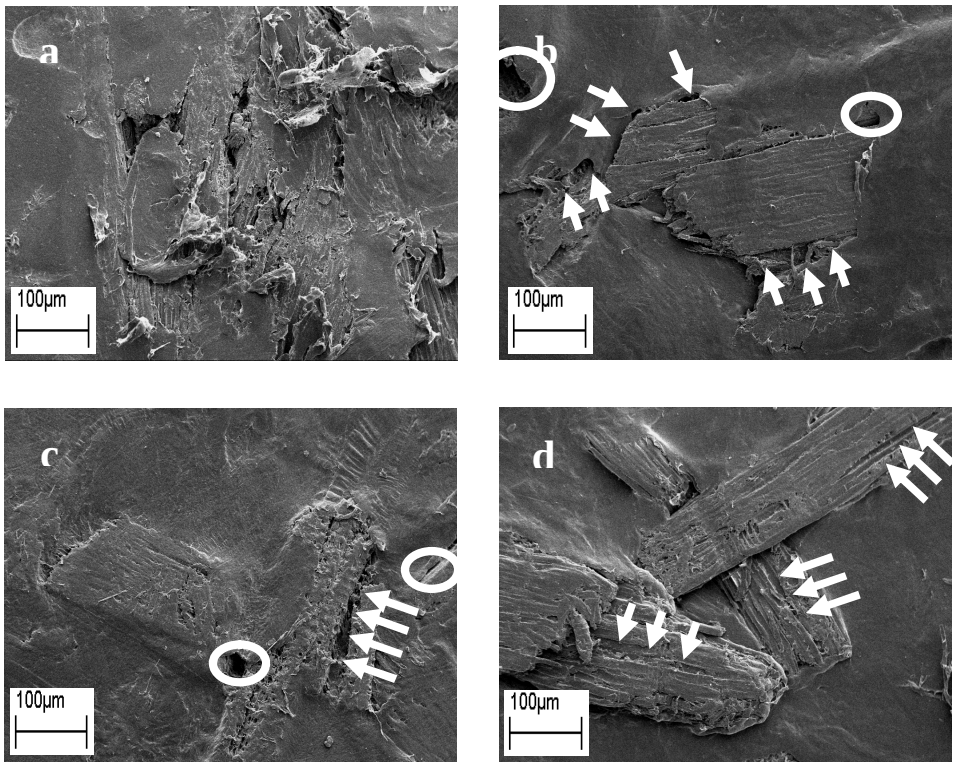

Figure 8.15 SEM micrographs of the fractured surfaces of a) PEW30, b) PEOH1W30, c) PEOH2W30 and d) PEOH3W30 (Mag. 100x).

SEM micrographs of the fractured surfaces of the composites with 30% wood content confirmed the formation of aggregation in these composites. As shown in Figure 8.15, PEOH3W30 (Figure 8.15d) exhibited better compatibility and interfacial adhesion between the wood particle and the matrix than PEOH1W30 (Figure 8.15b) and PEOH2W30 (Figure 8.15c). Although the aggregation clearly presented in PEOH3W30 (Figure 8.15d), PEOH3W30 appeared to have no voids or gaps between wood particle and the PEOH3 matrix. In addition to the aggregation there are distinct gaps between the wood particles and the PEOH1 and PEOH2 matrices in the PEOH1W30 and PEOH2W30 (see the circles in Figure 8.15b and 8.15c). This can be taken as an indication of the better properties of PEOH3W30 in comparison to PEOH1W30 and PEOH2W30.

8.4 Conclusions

PE and three functionalised PEs with varying numbers of hydroxyl groups were successfully synthesisd by copolymerizing ethylene and 10-undecen-1-ol with a soluble metallocene/MAO catalyst bis(tert-buCp)$_2$ZrCl$_2$/MAO at room temperature. The copolymerisations and characterisations of the products were confirmed by NMR, FTIR, GPC and DSC. The incorporation of functional groups increased with increasing the comonomer content. The broadening of MW and crystallinity decreased with increasing the comonomer content.

The PE and functionalised PEs was used to prepare WPCs with 10 and 30% wood content without any treatment or using any type of compatibiliser. Composites prepared with functionalised PEs showed better mechanical, thermal and morphological properties than composites prepared with neat PE. In both cases (composites with 10 and 30% wood content), improvements in the mechanical, thermal and morphological properties increased with increasing the number of hydroxyl groups in the functionalised PE. Composites with 10% wood content exhibited better properties and performance than composites with 30% wood content. This is because the number of hydroxyl groups in all the functionalised PEs is relatively small to impart adequate compatibility and interfacial adhesion between the wood particle and the polymer matrix at high levels of wood content. The deviation in the above properties at a large wood content (30%) in comparison to a low wood content (10%) was found to be due to structural effects, possibly due to particle aggregation and the presence of gaps or voids. Properties of WPCs often deteriorate at high filler content.

References

1. Aaltonen P., Löfgren B., Macromolecules, 28, 5353-5357, 1995.
2. Bruzaud S., Cramail H., Duvignac L., Deffieux A., Macromolecular Chemistry and Physics, 198, 291-303, 1997.
3. Aaltonen P., Löfgren B., European Polymer Journal, 33, 1187-1190, 1997.
4. Aaltonen P., Fink G., Löfgren B., Seppälä J., Macromolecules, 29, 5255-5260, 1996.
5. Dong J., Hu Y., Coordination Chemistry Reviews, 250, 47-65, 2006.
6. Schellekens M., Klumperman B., Polymer Reviews, 40, 167-192, 2000.
7. Amin S., Marks T., Angewandte Chemie, International Edition, 47, 2006-2025, 2008.
8. Chung T., Lu H., Janvikul W., Polymer, 38, 1495-1502, 1997.
9. Chung T., Janvikul W., Journal of Organometallic Chemistry, 581, 176-187, 1999.
10. Geldenhuys M., Metallocene Catalyzed Branched Polyethylene Copolymers, MSc thesis, University of Stellenbosch, South Africa, 1999. 1-9.
11. Resconi L., Cavallo L., Fait A., Piemontesi F., Chemical Reviews, 100, 1253-1345, 2000.
12. Brapaya N., Strelets V., Dzhabieva Z., Babkina O., Maryin V., Russian Chemical Bulletin, 47, 1491-1497, 1998.
13. Talja M., Aminopyridinato Complexes as Possible Alternatives for Metallocenes in Ethylene Polymerisation, PhD thesis, University of Helsinki, Finland, 2007. 12-25.
14. Talsi E., Bryliakov K., Semikolenova N., Zakharov V., Bochmann M., Kinetics and Catalysis, 48, 490-504, 2007.
15. Alder K., Ache H., Chemische Berichte, 95, 503-508, 1962.
16. Welborn H., Speed C., U.S. Patent 5,084,534, 1992.
17. Nesmeyanov A., Materikova1 R., Brainina1 E., Kochetkova1 N., Russian Chemical Bulletin, 18, 1220-1222, 1969.
18. Azimfar A., Kohsari I., Pourmortazavi S., Journal of Inorganic and Organometallic Polymers and Materials, 19, 181-186, 2009.
19. Uotila R., Hippi U., Paavola S., Seppälä J., Polymer, 46, 7923-7930, 2005.
20. Lai S., Yeh F., Wang Y., Chan H., Shen H., Journal of Applied Polymer Science, 87, 487-496, 2003.
21. Hristov V., Vlachopoulos J., Macromolecular Materials and Engineering, 292, 608-619, 2007.
22. Dányádi L., Janecska T., Szabo Z., Nagy G., Moczo J., Pukánszky B., Composites Science and Technology, 67, 2838-2846, 2007.
23. Joe D., Wu C., Bok T., Lee E., Lee C., Han W., Kang S., Lee B., Dalton Transactions, 33, 4056-4062, 2006.

24. Marcovich N., Villar, M., Journal of Applied Polymer Science, 90, 2775-2784, 2003.
25. Oksman K., Clemons C., Journal of Applied Polymer Science, 67, 1503-1513. 1998.
26. Georgopoulos S., Tarantili P., Avgerinos E., Andreopoulos A., Koukios E., Polymer Degradation and Stability, 90, 303-312, 2005.
27. Dányádi L., Renner K., Moczo J., Pukánszky B., Polymer Engineering and Science, 47, 1246-1255, 2007.
28. Sanjeev S., Mohanty A., Composites Science and Technology, 67, 1753-1763, 2007.
29. Ferran M., Francisco V., Amparo R., Adolfo B., Concha S., Journal of Applied Polymer Science, 99, 1823-1831, 2006.
30. Rials T., Wollcott M., Journal of Materials Science Letters, 17, 317-319, 1998.
31. Kim H., Kim S., Kim H., Yang H., Thermochimica Acta, 451, 181-188, 2006.
32. Hamdan S., Talib Z., Rahman M., Ahmed A., Islam M., BioResources, 5, 324-342, 2010.
33. Liu H., Wu Q., Han G., Yao F., Kojima Y., Suzuki S., Composites: Part A, 39, 1891-1900, 2008.
34. Hristov V., Vlachopoulos J., Macromolecular Materials and Engineering, 288, 798-806, 2003.
35. Dominick V., Donald V., Marlene G., Injection Moulding Handbook, 3rd edition, Kluwer Academic Publishers, USA, 2000. 528.
36. Wilkes C., Summers J., Daniels C., Berard M., PVC Handbook, 1st edition, Hanser Verlag, USA, 2005. 260.
37. Lu X., Zhang M., Rong M., Shi G., Yang, G., Composites Science and Technology, 63, 177-186, 2003.
38. Dányádi L., Moczo J., Pukánszky B., Composites: Part A, 41, 199-206, 2010.
39. Bengtsson M., Gatenholm P., Oksman K., Composites Science and Technology, 65, 1468-1479, 2005.
40. Sretenovic A., Müller U., Gindl W., Composites: Part A, 37, 1406-1412, 2003.

Chapter 9
Synopsis, conclusions and recommendations

9.1 Synopsis and conclusions

The focus of this study in the field of WPCs was to consider the relationship between the macromolecular composition and content of wood, and the properties, and performance of WPCs and their applications. The macromolecular composition and content of woods is of considerable importance to many wood-using industries. This is because the properties of wood vary from species to species due to the variability of the macromolecular composition and content between wood species. We believe that the choice of wood can make a significant difference to the properties and quality of the produced WPCs when the most suitable type and optimum amount of compatibilisers and matrices, are used. Therefore, the effect of different wood species with different macromolecular composition and content on the properties and performance of WPCs was investigated. The results obtained from this study demonstrate a profound impact of the macromolecular composition and content of wood on the properties and performance of WPCs. Four different wood species, namely *A. cyclops* (acacia), *E. grandis* (eucalyptus), *P. radiata* (pine) and *Q. alba* (oak), with different macromolecular composition and contents and average wood particle length were used, and led to the production WPCs with different properties and performance.

Although there are no new theories or fundamental concepts in the first part of our study, a set of useful quantitative structure-property relationships is offered. This can be used to predict many properties, and subsequently suitable applications, of the obtained WPC. In reality, some of these properties can be predicted with great accuracy, while others only approximately. Basically, knowing the macromolecular composition and content of wood, suitable applications of WPCs prepared using this type of wood can be expected. The success will however also depend upon processing methods and conditions, polymer matrix, type and amount of compatibiliser and length and size of wood particles. For example, better processing can be a solution for achieving better compatibility between the WPC components, besides noncompatibilisation. In the IM process, particles are known to align in the main flow direction. The differences in mechanical behaviour depending on the processing method used are due to the composite density and particle alignment. It is for this reason that IM composites showed better tensile strength, EAB and thermal stability than pressed

composites. On the other hand, IM composites exhibited lower hardness than pressed composites. This is because IM composites have smooth and polymer-rich surfaces, while pressed composites have fibre-rich surfaces.

In the second part, two planned approaches to attain ecological and economical improvements were successfully carried out. In the first approach, we demonstrated that degraded LLDPE can be used as a compatibilizer in a WPC system. This approach indicates that it is possible to convert polymer waste to useful products and to reduce the production cost of WPCs. This could be very useful in dealing with weathered waste plastics. In the second approach, we showed that a functionalized PE can be used as a compatibilizer and matrix in a WPC system without any treatment or using type of compatibiliser. This helps to minimise the raw materials in WPC system.

The following conclusions can be drawn from this study:

1. The use of different wood species with different macromolecular composition and contents led to produce WPCs with different properties and performance.
    - Hardwood species (*A. cyclops*, *E. grandis* and *Q. alba*) produced better wood-LLDPE composites than softwood species (*P. radiata*) in terms of mechanical properties, thermal properties and resistance to UV degradation. This therefore restricts the use of softwood composites in construction materials and in some industrial applications.
    - Superior mechanical properties such as tensile strength, EAB, impact strength and MOE were achieved when wood from *A. cyclops*. This is due to its higher cellulose and lignin contents, and size, length and average particle length/ size of particles.
    - Better thermal stability was achieved when wood with a higher cellulose and lignin content, such as *A. cyclops*, was used.
    - *A. cyclops* produced WPCs with better resistance to UV degradation due to higher lignin and extractives contents. In the light of the above conclusions, *A. cyclops* composites can be used in some indoor and outdoor construction, industrial and infrastructure applications where there is no contact with water. These composites can also be used in some automotive applications where very good impact strength is required. Product examples are door trim panels or instrument panels.

- A lower WA and TS rate in WPCs was achieved when wood from *P. radiata*. This is due to its lower cellulose content: a lower cellulose and hemicelluloses content probably presents fewer free hydroxyl groups in the WPC. Hence, *P. radiata* composites could be used in some indoor applications that might involve contact with water, such as some internal finishes, especially in the kitchen or bathroom (e.g. decorative profiles, interior panels, cabinets, laminate flooring, shelving, etc.).

2. All wood-LLDPE composites, prepared with compatibilisers, that exhibited better mechanical and thermal properties had better compatibility and interface adhesion. This means that controlling the interface to ensure better compatibility between the wood particles and polymer matrices via compatibilisers is therefore an important aspect when developing WPCs.

    - Less compatibility between the polymer matrix and wood particles can be due to the lower cellulose content and the presence of very small and oversized wood particles.

3. Using woods without extractives as fillers in WPCs resulted in improved thermal properties and a reduced WA rate. The improvement in thermal stability and WA behaviour of composites made with woods without extractives over the composites made with unextracted woods was found not to be due to the improvement in the compatibility and interfacial adhesion between the wood particle and polymer matrix via compatibiliser, but to the absence of wood extractives. The positive and negative effects of the complete removal of wood extractives on the properties and performance of WPCs was more pronounced than the effects of the removal of the polar and nonpolar extractives, respectively. However, extraction processes involve removal of greater amounts of materials, shrinkage of the wood particle size, and an increase in the production time and the cost of WPCs.

Hence, using extracted woods as reinforcement in WPC systems is more favourable in terms of mechanical properties, economic aspects and weatherability than using woods without extractives. After considering the results of the above objectives, *A. cyclops* was chosen for further studies.

4. The number of functionality of the compatibiliser and the number of hydroxyl groups available on the wood surface plays a dominate role in the creation of a strong contact areas or interfaces between the wood particles and polymer matrix. The availability of

hydroxyl groups on the wood surface is dependent on the macromolecular composition and content of wood particles and their length and size.

- It appeared that as the particle size and average particle length of the wood increases, an EVOH with higher hydroxyl content is required.
- *A. cyclops* with small particle size (180 μm) and average particle length (0.225 mm) offered better improvements in the properties of *A. cyclops*-LLDPE composites than *A. cyclops* with larger particle size (250 and 450 μm) and average particle length (1.220 and 3.240 mm).

5. Degraded LLDPE played an important role in improving interfacial adhesion and compatibility between wood particles and a LLDPE matrix at levels of 10, 30 and 50% wood contents. Mechanical properties such as tensile strength and hardness, and thermal and morphological properties of the compatibilised composites were better than those of the noncompatibilised composites and virgin LLDPE.
   - EAB and impact properties of compatibilised composites were worse than that of virgin LLDPE, but higher than those of noncompatibilised composites. Each level of wood content in WPC systems required its own optimal amount of degraded LLDPE to produce WPC systems with better properties and performance.
6. PE and different functionalised PEs with different hydroxyl contents were successfully synthesised by copolymerising ethylene and 10-undecen-1-ol using a soluble bis(tert-buCp)$_2$ZrCl$_2$/MAO catalyst at room temperature. PE and different functionalised PEs were then used as matrices in WPC systems without any treatment or using any type of compatibiliser. According to the results from the above objectives, *A. cyclops* with particle size 180 μm was used to prepare composites with 10 and 30% wood content without any treatment or using any type of compatibiliser. Composites prepared with functionalised PEs showed better mechanical, thermal and morphogical properties than composites prepared with PE.
   - Improvements in the mechanical, thermal and morphogical properties increased with an increase in the number of hydroxyl groups in the functionalised PE.
   - Composites with 10% wood content exhibited better properties and performance than composites with 30% wood content. This is because the number of hydroxyl groups in all functionalised PEs is relatively small to

impart adequate compatibility and interfacial adhesion between the wood particle and the polymer matrix at high level of wood content. The deviation in the properties at high wood contents (30%) was found to be due to structural effects, which is possibly due to the particles aggregation and the presence of gaps or voids. Properties of WPCs often deteriorate at high filler contents.

Hence, these approaches (using degraded polyolefin as compatibiliser and using functionalised PE as a matrix without any treatment or using any type of compatibiliser) can be used to convert the polymer waste into useful products and reduce the production cost of WPCs. Simply; these approaches can impart more attractive ecological and economical advantages to WPCs.

9.2 Recommendations for future work

In order to gain yet further understanding about the effect of wood's macromolecular composition and content on the properties and performance of WPCs, the hemicelluloses, cellulose and lignin components should be isolated separately from the wood and used as fillers in WPC systems. Then comparisons between WPC filled with these components and WPC filled with the original wood can made in order to determine the effect of these respective components on the properties and performance of WPCs.

Further information on using degraded LLDPE as a compatibiliser in WPCs is required. Hence, further investigations into the use of different LLDPEs with different degrees of degradation as compatibiliser in WPC systems should be carried out. The difference between the use of LLDPE degraded by thermal degradation and LLDPE degraded by UV irradiation in terms of the noncompatibilisation effect in WPC systems should also be determined. Comparisons between using degraded LLDPE and other degraded polyolefins, e.g. LDPE, HDPE, PP, etc., as compatibilisers in WPC systems could also be carried out.

Appendix A: XRD data

- XRD data from Chapter 3

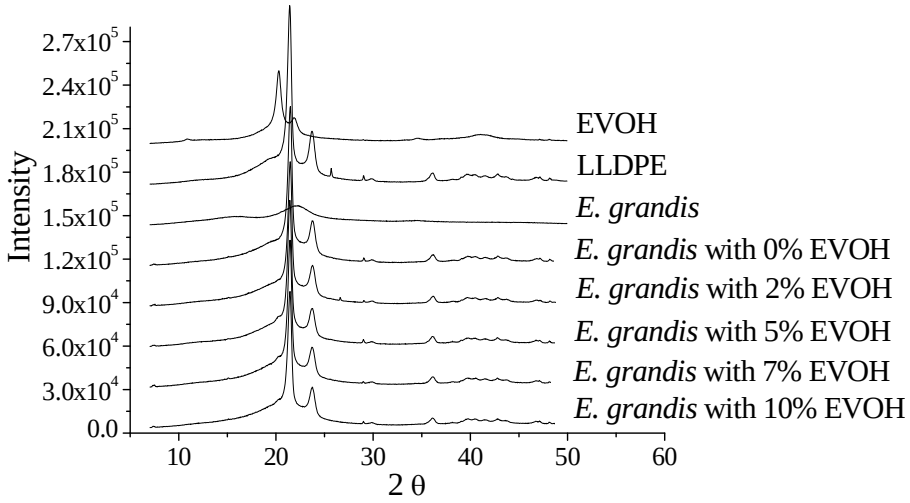

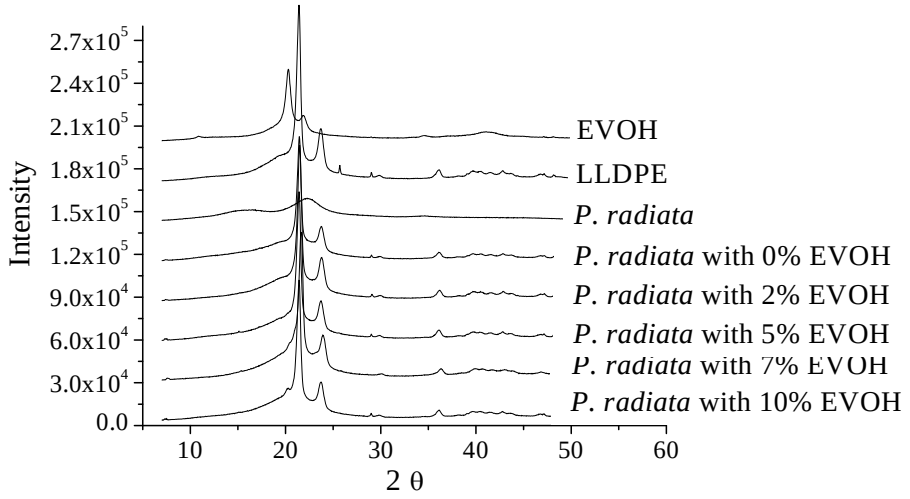

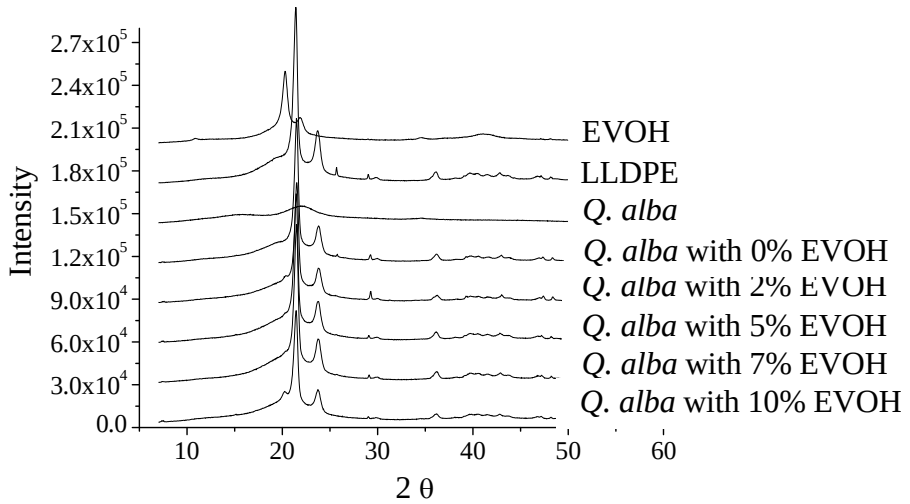

- XRD data from Chapter 5

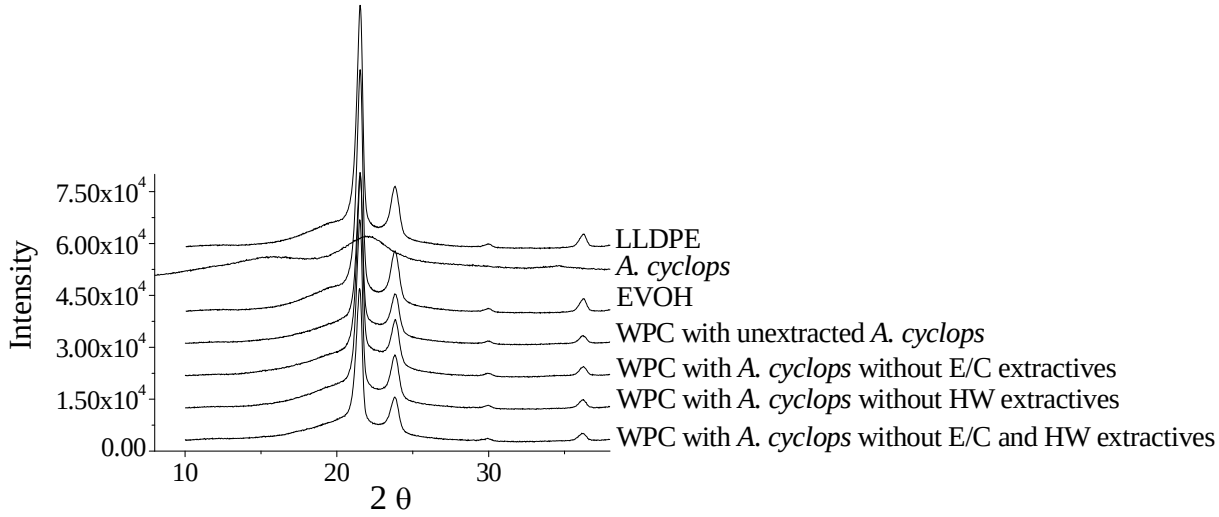

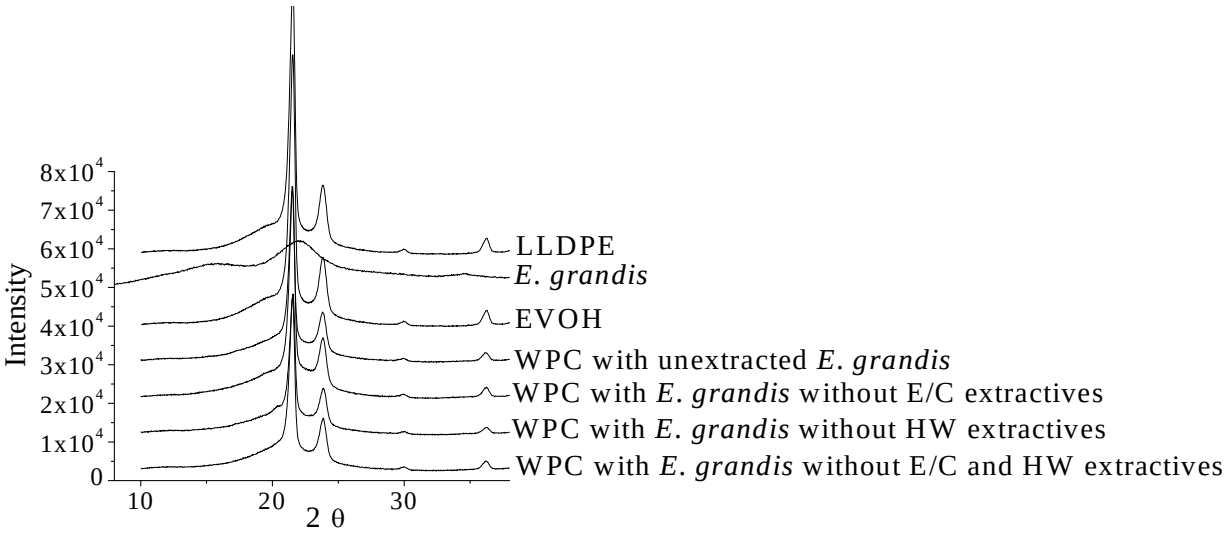

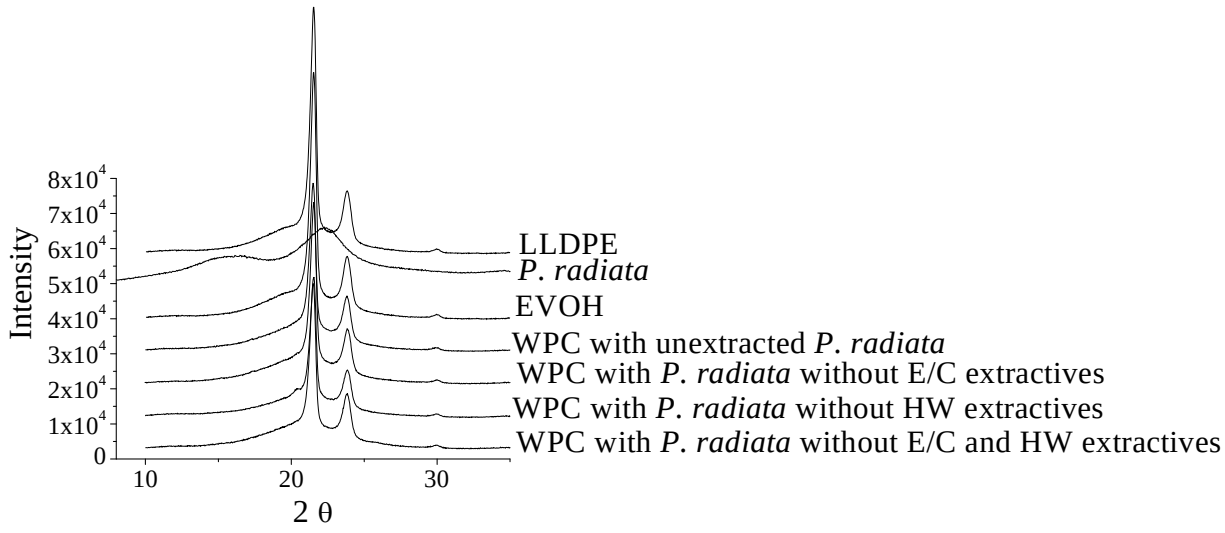

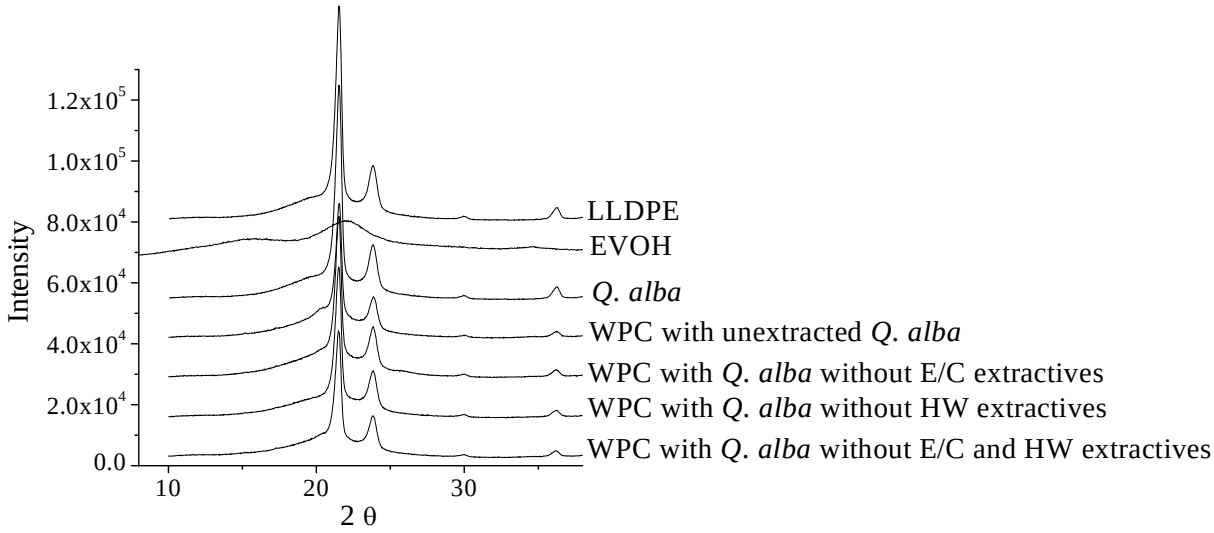
Intensity
1.2x10^5
1.0x10^5
8.0x10^4
6.0x10^4
4.0x10^4
2.0x10^4
0.0
10
20
30
2 θ
LLDPE
EVOH
Q. alba
WPC with unextracted Q. alba
WPC with Q. alba without E/C extractives
WPC with Q. alba without HW extractives
WPC with Q. alba without E/C and HW extractives

Appendix B: DMA data (stress-strain curves)

- **Stress-strain curves data from Chapter 3**

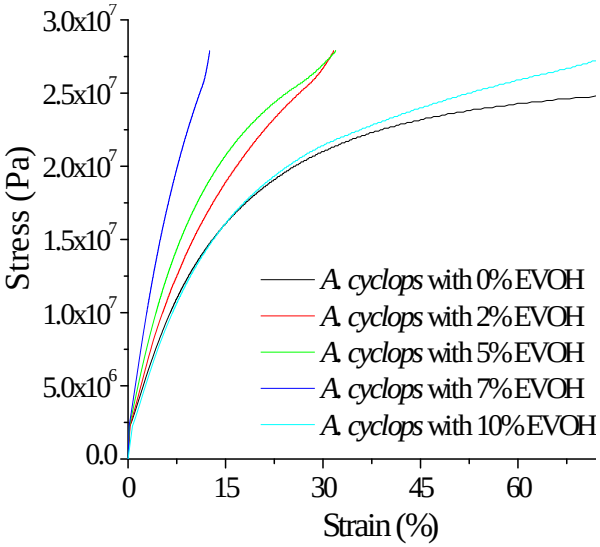

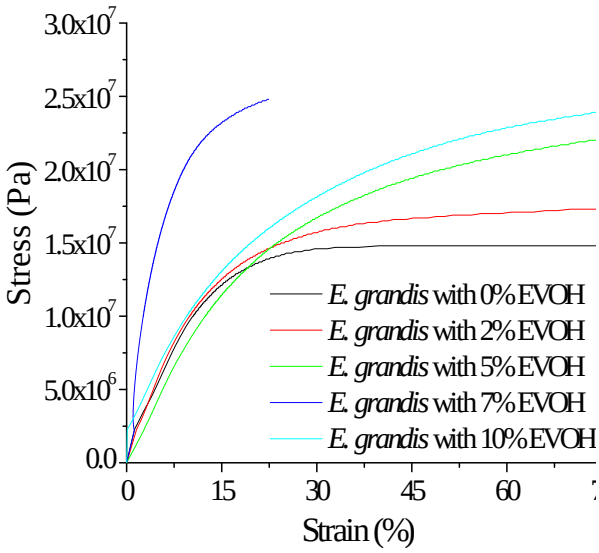

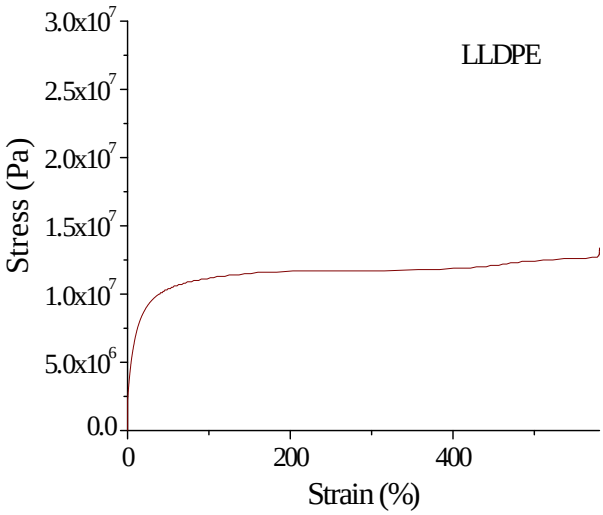

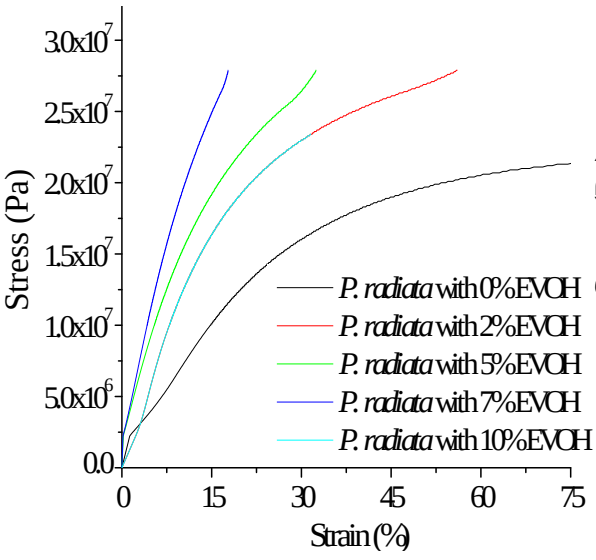

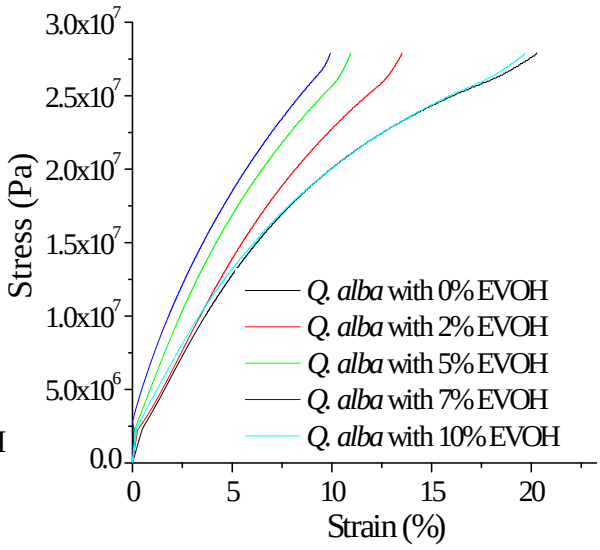

Appendix C: DSC data

- DSC data from Chapter 3

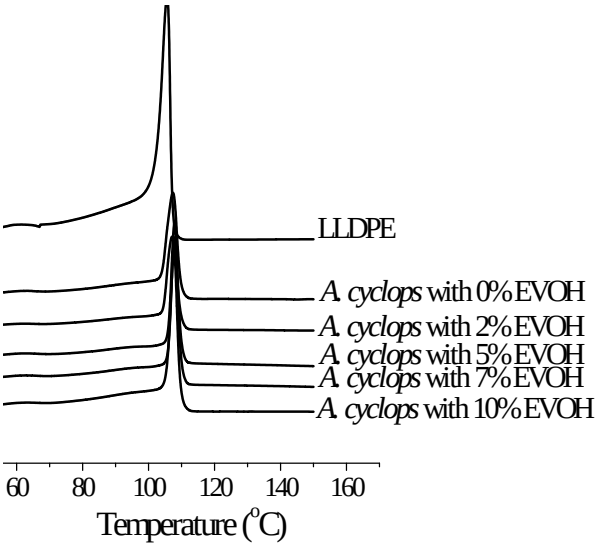

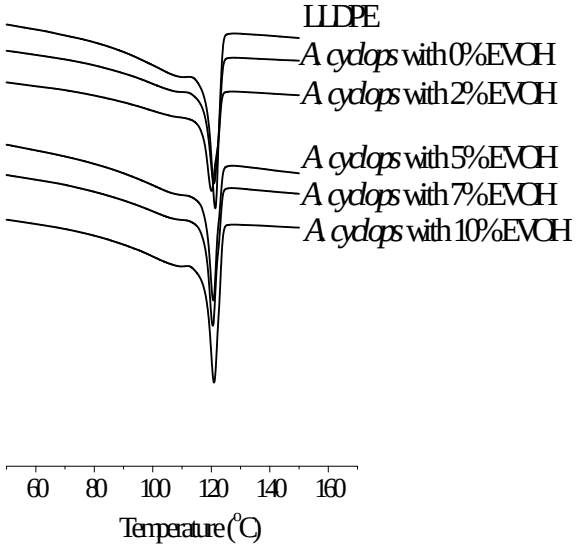

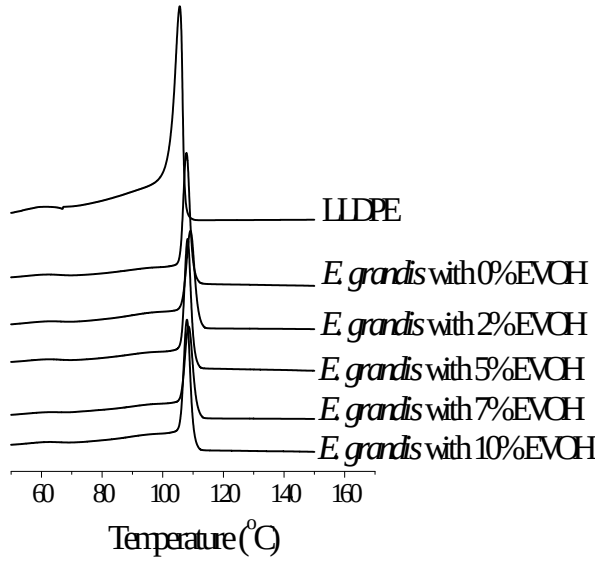

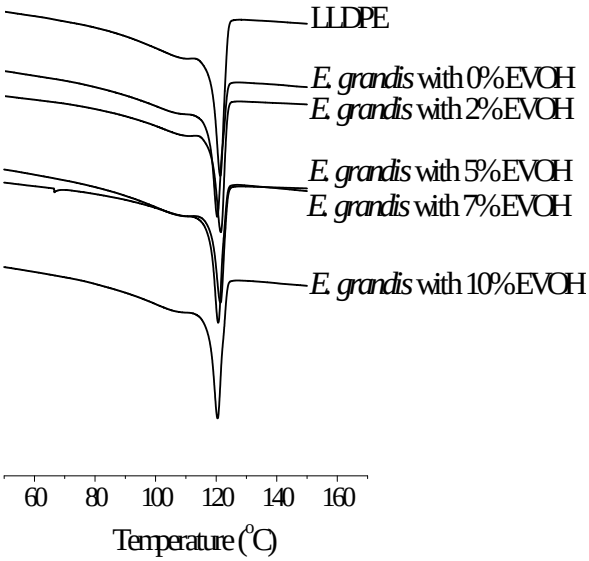

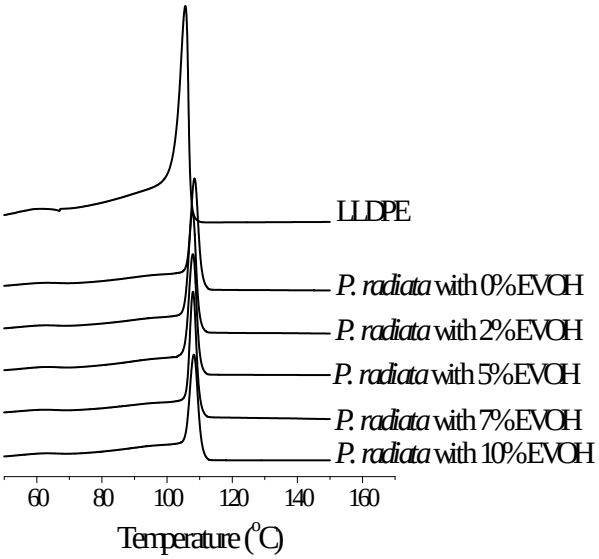

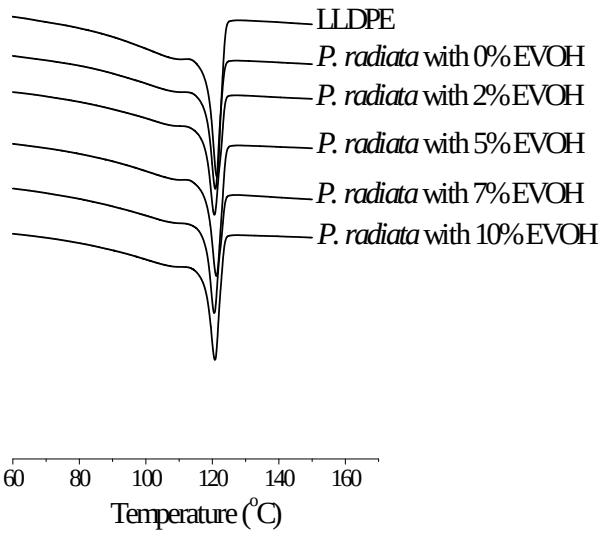

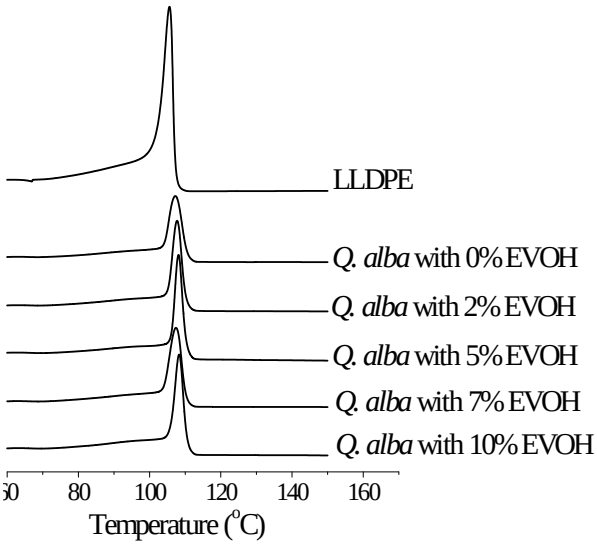

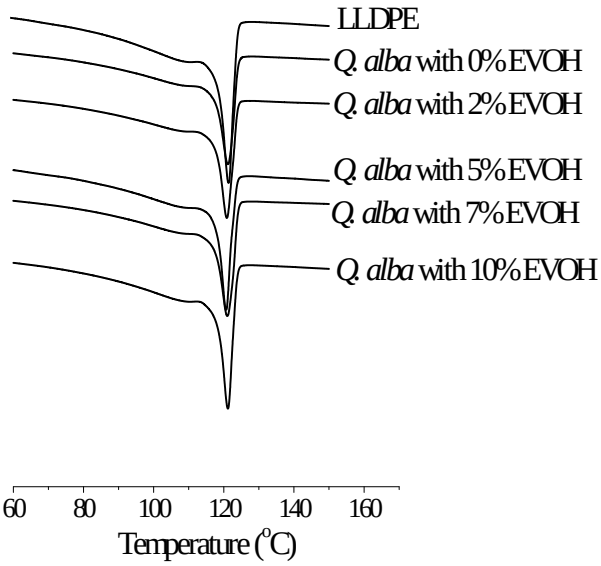

- **DSC data from Chapter 5**

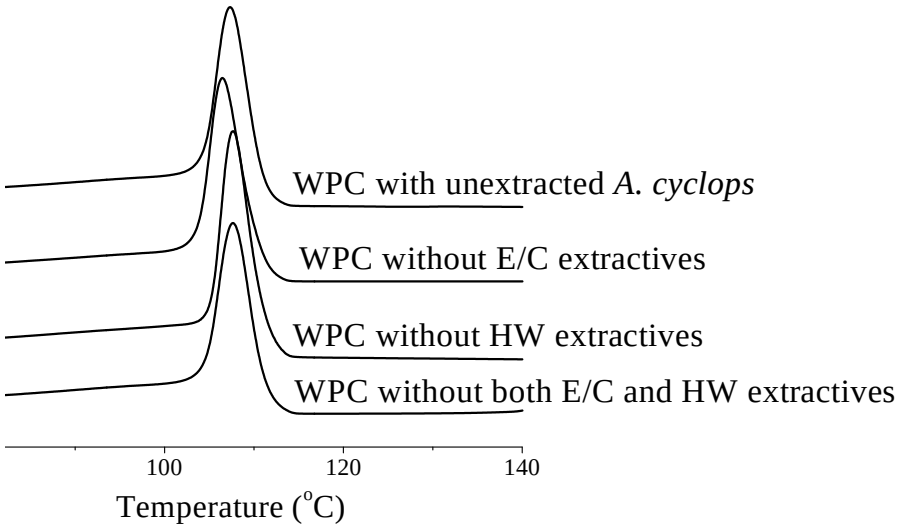

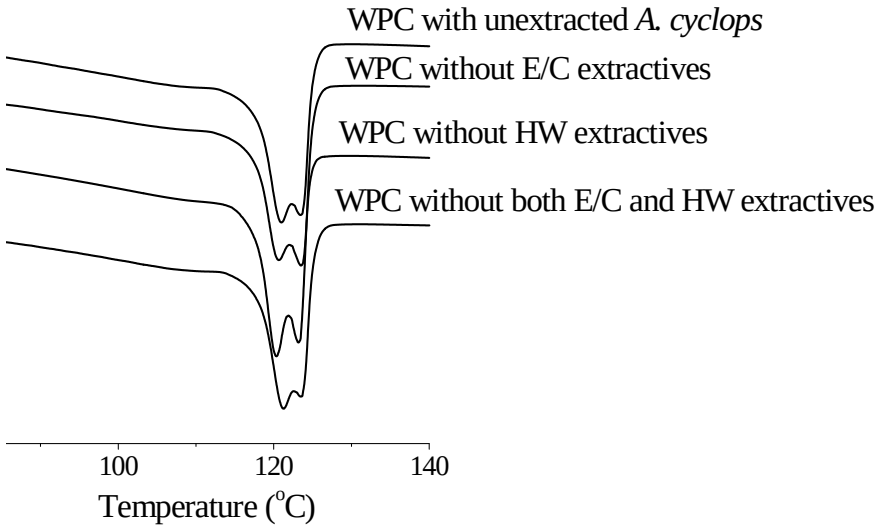

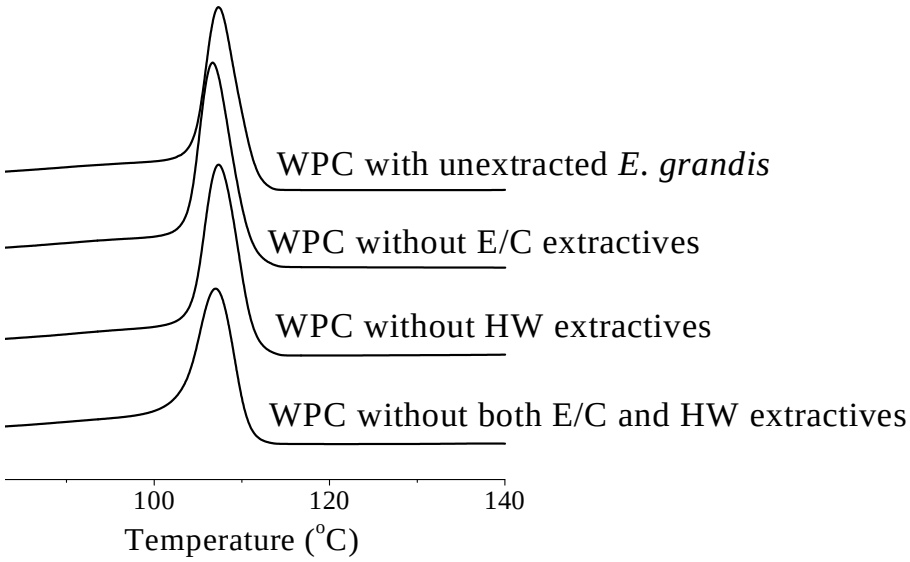
WPC with unextracted *E. grandis*
WPC without E/C extractives
WPC without HW extractives
WPC without both E/C and HW extractives
100
120
140
Temperature (°C)

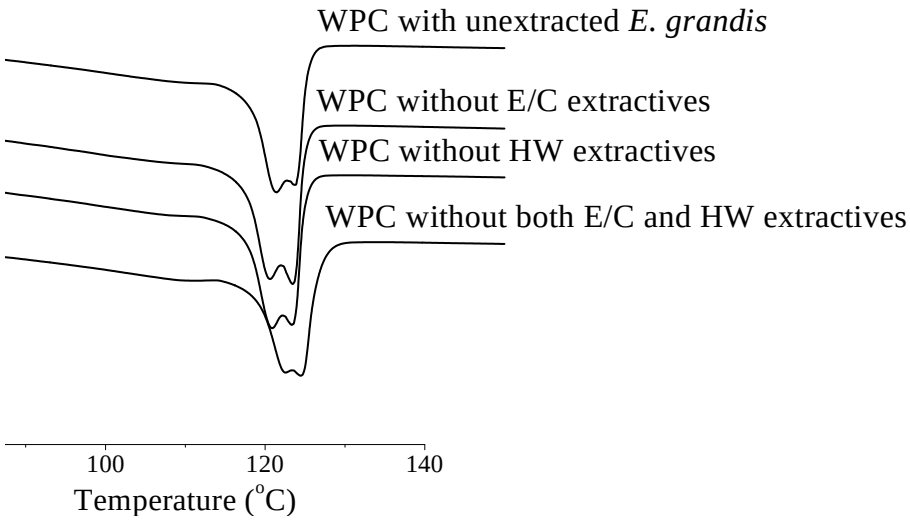
WPC with unextracted *E. grandis*
WPC without E/C extractives
WPC without HW extractives
WPC without both E/C and HW extractives
100
120
140
Temperature (°C)

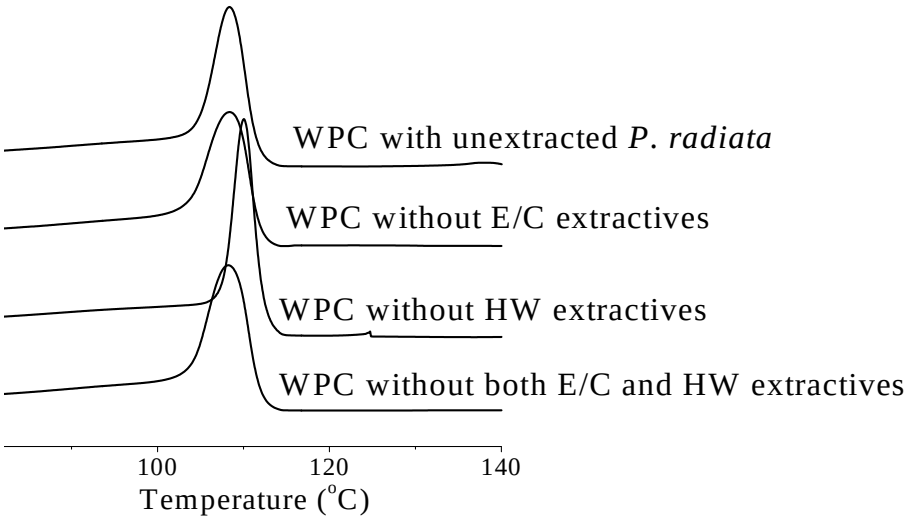
WPC with unextracted *P. radiata*
WPC without E/C extractives
WPC without HW extractives
WPC without both E/C and HW extractives
100
120
140
Temperature (°C)

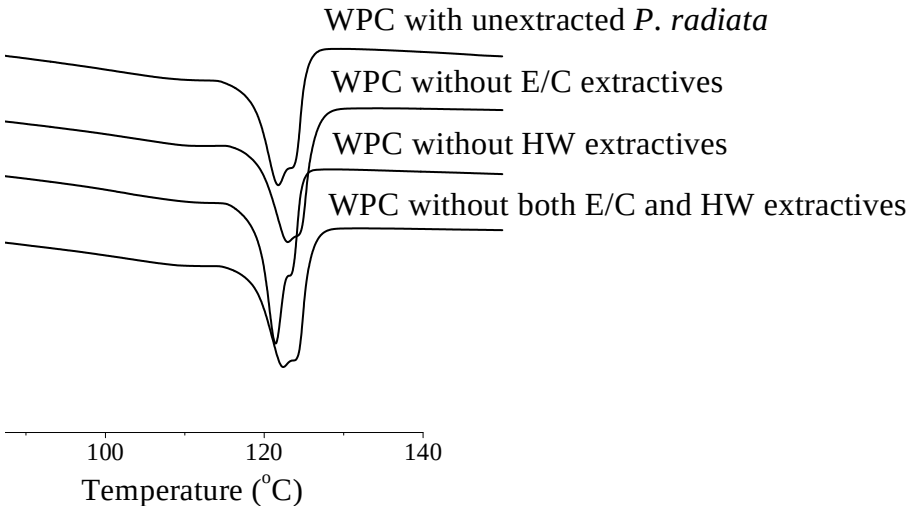
WPC with unextracted *P. radiata*
WPC without E/C extractives
WPC without HW extractives
WPC without both E/C and HW extractives
100
120
140
Temperature (°C)

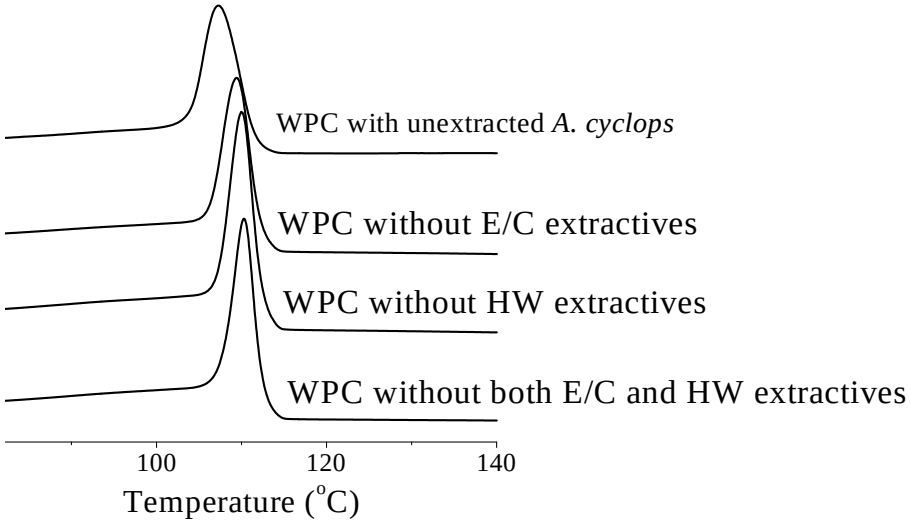
WPC with unextracted *A. cyclops*
WPC without E/C extractives
WPC without HW extractives
WPC without both E/C and HW extractives
100
120
140
Temperature (°C)

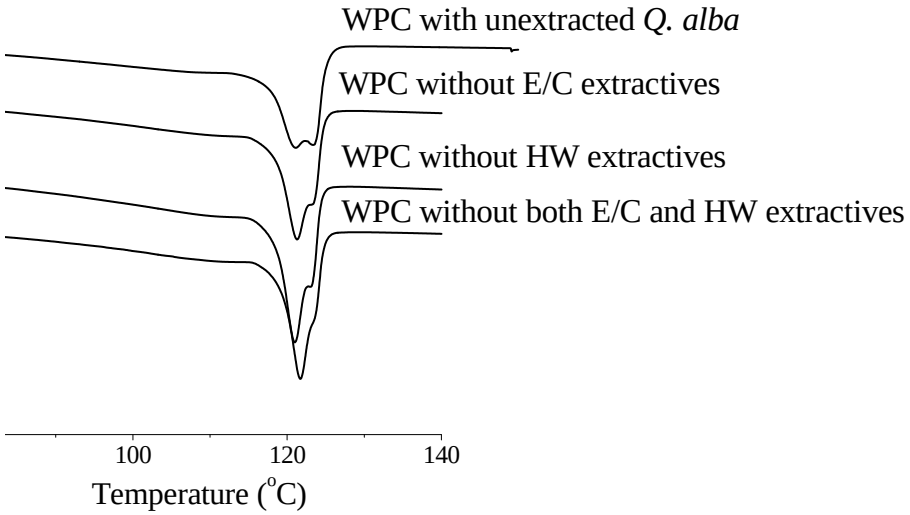
WPC with unextracted *Q. alba*
WPC without E/C extractives
WPC without HW extractives
WPC without both E/C and HW extractives
100
120
140
Temperature (°C)

- DSC data from Chapter 6

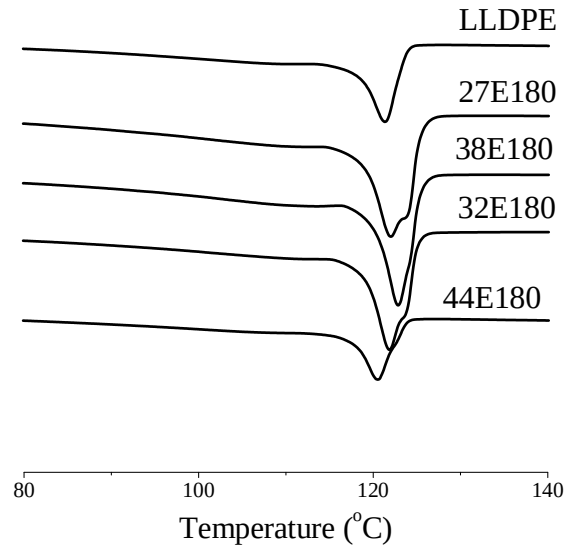

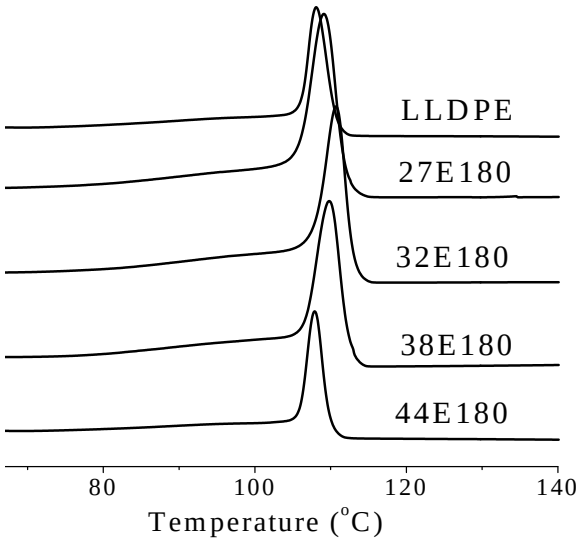

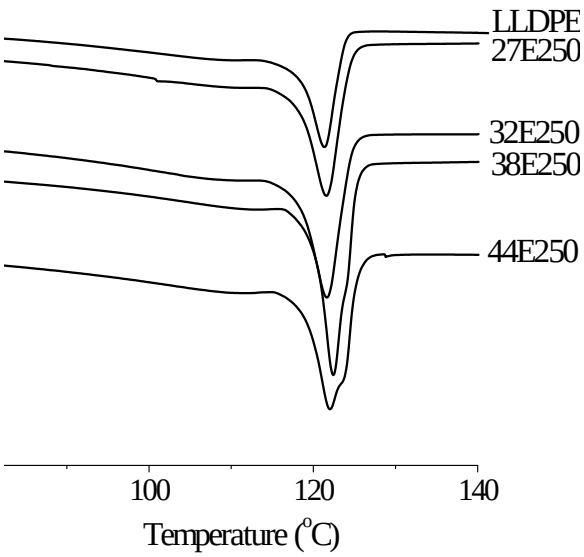

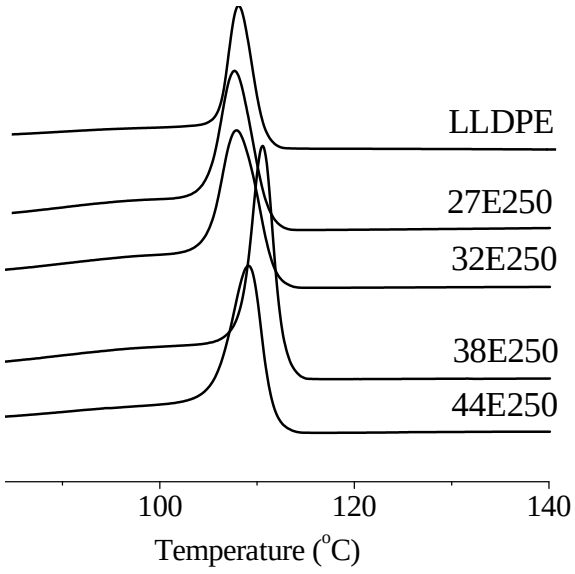

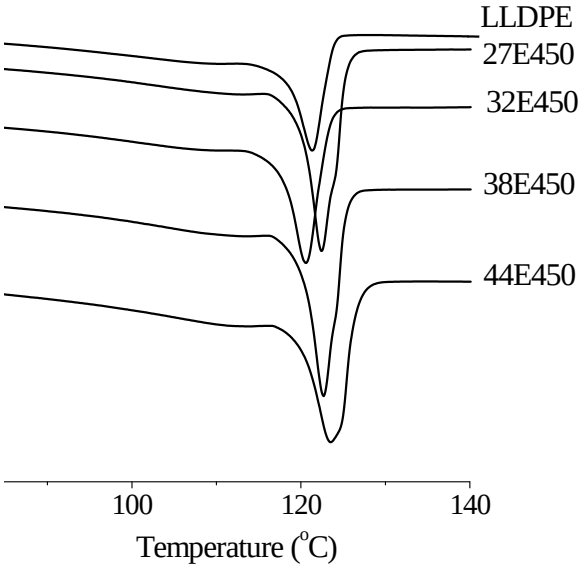

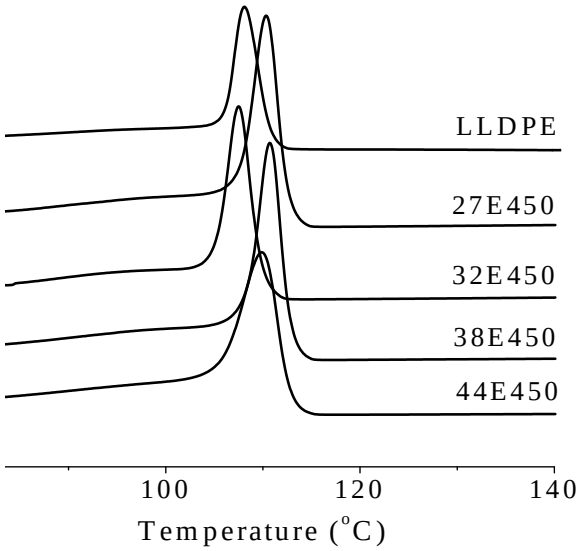

- **DSC data from Chapter 7**

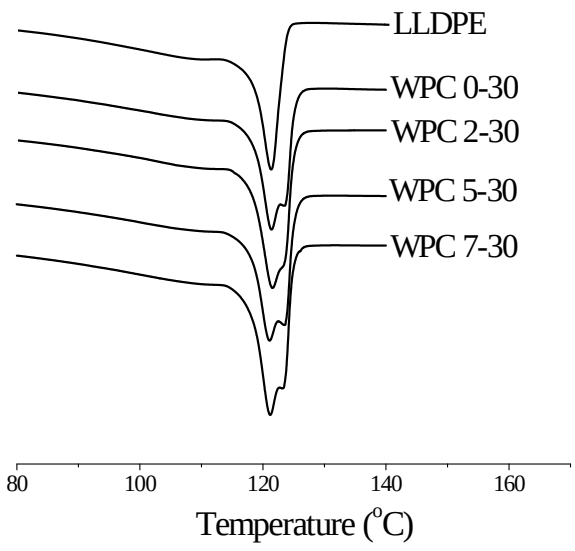

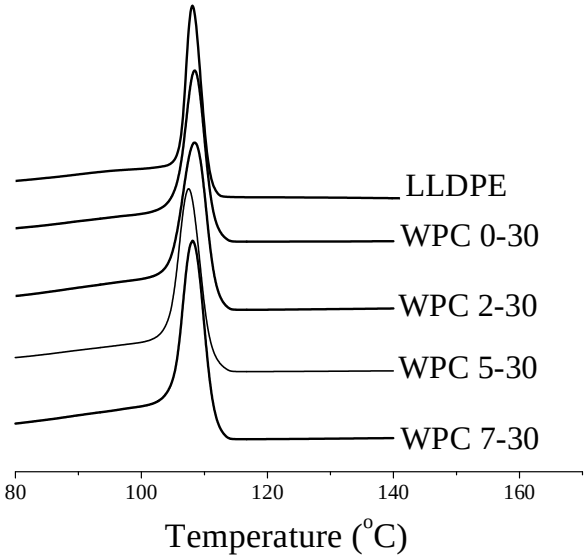

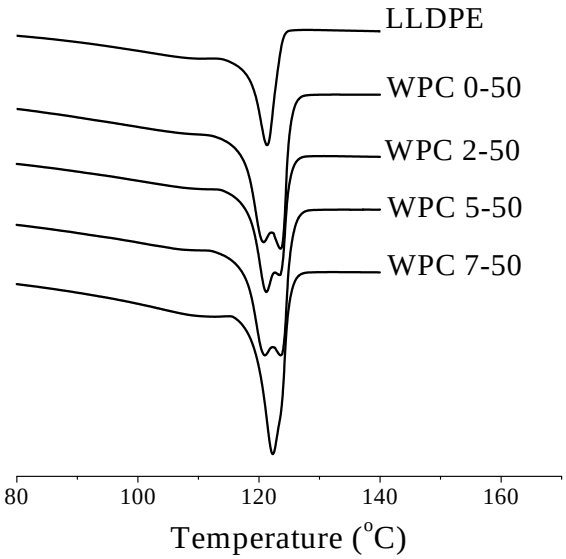

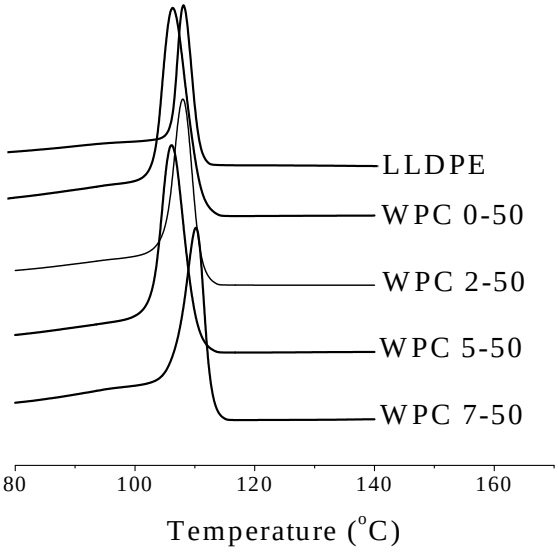

Appendix D: Optical micrographs

- **Optical micrographs from Chapter 3 (circles = aggregation or voids)**

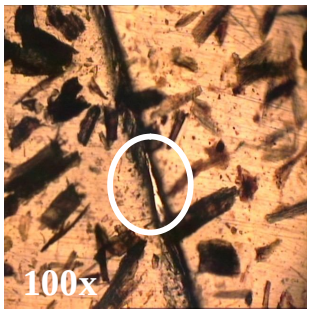

A. cyclops composite with 0% EVOH

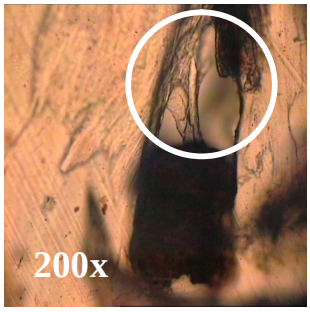

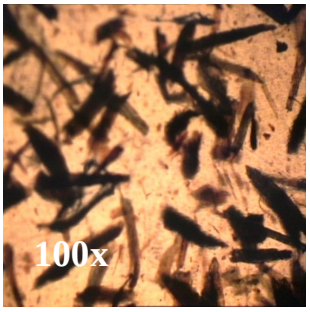

A. cyclops composite with 2% EVOH

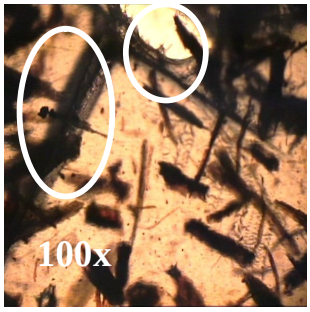

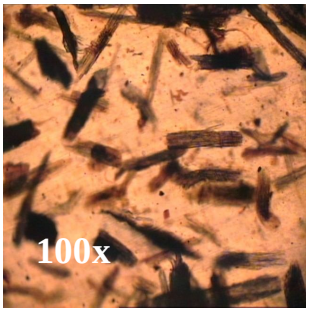

A. cyclops composite with 5% EVOH

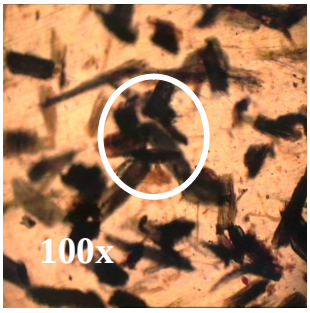

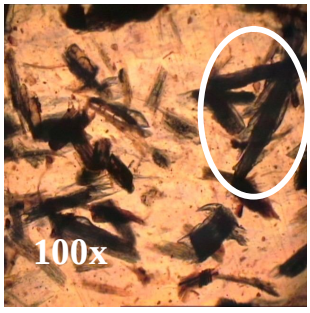

A. cyclops composite with 10% EVOH

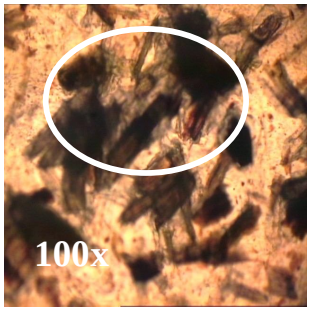

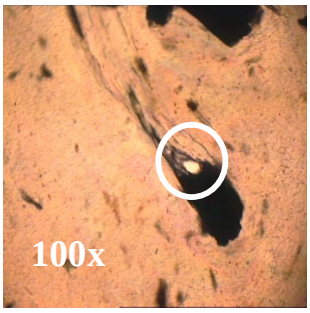

E. grandis composite with 0% EVOH

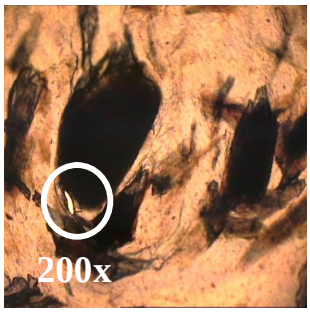

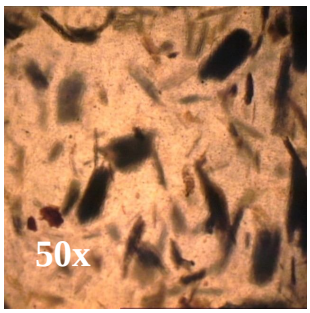

E. grandis composite with 2% EVOH

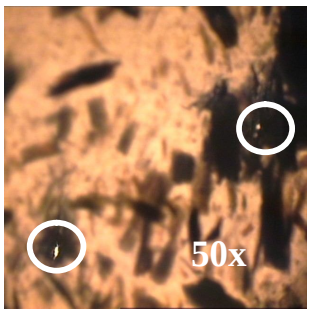

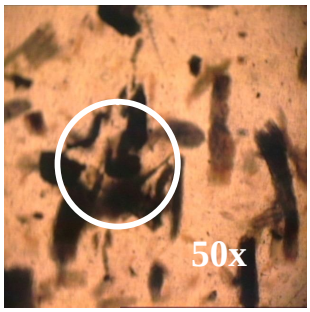

E. grandis composite with 5% EVOH

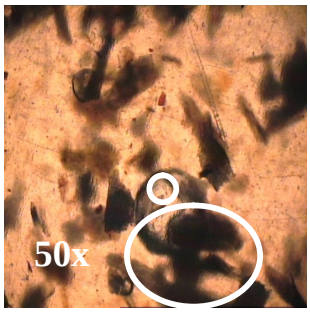

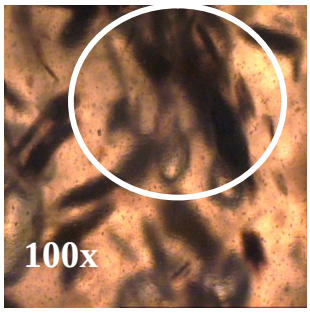

E. grandis composite with 10% EVOH

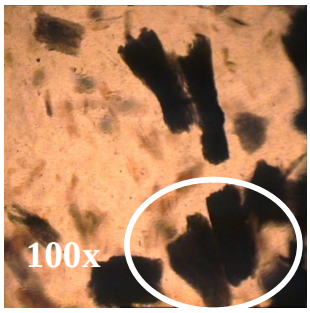

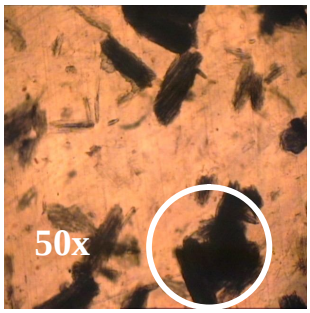

P. radiata composite with 0% EVOH

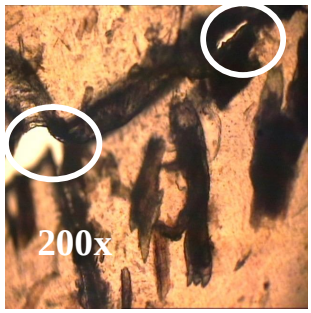

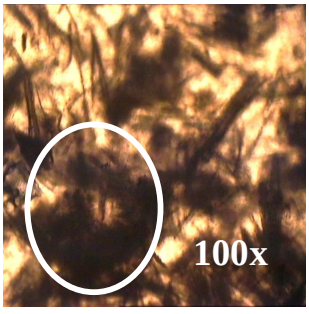

P. radiata composite with 2% EVOH

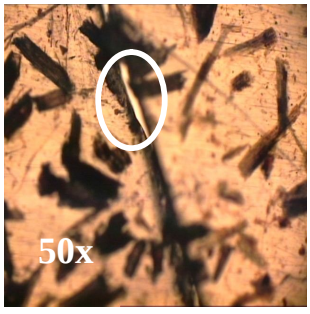

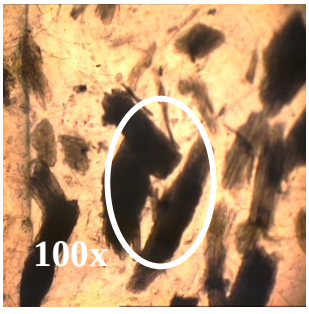

P. radiata composite with 5% EVOH

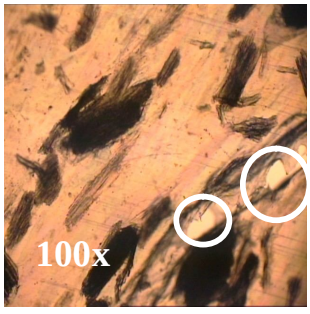

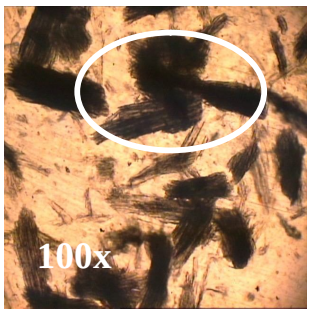

P. radiata composite with 10% EVOH

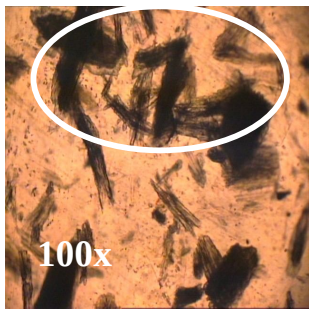

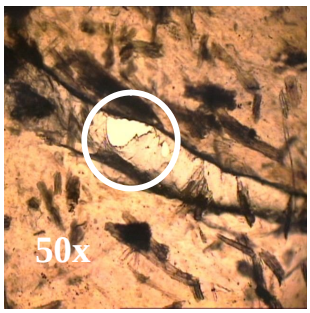

Q. alba composite with 0% EVOH

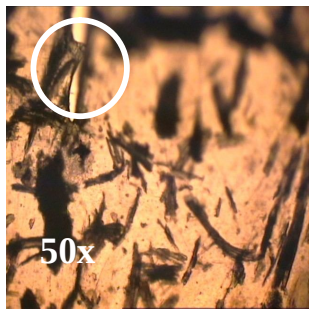

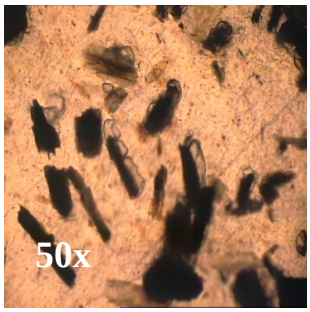

Q. alba composite with 2% EVOH

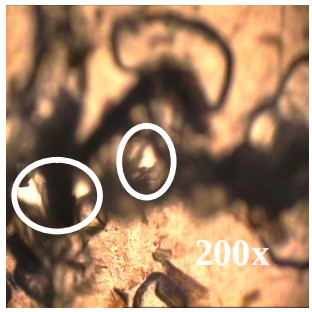

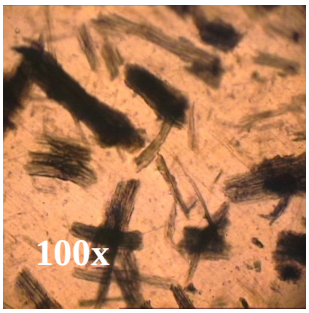

Q. alba composite with 5% EVOH

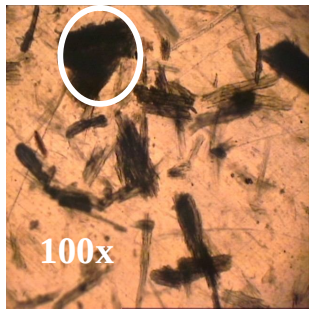

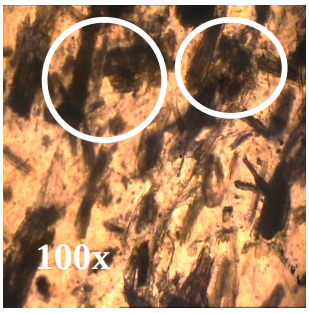

Q. alba composite with 10% EVOH

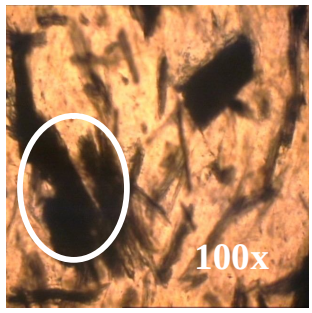

- Optical micrographs after UV degradation from Chapter 3

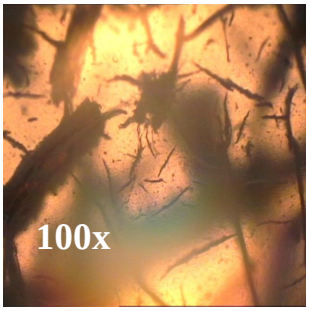

A. cyclops composite with 2% EVOH

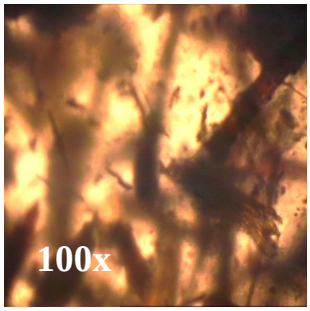

A. cyclops composite with 5% EVOH

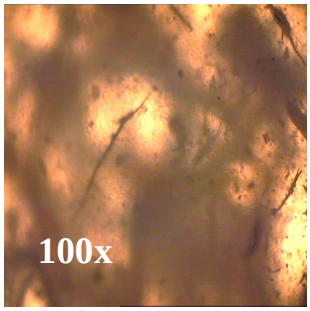

A. cyclops composite with 10% EVOH

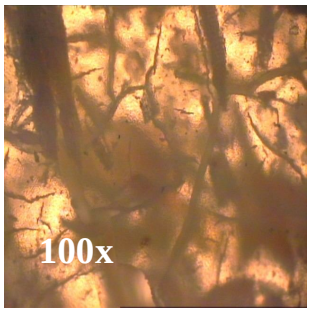

E. grandis composite with 2% EVOH

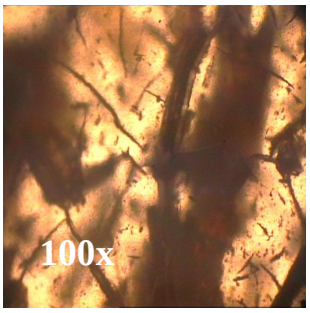

E. grandis composite with 5% EVOH

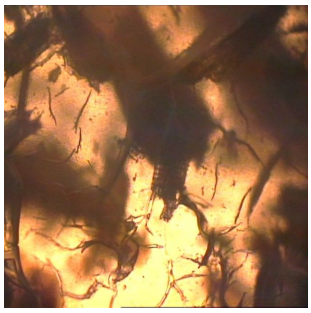

E. grandis composite with 10% EVOH

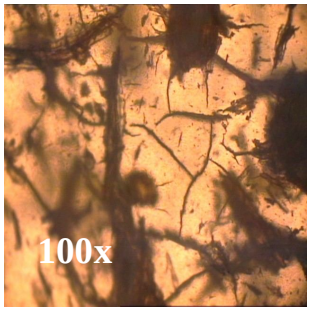

P. radiata composite with 2% EVOH

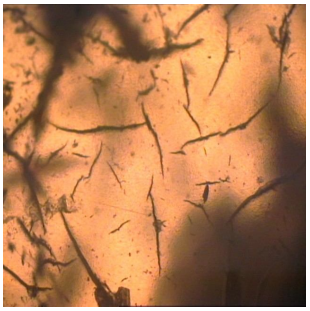

P. radiata composite with 5% EVOH

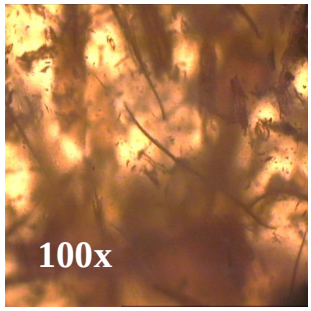

P. radiata composite with 10% EVOH

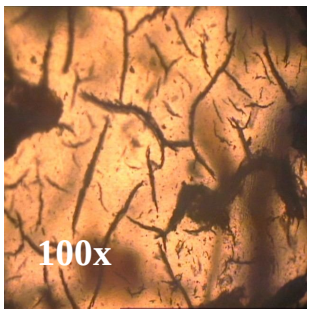

Q. alba composite with 2% EVOH

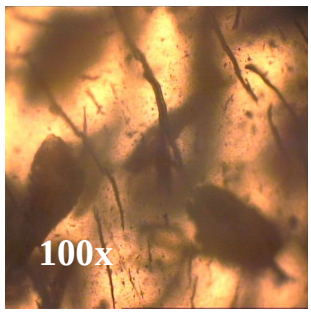

Q. alba composite with 5% EVOH

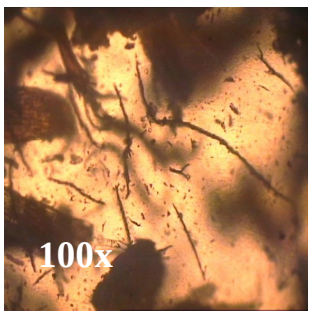

Q. alba composite with 10% EVOH

- Optical micrographs from Chapter 5

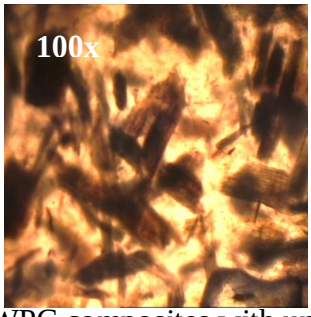

WPC composites with un-extracted *E. grandis*

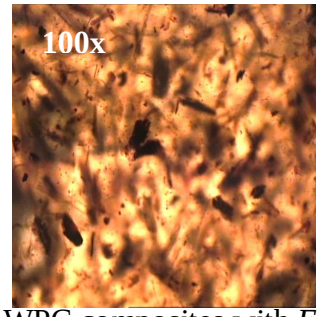

WPC composites with *E. grandis* without E/C extractives

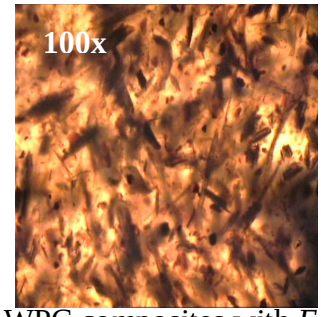

WPC composites with *E. grandis* without HW extractives

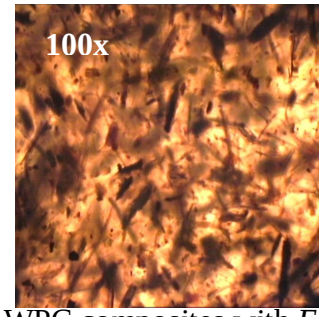

WPC composites with *E. grandis* without both HW and E/C extractives

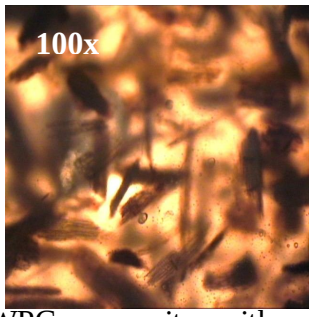

WPC composites with un-extracted *P. radiata*

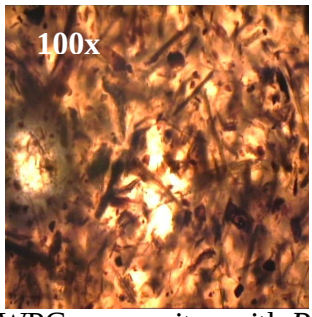

WPC composites with *P. radiata* without E/C extractives

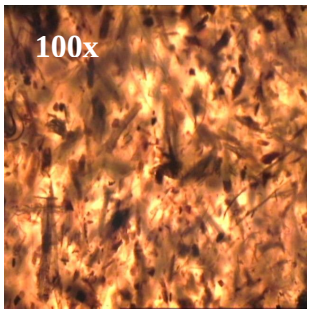

WPC composites with *P. radiata* without HW extractives

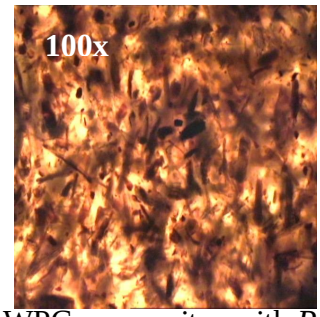

WPC composites with *P. radiata* without both HW and E/C extractives

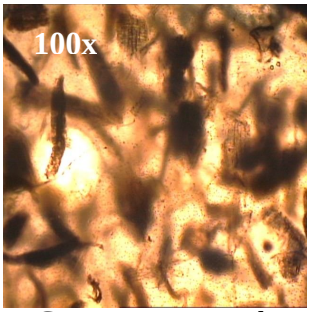

WPC composites with un-extracted *Q. alba*

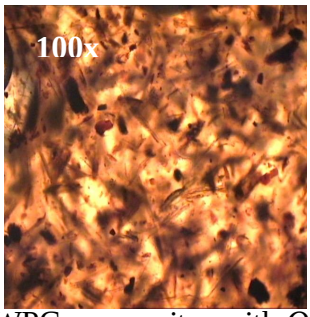

WPC composites with *Q. alba* without E/C extractives

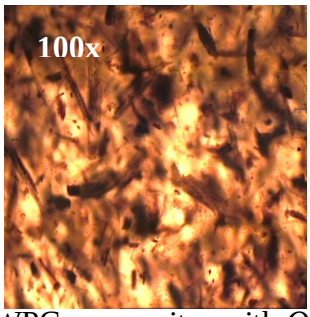

WPC composites with *Q. alba* without HW extractives

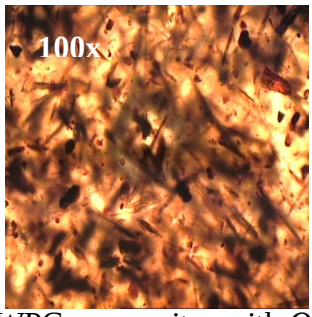

WPC composites with *Q. alba* without both HW and E/C extractives

- Optical micrographs from Chapter 7

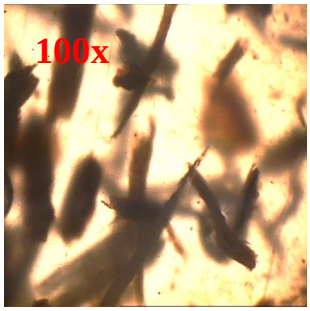

WPC 0-10

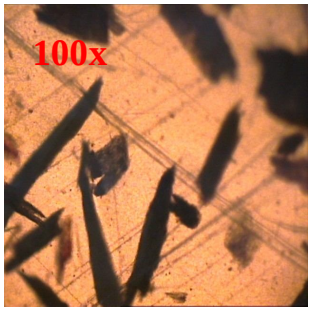

WPC 2-10

WPC 5-10

WPC 7-10

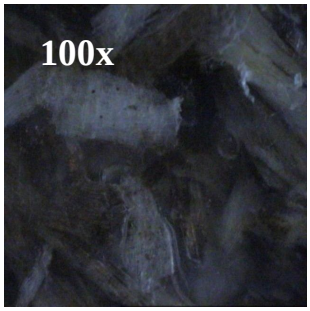

WPC 0-30

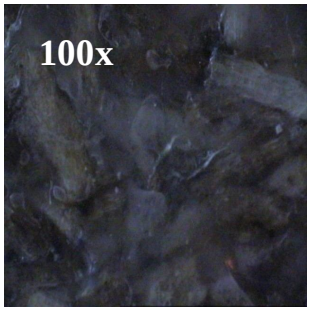

WPC 2-30

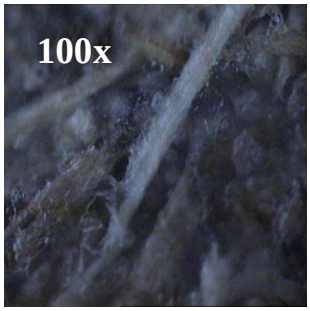

WPC 5-30

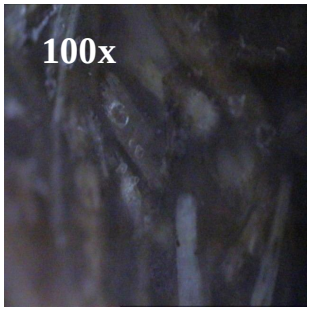

WPC 7-30

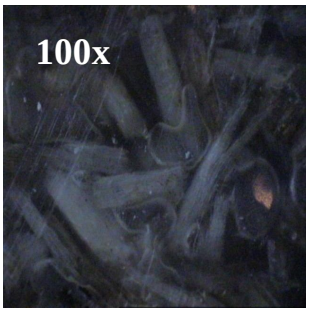

WPC 0-50

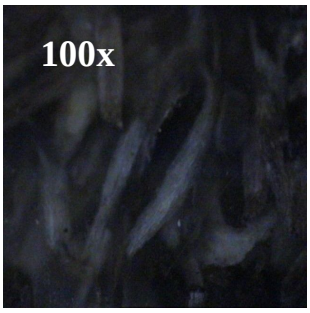

WPC 2-50

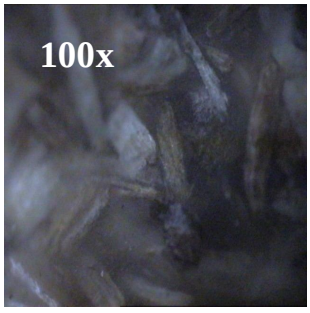

WPC 5-50

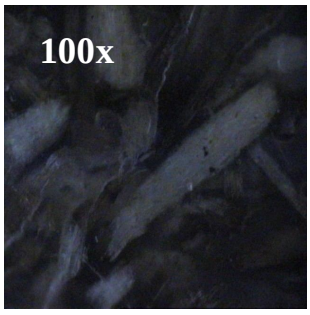

WPC 7-50

- **Optical micrographs from Chapter 8**

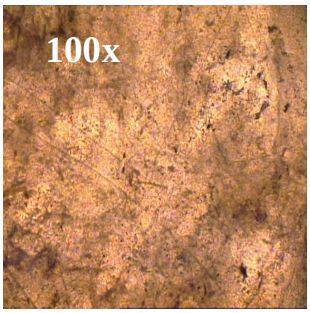

PE

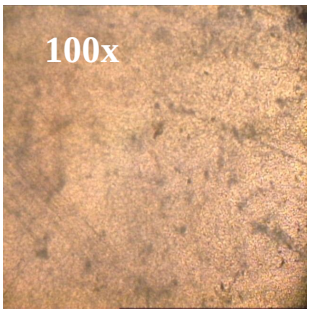

PEOH1

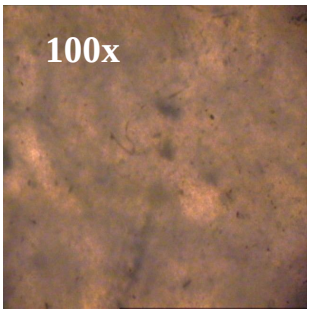

PEOH2

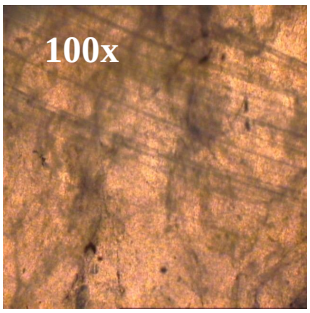

PEOH3

Appendix E: SEM images

- **SEM images of fractured surfaces from Chapter 6**

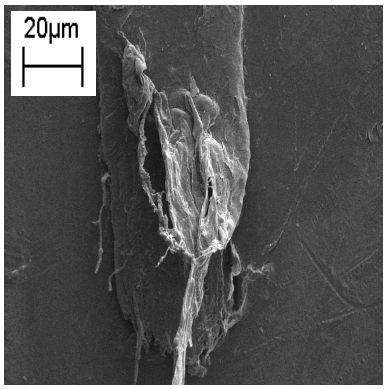

27E180 (Mag. 300x)

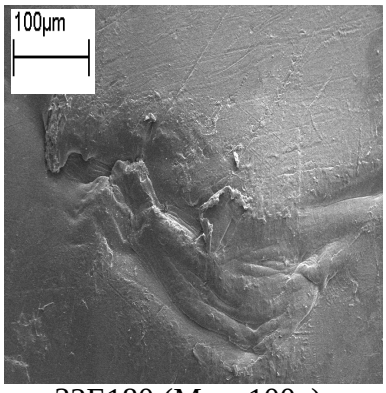

32E180 (Mag. 100x)

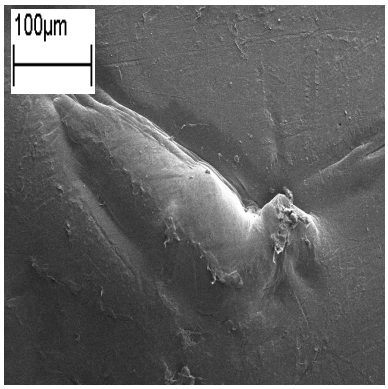

38E180 (Mag. 100x)

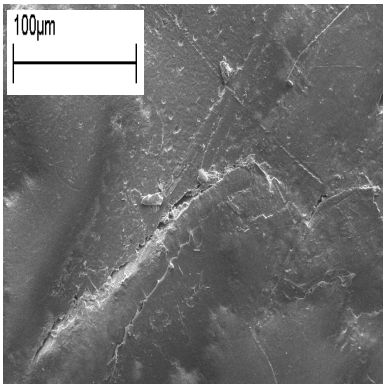

27E250 (Mag. 200x)

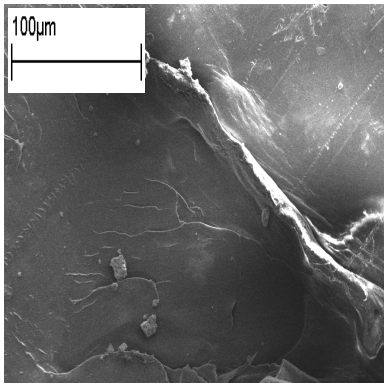

32E250 (Mag. 200x)

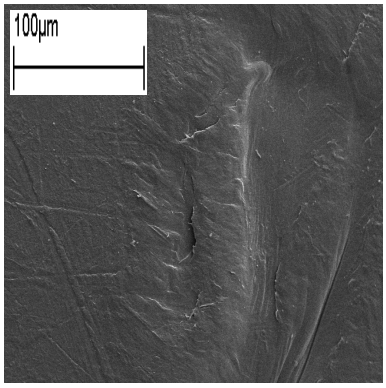

44E250 (Mag. 200x)

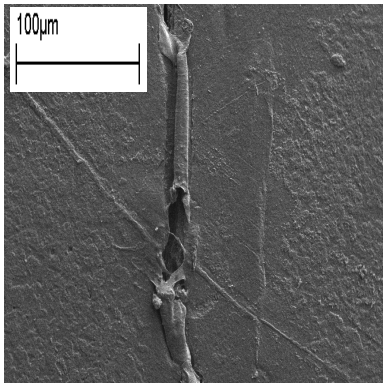

32E450 (Mag. 200x)

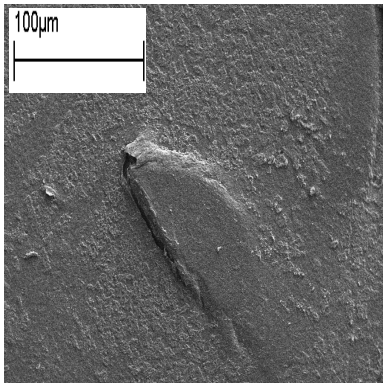

38E450 (Mag. 200x)

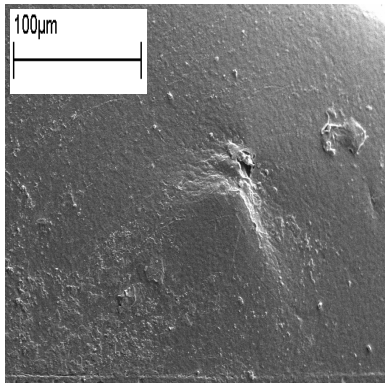

44E450 (Mag. 200x)

Appendix F: FTIR data

- **FTIR data from Chapter 8**